Die Bedeutung der H-Untereinheit des Reaktionszentrums bei der Assemblierung des Lichtsammelkomplexes LH1 in *Rhodospirillum rubrum*

Domenico Lupo

Die Bedeutung der H-Untereinheit des Reaktionszentrums bei der Assemblierung des Lichtsammelkomplexes LH1 in *Rhodospirillum rubrum*

Von der Fakultät Geo- und Biowissenschaften zur Erlangung der Würde eines Doktors der Naturwissenschaften (*doctor rerum naturalium*, Dr. rer. nat.) genehmigte Abhandlung

Vorgelegt von

Domenico Lupo

aus

Bietigheim-Bissingen

Hauptberichter:	Prof. Dr. R. Ghosh
Mitberichter:	Prof. Dr. H. Jeske
Tag der mündlichen Prüfung:	28.01.2005

Biologisches Institut
Abteilung Bioenergetik
Universität Stuttgart
2005

WIDMUNG

Dedico questa tesi ai miei genitori che:

con grandi sacrifici mi hanno permesso di condurre i miei studi,

con grande forza ed energia mi hanno sostenuto in questa impresa,

con grande amore ed affetto mi hanno formato trasmettendomi dei valori veri,

e ringrazio Dio anche per tutti coloro che fanno parte di quella grande ed inesauribile fonte d'energia chiamata famiglia.

Vi voglio un mondo di bene.

Il vostro Domenico

ERKLÄRUNG

Hiermit versichere ich, die vorliegende Arbeit selbständig und unter ausschließlicher Benutzung der angegebenen Hilfsmittel durchgeführt und angefertigt zu haben.

Stuttgart, den 21.12.2004

_____

Domenico Lupo

VORWORT

Die vorliegende Doktorarbeit wird entsperchend dem kumulativen Verfahren vorgelegt. Sie enthält fünf in englischer Sprache verfasste Manuskripte, die zusammen alle Ergebnisse dieser Arbeit umfassen. Davon liegen zwei Manuskripte schon als Publikationen vor:

> Lupo D. and R. Ghosh. 2004. The reaction center H subunit is not required for high levels of light-harvesting complex 1 in *Rhodospirillum rubrum* mutants. J. Bacteriol. 186:5585-5595.
>
> Gerken U., D. Lupo, C. Tietz, J. Wrachtrup, and R. Ghosh. 2003. Circular symmetry of the light-harvesting 1 complex from *Rhodospirillum rubrum* is not perturbed by interaction with the reaction center. *Biochemistry* 42, 10354-10360.

Von den weiteren Manuskripten werden zwei zur Publikation eingereicht und eines wird als Übersichtsartikel in einer Spezialausgabe der Zeitschrift Photosynthesis Research, für den dreizehnten internationalen Photosynthese-Kongress in Montreal, *PS 2004 Light-Harvesting Systems Workshop*, erscheinen. Diesen Manuskripten sind eine deutschsprachige Einleitung, sowie eine Zusammenfassung in den Sprachen Deutsch, Englisch und Italienisch vorangestellt.

Das gesamte Forschungsvorhaben wurde durch ein Stipendium der Landesgraduierten-förderung Baden-Württemberg (Aktenzeichen 7631.2), vom 01.09.2001 bis zum 31.12.2003, finanziell unterstützt.

Die Arbeit zur Isolierung und Aufreinigung der photosynthetischen Einheit wurde im Rahmen des gemeinsamen Projektes mit dem 3. Physikalischen Institut der Universität Stuttgart (*Energierelaxation eines bakteriellen LH1 Komplexes in definierten Komplex-Strukturen und Schichten*) mit einer Doktorandenstelle (vom 01.02.2004 bis 30.11.2004) durch die Deutsche Forschungsgemeinschaft finanziert (Aktenzeichen WR28/13-1).

Beiden Institutionen gilt mein aufrichtiger Dank für das entgegengebrachte Vertrauen in dieses Forschungsvorhaben.

Dezember 2004, Domenico Lupo

ERLÄUTERUNG

Die einzelnen Leistungen und Beiträge zu den Publikationen und Manuskripten werden im folgenden näher erläutert. Dies erfolgt aus Gründen der Klarheit vor allem für diejenigen Arbeiten, an denen mehrere Autoren beteiligt waren.

Publikation zum Deletions/Komplementationssystem:

Mithilfe und Unterstützung bei der Herstellung der elektronenmikroskopischen Schnitte und Aufnahmen durch Dr. Michael Schweikert (Abt. Zoologie, Biologisches Institut, Universität Stuttgart).

Unterstützung bei den ESR-Messungen durch Wolfgang Schmidt (3. Physikalisches Institut, Universität Stuttgart).

Alle weiteren Arbeiten wurden von mir durchgeführt.

Manuskript zur Mutagenese der H-Untereinheit:

Die Berechnung des RC-Modells wurde von Felix Autenrieth (Abt. Bioenergetik, Biologisches Institut, Universität Stuttgart) in der Gruppe von Prof. Dr. K. Schulten (Beckman Institute, University of Illinois) durchgeführt.

Die weiteren Arbeiten wurden von mir durchgeführt.

Publikation zur Einzelmolekülspektroskopie der PSU:

Die spektroskopischen Messungen, die Auswertung der Spektren und die Berechnung der Autokorrelationsfunktion erfolgten durch Dr. Uwe Gerken (ehemals 3. Physikalisches Institut, Universität Stuttgart; derzeit am Institut für Mikrobiologie, Universität Hohenheim).

Kultivierung der Bakterien und fraktionierter Zellaufschluss, sowie die Isolierung, die Aufreinigung, die Rekonstitution und die Qualitätsanalyse der PSU wurden von mir durchgeführt.

Manuskript zur Charakterisierung und Kristallisation der PSU:

Die Isolierung und Aufreinigung der H-LH1-Komplexe aus *R. rubrum* GKΔLM wurde durch Katharina Kittelmann im Rahmen ihrer Studienarbeit in der Abt. Bioenergetik durchgeführt.

Die Massenspektrometrie wurde von Bianca Naumann und Prof. Dr. Michael Hippler durchgeführt (Dep. of Biology, University of Pennsylvania).

Alle weiteren Arbeiten wurden von mir durchgeführt.

Übersichtsartikel:

Dieser Artikel bezieht sich hauptsächlich auf die oben aufgeführten Publikationen.

INHALTSVERZEICHNIS

ZUSAMMENFASSUNG

Das photosynthetische Bakterium *Rhodospirillum rubrum* gehört zur Familie der Nichtschwefelpurpurbakterien (*Rhodospirillaceae*). Es zeichnet sich durch seinen vielfältigen Stoffwechsel aus, darunter die Fähigkeit fakultativ photosynthetisch zu wachsen. Dabei vollzieht es eine sogenannte anaerobe, anoxygene Photosynthese; dazu dient der photosynthetische Apparat (PSA). Dieser PSA befindet sich in spezialisierten Membranen, die aus der inneren Membran des Bakteriums durch Einstülpung hervorgehen und intracytoplasmatische Membranen (ICM) genannt werden. Die Produktion der ICM unterliegt der Regulation durch ein Netzwerk verschiedener Komponenten, die hauptsächlich auf den Sauerstoffpartialdruck ansprechen. Sobald dieser unter den Schwellenwert von 1% sinkt werden sogar im Dunkeln ICM produziert. Die Hauptkomponente des PSA ist die photosynthetische Einheit (PSU). Sie besteht aus einem Lichtsammelkomplex LH1 und dem photosynthetischen Reaktionszentrum RC. Der LH1 aus *R. rubrum* besteht aus 16 Heterodimeren, wobei jedes Heterodimere aus zwei kleinen Polypeptiden α und β aufgebaut ist, an die zwei Bakteriochlorophyllmoleküle und ein Carotinoid gebunden sind. Die LH1 bilden, wie Strukturanalysen aus *R. rubrum* bei mittlerer Auflösung ergaben, eine geschlossene Struktur um das RC aus. Vom RC aus *R. rubrum* gibt es keine Strukturdaten, aber es sind Strukturen aus verwandten Arten vorhanden, die durch Röntgenbeugungsanalysen an RC-Kristallen erhalten worden waren. Diese RC-Strukturen zeigen alle den gleichen Aufbau: Sie bestehen, wie schon früher biochemisch festgestellt, aus drei Untereinheiten (H, M und L). Die Konformation der Heterotrimeren ist identisch und bestätigt frühere Untersuchungen, dass nur die M- und die L-Untereinheit die photosynthetisch relevanten Cofaktoren binden: Vier Bakteriochlorophyllmoleküle, zwei Bakteriophaeophytine, ein Carotinoid, zwei Ubichinonmoleküle und ein Eisenatom. Die Funktion der H-Untereinheit dagegen wurde später durch biochemische, molekularbiologische und strukturbiologische Methoden näher charakterisiert. Die Ergebnisse zeigten für die H-Untereinheit eine wichtige Rolle beim Zusammenbau des RC bzw. der PSU, sowie eine Beteiligung am Primärprozess der Photosynthese: Das Fehlen der H-Untereinheit äußerte sich in der Abwesenheit funktioneller RCs, der Unfähigkeit zur Photosynthese und drastisch verminderten LH1- und ICM-Mengen. Dabei waren aber in einigen Studien, darunter die an *R. rubrum*, nicht nur das Gen für die H-Untereinheit (*puhA*) deletiert, sondern auch flankierende Gensequenzen entfernt worden. In neueren Arbeiten wurde der mehrteilige Aufbau der H-Untereinheit untersucht und den einzelnen Domänen Funktionen zugeordnet.

In der vorliegenden Arbeit wurden verschiedene Projekte mit folgenden Zielsetzungen bearbeitet:

- Die genauere Charakterisierung von H-Untereinheitsmutanten aus *R. rubrum*, die durch einen präzisen genetischen Eingriff hergestellt wurden, und deren Rückführung in den ursprünglichen Elternstatus, mit dem Ziel ein Deletions/Komplementations-system zu etablieren.
- Darauf aufbauend sollten durch zielgerichteter Mutagenese an der H-Untereinheit Domänen definiert und deren Funktion untersucht werden. Das Ziel war die minimale Komponente der H-Untereinheit zu definieren, die in den oben genannten Mutanten den Elternstatus wiederherstellte.
- Das Protokoll zur Isolierung und Aufreinigung der PSU aus *R. rubrum* sollte modifiziert und optimiert werden. Angestrebt war eine einfachere und kostengünstige-re Methode, um große Mengen an reiner PSU zu erhalten.
- Die aufgereinigte PSU aus *R. rubrum* sollte biophysikalisch, biochemisch und strukturbiologisch untersucht werden, um die Geometrie des LH1 in der PSU zu klären, die Komponenten der isolierten PSU zu identifizieren und die PSU zu kristallisieren.

Die genaue Charakterisierung der Mutanten der H-Untereinheit zeigte, dass die durch die Abwesenheit der H-Untereinheit verursachte Reduktion der LH1- und ICM-Mengen aufgehoben werden konnte. Erreicht wurde dies durch die Kultivierung der H-defizienten Stämme in Medien verschiedener Zusammensetzung. Das Deletions/Komplementations-system konnte etabliert werden, indem der ursprüngliche Elternstatus durch ein Plasmid wiederhergestellt wurde, welches das Gen für die H-Untereinheit besaß.

Von diesem Plasmid ausgehend, konnte durch ein molekularbiologisches Design die H-Untereinheit erfolgreich in zwei Domänen getrennt werden. Zum ersten Mal wurde gezeigt, dass die getrennten, aber gemeinsam exprimierten Domänen die Funktion eines intakten H-Proteins beibehalten und somit in der Lage waren, den ursprünglichen Elternstatus in H-defizienten Stämmen hervorzurufen. Durch den einzigartigen Befund, dass jede Domäne für sich, selbständig exprimiert, in der Lage war, RC-Komplexe zu bilden und photosynthetisches Wachstum zu ermöglichen, konnten gleich zwei verschiedene minimale Komponenten definiert werden. Die genetischen Konstrukte, sowie die erhaltenen Expressionsstämme stellen die Grundlage für zukünftige Projekte dar. In diesen soll eine Beteiligung der H-Untereinheit am Regulationsnetzwerk untersucht bzw. dessen Einfluss auf die Sauerstoffempfindlichkeit der generierten Stämme systembiologisch geklärt werden.

Das alte Protokoll zur Isolierung und Aufreinigung der PSU aus *R. rubrum* konnte in seinem Ablauf deutlich vereinfacht werden. Durch die Wahl eines geeigneten Detergenz bzw. des Säulenmaterials für die Chromatographie wurde eine wesentliche Kosteneinsparung erreicht. Mit dem neuentwickelten Protokoll können bei gleicher Ansatzgröße, im Vergleich zum alten, zehnfach höhere Mengen an PSU isoliert werden. Das Absorptionsspektrum dieser PSU-Präparation entsprach dem unbehandelter ICM und die biochemische Analyse mittels Gelelektrophorese zeigte das gleiche Profil wie PSU-Präparationen nach dem alten Protokoll. Die in den PSU enthaltenen Proteine wurden durch Aminosäuresequenzierung mit Hilfe der Massenspektrometrie identifiziert. Dabei handelt es sich um die erste Studie, in der Komponenten der isolierten PSU mit dieser Methode charakterisiert werden. Zusätzlich zu den Komponenten des RC und LH1 wurde ein Protein der äußeren Membran, Porin 41, in der PSU-Präparation gefunden, welches in intensiver Wechselwirkung mit der PSU steht. In zukünftigen Projekten soll geklärt werden, ob dieses Porin ein echter Bestandteil der PSU ist oder aber ein Reinigungsartefakt; wobei im ersten Fall natürlich die Frage nach der Funktion des Porins zu beantworten sein wird. Zur Klärung der Geometrie des LH1 in der PSU wurden Einzelmolekülspektroskopiemessungen durchgeführt und ergaben einen eindeutig zirkular-symmetrischen Aufbau des LH1 um das RC. Dieser Befund galt für detergenz-solubilisierte PSU, aber auch für PSU, die erstmals in Lipidvesikeln rekonstituiert worden waren. Diese Ergebnisse stehen im Gegensatz zu jenen anderer Arbeitsgruppen, die alle elliptisch deformierte LH1-Komplexe in ihren PSU-Präparationen fanden. Die zweidimensionale Kristallisation zur Aufklärung der PSU-Struktur wurde soweit optimiert, dass Kristalle in reproduzierbarer Qualität erhalten wurden. Deren Auflösung lag im mittleren Bereich und ist weiter zu verbessern. Auch die dreidimensionale Kristallisation der PSU kann nunmehr in Angriff genommen werden, da die benötigte Proteinmenge mit dem neuen Protokoll erreicht wird. Mit dem neuentwickelten Reinigungsverfahren konnte ein Protokoll etabliert werden, um PSU aus verschiedenen *R. rubrum* Stämmen routinemäßig zu isolieren. Diese können nicht nur bezüglich ihrer Zusammensetzung, Konformation oder Struktur untersucht, sondern auch zur Aufklärung des Energietransfermechanismus weiter analysiert werden.

SUMMARY

The facultative photosynthetic bacterium *Rhodospirillum rubrum* belongs to the non-sulfur purple bacteria (*Rhodospirillaceae*). It is characterised by its versatile metabolism, which enables growth under either aerobic or anaerobic conditions or to perform an anaerobic anoxygenic photosynthesis. The *R. rubrum* cells produce the photosynthetic apparatus (PSA), which is embedded in specialised membranes derived from invaginations of the inner membrane and designated intracytoplasmic membranes (ICM) or, in isolated form, chromatophores. Expression of ICM is highly regulated by a signal transduction network of multiple components, which responds primarily to the oxygen partial pressure, but is also modulated by changes in light intensity. This bacterium produces ICM even in the dark as soon as the oxygen partial pressure drops below 1%. The main component of the PSA is the photosynthetic unit (PSU) consisting of a light-harvesting complex (LH1) and the photosynthetic reaction centre (RC). LH1 from *R. rubrum* has an hexadecameric structure consisting of heterodimeric α/β-polypeptide subunits, which bind two bacteriochlorophyll a (BChla) and one carotenoid molecule, respectively. Structural analysis at medium resolution revealed that the LH1 from *R. rubrum* encircles the RC in a closed conformation. The structure of the RC of *R. rubrum* is not yet solved, in contrast to the RCs of other species of purple bacteria for which high resolution data from X-ray crystallography are available. These latter data confirmed previous biochemical studies, which showed the RC to consist of three subunits, the H-, M-, and L-polypeptides, with the latter two binding all the cofactors needed for photosynthesis: 4 BChla, 2 bacteriophaeophytin, 2 ubiquinone molecules, one carotenoid and one iron atom. The function of the H subunit was defined only at a later date using biochemical, molecular biological and structural biological approaches. The results assigned the H-subunit to have an essential role in RC assembly and to participate in the primary process of photosynthesis. In previous studies from other groups deletion of the H-subunit resulted in the absence of functional RC, lack of photosynthetic growth and drastically reduced amounts of LH1 and ICM. In a previous study using *R. rubrum*, or other related photosynthetic bacteria, the strategy to obtain H-subunit deletion strains produced not only deletions in the gene encoding the H-subunit (*puhA*), but also in the flanking sequences of *puhA*. In recent studies, the multipartite structure of the H-subunit was analysed and the probable function of each domain was defined.

The present thesis contains following projects and goals:

- A further characterisation of the H-subunit deletion mutants of *R. rubrum*, which were generated by a precise site-directed interposon mutagenesis. Finally, by complementing these strains to the wild-type phenotype, a deletion/complementation system was to be established.
- Based on the above-mentioned system the putative H-subunit domains, indicated by molecular modelling, were to be experimentally characterised by site-directed mutagenesis. The goal was to generate a minimal domain of the H-subunit, which could restore the wild-type phenotype in the deletion strains.
- The protocol present in our laboratory for the isolation and purification of PSU from *R. rubrum* was to be modified and optimised. A further goal was to establish a simpler method, than previously employed, for obtaining a high yield of pure PSU, avoiding large quantities of expensive chemicals.
- The purified PSU from *R. rubrum* was to be characterised biophysical and biochemical techniques, and structural analysis to be performed for answering the question of LH1 geometry, the composition of the PSU and to also obtain structural data.

The characterisation of H subunit deletion mutants performed in this study revealed that the reduced levels of LH1 and ICM due to the absence of the H-subunit could be circumvented by cultivation in high expression growth media containing a combination of carbon sources. Complementation of the deletion strains with a broad-host range vector carrying a fragment encoding solely the H-subunit completely restored the wild-type phenotype, thus establishing successfully the deletion/complementation system.

The H-subunit was separated into two macrodomains by a sophisticated site-directed mutagenesis strategy. It is the first study so far, to show that co-expression of the separated domains still leads to a functional H-subunit and restores the wild-type phenotype in H-subunit deletion strains. Unexpectedly, both domains were able to assemble RC complexes when expressed singly in H-subunit deficient strains, so that we could define two different minimal domains of the H subunit sufficient to allow photosynthetic growth. The palette of plasmids and mutants generated in this study will also provide a number of new of further projects, to analyse the role of the H-subunit in the regulation of the PSA, and its influence upon the observed oxygen susceptibility of the mutant strains, respectively.

The PSU purification strategy published previously could be simplified and optimised. A reduction of costs was achieved by changing the solubilising detergent and also the chromatography matrix employed. The application of this new protocol with amounts of chromatophores equivalent to those used previously with the published procedure, showed an increased yield of purified PSU by up to 10-fold. The analysis of the PSU preparations by either spectroscopy or SDS-PAGE showed them to be identical to those obtained using the previous protocol. Proteins of the purified PSU were identified by amino acid sequencing using mass spectrometry. This is the first study to analyse components of isolated PSU by this technique. In addition to the expected proteins of the RC and LH1, a protein of the outer membrane, Porin41, was found in the PSU preparation. Our biochemical analysis indicated, that this porin is tightly associated with the PSU. In future projects it should be established if the binding of Porin41 to the RC is an artefact due to the isolation and purification protocol applied or whether the association has a physiological role. The LH1 geometry of the PSU was examined by single molecule fluorescence spectroscopy. The results indicated clearly that the LH1 surrounding the RC is present in a circularly symmetric conformation. This result was obtained for both detergent-solubilised PSU and also for PSU reconstituted into lipid vesicles. In contrast to these findings, studies performed by other groups have indicated that the LH1 in their PSU preparations is present in an elliptical conformation. Our results, performed using PSUs diluted in lipid bilayers, suggest that the elliptical deformation in the latter studies is mainly due to packing effects within 2D crystals, or that the detergent used for isolation leads to partial dissociation of the complex. Two-dimensional crystallisation of the PSU was optimised so that a procedure was established for obtaining crystals of reproducible quality. By further optimisation steps, the attainable resolution of the crystals will probably be enhanced. The higher amount of protein using the new developed protocol now allows also three-dimensional crystallisation trials to be feasible. Finally, the new protocol for the isolation and purification of PSU established a method, which allows the extraction of PSU from various *R. rubrum* mutants to be done routinely. Not only the aspects of composition, conformation or structure but also the analysis of energy transfer mechanism within the complex will be of great interest.

SOMMARIO

Rhodospirillum rubrum é un batterio fotosintetico appartenente alla famiglia delle *Rhodospirillaceae*. È caratterizzato da un metabolismo molto versatile e dalla capacità di svolgere la così detta fotosintesi anaerobica e anossigenica tramite l'apparato fotosintetico (PSA). Quest'ultimo é localizzato nelle membrane specializate che derivano da invaginazioni delle membrane interne dei batteri, e che vengono denominate membrane intracitoplasmatiche (ICM) oppure cromatofori. La produzione delle ICM è fortemente regolata da una rete proteica che risponde soprattutto alla pressione parziale dell'ossigeno e che viene attivata anche al buio qualora la pressione scenda sotto l'1%. Il PSA è composto da un'unità fotosintetica (PSU) a sua volta costituita dal collettore di luce (LH1) e dal centro di reazione fotosintectico (RC). Nel batterio *R. rubrum,* LH1 è un complesso di sedici unità eterodimeriche composte da due piccole proteine α e β associate a due molecole di batterioclorofilla ed una di carotinoide. Secondo le analisi strutturali a media risoluzione, questo colletore di luce forma una struttura circoscritta attorno al RC. La struttura del RC di *R. rubrum* rimane tuttora sconosciuta, a differenza di quella di altre specie appartenenti alla stessa famiglia per le quali la struttura è stata dettagliatamente descritta attraverso le analisi cristallografiche a raggi X. Queste analisi, confermate anche da precedenti studi biochimici, hanno mostrato che il RC è composto da tre subunitá polipeptidiche H, M ed L, delle quali le ultime due in grado di legare tutti i co-fattori necessari per la fotosintesi: quattro molecole di batterioclorofilla, due di batteriofeofitina, una di carotinoide, due ubichinoni ed un atomo di ferro. In seguito è stata definita anche la funzione della componente H usando metodi biochimici, genetici e strutturali. Dai risultati si è concluso, che la proteina H svolge un ruolo importante nell'assemblaggio del RC ed é implicata nel processo stesso della fotosintesi: l'eliminazione della subunitá H porta infatti ad un'alterazione del RC, con conseguente compromissione della fotosintesi e drastica riduzione nei livelli d'espressione di LH1 ed ICM. In alcuni studi, fra i quali anche uno condotto su *R. rubrum*, nel processo di eliminazione della subunitá H non è stato eliminato solo il gene per la proteina H (*puhA*) ma anche le sequenze adiacenti (flanking sequences). Studi più recenti hanno analizzato la struttura complessa della proteina H assegnando ai singoli domini le rispettive funzioni.

Gli obbiettivi delle ricerche e le tematiche contenute nella presente tesi sono riportati di seguito:

- Caratterizzazione dettagliata di ceppi di *R. rubrum* mutanti privati della proteina H, ottenuti attraverso un intervento di mutagenesi mirata, e da questi il ripristino delle condizioni originali dei batteri, ottenendo così un sistema di delezione/complementazione.
- Mutagenesi mirata della proteina H per definirne i domini e le relative funzioni, basandosi sul modello di cui sopra allo scopo di definire una proteina H minima che sia in grado di riportare i batteri mutanti allo stato originale.
- Modificazione ed ottimizzazione del protocollo usato finora per l'isolamento e la purificazione della PSU di *R. rubrum* al fine di semplificare la procedura, abbassare i costi ed aumentare l'efficienza di estrazione.
- Analisi della PSU di *R. rubrum* attraverso metodi biofisici, biochimici e strutturali per definire la geometria del LH1 nella PSU, identificare ed isolare le componenti della PSU ed infine cristallizzare la PSU stessa.

In questo studio, la caratterizzazione dei batteri *R. rubrum* privati della componente H ha dimostrato che la riduzione del LH1 e delle ICM causata dall'assenza della proteina H può essere compensata coltivando i batteri in mezzi di coltura differenti, contenenti una combinazione di diverse fonti di carbonio. Il sistema di delezione/complementazione è stato ristabilito usando un vettore (plasmide) che trasporta il frammento codificante per la proteina H nei batteri deficienti, ripristinando in tal modo il loro stato originale.

La proteina H derivata dal plasmide è stata separata con successo in due domini, utilizzando una tecnica di biologia molecolare molto sofisticata. In questo studio é stato dimostrato per la prima volta, che la co-espressione di questi domini conserva la funzione di una proteina H integra, in grado di restaurare lo stato originale nei ceppi mutanti. Inaspettatamente, si è visto anche che ogni singolo dominio, separatamente, é in grado di provocare l'assemblaggio di una RC in grado di fotosintetizzare, permettendo cosí l'identificazione di ben due diverse componenti proteiche minime. I ceppi batterici mutanti ed i plasmidi generati in questo studio costituiranno la base di partenza per progetti che analizzeranno il ruolo della proteina H nella rete regolatoria della PSA nonché l'influenza sulla suscettibilità all'ossigeno dei ceppi mutanti.

Il vecchio protocollo per l'isolamento e la purificazione di PSU dal batterio *R. rubrum* é stato notevolmente semplificato ed i costi sono stati notevolmente abbassati attraverso la scelta di un detergente e di una matrice cromatografica differenti. Inoltre, a paritá di condizioni, la

quantità di PSU isolate è stata aumentata di dieci volte rispetto al vecchio protocollo. Il profilo spettroscopico di questa preparazione rispecchia esattamente quello delle ICM native ed il profilo biochimico (SDS-PAGE) è identico alle PSU estratte secondo il vecchio protocollo. I componenti costituenti della PSU furono identificati sequenziando la loro composizione di aminoacidi usando la spettrometria di massa. La caratterizzazione dei componenti della PSU attraverso questo metodo rimane finora l'unica esistente. Oltre alle proteine del RC e LH1, nella PSU è stata identificata una proteina appartenente alle membrane esterne, chiamata porina 41, che si è mostrata essere strettamente associata alla PSU. In futuro dovrà essere chiarito se si tratta di un artefatto dovuto al protocollo utilizzato oppure di un vero elemento della PSU; in tal caso ovviamente dovrà essere chiarita anche la funzione della porina 41. La geometria del LH1 nelle PSU è stata definita usando la spettroscopia su singole molecole, la quale ha evidenziato la struttura circolare simmetrica del LH1 attorno alla PSU. Questo risultato si è rivelato valido sia per le PSU solubilizzate col detergente, che per le PSU ricostituite per la prima volta in vescicole lipidiche, ed é in contrasto con i risultati pubblicati da altri gruppi i quali hanno sempre osservato una deformazione elittica del LH1. La cristallizzazione bidimensionale, usata per definire la struttura della PSU è stata ottimizzata a tal punto, che si possono ottenere cristalli di qualità riproducibili. Future ottimizzazioni del metodo porteranno certamente ad un miglioramento della risoluzione media. Attraverso il nuovo protocollo è ora possibile anche la cristallizzazione tridimensionale, grazie ad un aumento delle quantità prodotte. Infine, l'applicazione di questa nuova procedura consente l'estrazione di routine delle PSU da varie specie di *R. rubrum* le quali potranno poi essere sottoposte ad analisi non soltanto qualitative e strutturali ma anche di studio del meccanismo di trasferimento energetico.

EINLEITUNG

1. Allgemeines

Organismen, die Photosynthese betreiben, nutzen die Energie des Lichtes für ihr Wachstum. Zu diesen Organismen gehören photosynthetische Bakterien, Algen sowie höhere Pflanzen. Dabei wird die Lichtenergie in biochemische Energie umgewandelt (Abb. 1.1 und Abb. 1.2). Das geschieht mit Hilfe von Pigmentmolekülen aus der Familie der Tetrapyrrole

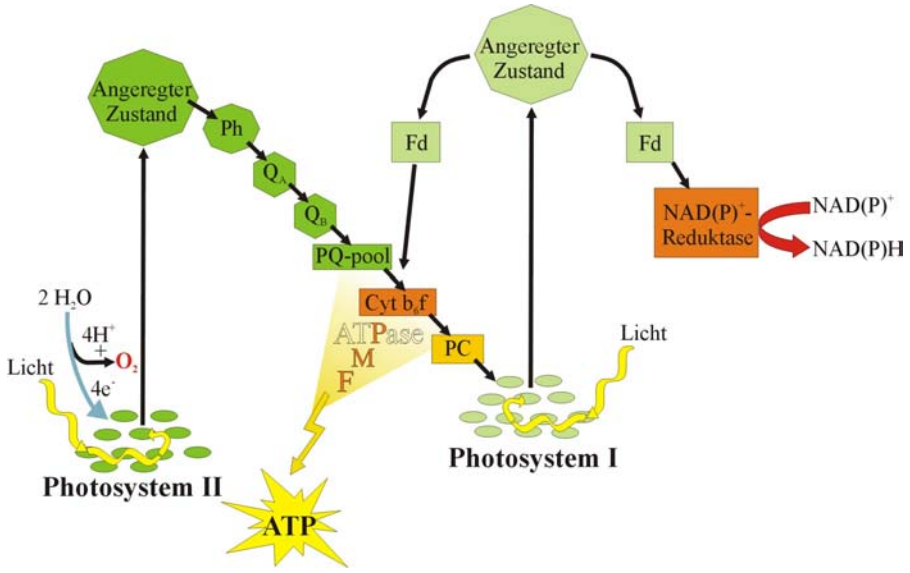

Abb. 1.1: Kopplung von Elektronentransfer und Energiegewinnung in Pflanzen. Die durch Licht angeregten Elektronen der Chlorophylle im Photosystem II (links) werden zum Photosystem I (rechts) geleitet; sogenanntes Z-Schema. Hier erfolgt durch Licht ebenso eine Anregung der Elektronen, die zur Reduktion von NADPH genutzt werden. Auf der Stufe von Cytochrom b_6f wird, wie auch an anderen Stellen, ein Protonengradient (PMF) aufgebaut, der zur ATP-Synthese durch die ATPase dient. Das oxidierte Photosystem II regeneriert sich durch die Spaltung von Wasser, wobei Sauerstoff freigesetzt wird.
Abkürzungen: Phaeophytin (Ph), Plastochinone (Q_A, Q_B und PQ), Plastocyanin (PC) und Ferredoxin (Fd).

(Chlorophylle), welche die absorbierte Lichtenergie durch Ladungstrennung und Abgabe eines Elektrons nutzen. Die Elektronen werden durch bewegliche Moleküle (Chinone oder Ferredoxine) auf Cytochrome übertragen. Diese haemgruppenhaltige Proteinkomplexe nutzen die freiwerdende Energie aus der Redoxreaktion, um zum Aufbau eines Protonengradienten beizutragen. Letzterer dient der Adenosintriphosphatsynthase (ATPase) zur Bildung von Adenosintriphosphat (ATP), welches als sogenannte “Energiewährung“ benutzt wird. Alle beschriebenen Prozesse vollziehen sich in spezialisierten Membranen und werden von Proteinkomplexe der Membran bzw. von membranassoziierten Proteinen durchgeführt.

Im Vergleich zu den komplexen Photosystemen I und II aus Cyanobakterien und Pflanzen, die aus vielen verschiedenen Proteinuntereinheiten aufgebaut sind, sind die Photoeinheiten der Purpurbakterien aus wenigen Baueinheiten zusammengesetzt. Diese Proteinkomplexe

sind Forschungsobjekt der Physiologie, der Biochemie, der Biophysik und der Strukturbiologie mit dem Ziel, den Prozess der Photosynthese auf molekularer Ebene erklären und beschreiben zu können. Der erste Komplex von Membranproteinen, dessen Struktur

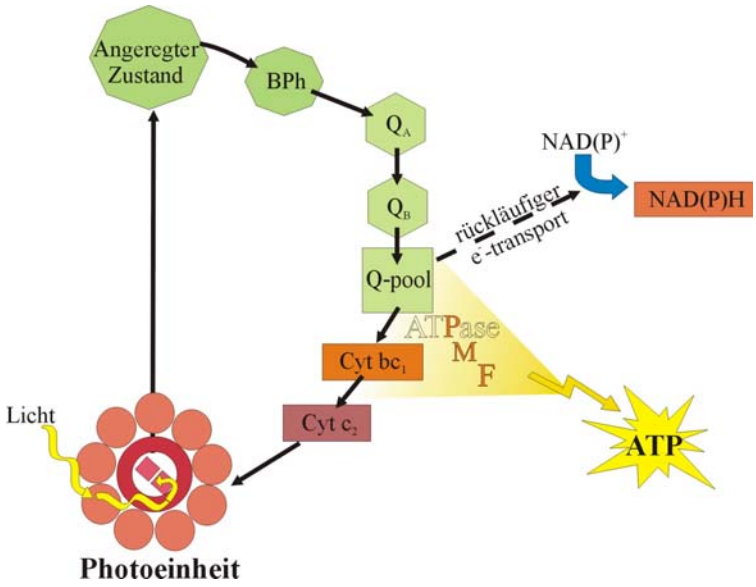

Abb. 1.2: Zyklischer Elektronentransport in Purpurbakterien. Die Bakteriochrorophyllmoleküle der Photoeinheit werden durch Licht angeregt und geben ihre Elektronen an Bakteriophaeophytin (BPh) ab. Diese Elektronen werden über Chinonmoleküle (Q_A, Q_B) und Cytochrome (Cyt bc_1 und Cyt c_2) zur Photoeinheit zurückgeleitet. Die dabei freiwerdende Energie wird durch Cyt bc_1 in einem Protonengradienten (PMF) umgewandelt. Zur Herstellung von NADH müssen die Elektronen in einem rückläufigem Transport energetisch angehoben werden.

aufgeklärt wurde war das photosynthetische Reaktionszentrum (RC) aus *Blastochloris viridis* [Dei85]. Es folgten der Lichtsammelkomplex LH2 aus *Rhodopseudomonas acidophila* [McD95] und *Phaeospirillum molischianum* [Koe96] und kürzlich die Strukturaufklärung der Photosysteme I [Jor01] und II [Fer04] aus *Synechochoccus elongatus*, des Photosystems I aus *Pisum sativum* [Ben03] und des Lichtsammelkomplexes LHCII aus *Spinacia oleracea* [Liu04]. Weitere Bestrebungen sollen zur Aufklärung der Struktur des supramolekularen Komplexes (Reaktionszentrum und Lichtsammelkomplex) führen. Von besonderer Aktualität ist auch die Beschreibung der Dynamik des Zusammenbaus (Assemblierung).

Einen umfassenden Überblick über alle Themenbereichen mit Querverweisen zu Arbeitsgruppen und historischen Entwicklungen der Photosyntheseforschung findet man im Internet [Int1].

2. Die Anoxygene Photosynthese

Im Gegensatz zur pflanzlichen Photosynthese betreiben Purpurbakterien eine anoxygene Photosynthese, die also nicht zur Freisetzung von Sauerstoff durch die Spaltung von Wasser führt. Diese Form von photosynthetischer Energiegewinnung ist durch einen zyklischen Elektronentransport charakterisiert (Abb. 2.1). Die Ladungsspaltung findet im bakteriellen

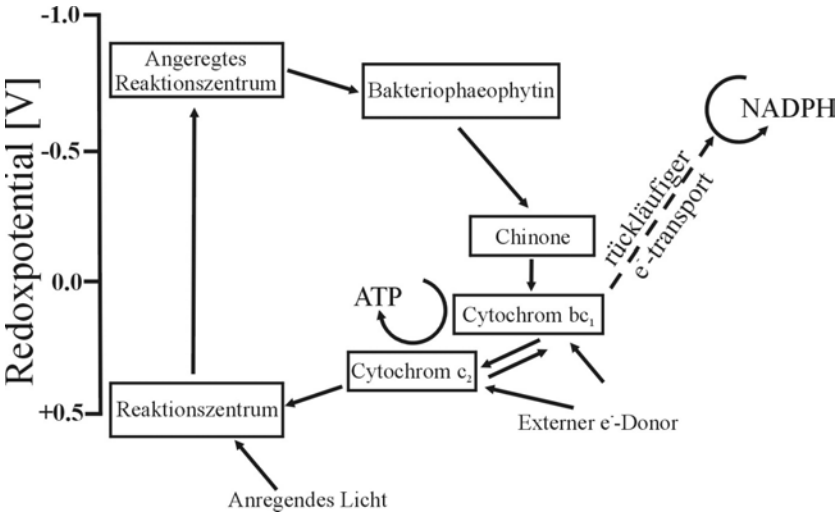

Abb. 2.1: Elektrochemisches Potentialdiagramm. Das Redoxpotential der am zyklischen Elektronentransport beteiligten Komponenten in der anoxygenen Photosynthese ist in Volt dargestellt (Genauere Erklärung im Text).

Reaktionszentrum (RC) am sogenannten "Spezial-Paar" statt; dies sind zwei eng benachbarte Bakteriochlorophyllmoleküle (BChla), die ein Elektron abgeben können. Das abgespaltene Elektron wird über akzessorische BChla- und Bakteriophaeophytinmoleküle (BPh) zuerst zum unbeweglichen Chinon (Q_A) und schließlich zum beweglichen Chinon (Q_B) übertragen. Dieser Vorgang entspricht völlig demjenigen am PSII der Pflanzen. Q_B kann durch die Lipidmembran diffundieren und vom membranständigen Cytochrom bc_1-Komplex oxidiert werden. Da die Reduktion bzw. Oxidation mit der Protonierung und Deprotonierung des Chinons einhergeht, wird an dieser Stelle ein Protonengradient aufgebaut; das Elektron wird an Cytochrom c_2 abgegeben. Dieser bewegliche Elektronentransporter wandert durch das Periplasma zum RC, wo es den Zyklus durch Regeneration des oxidierten RCs schließt. Das RC ist nach seinem Redoxpotenzial nicht im Stande, Wasser als Elektronendonator zu nutzen. Der aufgebaute Protonengradient dient der Energiegewinnung über das membrangebundene ATPase-System. Da die Bakterien aber auch Reduktionsäquivalente benötigen, um Kohlendioxid (CO_2) und Stickstoff (N_2) zu fixieren, wird ein Teil der Elektronen in einem energieverbrauchenden rückläufigen Transport abgezweigt, um Nikotinamidadenindinukleotid NAD(P) zu reduzieren. Diese Reaktion findet nur bei Abwesenheit von Sauerstoff statt, weshalb man von anaerober Photosynthese spricht. Außerdem ist ein externer Elektronendonator erforderlich, um den zyklischen Elektronentransport aufrecht zu erhalten. Als solcher

kann Wasserstoff oder Schwefelwasserstoff fungieren; dann wachsen die Purpurbakterien photoautotroph. Falls diese Donatoren nicht zur Verfügung stehen, sind sie von oxidierbaren Kohlenstoffverbindungen, wie Zucker oder Säuren, abhängig; dann spricht man von photoheterotrophem Wachstum.

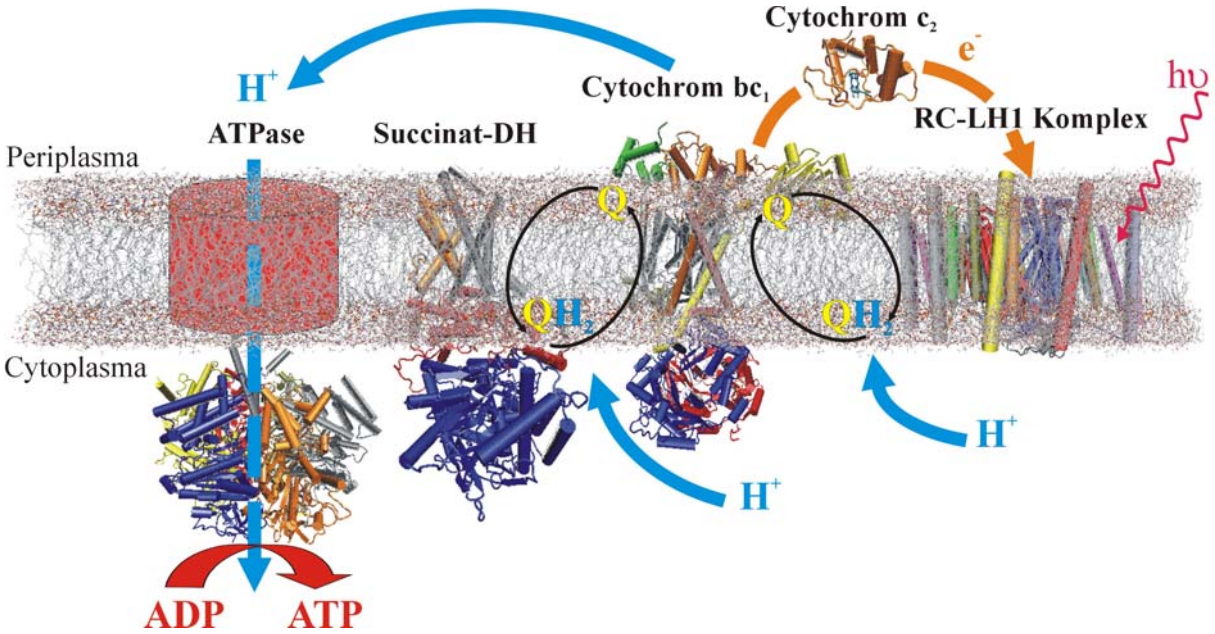

Abb. 2.2: Aufbau der photosynthetischen Membran der Purpurbakterien. Die Hauptkomponenten, die bei der anoxygenen Photosynthese und beim zyklischen Elektronentransport beteiligt sind, wurden, soweit bekannt [Ber00 und Int2], durch genaue Strukturmodelle dargestellt: Lipidmembran (Flüssige Phase, fluid.pdb [Hel93 und Int3]), F1-ATPase (1WOK.pdb [Kag04]), Succinatdehydrogenase (1NEK.pdb [Yan03]), Cytochrom bc_1 (1BCC.pdb [Zha98]), Cytochrom c_2 (3C2C.pdb, Bha81]) und RC-LH1-Komplex (1PYH.pdb, [Ros03]). Die Moleküle wurden mit dem Programm VMD dargestellt [Hum96].

Alle Aspekte der anoxygenen, phototrophen Bakterien, von denen die wichtigsten im folgenden vorgestellt werden, wurden in einer Buchpublikation zusammengefasst [Var95], die allerdings nicht mehr den neuesten Stand enthält.

3. Das Nichtschwefelpurpurbakterium *Rhodospirillum rubrum*

Das α-Proteobakterium *Rhodospirillum rubrum* (Abb. 3.1) aus der Familie der Nichtschwefelpurpurbakterien (*Rhodospirillaceae*) weist eine hohe metabolische Versatilität auf. Neben der Fähigkeit zur anaeroben, anoxygenen Photosynthese ist es in der Lage, bei Dunkelheit durch andere Formen der Energiegewinnung seinen Energiebedarf anaerob zu decken: Es kann anaerob fermentieren oder Nitrat "veratmen", d. h. als Elektronenakzeptor nutzen. Unter aeroben Bedingungen dagegen vollzieht es die normale oxidative Phosphorylierung über den Tricarbonsäurezyklus und Atmungskette. Eine ungewöhnliche Eigenart dieses Bakteriums, wie auch seiner Verwandten, ist die Bildung der spezialisierten Membranen mit dem photosynthetischem Apparat (PSA) und den anderen Komponenten, die für das photosynthetische Wachstum notwendig sind, unter semiaeroben Bedingungen im Dunkeln. Darunter versteht man, dass bei sehr geringem Sauerstoffpartialdruck ($pO_2 \leq 1\%$) sich Einstülpungen in der cytoplasmatischen Membran bilden, die Chromatophoren oder intracytoplasmatische Membranen (ICM) genannt werden und lamelläre, tubuläre oder vesikuläre Form besitzen [Dre78]. Diese Eigenschaft der Bakterien wird aus ihrer ökologischen Nische verständlich. Denn unterhalb der Chemokline (im Hypolimnion) aquatischer Lebensräume müssen diese Organismen auf sich ständig verändernde Umweltbedingungen reagieren. Bei der Laborkultivierung macht man sich diese Eigenschaft zu nutze, um unter semiaeroben Bedingungen Chromatophoren zu produzieren. Heute ist man in der Lage, aus *R. rubrum* unter semiaerober Kultivierung in optimiertem Medium [Gho94], ICM-Mengen zu isolieren, die man sonst nur unter anaeroben, "photosynthetischen" Bedingungen erhielte. Das macht diese Bakterien zu ausgezeichneten Versuchsorganismen, um die Komponenten des PSA und deren Regulation zu untersuchen, da Veränderungen bei photosynthetisch relevanten Genen unter nicht-photosynthetischen Bedingungen analysierbar und Eingriffe möglich sind.

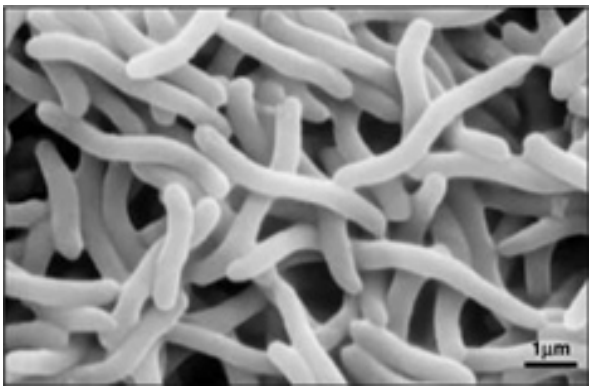

Abb. 3.1: Elektronenmikroskopische Aufnahme von *Rhodospirillum rubrum* [aus Int4].

4. Regulation des Photosyntheseapparates

Neben Licht ist Sauerstoff der Hauptparameter, der die Produktion des PSA beeinflusst. Die Expression der photosynthetischen Komponenten wird durch ein komplexes Signaltransduktions- und Regulationsnetzwerk kontrolliert [Pem98, Zei98, Oh01 und Zei04]. Dabei werden die Umweltfaktoren entweder direkt von Regulatorproteinen registriert oder ihre Änderung als Redoxsignale weitergegeben (Abb. 4.1). Eine zentrale Rolle spielt dabei das Zweikomponentenregelwerk [Jos96], bestehend aus einer membranständigen Sensor-Histidinkinase (RegB) [Mos94] und dem DNA-bindenden Regulatorprotein (RegA) [Sga92]. Als Signal dient dabei der vom cbb_3-Komplex, einer Cytochromoxidase, stammende Elektronenfluss, welcher bei hohen Sauerstoffpartialdrücken stärker ist und bei umgekehrten Verhältnissen zur Phosphorylierung des RegA-Proteins durch RegB führt[Oh00], was die Aktivierung der Genexpression auslöst. Eine Reihe von Repressor/Antirepressor-Systemen sorgt für die Feinregulierung der Genexpression [Zei98]. Das ausgefeilteste Regulationssystem zeigt das PpsR/ AppA Repressor/Antirepressorpaar [Mas02]. PpsR reprimiert in Anwesenheit von Sauerstoff die Genexpression und wird bei sinkendem O_2-Partialdruck von AppA reduziert. Dadurch werden strukturerhaltende Disulfidbrücken gelöst und PpsR kann von AppA in zwei Dimere getrennt werden, die an je einen Antirepressor gebunden bleiben. Dies führt zur Aufhebung der Repression. Bei hohen Blaulichtintensitäten kommt es aber zu einer Konformationsänderung des Flavoproteins AppA, die zur Freisetzung von PpsR und somit zur erneuten Repression der kontrollierten Gene führt.

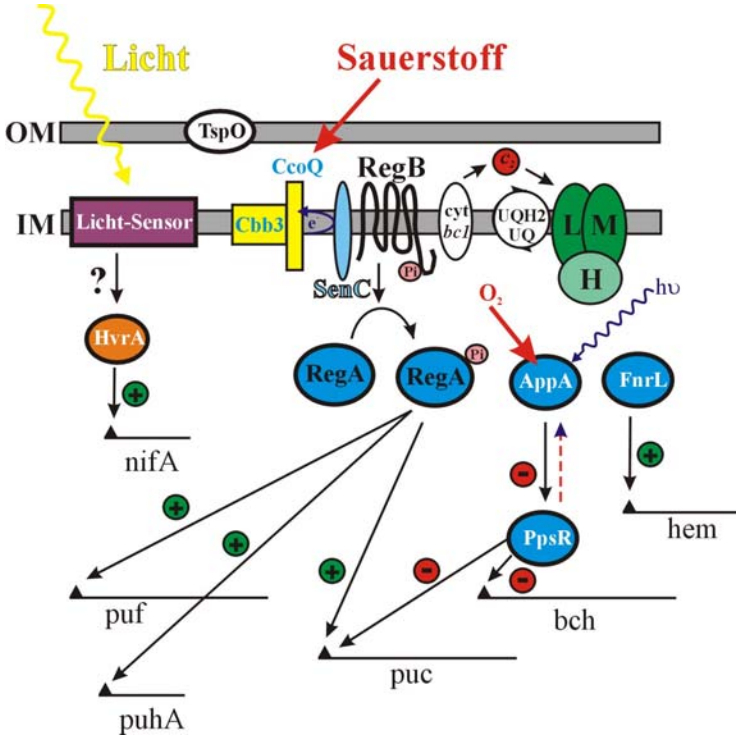

Abb. 4.1: Signaltransduktionsnetzwerk und Komponenten zur Regulation der Photosynthesegene. Alle bis heute bekannten Komponenten des Regulationsnetzwerkes sind aufgeführt: HvrA [Bug94], TspO [Yel95], Cbb3/CcoQ [Oh00], SenC [Era00], RegA/RegB [Swe01], PpsR [Pon95], AppA [Gom95] und FnrL [Zei95]. Die Funktionen der einzelnen Komponenten sind durch Pfeile mit Plus- oder Minuszeichen dargestellt (induzierende oder inhibierende Wirkung auf die verschiedenen Gengruppen (siehe Abb. 4.2); weitere Erläuterungen im Text).

Da sich alle Gene, die für das photosynthetische Wachstum notwendig sind, unter der Kontrolle dieses Netzwerkes befinden, findet man in vielen Vertretern der Nichtschwefelpurpurbakterien eine benachbarte Lage aller dieser Gene. Dieser Genomabschnitt wird als photosynthetischer Gencluster (PGC) bezeichnet (Abb. 4.2), ist 40 bis 50 Kilobasen groß und kodiert sowohl für die PSA-Komponenten als auch für die Enzyme der Pigmentbiosynthese und für die Regulatoren selber [Nay99 und Iga01]. Die meisten dieser Gene befinden sich in kleinen Transkriptionsgruppen (Operons) oder großen Superoperons. Dies gewährleistet den schnellen und koordinierten Aufbau des PSA. Diese Gengruppierungen sind sogar in *R. rubrum* unverändert vorhanden, obwohl es kein solches PGC besitzt [Int4].

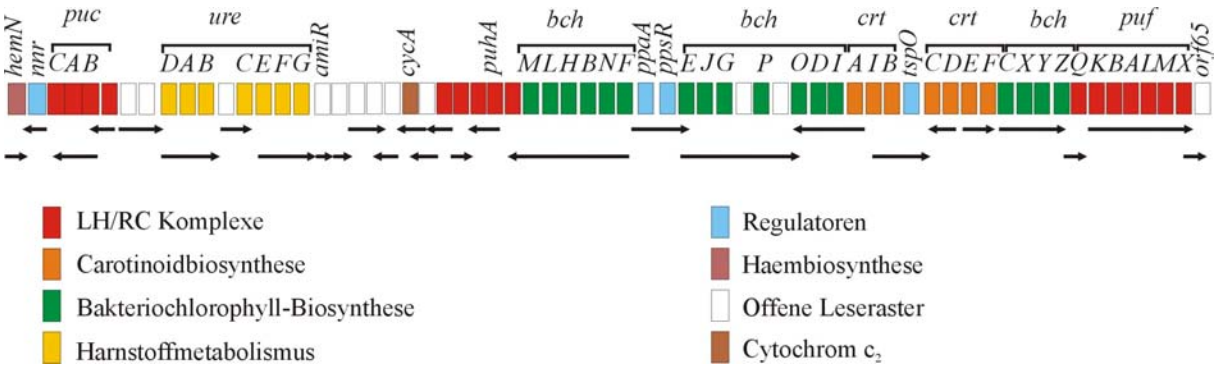

Abb. 4.2: Aufbau des photosynthetischen Genclusters aus *Rhodobacter sphaeroides* (PGC). Die Pfeile stellen Gruppen von Genen dar, die gemeinsam abgelesen werden. Die Leserichtung wird durch den Pfeilkopf angezeigt. Die Farbkodierung in der Legende zeigt die funktionellen Gruppen an.

5.Funktion und Aufbau des Photosyntheseapparates

Der PSA von *R. rubrum* besteht nur aus der photosynthetischen Kerneinheit (PSU), die vom Reaktionszentrum (RC oder B800) und vom Antennen- bzw. Lichtsammelkomplex 1 (LH1 oder B875/880) gebildet wird. Andere Spezies der *Rhodospirillaceae* besitzen dagegen weitere Lichtsammelkomplexe, wie LH2 (B800-850), LH3 (B800-820) [McL01] oder LH4 (B800) [Har02]. Alle aufgeführten photosynthetischen Komponenten können spektroskopisch voneinander unterschieden werden und jegliche Eingriffe, auf molekularbiologischer (Mutanten) oder biochemischer (Dissoziation) Ebene, äußern sich in Veränderungen dieser physikalischen Eigenschaft; was diese Bakterien zu idealen Versuchsobjekten gemacht hat.

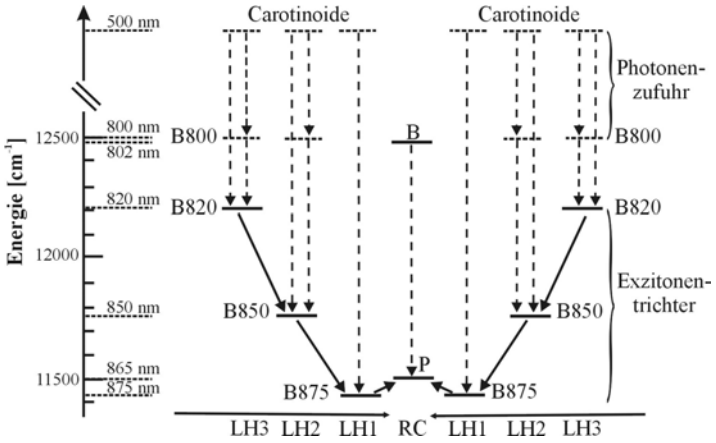

Abb. 5.1: Energietransfer im Photosyntheseapparat von Purpurbakterien. Die Energiezustände der Photosynthesekomponenten sind als horizontale Linien dargestellt und mit der entsprechenden Wellenlänge ihres Absorptionsmaximums bezeichnet. Die gestrichelten Pfeile zeigen innermolekularen und die durchgezogenen Pfeile zwischenmolekularen Energietransfer an. Modifiziert aus [Hu02].

Von den Pigmentmolekülen der Lichtsammelkomplexe wird die absorbierte Lichtenergie in einem extrem kurzen Zeitintervall als Anregungsenergie (Exziton) ins RC geschleust, in dem der photosynthetische Primärprozess der Ladungstrennung stattfindet. Dieser schnelle Exzitonentransfer ist das Ergebnis der verschiedenen Energiezustände der Pigmentmoleküle, die ein Energiegefälle (Abb. 5.1) zum RC aufweisen [Hu02]. Da die Rückreaktion vom RC zum LH1 schneller abläuft [Kat03] als die Lebenszeit des LH-Anregungszustandes (1 ns),

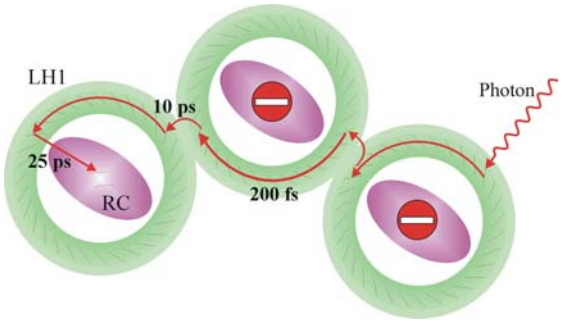

Abb. 5.2: Energietransfer in photosynthetischen Kerneinheiten (PSU). Die aus einem Photon stammende Energie wird solange über benachbarte PSUs weitergeleitet bis ein freies RC erreicht ist, das die Energie in eine Ladungsspaltung umsetzt. Bild modifiziert aus [Ger03].

können die Exzitonen weitergeleitet werden, bis ein empfangsbereites RC erreicht wird (Abb 5.2). Dies resultiert in sehr hohen Energieausbeuten (fast 100% Effizienz), die auf die speziellen Pigmentmolekülanordnungen zurückzuführen sind.

In LH2-Molekülen, dessen Struktur aufgeklärt wurde, findet man eine ringförmige Bakteriochlorophyllanordnung (Abb. 5.3). Diese variiert je nach Spezies zwischen acht [Koe96] und neun Dimeren [McD95]. Auch die LH1 Komplexe bilden, wie die Studien an

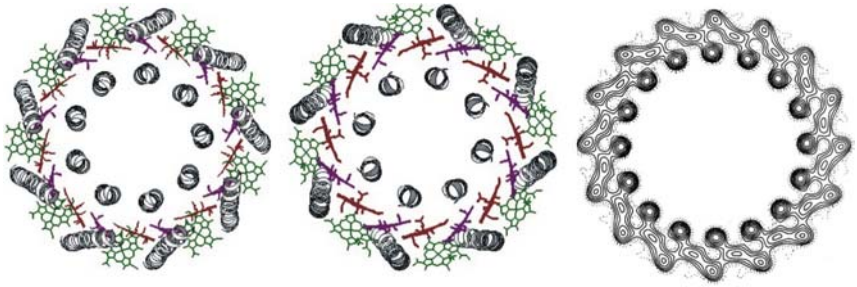

Abb. 5.3: Strukturen der Lichtsammelkomplexe. Links die Kristallstruktur des LH2 aus *Rps. acidophila* (1KZU.pdb, [McD95]). In der Mitte die LH2 Struktur aus *Phs. molischianum* (1LGH.pdb, [Koe96]). Rechts die Elektronendichteverteilung in zweidimensionalen Kristallen des

zweidimensionalen Kristallen [Kar95] und biophysikalischen Analysen zeigten [Sch03], ringförmige Strukturen aus, die aber aus 16 Dimeren bestehen (Abb. 5.3). Jedoch weisen Strukturuntersuchungen an photosynthetischen Einheiten, also RC-LH1-Komplexe (Abb. 5.4 und Abb. 5.5), unterschiedliche Anordnungen auf, die vom geschlossenem LH1-Ring [Jam02], über offene, "S"-förmige RC-LH1-Dimere [Jun99 und Sch04] bis hin zu fast geschlossenen LH1-Ellipsen um ein RC reichen [Ros03].

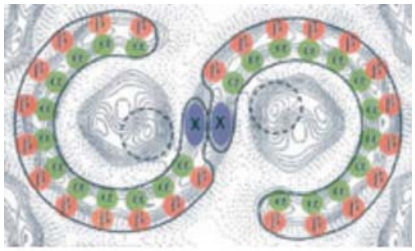

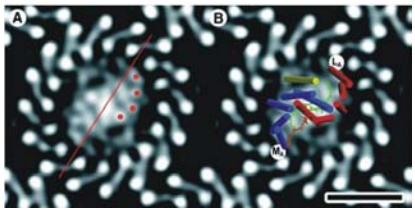

Abb. 5.4: Zweidimensionale Kristalle der PSU.

Oben: Elektronendichteverteilung der "S"-förmigen PSU aus *Rb. sphaeroides* bei 26 Å Auflösung [Sch04].

Unten: Elektronendichteverteilung von RC-LH1 Komplexe aus *R. rubrum* aufgelöst bei 8.5 Å [Jam02].

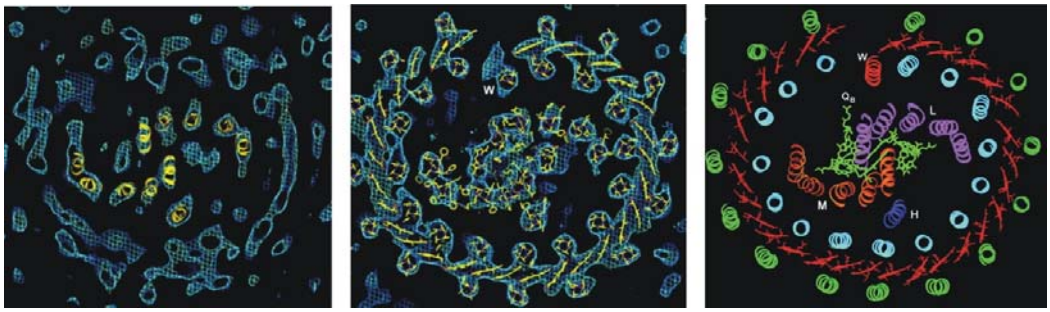

Abb. 5.5: Kristallstruktur der PSU aus *Rhodopseudomonas palustris*. Links: Elektronendichteverteilung mit den transmembranspannenden α-Helices des RC (in gelb); berechnet nach der "molecular replacement" Methode mit einer Auflösung von 4.8 Å. Mitte: Weitere Bestandteile wie LH1-Polypeptide und Farbstoffmoleküle wurden hinein modelliert. Rechts: Schematisches Modell der PSU mit allen Komponenten (1PYH.pdb). Abbildung stammt aus [Ros03].

Vom RC dagegen gibt es drei Strukturen auf der Basis der Röntgenanalyse von Kristallen [Dei85, All86 und Nog00], darunter die aus *Blc. viridis* [Dei85], die als erste Membranproteinstruktur aufgeklärt wurde und 1988 mit dem Nobelpreis ausgezeichnet wurde. Das RC besteht aus drei Proteinuntereinheiten, die auf grund ihres elektrophoretischen Verhaltens mit H ("heavy"), M ("middle") und L ("light") bezeichnet werden. Diese Polypeptidketten besitzen zu 50%-80% gleiche Aminosäurenzusammensetzung, ihre dreidimensionale Faltung und ihre räumliche Anordnung sind aber fast identisch (Abb. 5.6). Während die Funktion der L- und M-Polypeptide aus der nicht-kovalenten Bindung aller Pigmentmoleküle und Cofaktoren besteht [Oka74] und durch die Strukturen auf molekularer Ebene ersichtlich wird (Abb. 5.6), war die Funktion der H-Untereinheit noch weitgehend unklar.

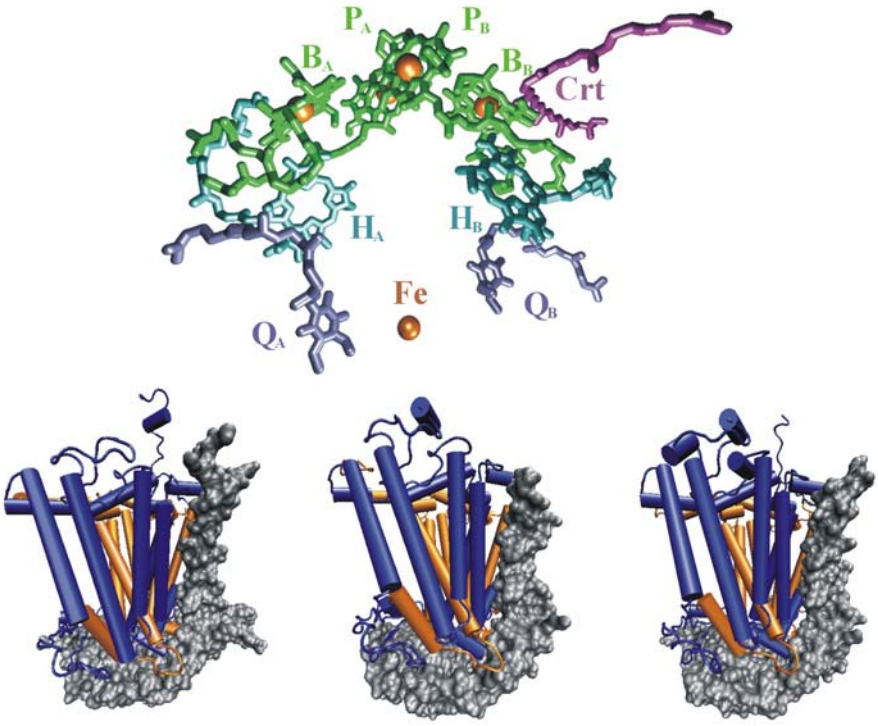

Abb. 5.6: Struktur des photosynthetischen Reaktionszentrums (RC). Oben: Anordnung der Cofaktoren im RC; "Spezial-Paar" (P_A und P_B), akzessorische Bakteriochlorophylle (B_A und B_B), Bakteriophaeophytine (H_A und H_B) Chinone (Q_A und Q_B), Carotinoid (Crt) und Eisen (Fe). Unten: Links – Struktur des RC aus *Blc. viridis* (1PRC.pdb, [Dei95]). Mitte – RC aus *Rb. sphaeroides* (1PCR.pdb, [Erm94]) und Rechts – RC aus *Thermochromatium tepidum* (1EYS.pdb, [Nog00]). H-, M- und L-Untereinheiten sind in Grau, Blau und Orange gefärbt. Zur besseren Übersicht wurden M und L schematisch und H mit ausgefüllten Atomradien dargestellt. Die Moleküle wurden mit dem Programm VMD dargestellt [Hum96].

6. Erkenntnisse über die Funktion der H-Untereinheit

Die ersten *in vitro* Studien zeigten, dass dieses Protein zwar aus dem RC-Komplex abgetrennt werden konnte, ohne den primären Prozess der Ladungstrennung zu beeinflussen [Oka74 und Vad79]. Die Reduktion des mobilen Elektronentransporters Q_B wurde dadurch aber drastisch herabgesetzt [Deb85 und Har98]. Auch andere Eigenschaften des RC, wie die Affinität zum Q_B und die Wiederstandsfähigkeit gegenüber denaturierenden Stoffen wurde stark vermindert. Das führte zu dem Schluss, dass die H-Untereinheit die Umgebung der Q_B-Bindestelle beeinflusse, vielleicht durch die Wechselwirkung mit speziellen Membranlipiden [McA99 und Cam02]. Diese Aussage wurde durch Strukturaufklärung höherer Auflösung [Dei95] zum einen gestützt und zum anderen erweitert, denn für die H-Untereinheit ergab sich dabei eine Beteiligung an der Ausbildung eines Protonenkanals, welcher vom Cytoplasma zur Q_B-Bindestelle reicht [Sto97]. Durch gezielten Aminosäurenaustausch in der H-Untereinheit konnte diese Funktion bestätigt werden [Tak96 und Abr98]. Das Fehlen der H-Untereinheit, das auf gentechnischem Wege erreicht wurde [Soc89], hatte weitreichende Folgen. Die Entfernung des *puhA* Gens (kodiert für das H-Protein) äußerte sich in der Abwesenheit eines funktionellen RC und somit in einer Unfähigkeit der veränderten Stämme photosynthetisch zu wachsen. Genauere Untersuchungen mit hilfe präziserer genetischer Eingriffe, lieferten weitere Befunde zur Funktion der H-Untereinheit sowie der *puhA* umgebenden Gene [Won96, You98 und Akl00]. Zusammen mit den Ergebnissen aus einer Studie an *R. rubrum* [Che00] kam man zu der Auffassung, dass die H-Untereinheit als Gerüstprotein dient, die den Einbau der L- und M-Untereinheiten in die Membran erleichtert (wie ein Chaperon); ihre Abwesenheit bewirkte eine drastische Abnahme der LH1- und ICM-Mengen. Die neueste Untersuchung zur Funktion der H-Untereinheit und zum Zusammenbau des RC zeigt aber ein völlig anderes Bild [Teh04]. Danach wirkt die M-Untereinheit als Basisprotein, dessen Wechselwirkung mit der L-Untereinheit erst den Einbau der H-Untereinheit in die Membran ermöglicht. Jedoch ist der LM-Komplex in Abwesenheit der H-Untereinheit einem schnellen Abbauprozess unterworfen. Außerdem kann ohne die H-Untereinheit die notwendige Anhäufung der L- und M-Proteine im Cytoplasma nicht stattfinden. Diese Ergebnisse ergänzen eine frühere Arbeit der gleichen Gruppe [Teh03], die den molekularen Aufbau der H-Untereinheit und dessen Funktion klären sollte. Aus Strukturvergleichen der verschiedenen H-Untereinheiten war bekannt [Fat01], dass dieses Protein zwei bzw. drei Domänen aufweist; einen periplasmatischen Anteil, einen Transmembranteil (manchmal mit dem periplasmatischen Anteil als Einheit angesehen) und einen cytoplasmatischen Teil (Abb. 6.1). Die größere

ist die cytoplasmatische Domäne, die wie ein “Kochlöffelkopf“ herausragt und den LM-Komplex einfasst. Diese Domäne besitzt ein 80 Aminosäuren langes Strukturmotiv, ein PRC-H β-Fass, welches als Prototyp einer neuen Proteinstruktur-Überfamilie definiert wurde [Ana02] und in Archaebakterien, Eubakterien und Pflanzen weit verbreitet ist. Man findet dieses PRC-H β-Fass unter anderem in Proteinen, die an Elektronentransferreaktionen, am RNA-Metabolismus und an Protein-Protein-Wechselwirkungen beteiligt sind. In der obengenannten Arbeit [Teh03] wurden die drei Domänen der H-Untereinheit aus *Rb. sphaeroides* gegen die Domänen aus *Blc. viridis* systematisch ausgetauscht und die Effekte in einem H-defizienten Stamm untersucht. Nur die Transmembrandomäne tolerierte den Interspeziesaustausch, bildete jedoch nur noch 65% an RC aus. Der Austausch der beiden anderen Domänen zeigte, dass diese zwar einen speziesbedingten Einbau der H-Untereinheit vermittelten, der aber vom genetischen Hintergrund abhing. Die H-Untereinheit mit dem

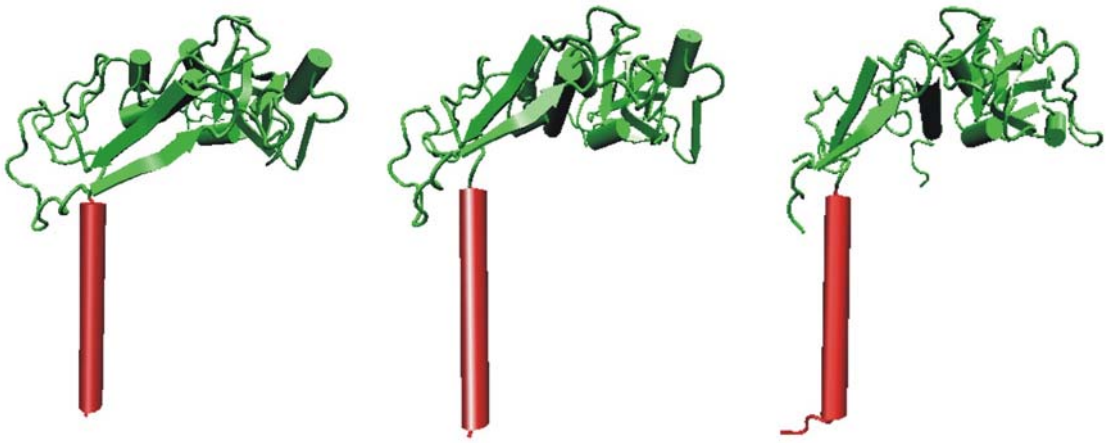

Abb. 6.1: Strukturvergleich der H-Untereinheiten. Alle H-Untereinheiten zeigen den gleichen, zweigeteilten Aufbau: Eine Transmembran-Domäne (als roter Zylinder dargestellt), die die H-Untereinheit in der Membran verankert und eine cytoplasmatische Domäne (grünfarben), die auf den L- und M-Proteinen sitzt. Quelle der Kristallstrukturen wie in Abb. 5.6 angegeben und dargestellt mit dem Programm VMD [Hum96].

“fremden“ periplasmatischen Anteil führte nur in Stämmen mit zusätzlichen LH2-Komplexen zu photosynthetischem Wachstum. Dagegen waren H-Untereinheiten mit ausgetauschten cytoplasmatischen Domänen in allen Fällen unfähig, photosynthetisches Wachstum zu vermitteln.

Das Verständnis der Funktion der H-Untereinheit wurde zwar durch die aufgeführten Studien im Laufe der Zeit immer besser, bleibt aber nach über zwei Jahrzehnten noch immer unvollständig und in Details rätselhaft.

7. Zielsetzungen

A. **Etablierung eines Deletions/Komplementationssystems**
   Vorhandenen *R. rubrum*-Stämme war durch zielgerichtete Mutagenese die H-Untereinheit entfernt und durch eine Antibiotikaresistenz ausgetauscht worden [Lup00]. Diese Stämme waren zunächst genauer zu charakterisieren. Danach sollten diese Deletionsmutanten wieder in den ursprünglichen "Elternstatus" versetzt werden. Dafür war ein Plasmid zu konstruieren, das nur für die H-Untereinheit kodierte und in diese Stämme transferiert werden konnte. Die Wiederherstellung des Elternstatus sollte gewährleistet werden.

B. **Mutagenese der H-Untereinheit**
   Vom etabliertem Deletions/Komplementationssystems ausgehend sollte eine minimale H-Untereinheit hergestellt werden, mit der die Ausbildung eines funktionellen RC und damit die Photosynthese möglich ist. Die erhaltenen Stämme sollten biochemisch und biophysikalisch untersucht werden.

C. **Isolierung und Aufreinigung der photosynthetischen Einheit**
   Das vorhandene Protokoll [Sta98] sollte verbessert werden, um größere Ausbeuten an PSU zu erreichen. Angestrebt war eine kostengünstige Vereinfachung mit größtmöglichem Ertrag.

D. **Biophysikalische und biochemische Charakterisierung der isolierten PSU**
   Die isolierten und aufgereinigten PSU sollten spektroskopisch untersucht werden. Diese Qualitätskontrolle zeigt sehr rasch jegliche Veränderungen auf molekularer Ebene an. Ferner sollte die Zusammensetzung der PSU-Komponenten biochemisch geklärt werden.

E. **Strukturuntersuchung und zweidimensionale Kristallisation der PSU**
   Durch Einzelmolekülspektroskopie an in Detergenz gelösten, sowie in Lipidvesikeln eingebetteten PSU sollte die Form dieses Komplexes untersucht werden. Zur Strukturaufklärung sollte ein Protokoll etabliert werden, welches zweidimensionale Kristalle der PSU in reproduzierbarer Qualität liefern sollte.

8. Ergebnisse

Zu A. Das Deletions/Komplementationssystem konnte etabliert werden. Alle Stämme wurden durch zahlreiche Untersuchungsmethoden charakterisiert und die Ausfallerscheinungen infolge Fehlens der H-Untereinheit beschrieben. Die Deletionsmutanten besaßen kein RC und waren somit unfähig, photosynthetisch zu wachsen. Im Gegensatz zu anderen Studien [Soc89, Won96 und Che00] waren die LH1- und ICM-Mengen nicht reduziert, wenn die Zellen in M2SF-Medium [Gho94] gezüchtet wurden. Da dieses Medium den Redoxstatus der Zellen, welcher ein Regulationsfaktor für die Expression der photosynthetischen Gene ist, verändert [Gra03], könnte die H-Untereinheit mit der Vermittlung dieses Signals in Zusammenhang stehen. Der ursprüngliche Elternzustand konnte vollständig wiederhergestellt werden. Dies wurde durch ein besonderes genetisches Konstrukt erreicht. Es bestand aus einem "broad host range"- Vektor, der in vielen verschiedenen Bakterien vermehrt werden kann und dem *puhA*-Gen. Im Gegensatz zu den erwähnten Studien stand dabei die Expression der H-Untereinheit unter der Kontrolle ihres eigenen, natürlichen Promotors.

⇒ **Publikation zum Deletions/Komplementationssystem**

Zu B. In der vorliegenden Arbeit wurde zum ersten Mal die H-Untereinheit in zwei Makrodomänen, einer transmembran Domäne (TM) und einer cytoplasmatischen Domäne (CY), getrennt. Deren gemeinsame Expression in den Deletionsstämmen konnte den Elternzustand mit funktionellem RC und photosynthetischem Wachstum wiederherstellen. Keine der beiden Domänen konnte einzeln exprimiert eine solche Wiederherstellung erreichen. Jedoch waren die einzelnen Domänen in der Lage, unter semiaeroben Bedingungen in M2SF-Medium, die RC-Mengen zu steigern. Diese Module können unabhängig von einander Strukturen bilden, die zur Bildung von RC-Komplexen führen. Diese sind jedoch funktionsuntüchtig. Demnach besitzen beide Domänen wichtige Bereiche, die gemeinsam vorhanden sein müssen, um ein funktionelles RC zu bilden. Diese Ergebnisse werden im Rahmen der oben erwähnten Studie [Teh03] diskutiert.

⇒ **Manuskript zur Mutagenese der H-Untereinheit**

Zu C. Das Protokoll zur Isolierung und Aufreinigung der PSU [Sta98] wurde in seinem Ablauf vereinfacht und durch die Benutzung von n-Octyl-β-Glukopyranosid (β-OG) und DEAE-Cellulose anstelle von Diheptanoylphosphatidylcholin (DHPC) und DEAE-Sepharose auch kostengünstiger. Dieses neue Verfahren lieferte im Vergleich zum alten deutlich höhere Mengen. Die Zusammensetzung der isolierten PSU entsprach vom Gelprofil her demjenigen aus der erwähnten Veröffentlichung [Sta98].

⇒ **Manuskript zur biochemischen Charakterisierung und Kristallisation der PSU**

Zu D. Auf jeder Reinigungsstufe wurde ein Absorptionsspektrum aufgenommen, dessen Profil immer identisch mit dem isolierter Chromatophoren war. Das bedeutete, dass die Pigment-Protein-Anordnung in den gereinigten PSU in keiner Weise gestört war. Aus einem präparativem Elektrophoresegel wurden die größeren Komponenten der isolierten PSU herausgeschnitten und mit Hilfe der Massenspektrometrie die Aminosäurenzusammensetzung analysiert. Dabei handelt es sich um die erste Studie, die PSU-Komponenten proteinchemisch charakterisiert. Diese Proteinsequenzierung zeigte, dass Proteine aus der äußeren Membran, wie Por39 oder Por41, mit den PSU aufgereinigt wurden. Durch anschließende biochemische Untersuchungen wurde nachgewiesen, dass diese eng mit dem RC-LH1-Komplex verbunden sind und in einem unerwartet großem Mengenverhältnis vorliegen.

⇒ **Manuskript zur biochemischen Charakterisierung und Kristallisation der PSU**

Zu E. Die Ergebnisse aus den Einzelmolekülspektroskopiemessungen an den isolierten PSU zeigten eindeutig, dass der LH1-Ring eine zirkularsymmetrische Form um das RC besitzt. Diese Ergebnisse stehen im Widerspruch zu anderen Veröffentlichungen [Ket02], die stets eine elliptische Verformung der LH1-Komplexe fanden. Vermutlich liegen die Unterschiede in der Wahl des Detergens und in der Präparationsmethode.

Das Protokoll für die zweidimensionalen Kristallisation der PSU wurde soweit optimiert, dass Kristalle in reproduzierbarer Qualität erhalten werden konnten.

⇒ **Publikation zur Einzelmolekülspektroskopie der PSU**

⇒ **Manuskript zur biochemischen Charakterisierung und Kristallisation der PSU**

9. Ausblick

Die vorliegende Arbeit hat den Grundstein für einige zukünftige Projekte gelegt:

- Die Stämme aus dem Deletions/Komplementationsexperiment, sowie aus der H-Untereinheitsmutagenese können geeignete Versuchsobjekte von systembiologischen und Signaltransduktionsuntersuchungen werden.
- Die isolierten Chromatophoren der oben erwähnten Stämme sollen zur Aufklärung der Energietransferreaktion dienen. Die ersten Vorversuche durch transiente Absorptions-spektroskopie zeigten sehr interessante Ergebnisse.
- Das hochflexible und modulare Design der Mutageneseplasmide kann für die Konstruktion von Expressionsvektoren bis hin zu Reportergensystemen ausgebaut werden. Ein erstes Fusionskonstrukt mit einem fluoreszierenden Protein liegt schon vor und soll in Fluoreszenzenergietransferexperimente (FRET) eingesetzt werden. Damit soll zum einen die Lage der H-Untereinheit in bezug auf den LH1-Komplex geklärt werden, zum anderen, ob die Genprodukte (die auch fluoreszenzmarkiert werden) des *puh*-Operons in der PSU vorhanden sind. Diese Fragestellungen können mit Hilfe der Einzelmolekülspektroskopie beantwortet werden. Ergänzt wird es durch das Vorliegen weiterer Konstrukte. Diese besitzen einen Aminosäureaustausch in der CY-Domäne (Threonin 104 wurde gegen ein Cystein ausgetauscht) der intakten, sowie der getrennten H-Untereinheit. Damit können FRET-Analysen durch Kopplung eines Fluoreszenzfarbstoffes oder Quervernetzungsexperimente (“cross linking“) durchge-führt werden.
- Mit dem neuen Protokoll für die Isolierung und Aufreinigung der PSU können zum einen routinemäßige Präparationen für die Einzelmolekülspektroskopie durchgeführt werden, zum anderen sind die erhaltenen Mengen nicht nur ausreichend, um in größeren Versuchsreihen die 2D-Kristallisationsbedingungen zu optimieren, sondern auch um dreidimensionale Kristallisationsversuche durchzuführen.
- Die Identifizierung von äußeren Membranproteinen, wie Por39 und Por41, die eng mit der PSU assoziiert sind, bedingt neue Experimente. In diesen muss vor allem die Beteiligung der Porine beim Aufbau der PSU geklärt werden und ob diese an der Funktion des photosynthetischen Prozesses teilhaben.

10. Quellenangaben

[Abr98] Abresch E.C., M. L. Paddock, M. H. B. Stowell, T. M. McPhillips, H. L. Axelrod, S. M. Soltis, D. C. Rees, M. Y. Okamura and G. Feher. 1998. Identification of proton transfer pathways in the X-ray crystal structure of the bacterial reaction center from *Rhodobacter sphaeroides*. Photosyn. Res. **55:**119-125.

[Akl00] Aklujkar M., A. L. Harmer, R. C. Prince and J. T. Beatty. 2000. The *orf162b* sequence of *Rhodobacter capsulatus* encodes a protein required for optimal levels of photosynthetic pigment-protein complexes. J. Bacteriol. **182:**5440-5447.

[All86] Allen J. P., G. Feher, T. O. Yeates, D. C. Rees, J. Deisenhofer, H. Michel and R. Huber. 1986. Structural homology of reaction centers from *Rhodopseudomonas sphaeroides* and *Rhodopseudomonas viridis* as determined by X-ray diffraction. Proc. Natl. Acad. Sci. U S A. **83:**8589-93.

[Ana02] Anantharaman V. and L. Aravind. 2002. The PRC-barrel: A widespread, conserved domain shared by photosynthetic reaction center subunits and proteins of RNA metabolism. Genome Biol. **3:**0061.1-0061.9.

[Ben03] Ben-Shem A., F. Frolow and N. Nelson. 2003: Crystal structure of plant photosystem I. Nature **426:**630-635.

[Ber00] Berman H.M., J. Westbrook, Z. Feng, G. Gilliland, T. N. Bhat, H. Weissig, I. N. Shindyalov and P. E. Bourne. 2000: The protein databank. Nucleic Acids Res. **28:**235-242.

[Bha81] Bhatia G. E. 1981: Refinement of the crystal structure of oxidized *Rhodospirillum rubrum* cytochrome c_2. Ph.D. thesis, University of California San Diego, USA.

[Bug94] Buggy J. J., M. W. Sganga and C. E. Bauer. 1994: Characterization of a light-responding trans-activator responsible for differentially controlling reaction center and light-harvesting-I gene expression in *Rhodobacter capsulatus*. J. Bacteriol. **176:**6936-6943.

[Cam02] Camara-Artigas A., D. Brune and P. Allen. 2002: Interaction between lipids and bacterial reaction centres determined by protein crystallography; Proc. Natl. Acad. Sci. U S A. **99:**11055-11060.

[Che00] Cheng Y. S., C. A. Brantner, A. Tsapin and M. L. P. Collins. 2000. Role of the H protein in assembly of the photochemical reaction center and intracytoplasmic membrane in *Rhodospirillum rubrum*. J. Bacteriol. **182:**1200-1207.

[Deb85] Debus R. J., G. Feher and M. Y. Okamura. 1985. LM complex of reaction centers from *Rhodopseudomonas sphaeroides* R-26: characterization and reconstitution with the H subunit. Biochemistry. **24:**2488-2500.

[Dei95] Deisenhofer J., O. Epp, I. Sinning and H. Michel. 1995. Crystallographic refinement at 2.3 Å resolution and refined model of the photosynthetic reaction centre from *Rhodopseudomonas viridis*. J. Mol. Biol. **246:**429-457.

[Dei85] Deisenhofer J., O. Epp, K. Miki, R. Huber and H. Michel. 1985. Structure of the protein subunits in the photosynthetic reaction centre of *Rhodopseudomonas viridis* at 3 Å resolution. Nature **318:**618-624.

[Dre78] Drews G. 1978. Structure and development of the membrane system of photosynthetic bacteria. Curr. Top. In Bioenergetics. **8B:**161-207.

[Era00] Eraso J. M. and S. Kaplan. 2000: From redox flow to gene regulation: role of the PrrC protein of *Rhodobacter sphaeroides* 2.4.1. Biochemistry. **39:**2052-2062.

[Erm94] Ermler U., G. Fritzsch, S. K. Buchanan and H. Michel. 1994: Structure of the photosynthetic reaction centre from *Rhodobacter sphaeroides* at 2.65 Å resolution: cofactors and protein-cofactor interactions. Structure **2:**925-936.

[Fat01] Fathir I., T. Mori, T. Nogi, M. Kobayashi, K. Miki and T. Nozawa. 2001 Structure of the H subunit of the photosynthetic reaction center from the thermophilic purple sulfur bacterium, *Thermochromatium tepidum*. Implications for the specific binding of the lipid molecule to the membrane protein complex. Eur. J. Biochem. **268:**2652-7.

[Fer04] Ferreira K. N., T. M. Iverson, K. Maghlaoui, J. Barber and S. Iwata. 2004: Architecture of the photosynthetic oxygen-evolving center. Science **303:**1831-1838.

[Ger03] Gerken U. 2003. Spektroskopische Untersuchungen an einzelnen Lichtsammelkomplexen des Purpurbakteriums *R. rubrum*. Doktorarbeit, Universität Stuttgart, Deutschland.

[Gho94] Ghosh R., A. Hardmeyer, I. Thoenen and R. Bachofen. 1994. Optimization of the Sistrom culture medium for large-scale batch cultivation of *Rhodospirillum rubrum* under semi-aerobic conditions with maximal yield of photosynthetic membranes. Appl. Environ. Microbiol. **60:**1698-1700.

[Gom95] Gomelsky M. and S. Kaplan. 1995: appA, a novel gene encoding a trans-acting factor involved in the regulation of photosynthesis gene expression in *Rhodobacter sphaeroides* 2.4.1. J. Bacteriol. **177:**4609-4618.

[Gra03] Grammel H., E. D. Gilles and R. Ghosh. 2003. Microaerophilic cooperation of reductive and oxidative pathways allows maximal photosynthetic membrane biosynthesis in *Rhodospirillum rubrum*. Appl. Environ. Microbiol. **69:** 6577-6586.

[Har98] Hara M., T. Kaneko, C. Nakamura, Y. Asada and J. Miyake. 1998. Redox properties of an H-subunit-depleted photosynthetic reaction center from *Rhodopseudomonas viridis*. Biochim. Biophys. Acta. 1998 **1363:**199-208.

[Har02] Hartigan N., H. A. Tharia, F. Sweeney, A. M. Lawless, and M. Z. Papiz. 2002. The 7.5 Å electron density and spectroscopic properties of a novel low-light B800 LH2 from *Rhodopseudomonas palustris*. Biophys. J. **82:**963-977.

[Hel93] Heller H. 1993: Simulation einer Lipidmembran auf einem Parallelrechner, Doktorarbeit Technische Universität München, Deutschland.

[Hel93] Heller H., M. Schäfer and K. Schulten. 1993: Molecular dynamics simulation of a bilayer of 200~lipids in the gel and in the liquid crystal phases. J. Phys. Chem. **97:**8343-8360.

[Hu02] Hu X., T. Ritz, A. Damjanovic, F. Autenrieth and K. Schulten. 2002: Photosynthetic apparatus of purple bacteria. Q. Rev. Biophys. **35:**1-62.

[Hum96] Humphrey W., A. Dalke and K. Schulten. 1996: VMD: visual molecular dynamics. J. Mol. Graph. **14:**33-38.

[Iga01] Igarashi N., J. Harada, S. Nagashima, K. Matsuura, K. Shimada and K. V. Nagashima. 2001: Horizontal transfer of the photosynthesis gene cluster and operon rearrangement in purple bacteria. J. Mol. Evol. **52:**333-341.

[Jam02] Jamieson S. J., P. Wang, P. Quian, J. Y. Kirkland, M. J. Conroy, C. N. Hunter and P. A. Bullough. 2002. Projection structure of the photosynthetic reaction centre-antenna complex of *Rhodospirillum rubrum* at 8.5 Å resolution. EMBO J. **21:**3927-3935.

[Jor01] Jordan P., P. Fromme, H. T. Witt, O. Klukas, W. Saenger and N. Krauss. 2001: Three-dimensional structure of cyanobacterial photosystem I at 2.5 A resolution. Nature **411:**909-917.

[Jos96] Joshi H. M. and F. R. Tabita. 1996: A global two component signal transduction system that integrates the control of photosynthesis, carbon dioxide assimilation, and nitrogen fixation. Proc. Natl. Acad. Sci. U S A. **93:**14515-14520.

[Jun99] Jungas C., J. L. Ranck, J. L. Rigaud, P. Joliot, A. Vermeglio. 1999: Supramolecular organization of the photosynthetic apparatus of *Rhodobacter sphaeroides*. EMBO J. **18:**534-542.

[Kag04] Kagawa R., M. G. Montgomery, K. Braig, A. G. Leslie and J. E. Walker. 2004: The structure of bovine F(1)-ATPase inhibited by ADP and beryllium fluoride. EMBO J. **23:**2734-2744.

[Kar95] Karrasch S., P. A. Bullough and R. Ghosh. 1995. The 8.5 Å projection map of the light-harvesting complex I from *Rhodospirillum rubrum* reveals a ring composed of 16 subunits. EMBO J. 14:631-638.

[Kat03] Katiliene Z., E. Katilius, N. W. Woodbury. 2003. Energy trapping and detrapping in reaction center mutants from *Rhodobacter sphaeroides*. Biophys J. **84:**3240-3251.

[Ket02] Ketelaars M., C. Hofmann, J. Köhler, T. D. Howard, R. J. Cogdell, J. Schmidt and T. J. Aartsma. 2002: Spectroscopy on individual light-harvesting 1 complexes of *Rhodopseudomonas acidophila*. Biophys. J. **83:**1701-15.

[Koe96] Koepke J., X. Hu, C. Muenke, K. Schulten and H. Michel. 1996: The crystal structure of the light-harvesting complex II (B800-850) from *Rhodospirillum molischianum*. Structure. **4:**581-597.

[Liu04] Liu Z., H. Yan, K. Wang, T. Kuang, J. Zhang, L. Gui, X. An and W. Chang. 2004: Crystal structure of spinach major light-harvesting complex at 2.72 Å resolution. Nature **428:**287-292.

[Lup00] Lupo D. 2000: Funktion der H-Untereinheit des photosynthetischen Reaktionszentrums aus *Rhodospirillum rubrum*. Diplomarbeit, Universität Stuttgart, Deutschland.

[Mas02] Masuda S. and C. E. Bauer. 2002: AppA is a blue light photoreceptor that antirepresses photosynthesis gene expression in *Rhodobacter sphaeroides*. Cell. **110:**613-623.

[McA99] McAuley K. E., P. K. Fyfe, J. P. Ridge, N. W. Isaacs, R. J. Cogdell and M. R. Jones. 1999: Structural details of an interaction between cardiolipin and an integral membrane protein. Proc. Natl. Acad. Sci. U S A. **96:**14706-14711.

[McD95] McDermott G., S. M. Prince, A. A. Freer. A. M. Hawthornthwaite-Lawless, M. Z. Papiz, R. J. Cogdell and N. W. Isaacs. 1995: Crystal structure of an integral membrane light-harvesting complex from photosynthetic bacteria Nature **374:**517-521.

[McL01] McLuskey K., M. Prince, R. J. Cogdell, and N. W. Isaacs. 2001. The crystallographic structure of the B800-820 LH3 light-harvesting complex from the purple bacteria *Rhodopseudomonas acidophila* strain 7050. Biochemistry. **40:**8783-8789.

[Mos94] Mosley C. S., J. Y. Suzuki and C. E. Bauer. 1994: Identification and molecular genetic characterization of a sensor kinase responsible for coordinately regulating light harvesting and reaction center gene expression in response to anaerobiosis. J. Bacteriol. **176:**7566-7573.

[Nay99] Naylor G. W., H. A. Addlesee, L. C. D. Gibson and C. N. Hunter. 1999: The photosynthesis gene cluster of *Rhodobacter sphaeroides*. Photosyn. Res. **62:**121–139.

[Nog00] Nogi T., I. Fathir, M. Kobayashi, T. Nozawa and K. Miki. 2000. Crystal structures of photosynthetic reaction center and high-potential iron-sulfur protein from *Thermochromatium tepidum*: Thermostability and electron transfer. Proc. Natl. Acad. Sci. U S A. **97:**13561-6.

[Oh00] Oh J. I. and S. Kaplan. 2000: Redox signaling: globalization of gene expression. EMBO J. **19:**4237-4247.

[Oh01] Oh J. I. and S. Kaplan. 2001: Generalized approach to the regulation and integration of gene expression. Mol. Microbiol. **39:**1116-1123.

[Oka74] Okamura M. Y., L. A. Steiner and G. Feher. 1974: Characterization of reaction centers from photosynthetic bacteria. I. Subunit structure of the protein mediating the primary photochemistry in *Rhodopseudomonas spheroides* R-26. Biochemistry. **13:**1394-1403.

[Pem98] Pemberton J. M., I. M. Horne, and A. G. McEwan. 1998: Regulation of photosynthetic gene expression in purple bacteria. Microbiology **144**:267 - 278.

[Pon95] Ponnampalam S. N., J. J. Buggy and C. E. Bauer. 1995: Characterization of an aerobic repressor that coordinately regulates bacteriochlorophyll, carotenoid, and light harvesting-II expression in *Rhodobacter capsulatus*. J. Bacteriol. **177:**2990-2997.

[Ros03] Roszak A. W., T. D. Howard, J. Southall, A. T. Gardiner, C. J. Law, N. W. Isaacs, R. J. Cogdell. 2003: Crystal structure of the RC-LH1 core complex from *Rhodopseudomonas palustris*. Science. **302:**1969-1972.

[Sch04] Scheuring S., F. Francia, J. Busselez, B. A. Melandri, J. L. Rigaud and D. Levy. 2004: Structural role of PufX in the dimerization of the photosynthetic core complex of *Rhodobacter sphaeroides*. J. Biol. Chem. **279:**3620-3626.

[Sch03] Scheuring S., J. Seguin, S. Marco, D. Levy, B. Robert and J. L. Rigaud. 2003: Nanodissection and high-resolution imaging of the *Rhodopseudomonas viridis* photosynthetic core complex in native membranes by AFM. Atomic force microscopy. Proc. Natl. Acad. Sci. U S A. **100:**1690-1693.

[Sga92] Sganga M.W. and C. E. Bauer. 1992: Regulatory factors controlling photosynthetic reaction center and light-harvesting gene expression in *Rhodobacter capsulatus*. Cell. **68:**945-954.

[Soc89] Sockett R. E., T. J. Donohue, A. R. Varga and S. Kaplan. 1989. Control of photosynthetic membrane assembly in *Rhodobacter sphaeroides* mediated by *puhA* and flanking sequences. J. Bacteriol. **171:**436-446.

[Sta98] Stahlberg H., J. Dubochet, H. Vogel and R. Ghosh. 1998. Are the light-harvesting I complexes from *Rhodospirillum rubrum* arranged around the reaction centre in a square geometry? J. Mol. Biol. **282:**819-831.

[Sto97] Stowell M. H. B., T. M. McPhillips, D. C. Rees, S. M. Soltis, E. Abresch and G. Feher. 1997. Light induced structural changes and the mechanism of electron/proton transfer in the photosynthetic reaction center. Science **276:**812–816.

[Swe01] Swem L. R., S. Elsen, T. H. Bird, D. L. Swem, H. G. Koch, H. Myllykallio, F. Daldal and C. E. Bauer. 2001: The RegB/RegA two-component regulatory system controls synthesis of photosynthesis and respiratory electron transfer components in *Rhodobacter capsulatus*. J. Mol. Biol. **309:**121-138.

[Tak96] Takahashi E. and C. A. Wraight. 1996. Potentiation of proton transfer function by electrostatic interactions in photosynthetic reaction centers from *Rhodobacter sphaeroides*: First results from site-directed mutation of the H subunit. Proc. Natl. Acad. Sci. U S A. **93:**2640-5.

[Teh04] Tehrani A. and J. T. Beatty. 2004: Effects of precise deletions in *Rhodobacter sphaeroides* reaction center genes on steady-state levels of reaction center proteins: a revised model for reaction center assembly. Photosyn. Res. **79:**101-108.

[Teh03] Tehrani A., R. C. Prince and J. T. Beatty. 2003. Effects of photosynthetic reaction center H protein domain mutations on photosynthetic properties and reaction center assembly in *Rhodobacter sphaeroides*. Biochemistry **42:**8919-8928.

[Vad79] Vadeboncoeur C., M. Mamet-Bratley and G. Gingras. 1979: Photoreaction center of photosynthetic bacteria. 2. Size and quaternary structure of the photoreaction

centers from *Rhodospirillum rubrum* strain G9 and from *Rhodopseudomonas sphaeroides* strain 2.4.1. Biochemistry. **18:**4308-4314.

[Var95] Various authors. 1995: In R. E. Blankenship, M. T. Madigan, and C. E. Bauer (ed.) Anoxygenic photosynthetic bacteria. Kluwer Academic Publishers, Dordrecht, The Netherlands.

[Won96] Wong D. K.-H., W. J. Collins, A. Harmer, T. G. Lilburn and J. T. Beatty. 1996. Directed mutagenesis of the *Rhodobacter capsulatus puhA* gene and *orf214*: pleiotropic effects on photosynthetic reaction center and light-harvesting 1 complexes. J. Bacteriol. **178:**2334-2342.

[Yan03] Yankovskaya V., R. Horsefield, S. Tornroth, C. Luna-Chavez, H. Miyoshi, C. Leger, B. Byrne, G. Cecchini and S. Iwata. 2003: Architecture of succinate dehydrogenase and reactive oxygen species generation. Science **299:**700-704.

[Yel95] Yeliseev A. A. and S. Kaplan. 1995: A sensory transducer homologous to the mammalian peripheral-type benzodiazepine receptor regulates photosynthetic membrane complex formation in *Rhodobacter sphaeroides* 2.4.1. J. Biol. Chem. **270:**21167-21175.

[You98] Young C. S., R. C. Reyes and J. T. Beatty. 1998. Genetic complementation and kinetic analyses of *Rhodobacter capsulatus orf1696* mutants indicate that the Orf1696 protein enhances assembly of the light-harvesting I complex. J. Bacteriol. **180:**1759-1765.

[Zei95] Zeilstra-Ryalls J. H. and S. Kaplan. 1995: Aerobic and anaerobic regulation in *Rhodobacter sphaeroides* 2.4.1: the role of the fnrL gene. J. Bacteriol. **177:**6422-6431.

[Zei04] Zeilstra-Ryalls J. H. and S. Kaplan. 2004: Oxygen intervention in the regulation of gene expression: the photosynthetic bacterial paradigm. Cell. Mol. Life Sci. **61:**417-436.

[Zei98] Zeilstra-Ryalls J., M. Gomelsky, J. M. Eraso, A. Yeliseev, J. O'Gara and S. Kaplan. 1998: Control of photosystem formation in *Rhodobacter sphaeroides*. J. Bacteriol. **180:**2801-2809.

[Zha98] Zhang Z., L. Huang, V. M. Shulmeister, Y. I. Chi, K. K. Kim, L. W. Hung, A. R. Crofts, E. A. Berry and S. H. Kim. 1998: Electron transfer by domain movement in cytochrome bc1. Nature. **392:**677-684.

Internetquellen:

[Int1] Alles zur Photosynthese.
http://www.life.uiuc.edu/govindjee/
http://www.life.uiuc.edu/govindjee/Part1/Part1.html
http://www.life.uiuc.edu/govindjee/Part2/Part2.html
http://www.life.uiuc.edu/govindjee/Part3/Part3.html

[Int2] Protein Datenbank.
http://www.rcsb.org/pdb/index.html

[Int3] Membranstrukturen.
http://www.lrzmuenchen.de/~heller/membrane/membrane.html

[Int4] *Rhodospirillum rubrum* Genomprojekt.
http://genome.jgi-psf.org/draft_microbes/rhoru/rhoru.home.html

DELETIONS/KOMPLEMENTATIONSSYSTEM

Running title: Reaction center H-subunit and LH1 formation

The reaction center H-subunit is not required for high levels of light-harvesting complex 1 in *Rhodospirillum rubrum* mutants

Domenico Lupo and Robin Ghosh*

Department of Bioenergetics
Institute of Biology
University of Stuttgart
Pfaffenwaldring 57
D-70550 Stuttgart
Germany

*corresponding author: Tel. +49711/685-5047; Fax:+49711/685-5096;
E-mail: robin.ghosh@bio.uni-stuttgart.de

JOURNAL OF BACTERIOLOGY; 2004; 186 (17); p. 5585–5595.

DOI: 10.1128/JB.186.17.5585–5595.2004

ABSTRACT

The gene (*puhA*) encoding the H subunit of the reaction center (RC) was deleted by site-directed interposon mutagenesis by using a kanamycin resistance cassette lacking transcriptional terminators to eliminate polar effects in both the wild-type strain *Rhodospirillum rubrum* S1 and the carotenoid-less strain *R. rubrum* G9. The *puhA* interposon mutants were incapable of photoheterotrophic growth but grew normally under aerobic chemoheterotrophic conditions. Absorption spectroscopy and sodium dodecyl sulfate-polyacrylamide gel electrophoresis showed that the RCs were absent. In minimal medium and also in modified medium containing succinate and fructose, the light-harvesting 1 complex (LH1) levels of the S1-derived mutants were about 70 to 100% of the wild-type levels in the same media. The correct assembly of LH1 in the membrane and the pigment-pigment interaction were confirmed by near-infrared circular dichroism spectroscopy. LH1 formation was almost absent when the carotenoid-less G9-derived *puhA* mutants were grown in standard minimal medium, suggesting that carotenoids may stabilize LH1. In the fructose-containing medium, however, the LH1 levels of the G9 mutants were 70 to 100% of the parental strain levels. Electron micrographs of thin sections of *R. rubrum* revealed photosynthetic membranes in all mutants grown in succinate-fructose medium. These studies indicate that the H subunit of the RC is necessary neither for maximal formation of LH1 nor for photosynthetic membrane formation but is essential for functional RC assembly.

INTRODUCTION

It is well established that in phototrophic purple bacteria the photosynthetic unit is expressed in a specialized intracytoplasmic membrane (ICM) (16, 18) and is composed of a reaction center (RC) surrounded by a light-harvesting complex (1, 17, 44). Although most phototrophic bacteria contain two kinds of light-harvesting complexes, light-harvesting complex 1 (LH1) and light-harvesting complex 2 (LH2), only one of these, LH1, is in intimate contact with the RC. Recent structural studies (6, 20, 22, 25, 31, 36, 37, 43, 59–61) have indicated that the component αβ dimers of LH1, each of which binds two bacteriochlorophyll (BChl) molecules and at least one molecule of carotenoid, form a ring around the RC. For *Rhodospirillu rubrum* (33, 37, 59, 61) and *Blastochloris viridis* (previously called *Rhodopseudomonas viridis*) (60), both of which contain only a single light-harvesting complex, LH1 appears to completely surround the RC. In *Rhodobacter sphaeroides*, however, recent electron micrographic evidence (36) has suggested that the LH1 in this organism may not be completely closed, although the low resolution of the data in this study may not have been sufficient to allow a definite conclusion to be drawn. In all cases, however, it appears that the assembly of RCs and LH1 in vivo is always perfectly coordinated, and neither biochemical nor spectroscopic evidence has indicated the presence of empty LH1 rings or incorrectly assembled RCs. A continuing puzzle, therefore, concerns the mechanism of assembly of this coordinately regulated supramolecular aggregate.

Genetic studies with *Rhodobacter sphaeroides* (14, 56), *Rhodobacter capsulatus* (2, 64–66), and *R. rubrum* (9) have indicated that the genes of the *puh* operon play an important role in the targeting of the RCs to the LH1 and also in the assembly of the LH1 per se. Early studies by Sockett and coworkers (57) indicated that the H subunit of the RC plays a major role in LH1 assembly. Thus, Sockett et al. (57) deleted the *puhA* gene together with a small part of the upstream flanking region in *Rhodobacter sphaeroides*, which prevented the formation of LH1. This group proposed that the H subunit, which is the only RC subunit to be expressed at low levels under aerobic conditions, may form an assembly point for the LH1. Subsequently, however, Young et al. showed that in *Rhodobacter capsulatus* (65) the upstream gene flanking *puhA*, previously designated *orf1696* and now designated *lhaA*, is also involved in enhancing LH1 formation (65, 66), as are the two open reading frames immediately

downstream of the *puhA* gene. In particular, Beatty and coworkers showed that the downstream genes, designated *orf214* and *orf162b* in *Rhodobacter capsulatus*, are expressed as an operon (2, 64) and that deletion of either gene reduces the levels of LH1 and RC formation to less than 20% of the wild-type levels. The homology of the genes flanking *puhA* and the similarity of the gene organization in *Rhodobacter sphaeroides*, *Rhodobacter capsulatus*, and *R. rubrum* are striking (4), so that similar functions for these genes are implied. Independently, Cheng and coworkers (9) deleted the *puhA* gene of *R. rubrum* and part of the flanking upstream gene, *G115* (which shows homology to *lhaA*), and on the basis of their results suggested that the H subunit is important for LH1 formation. In the latter study, however, the *G115-puhA* deletion mutants still expressed about 30% of the wild-type LH1 levels under semiaerobic conditions, suggesting that these genes may not be necessary for LH1 formation. This group also proposed that in *R. rubrum* the H subunit plays a major role in the formation of the ICM, which was reduced in the *G115-puhA* deletion mutants grown semiaerobically.

In this study we reexamined the role of *puhA* in the assembly of LH1 and RCs in *R. rubrum* by precisely deleting the *puhA* gene without affecting the open reading frames of the flanking genes. We found that in the H-subunit deletion mutants, in contrast to the conclusions of Cheng and coworkers (9), *puhA* is not necessarily important for high-level LH1 formation (i.e., the level present during photoheterotrophic growth in low light) or for ICM formation under particular growth conditions. In contrast to *Rhodobacter sphaeroides* and *Rhodobacter capsulatus*, growth of *R. rubrum* with a special medium (M2SF), containing both succinate and fructose, allows highlevel expression of the photosynthetic membranes with associated LH1 at levels previously observed only in anaerobic phototrophic cultures (23, 28). This medium provides a unique tool for examining the phenotypes of mutants with lesions in genes involved in photosynthesis and was employed here for the first time for this purpose. In addition, we deleted *puhA* using the wild-type strain *R. rubrum* S1 and the carotenoid-less strain *R. rubrum* G9. A comparison of the results for these two strains indicated that carotenoids have a stabilizing role for LH1 formation in the absence of the H subunit.

MATERIALS AND METHODS

Growth of bacteria. Bacterial strains and plasmids are listed in Table 1. *Escherichia coli* cultures were grown in Luria-Bertani medium (52) at 37°C. Antibiotics were added as required at the following concentrations: Na-ampicillin 100 µg/ml; kanamycin sulfate 50 µg/ml and tetracycline-HCl 10 µg/ml. *R. rubrum* strains were grown at 30°C in either Sistrom minimal medium A (M-medium, containing K-succinate (20 mM) and added glutamic acid (0.7 mM) and aspartic acid (0.3 mM)) as described previously (56) with antibiotics added as required in the following concentrations: kanamycin sulfate, 20 µg/ml; and tetracycline-HCl, 4 µg/ml or in M2S (M-medium with following modifications, 40 mM NH_4^+-succinate (replaces K-succinate), 40 mM Na-phosphate and 20 mM HEPES) or M2SF (M2S-medium containing additionally 0.3 % (16.7 mM) fructose) (23).

Cultures were cultivated phototrophically in closed bottles (Pyrex) using M-medium at 30°C. *R. rubrum* was grown chemoheterotrophically in the dark in 250 ml baffled Erlenmeyer flasks in one of the above media (100 ml) at 30°C, shaking at 150 rpm (Lab-Therm, 2 cm throw, Adolf Kühner Inc. Basel).
For anaerobic, photoheterotrophic growth on M-agar plates an anaerobic jar (Oxoid) was employed under a controlled CO_2/H_2 atmosphere (GasPack from Oxoid no. BR 038B).

Molecular biological techniques. Plasmid DNA was isolated using kits from Qiagen and BioRad and cloned by standard procedures (52). For Southern hybridization, DNA fragments were transferred to nylon filters (Hybond-N, Pharmacia) as described (52) and detected by using chemiluminescence as described (Roche Diagnostics) using digoxigenin-labelled probes.

PCR production of the *puh* operon. A cosmid pSC21-7 with a 20 kb insert, carrying the *puh* operon (Fig. 1) was isolated by complementation of a putative *bchL*$^-$ mutant of *R. rubrum* S1 (50). The insert could be excised as three *Hin*dIII fragments, two of which were subsequently subcloned into pBsKSII(+) to yield the plasmids pBsH2 and pBsH3 (Table 1). The 3.6 kb *Hin*dIII fragment encoding the *puh* operon (described previously (4))was cloned into pBsH2 .. This was confirmed initially by PCR amplification of a 321 bp fragment with PCR primers derived from the *puh* promotor sequence described by Bérard *et al.* (4, 5). The primers used for PCR were 5′-CTGGCCGATGAAACGGTC-3′ and 5′-ATTCATGAGAAGGCCTCC-3′

and the PCR was performed using the AmpliTaq Kit protocol (Perkin Elmer): 30 cycles, initial denaturation at 94°C, 1 min annealing at 52°C and a polymerization step of 1 min at 72°C. DNA sequence analysis yielded the final confirmation.

Generation of *puhA* deletion mutants. The *puhA* gene (771 bp) contained on pBsH2 was digested with *Mlu*I (53 bp downstream of the *puhA* ATG start codon) and *Bst*EII (23 bp upstream of the *puhA* TAA stop codon) to remove a 695 bp fragment. The 5.9 kb fragment was blunt-ended with the Klenow polymerase fragment and ligated to a blunt-ended kanamycin cassette (*npt* gene). The kanamycin cassette was obtained on a 1.5 kb *Hin*dIII-*Sal*I fragment from Tn*5* (3) and subcloned in pBsLGKAN, to obtain the plasmids pBsPUHK1 and pBsPUHK2, containing the kanamycin gene in the same and opposite direction with respect to the direction of *puh* transcription, respectively (Fig.1). A subsequent restriction digest of both plasmids with *Hin*dIII yielded *puh*-derived fragments (4.4 kb) which were blunt-ended with the Klenow polymerase fragment and then ligated to *Eco*RI-restricted and blunt-ended pSUP202 (55) to yield the plasmids pSUPPK1 and pSUPPK2, respectively. These plasmids were transferred separately either to *R. rubrum* S1 or *R. rubrum* G9 by triparental conjugation with *E. coli* RR28 (29), using the helper plasmid pRK2013 (19) contained in *E.coli* RR28, applying the filter-mating technique (63). The transconjugants, containing a chromosomal insertion, were selected by kanamycin resistance under aerobic dark conditions. Double crossover recombinants containing the *puhA-npt* construct were selected by the phenotype Kan^r Tet^s and confirmed by Southern hybridization.

Complementation of mutants. The 3.6 kb fragment was cloned into pRK404 (13) at the blunt-ended *Bam*HI site to yield the plasmid pRKOPUH1and was transferred to the *R. rubrum puhA* deletion mutants by triparental conjugation as described above. In a further construction, a 2.4 kb *Hin*dIII-*Eco*RI fragment containing full-length *G115-puhA* was inserted into pRK404 to yield the plasmid pRKGP (Fig. 1). Finally G115 was N-terminally truncated by removing a *Sph*I-*Eco*47III fragment, which removes approximately 58% (259 amino acids) of the protein. The truncated *Hin*dIII-*Eco*RI fragment inserted into pRK404 was designated pRKΔGP.

Isolation of chromatophores (intracytoplasmic membranes, ICM). The chromatophore preparation was performed as described previously (24) with the following modifications. Cells of semi-aerobic cultures (500 ml) grown in M2SF-medium to an OD_{660nm} (1cm path-

length) = 3 were harvested at 4°C and washed with 50 mM Na-phosphate buffer pH 7.0 (50P7). The washed cell paste was resuspended in 8 vol of 50P7 and the cells disrupted by three passages through a French-Press-type apparatus EmulsiFlex-C5 (Avestin Inc., Ottawa, Canada) in the presence of a few grains of DNAseI and the protease inhibitor phenyl-methyl-sulfonyl-fluoride (100 μM). The lysate was then centrifuged once at 3 000×g to remove unbroken cells and then recentrifuged at 40 000×g at 4°C for 20 min to remove cell fragments. The latter supernatant (water-soluble proteins and ICM) was then centrifuged at 100 000×g for 1h at 4°C to yield a supernatant (containing water-soluble proteins) and a pellet (containing the intracytoplasmic membrane fraction). The pellet was washed once in 50P7 containing 5 mM EDTA by homogenization and recentrifuged. Finally, the pellet was resuspended in 2 ml of 20 mM TrisHCl pH 8.0, frozen in liquid nitrogen and stored at –85°C.

Absorption spectra. The absorption spectrum of intact cells as well as of chromatophores was measured using 2 mm path-length cuvettes in a Jasco V-560 UV/VIS spectrophotometer, equipped with a photodiode detector for turbid samples. Intact cells were measured after suspension in M-medium containing 80% glycerol. For the absorption measurements equal amounts of cells and chromatophores were employed by adjusting the concentrations to yield the same absorption at λ = 660 nm (turbidity) or at λ = 275 nm (protein amount).

SDS-polyacrylamide gel electrophoresis (SDS-PAGE). SDS-PAGE was performed according to the method of Laemmli (41) using 12.5% acrylamide gels. In general, samples (20μg protein) were precipitated by the addition of 3 vol of methanol before solubilizing in SDS-PAGE sample buffer. This step is effective in reducing the BChl and lipid content of the sample, which can affect the final gel resolution. The gels were stained with Coomassie Brilliant Blue R250 (Pharmacia). Heme staining was performed according to Goodhew *et al.* (28). The protein determination was performed by the modified Lowry method of Peterson (46) using bovine serum albumin as standard.

Near-infrared (near-IR) circular dichroism (CD) spectroscopy. Near-IR CD spectra were recorded at room temperature using a Jasco 715 spectropolarimeter and a near-IR-sensitive photomultiplier (1 nm band width). Samples having an $A_{880nm(or\ 873nm)}$ of 1 (1 mm path-length) were used; the corresponding volume was diluted in 20 mM TrisHCl pH 8.0 containing 10 mM Na-ascorbate. Data were corrected by smoothing after subtraction of the baseline.

Electron spin resonance (ESR) spectroscopy. ESR spectra of chromatophores were recorded at room temperature on a Bruker pulsed-ESR spectrometer ESP 300. Both the light-induced and the dark signal were measured with samples (filled in 4 mm quartz capillaries) having the same absorption at λ = 880 nm (or 873 nm). Illumination of the samples was performed using a 150 W halogen light source. The ESR parameters were: microwave frequency, 9.45 GHz; frequency, 100 kHz; power, 20 dB (2 mW); field width, 50 G; conversion time, 80 ms; field modulation intensity, 8 G_{pp}; gain, $2x10^4$.

Electron micrographs. Cells obtained after cultivation with M2SF (as described above) were fixed with 2% glutaraldehyde and stained with 1% (w/v) OsO_4, dehydrated with a series of acetone extractions and embedded in Spurr´s resin (58). Ultra-thin sections were made with a Leica ultramicrotome UCT, counterstained with uranyl acetate and lead citrate and micrographs recorded on Zeiss EM10 electron microscope at 60 kV.

RESULTS

Gene deletion and Southern hybridization analysis. The genotypes of the S1-derived *puh-npt* double recombinants SPUHK1 and SPUHK2 and the G9-derived recombinants GPUHK1 and GPUHK2 were confirmed by Southern hybridization by using a NotI/EcoRI fragment (1.7 kb) containing the intact *puhA* gene and flanking regions (818 bp upstream and 77 bp downstream of *puhA*) and the isolated *npt* gene (1.5-kb HindIII/SalI fragment) as probes (data not shown).

Phenotypes of the deletion mutants. The double recombinants derived from S1, SPUHK1 and SPUHK2, appeared to be pale pink when they were grown aerobically in the dark on M agar plates, whereas the double recombinants derived from G9, GPUHK1 and GPUHK2, were essentially colorless. All mutants were incapable of photosynthetic growth but showed growth kinetics characteristic of the parental strains when they were grown aerobically. Initially, absorption spectra of the parental strains and the deletion mutants (Fig. 2) were obtained by using cell cultures grown semiaerobically in M (Sistrom) medium. M medium is essentially comparable to the modified medium of Ormerod et al. (45) employed by Cheng and coworkers (9), but it contains succinate instead of malate as the sole carbon source. For the deletion mutants obtained from S1, the absorption maximum (wavelength, 880 nm) due to LH1 was at least 70 to 90% of the absorption maximum observed for the wild-type strain. We noted that, as reported previously (23), the wild-type LH1 levels under semiaerobic growth conditions in M medium were only about 20% of the levels observed in the same medium when organisms were grown photosynthetically. The corresponding maximum (wavelength, 873 nm) for the deletion mutants obtained from G9 was essentially absent. For all deletions the absorption maxima at 760 and 802 nm arising from the bacteriopheophytin and accessory BChl of the RC in the wild type were absent. Above we describe modified Sistrom media (M2S and M2SF) (31) which enhance the levels of BChl and photosynthetic membranes in cells grown semiaerobically in the dark compared to the levels in cells grown under anaerobic, phototrophic conditions. For S1 and G9 growth in M2S led to approximately 3.7- and 10-fold increases in the levels of LH1, respectively, as judged from the LH1 absorption maximum, compared to the levels observed for M medium, whereas growth in M2SF (M2S containing 0.3% fructose) led to levels of LH1 and implicitly photosynthetic membrane production essentially equivalent to those observed for photoheterotrophic cultures grown under low light conditions. We noted that in contrast to *Rhodobacter sphaeroides* and

Rhodobacter capsulatus, in which the ICM composition is very variable, it is well established that the ICM composition in *R. rubrum* is remarkably constant under all growth conditions (12, 30). This enabled us to estimate the ICM levels on the basis of the near-IR absorption of the LH1 complex. In M2S, the LH1 near-IR maxima for both S1- and G9-derived *puhA* mutants were approximately 26 to 38% (5%) of the maxima for the parental strain (Table 2), whereas in M2SF, the LH1 near-IR intensities of S1 and G9 were enhanced approximately 5- and 14-fold, respectively, compared to the intensities observed in M medium. Strikingly, the LH1 near-IR intensities of both S1- and G9-derived mutants grown in M2SF were approximately 70 to 100% (5%) of the wild-type intensities (Table 2). For all of the mutants the peak at 802 nm corresponding to the accessory BChl *a* of the RC was not detectable, indicating that the RC was absent. The small peak at 760 nm observed for SPUHK1 cannot be interpreted at the present time, but we noted that it was also observable in the spectrum obtained by Wong et al. (64) from an $LH2^-$ (originating from a lesion in *pucC*) *puhA* mutant of *Rhodobacter capsulatus*. Finally, the relative absorption intensity of the LH1 maximum at 880 nm (or 873 nm) was independent of the orientation of the kanamycin cassette with respect to the direction of transcription of the *puh* operon. Thin sections (Fig. 3) of all *puhA* deletion mutants and their parental strains showed similar levels of ICM with essentially identical diameters and cellular distributions when organisms were grown semiaerobically with M2SF.

Complementation. All deletion mutants could be complemented by plasmid pRKOPUH1, which contained the complete *puh* operon (*G115*, *puhA*, *I2372*, and *I3087*), as well as with pRKGP, which contained only *G115-puhA*, and pRKΔGP, which contained only *puhA*, and produced colonies with the Kan^r Tet^r phenotype capable of photoheterotrophic growth. In all cases absorption spectra of the complemented strains showed absorption maxima at 760 and 802 nm due to the presence of intact RC complexes (data not shown). In addition, the ratios of the intensity of the near-IR LH1 absorption maximum to the intensities of the RC at 760 and 802 nm were identical to those of the parental strains, showing that the LH1-to-RC stoichiometry had been restored. The intensity of the near-IR peak at 880 nm, corresponding to LH1, obtained for the complemented mutants derived from *R. rubrum* S1 was 70% [SPUHK1(pRKOPUH1)] to 90% [SPUHK2(pRKOPUH1)] of that of the parental strain. This was also true when pRKGP was employed for complementation (Table 2). However, the corresponding intensities of the near-IR peak at 873 nm obtained from the complemented strains GPUHK1 (pRKOPUH1) and GPUHK2 (pRKOPUH1) grown phototrophically were

only about 50% of that of the parental strain, *R. rubrum* G9, indicating once again that there was a stabilizing effect due to the carotenoids. Under semiaerobic conditions in M2SF both SPUHK1(pRKGP) and S1(pRKGP) showed almost the same LH1 levels as the corresponding strains in the absence of a plasmid.

However, compared to the growth rate of wild-type strain S1, the growth rates of SPUHK1(pRKGP) and S1(pRKGP) showed a lag phase of up to 10 h before growth commenced (data not shown). To test the possibility that establishment of rare plasmid-chromosome recombinants might be responsible for the 10-h lag phase, we repeatedly (three times) employed inocula from cultures in the late exponential phase for further cultivation. The latter cultures also showed the characteristic 10-h lag phase, suggesting that plasmid-chromosome recombination had not occurred. We believe that the 10-h lag phase is due to the overexpression of G115 (the pRK derivatives are present at levels of about 10 copies per cell in *R. rubrum* [51]), which hydropathy analysis indicated is an integral membrane protein containing 12 putative transmembrane α-helices (4), as complementation with pRKΔGP did not show any lag phase under either aerobic or anaerobic conditions. In *E. coli* it is often observed that high to medium expression of integral membrane proteins leads to toxicity effects (53). The similar levels of LH1 observed for SPUHK1(pRKGP) and SPUHK1 (pRKΔGP) show that the overexpression of G115, which has been implicated in LH1 assembly (66), is not important for the *puhA* complementation described here.

Characterization of isolated chromatophores. Chromatophores were isolated from parental strains and mutants grown in M2SF. The isolated pellets from all mutants showed the intense pigmentation of the parental strains. The absorption spectra of resuspended chromatophores (equal amounts of membrane protein) from all of the mutants corresponded exactly to those of the parental strains with respect to the positions of the peak maxima of BChl and carotenoids (data not shown). The relative intensities of the individual spectral component LH1 Qy and the carotenoid main peak (Table 3) were also about 80 to 90% (10%) of the wild-type intensities. The isolated chromatophores of the mutants showed little or no intensity at either 760 or 802 nm due to the RC. An independent determination of the BChl content of S1 under semiaerobic conditions in M2SF yielded a value (32.7 4.4 nmol of BChl/mg of protein) almost identical to that reported by Cheng et al. (9) (34.1 4.73 nmol of BChl/mg of protein). However, in contrast to the findings of Cheng et al. (9), who obtained values of 9.52 nmol of BChl/mg of protein for their *G115-puhA* mutant grown under semiaerobic conditions in

modified medium of Ormerod et al. (45), semiaerobic cultures of SPUHK1 and SPUHK2 grown in M2SF in this study yielded values of 32.66 16 and 23.25 7.22 nmol of BChl/mg of protein, respectively, corresponding to 99% and 71% of the wild-type values, respectively. As expected, the percentage of variation observed for the BChl determination is very close to the LH1 variation (for a comparison with the parental strain under the same growth conditions) determined for the 880-nm absorption maximum (Table 3). An analysis of BChl extraction data for the G9-derived strains showed a similar correlation (data not shown). In addition, both protein determination and spectral analysis confirmed that the pigment-to-protein ratio of the mutants was approximately 90% that of the parental strains. SDS-PAGE analysis of the isolated chromatophores revealed that in all cases the 21- and 24-kDa bands corresponding to the L and M subunits of the RC, respectively, were not detectable in the mutants (Fig. 4). Precise densitometric analysis showed that the very weak band at approximately 30 kDa had a lower molecular mass than the H subunit and was therefore assigned to another component which serendipitously migrated at the same position (data not shown). A protein with a molecular mass of approximately 31 kDa, which stained positively for heme and was assigned to cytochrome *c*1 (40), was present at the same level in the mutants and in the parental strains. Interestingly, the SDS-PAGE profile of all of the mutant chromatophores, particularly those derived from *R. rubrum* G9, showed a strongly enhanced intensity for a 40-kDa protein, which might correspond to the predicted *G115* gene product.

The SDS-PAGE profiles of the water-soluble fractions of the parental and mutant strains were essentially identical, with the exception of an additional 30-kDa band observed only for the mutants (data not shown). We attributed this band to the *npt* gene product as it was also observed for the water-soluble fraction of the carotenoid-less mutant ST2, which was derived by Tn*5* mutagenesis of S1 (62).

The microscopic integrity of LH1 and associated pigments was analyzed by near-IR CD, which has previously been shown to be a fingerprint for pigment-pigment interactions in the Qy region (10, 24, 26, 47, 54). The near-IR CD spectra of isolated chromatophores from S1 grown anaerobically and semiaerobically (Fig. 5A) were essentially identical, having a peak maximum at 875 nm, a crossover point at 886 nm, and a peak minimum at 899 nm, which are characteristic of native LH1. The minor differences observed in the region which crossed over at 880 nm were due to the effects of slight differences in light scattering in different measurements and are within the usual experimental error observed for the same preparation.

In addition, a small S-shaped signal with a peak maximum at 807 nm, a crossover point at 813 nm, and a peak minimum at 820 nm, which were due to the RC (47), was also observed. Chromatophores isolated from both SPUHK1 and SPUHK2 grown semiaerobically with M2SF exhibited essentially an identical S-shaped signal in the 880-nm region due to the LH1, but the S-shaped signal at approximately 800 nm due to the RC was absent. The peak and trough intensities of the near-IR CD spectra obtained by using equivalent amounts of chromatophores (adjusted to an *A*880 or *A*873 [path length, 1 mm] of 1) were approximately equal. The carotenoid-less parental strain G9 grown anaerobically and ST2 grown semiaerobically in M2SF also yielded near-IR CD spectra that had the same features and relative intensities as the spectra of S1, although the maximum, crossover point, and minimum of the CD signal due to LH1 were blue shifted by approximately 10 nm, as expected from the absorption maximum of the LH1 Qy band (Fig. 5B). The CD spectra of the LH1 were identical to those reported previously (24). We included strain ST2 here to eliminate possible differences in the LH1 near-IR CD spectrum arising from undefined random mutations in G9. As observed for the CD spectra of S1 mutants, the CD spectra of G9, GPUHK1, and GPUHK2 showed the same general features as the features observed for the parental strain for the LH1 region, but the signal due to RC was absent. However, the relative intensities of the near-IR CD spectra of the isolated chromatophores of the mutants were only approximately 70% of those of G9, suggesting that the carotenoids had a stabilizing effect.

In the study of Cheng et al. (9) low-temperature ESR spectroscopy of total cells obtained from cultures of *G115-puhA* deletion mutants of *R. rubrum* R5 revealed a small amount (about 8% of the wild-type level) of a reversible light-inducible signal due to the special pair of the RC (39). We also performed ESR spectroscopy of isolated chromatophores, although we performed our analysis at room temperature. With chromatophores from S1, G9, and ST2 grown both anaerobically and semiaerobically in M2SF, the presence of RC was confirmed by light-inducible ESR spectra (data not shown). In contrast, no light-induced ESR signal due to RC was observed for chromatophores from any of the mutants grown under semiaerobic conditions, although the attainable signal-to-noise ratio was too low to accurately determine an RC signal that was less than 10% of the wild-type signal. However, even low functional expression of RC should allow mutants to be photosynthetically competent, which was not observed even after more than 3 weeks of anaerobic incubation under high light conditions.

DISCUSSION

In early studies in which point mutations were used to eliminate functional LH1 assembly in *Rhodobacter capsulatus*, Garcia et al. (21), Richter et al. (49), Bylina et al. (7), and Dörge et al. (15) indicated that the LH1 is not essential for RC formation. However, in many of these studies it was also shown that nonassembled α or β polypeptides were still present in the ICM, thus leaving their possible role in RC assembly uncertain. The study of Richter and Drews (48), who deleted either the *pufA* or *pufB* gene, showed the same result, although in this study the presence of a membrane-located β-polypeptide was also demonstrated. However, Jones and coworkers (34, 35) demonstrated unambiguously that a *pufBALMX* LH2_ deletion mutant could be complemented by a plasmid containing only *pufLM* so that the cells became photosynthetically competent and the absorption spectrum was characteristic only of functional RC complexes. This indicates that at least in *Rhodobacter capsulatus* and *Rhodobacter sphaeroides* and probably in all phototrophic bacteria the assembly of the RC into the membrane does not require the presence of an LH1 in the membrane or expression of the *pufBA* genes. Similarly, it seems that the formation of the LH1 does not require the presence of an intact RC. Thus, deletion of the L and M subunits of the RC appeared to have no effect upon the expression and assembly of the LH1 in *Rhodobacter sphaeroides* (32) or *R. rubrum* (R. Saegesser, R. Bachofen, and R. Ghosh, unpublished data), although a reduction of 55% was observed for an LM deletion mutant of *Rhodobacter capsulatus* (38). On the other hand, in all of the organisms mentioned above, deletion of the H subunit causes a significant reduction in the levels of LH1 when the organisms are grown in standard minimal media. In all cases, deletion of the H subunit almost abolished assembly of the RC into the membrane (9, 57, 64). The studies of Beatty and coworkers (2, 64–66), in particular, showed that not only *puhA* but also all of the *puh* operon genes, as well as the upstream gene *lhaA*, may be involved in regulating LH1 formation. It is important to note that all studies so far have shown that the levels of the *pufBA* and *pufBALM* transcripts remain unchanged in *puh* deletion mutants compared to the levels in the wild type (8, 57, 64), indicating that the regulation of LH1 assembly occurs posttranslationally.

An important aspect of our study is that we constructed *puhA* deletion mutants using a kanamycin cassette lacking a transcriptional terminator. The *npt* gene used was obtained from Tn*5*, in which it is the first gene of an operon that includes *npt*, a streptomycin resistance gene, and a bleomycin resistance gene (42). In addition and in contrast to the studies of

Sockett et al. (57) and Cheng et al. (9), we inserted the *npt* interposon precisely into the *puhA* gene without affecting the upstream flanking regions encoding the LhaA homolog, G115, which has been shown to be important for LH1 formation in *Rhodobacter capsulatus* (65, 66). Also, by employing strains with and without carotenoids, we examined the role of this component in LH1 formation with respect to the function of the H subunit.

The *puhA* deletion mutants derived from both the wild-type strain *R. rubrum* S1 and the carotenoid-less strain *R. rubrum* G9 were incapable of photosynthetic growth, which is consistent with the results obtained for precise transcriptionally neutral *puhA* deletion mutants of *Rhodobacter capsulatus* (64). When grown in standard minimal (Sistrom) medium (56), the absorption, near-IR CD, and ESR spectra of the *R. rubrum puhA* mutants showed that the RC signal was undetectable. Interestingly, only the *R. rubrum* S1-derived *puhA* deletion mutants showed an LH1 peak, whose level was almost 70 to 90% of the wild-type level under the same growth conditions, suggesting that the carotenoids present in these strains had a stabilizing effect. The amount of LH1 per cell (i.e., the amount normalized to the cell density) observed for Sistrom mediumgrown S1 *puhA* mutants is approximately 2.5- to 3-fold higher than that observed by Cheng et al. (9) for their *G115-puhA* deletion mutant. The lower level observed by Cheng et al. (9) was therefore probably due to the absence of *G115* (*lhaA*) in their strain, as a similar low level was observed for a transcriptionally neutral *lhaA* mutant of *Rhodobacter capsulatus* (66). However, in the latter strain, LH1 levels that were about 20% of the wild-type level were also observed for a transcriptionally neutral *puhA* mutant (64). The lower level observed in *Rhodobacter capsulatus* may have been due to the different genetic background, or the presence of LH2 might have stabilized the formation of LH1 in the absence of *puhA* in that strain. When organisms were grown semiaerobically in M2SF containing succinate and fructose, the LH1 levels in both S1- and G9-derived deletion mutants reached almost wild-type levels, although the characteristic 802-nm peak due to the RC remained undetectable. These results clearly demonstrate that the H subunit is not critical for maximal LH1 formation under certain growth conditions. In addition, it should be mentioned that all *puhA* deletion mutants obtained here and grown in M2SF had amounts of ICM structures corresponding to the amount of LH1 formed. Thus, the H subunit is also not important for ICM formation under certain growth conditions.

The presence of the characteristic absorption maximum for LH1 for the *puhA* deletion mutants grown in either M2S or M2SF deserves further discussion. In all of the structural and

biophysical studies performed with purified LH1 or RC-LH1 complexes in our laboratory so far (26, 59, 61), we have observed without exception that the absorption maximum at either 880 nm (for the wild-type strain *R. rubrum* S1) or 873 nm (for the carotenoid-less strain *R. rubrum* G9) is always correlated with a perfectly assembled closed ring of $\alpha\beta(BChl)_2$ dimers. It has also been demonstrated that this is true for LH1 reconstituted with phospholipids (59), and we believe that it is true for the in vivo situation. However, it is known that the absorption spectrum may not be sensitive enough to indicate if the microscopic pigment-pigment interaction is really identical to that of the wild type. To resolve this question, we employed near-IR CD spectroscopy, which is exquisitely sensitive to details of pigment-pigment interactions not indicated by a simple absorption spectrum. Thus, the near-IR CD spectra of the *puhA* deletion mutants grown in M2SF showed that the LH1 show only minor, if any, differences compared to the LH1 of the wild-type parental strains, indicating that the H subunit has little or no effect upon the assembly of the LH1 even at the microscopic level of pigment-pigment interaction.

In fact, in all of the studies of LH1 assembly in *Rhodobacter capsulatus* performed with the *puh* operon so far, a wild-type LH1 absorption spectrum, albeit at low level, was observed for almost every transcriptionally neutral deletion mutant with a mutation in *puh* operon genes (64–66); the only exception was a deletion mutant of *orf162b*, which showed levels of LH1 corresponding to about 15% of the wild-type level (2). This implies that none of the components are truly essential for LH1 formation but serve only to enhance it. This may not be true for *Rhodobacter sphaeroides*, however, as Sockett and coworkers (57) demonstrated that their *lhaA-puhA* deletion mutant lacked LH1 completely, and at least the α polypeptide could not be detected by using an anti-LH1α antibody.

The present study was the first study to examine the effect of carotenoids on the formation of LH1 in *puh* deletion mutants. In cultures grown semiaerobically in Sistrom medium, the effect of carotenoids is striking: in the presence of carotenoids *puhA* deletion mutants show a low level of LH1 comparable to that seen in the corresponding strains of *Rhodobacter capsulatus*, whereas in the absence of carotenoids no LH1 formation is observed. When the M2S and M2SF growth media were employed, increased levels of LH1 were observed for all *puhA* mutants, and the level in M2SF was comparable to the level obtained for the parental strain. These results clearly show that carotenoids have a stabilizing effect upon LH1 formation.

In all other studies so far in which *Rhodobacter capsulatus* (64) or *Rhodobacter sphaeroides* (57) has been used, deletion of *puhA* led to large reductions in the LH1 levels compared to the wild-type levels. Thus, *puhA* appeared to be important but not essential for LH1 formation. The situation seems to be different in wild-type carotenoid-containing *R*. *rubrum*, in which similar levels of LH1 were observed in both the parental (S1) and *puhA* deletion strains when both minimal medium (M medium) and M2SF were used. Thus, in carotenoid-containing strains, it seems that the presence of *puhA* is largely unimportant for LH1 formation. In the absence of carotenoids, however, the LH1 levels are always reduced (and in minimal medium abolished) compared to the levels in the corresponding carotenoid-containing strains, indicating that these molecules have an important stabilizing role. To our knowledge, this study is the first study to document the influence of carotenoids upon the phenotype of a *puh* operon deletion mutant and adds an additional level of complexity to the factors governing LH1 formation in vivo. Further studies to examine the effects of carotenoids on the phenotypes of other *puh* operon deletion mutants are in progress.

ACKNOWLEDGMENTS

We would like to thank Dr. Michael Schweikert from the Department of Zoology for his advice with the electron microscopy. We also thank Wolfgang Schmidt (Institute of Physics) for his help with the ESR spectroscopy and Prof. Dr. Andreas Kuhn for providing near-IR CD facilities and Prof. Dr. Holger Jeske for stimulating discussions. We acknowledge the Swiss National Science Foundation (grant no. 5002-39816), which financed the initial part of the work, and the German Ministry for Science and Technology (BEO/BMBF) (grant no. 0311820) and the Landesgraduiertenförderung (7631.2-01/2) for financial assistance.

REFERENCES

1. **Aargard, J., and W. R. Sistrom.** 1972. Control of synthesis of reaction center bacteriochlorophyll in photosynthetic bacteria. Photochem. Photobiol. **15:**209-225.
2. **Aklujkar, M., A. L. Harmer, R. C. Prince, and J. T. Beatty.** 2000. The *orf162b* sequence of *Rhodobacter capsulatus* encodes a protein required for optimal levels of photosynthetic pigment-protein complexes. J. Bacteriol. **182:**5440-5447.
3. **Beck, E., G. Ludwig, E. A. Auerswald, B. Reiss, and H. Schaller.** 1982. Nucleotide sequence of the neomycin phosphotransferase gene from transposon Tn*5*. Gene. **19:**327-336.
4. **Bérard, J., and G. Gingrás.** 1990. The *puh* structural gene coding for the H subunit of *Rhodospirillum rubrum* photoreaction center. Biochem. Cell Biol. **69:**122-131.
5. **Bérard, J., G. Bélanger, and G. Gingrás.** 1989. Mapping of the *puh* messenger RNAs from *Rhodospirillum rubrum* - evidence for tandem promoters. J. Biol. Chem. **265:** 10897-10903.
6. **Boonstra, A. F., R. W. Visschers, F. Calkoen, R. van Grondelle, E. F. J. van Bruggen, and E. J. Boekema.** 1994. Structural characterization of the B800-850 and B875 light-harvesting antenna complexes from *Rhodobacter capsulatus* by electron microscopy. Biochim. Biophys. Acta. **1142:**181-188.
7. **Bylina, E. J., S. J. Robles, and D. C. Youvan.** 1988. Directed mutations affecting the putative bacteriochlorophyll-binding sites in the light-harvesting I antenna of *Rhodobacter capsulatus*. Israel J. Chem. **28:**73-78.
8. **Chen, X. Y., Yurkov, V., M. L. Paddock, M. Y. Okamura and J. T. Beatty**. 1998. A *puhA* gene deletion and plasmid complementation system for facile site directed mutagenesis studies of the reaction center H protein of *Rhodobacter sphaeroides*. Photosynth. Res. **55:**369-373.
9. **Cheng, Y. S., C. A. Brantner, A. Tsapin, and M. L. P. Collins.** 2000. Role of the H protein in assembly of the photochemical reaction center and intracytoplasmic membrane in *Rhodospirillum rubrum*. J. Bacteriol. **182:**1200-1207.
10. **Cogdell, R., and H. Scheer.** 1985. Circular dichroism of light-harvesting complexes from purple photosynthetic bacteria. Photochem. Photobiol. **42:**669-678.
11. **Cohen-Bazire, G., W. R. Sistrom, and R. Y. Stanier.** 1956. Kinetic studies of pigment synthesis by non-sulfur purple bacteria. J. Cell. Comp. Physiol. **49:**25–68.

12. **DaPra, E., M. Snozzi, and R. Bachofen**. 1982. Distribution of phosphatidylethanolamine in the lipid bilayer of chromatophores of the photosynthetic bacterium *Rhodospirillum rubrum*. Arch Microbiol. **133:**23-27.
13. **Ditta, G., T. Schmidhauser, E. Yakobson, P. Lu, X.-W. Liang, D. R. Finlay, D. Guiney, and D. R. Helinski.** 1985. Plasmids related to the broad host range vector, pRK290, useful for gene cloning and for monitoring gene expression. Plasmid. **13:**149–153.
14. **Dörge, B., G. Klug, N. Gad'on, S. N. Cohen and G. Drews**. 1990. Effects on the formation of antenna complex B870 of *Rhodobacter capsulatus* by exchange of charged amino acids in the N-terminal domain of the α and β pigment-binding proteins. Biochemistry **29:**7754-7758.
15. **Donohue, J. T., J. H. Hoger, and S. Kaplan.** 1986. Cloning and expression of the *Rhodobacter sphaeroides* reaction center H gene. J. Bacteriol. **168:**953-961.
16. **Drews, G.** 1978. Structure and development of the membrane system of photosynthetic bacteria. Curr. Top. In Bioenergetics. **8B:**161-207.
17. **Drews, G., and J. R. Golecki.** 1995. Structure, molecular organization, and biosynthesis of membranes of purple bacteria, p. 231–257. *In* R. E. Blankenship, M. T. Madigan, and C. E. Bauer (ed.), Anoxygenic photosynthetic bacteria. Kluwer Academic Publishers, Dordrecht, The Netherlands.
18. **Drews, G., and J. Oelze.** 1981. Organization and differentiation of membranes of phototrophic bacteria. Adv. Microb. Physiol. **22:**1-92.
19. **Figurski, D. H., and D. R. Helinski.** 1979. Replication of an origin-containing derivative of plasmid RK2 dependent on a plasmid function provided *in trans*. Proc. Natl. Acad. Sci. USA**. 76:**1648-1652.
20. **Francke, C., and J. Amesz.** 1995. The size of the photosynthetic unit in purple bacteria. Photosyn. Res. **46:**347-352.
21. **Garcia, A. F., W. Mäntele, N. Gad'on, M. H. Tadros, and G. Drews.** 1991. Growth and photosynthetic activities of wild-type and antenna-deficient mutant strains of *Rhodobacter capsulatus*. Arch. Microbiol. **155:**205-209.
22. **Ghosh, R., and R. Bachofen.** 1989. Die molekulare Struktur der photosynthetischen Membranen bei anoxygenen phototrophen Bakterien. Forum Mikrobiologie. **12:**556-564.
23. **Ghosh, R., A. Hardmeyer, I. Thoenen, and R. Bachofen.** 1994. Optimization of the Sistrom culture medium for large-scale batch cultivation of *Rhodospirillum rubrum* under

semi-aerobic conditions with maximal yield of photosynthetic membranes. Appl. Environ. Microbiol. **60:**1698-1700.

24. **Ghosh, R., H. Hauser, and R. Bachofen.** 1988. Reversible dissociation of B873 light-harvesting complex from *Rhodospirillum rubrum* G9+. Biochemistry. **27:**1004-1014.
25. **Ghosh, R., A. Hoenger, A. Hardmeyer, D. Mihailescu, R. Bachofen, A. Engel, and J. P. Rosenbusch.** 1993. Two-dimensional crystallization of the light-harvesting complex from *Rhodospirillum rubrum*. J. Mol. Biol. **231:**501-504.
26. **Ghosh, R.**, **T. Rosatzin, and R. Bachhofen.** 1988. Subunit structure and reassembly of the light-harvesting complex from *Rhodospirillum rubrum* G9+, p. 93-102. *In* H. Scheer and S. Schneider (ed.), Photosynthetic light-harvesting systems. Walter de Gruyter and Co., Berlin-New York.
27. **Grammel, H., E. D. Gilles, and R. Ghosh.** 2003. Microaerophilic cooperation of reductive and oxidative pathways allows maximal photosynthetic membrane biosynthesis in *Rhodospirillum rubrum*. Appl. Environ. Microbiol. **69:** 6577-6586.
28. **Goodhew, C. F., K. R. Brown, and G. W. Pettigrew.** 1986. Haem staining in gels, a useful tool in the study of bacterial *c*-type cytochromes. Biochim. Biopys. Acta. **852:**288-294.
29. **Hennecke, H., I. Günther, and F. Binder.** 1982. A novel cloning vector for the direct selection of recombinant DNA in *E. coli*. Gene. **19:**231-234.
30. **Holt, S. C., and A. G. Marr**. 1965. Effect of light intensity on the formation of intracytoplasmic membrane in *Rhodospirillum rubrum*. J. Bacteriol. **52:**1421-1429.
31. **Hu, X., and K. Schulten.** 1998. A model for the light-harvesting complex I (B875) of *Rhodobacter sphaeroides*. Biophys. J. **75:**683-694.
32. **Hunter, C. N., R. van Grondelle, and R. J. van Dorssen.** 1989. The construction and properties of a mutant of *Rhodobacter sphaeroides* with the LH1 antenna as the sole pigment protein. Biochim. Biophys. Acta. **973:**383-389.
33. **Jamieson, S. J., P. Wang, P. Quian, J. Y. Kirkland, M. J. Conroy, C. N. Hunter and P. A. Bullough.** 2002. Projection structure of the photosynthetic reaction centre-antenna complex of *Rhodospirillum rubrum* at 8.5 Å resolution. EMBO J. **21:**3927-3935.
34. **Jones, M. R., G. J. S. Fowler, L. C. D. Gibson, G. G. Grief, J. D. Olsen, W. Crielaard, and C. N. Hunter**. 1992. Mutants of *Rhodobacter sphaeroides* lacking one or more pigment-protein complexes and complementation with reaction-centre, LH1 and LH2 genes. Mol. Microbiol. **6:**1173-1184.

35. **Jones, M. R., R. W. Visschers, R. van Grondelle, and C. N. Hunter.** 1992. Construction and characterization of a mutant of *Rhodobacter sphaeroides* with the reaction center as the sole pigment-protein complex. Biochemistry. **31:**4458-4465.
36. **Jungas, C., J. Ranck, J. Rigaud, P. Joliot, and A. Verméglio.** 1999. Supramolecular organization of the photosynthetic apparatus of *Rhodobacter sphaeroides*. EMBO J. **18:**534-542.
37. **Karrasch, S., P. A. Bullough, and R. Ghosh.** 1995. The 8.5 Å projection map of the light-harvesting complex I from *Rhodospirillum rubrum* reveals a ring composed of 16 subunits. EMBO J. **14:**631-638.
38. **Klug, G., and S. Cohen.** 1988. Pleiotropic effects of localized *Rhodobacter capsulatus puf* operon deletions on production of light-absorbing pigment-protein complexes. J. Bacteriol. **170:**5814-5821.
39. **Kohl, D. H., J. Townsend, B. Commoner, H. L. Crespi, R. C. Dougherty, and J. J. Katz.** 1965. Effects of isotopic substitution on electron spin resonance signals in photosynthetic organisms. Nature. **12:**1105-1110.
40. **Kriauciunas, A., L. Yu, C.-A. Yu, R. M. Wynn, and D. B. Knaff.** 1989. The *Rhodospirillum rubrum* cytochrome bc_1 complex: peptide composition, prosthetic group content and quinone binding. Biochim. Biophys. Acta. **976:**70-76.
41. **Laemmli, U. K.** 1970. Cleavage of structural proteins during the assembly of the head of bacteriophage T4. Nature. **227:**680-685.
42. **Mazodier, P., P. Cossart, E. Giraud, and F. Gasser.** 1985. Completion of the nucleotide sequence of the central region of Tn*5* confirms the presence of three resistance genes. Nucleic Acids Res. **13:**195-205.
43. **Miller, K. R.** 1982. Three-dimensional structure of a photosynthetic membrane. Nature. **300:**53-55.
44. **Monger, T., and W. W. Parson.** 1977. Singlet-triplet fusion in *Rhodopseudomonas sphaeroides* chromatophores. Biochim. Biophys. Acta. **460:**393-407.
45. **Ormerod, J. G., K. S. Ormerod, and H. Gest.** 1961. Light-dependent utilization of organic compounds and photoproduction of molecular hydrogen by photosynthetic bacteria; relationships with nitrogen metabolism. Arch. Biochem. Biophys. **94:**449–463.
46. **Peterson, G. L.** 1977. A simplification of the protein assay method of Lowry *et al.* which is more generally applicable. Anal. Biochem. **83:**346-356.

47. **Philipson, K. D., and K. Sauer.** 1973. Comparative study of the circular dichroism spectra of reaction centers from several photosynthetic bacteria. Biochemistry. **12:**535-539.

48. **Richter, P., and G. Drews**. 1991. Incorporation of light-harvesting complex I α and β polypeptides into the intracytoplasmic membrane of *Rhodobacter capsulatus*. J. Bacteriol. **173:**5336-5345.

49. **Richter, P., M. Brand, and G. Drews**. 1992. Characterization of LHI^- and LHI^+ *Rhodobacter capsulatus pufA* mutants. J. Bacteriol. **174:**3030-3041.

50. **Saegesser, R.** 1992. Identifikation und Charakterisierung des Photosynthese - Genclusters aus *Rhodospirillum rubrum*. Ph.D. thesis. University of Zurich, Switzerland.

51. **Saegesser, R., R. Ghosh, and R. Bachofen**. 1992. Stability of broad host range cloning vectors in the phototrophic bacterium *Rhodospirillum rubrum*. FEMS Microbiol. Lett. **95:** 7-12.

52. **Sambrook, J., E. F. Fritsch, and T. Maniatis.** 1989. Molecular Cloning: a laboratory manual, 2nd ed. Cold Spring Harbor Laboratory Press. Cold Spring Harbor, N.Y.

53. **Schertler, G. F. X**. 1992. Overproduction of membrane proteins. Curr. Opin Struct. Biol. **2:**534-544.

54. **Scherz, A., and W. W. Parson.** 1984. Oligomers of bacteriochlorophyll and bacteriopheophytin with spectroscopic properties resembling those found in photosynthetic bacteria. Biochim. Biophys. Acta. **766:**653-665.

55. **Simon, R., U. Priefer, and A. Pühler.** 1983. Vector plasmids for *in-vivo* and *in-vitro* manipulations of gram-negative bacteria, p. 98-105. *In* A. Pühler (ed.) Molecular genetics of the bacteria-plant interaction. Springer-Verlag Berlin Heidelberg.

56. **Sistrom, W. R.** 1960. A requirement for sodium in the growth of *Rhodopseudomonas sphaeroides*. J. Gen. Microbiol. **22:**778-785.

57. **Sockett, R. E., T. J. Donohue, A. R. Varga, and S. Kaplan.** 1989. Control of photosynthetic membrane assembly in *Rhodobacter sphaeroides* mediated by *puhA* and flanking sequences. J. Bacteriol. **171:**436-446.

58. **Spurr, A. R.** 1969. A low viscosity epoxy resin embedding medium for electron microscopy. J. Ultrastruct. Res. **26:**31-43.

59. **Stahlberg, H., J. Dubochet, H. Vogel, and R. Ghosh.** 1998. Are the light-harvesting I complexes from *Rhodospirillum rubrum* arranged around the reaction centre in a square geometry? J. Mol. Biol. **282:**819-831.

60. **Stark, W., W. Kühlbrandt, I. Wildhaber, E. Wehrli, and K. Mühlethaler.** 1984. The structure of the photoreceptor unit of *Rhodopseudomonas viridis*. EMBO J. **3:**777-783.
61. **Walz, T., and R. Ghosh.** 1997. Two-dimensional crystallization of the light-harvesting I-reaction centre photounit from *Rhodospirillum rubrum*. J. Mol. Biol. **265:**107-111.
62. **Wiggli, M.**, **L. Cornacchia, R. Saegesser, R. Bachofen, and R. Ghosh.** 1996. Characterization of *Rhodospirillum rubrum* ST2: a new Tn*5*-induced carotenoid-less mutant for functional studies. Microbiol. Res. **151:**57-62.
63. **Willetts, N.** 1984. Conjugation. Meth. Microbiol. **17:**33-59.
64. **Wong, D. K.-H., W. J. Collins, A. Harmer, T. G. Lilburn, and J. T. Beatty.** 1996. Directed mutagenesis of the *Rhodobacter capsulatus puhA* gene and *orf214*: pleiotropic effects on photosynthetic reaction center and light-harvesting 1 complexes. J. Bacteriol. **178:**2334-2342.
65. **Young, C. S., and J. T. Beatty.** 1998. Topological model of the *Rhodobacter capsulatus* light-harvesting complex I assembly protein LhaA (previously known as Orf1696). J. Bacteriol. **180:**4742-4745.
66. **Young, C. S., R. C. Reyes, and J. T. Beatty.** 1998. Genetic complementation and kinetic analyses of *Rhodobacter capsulatus orf1696* mutants indicate that the Orf1696 protein enhances assembly of the light-harvesting I complex. J. Bacteriol. **180:**1759-1765.

FIGURE LEGENDS

Figure 1: Construction map for the deletion of the *puhA* gene. The approximate position and relevant restriction sites of the *puh* operon (4) on the pVK100-derived cosmid pSC21-7 are shown (upper part of the figure). The lower part of the figure shows a magnification of the 3.6 kb fragment present on pBsH2, which encodes the *puhA* operon used for the deletion of the *puhA* open reading frame and the insertion of the kanamycin cassette to yield pBsPUHK1 and pBsPUHK2, respectively. The plasmids pRKGP and pRKΔGP used in the complementation experiment are also indicated. Relevant scale bars are indicated in the upper and lower part of the figure, respectively. Abbreviations: *B*, *Bam*HI; RI, *Eco*RI; *S*, *Sal*I; *P*, *Pst*I; *H*, *Hin*dIII; *Nt*, *Not*I; *Ml*, *Mlu*I; *Bt*, *Bst*EII; *Sph*, *Sph*I and *Ec*4, *Eco*47III.

Figure 2: Absorption spectra of total cells grown in different growth media. Left hand panels (A): Absorption spectra obtained for S1 (–) and mutants SPUHK1 (--) and SPUHK2 (··). Right hand panels (B): Absorption spectra of G9 (–), ST2 (–) and the *puhA* deletion mutants GPUHK1 (--) and GPUHK2 (··). Spectra were obtained from equal amounts of cells (A_{660nm}(1 cm) = 2.5) suspended in M-medium containing 80% (v/v) glycerol. A 2 mm path-length quartz cell was employed for the measurement. The corresponding growth media are indicated in the figure. The peak heights were measured by extrapolating the $A_{660\ nm}$ (due only to turbidity) to 880 nm and then subtracting this value from the measured 880 nm (or 873 nm) peak.

Figure 3: Electron micrographs of *puhA* deletion mutants and parental strains. Arrow indicates the ICM. Bar = 0.25 µm. All cultures were grown semi-aerobically using M2SF medium (see Materials and Methods).

Figure 4: SDS-PAGE analysis of isolated chromatophores of parental strains and mutants. Each lane contains 20 µg of protein and has been stained with Coomassie Blue. Growth conditions [aerobic (aer) and anaerobic (an)] are indicated as appropiate. Assignments of the known protein components, the H, M and L subunits of the RC as well as the cytochrome c_1 of the cytochrome bc_1 complex, and the LH1 complex (α and β polypeptides are not resolved

in this system) are indicated. The (?) symbol indicates an unknown protein with a mass corresponding to G115 (LhaA).

Figure 5: Near-IR CD spectra of isolated chromatophores obtained from parental strains and *puhA* deletion mutants. (A) Spectra obtained from S1 grown anaerobically (–) and semi-aerobically (–) as well as those obtained for the deletion mutants SPUHK1 (--) and SPUHK2 (--); (B) Spectra from G9 grown anaerobically (–), ST2 grown semi-aerobically (–) and from the *puhA* deletion mutants GPUHK1 (--) and GPUHK2 (--). Equal amounts, corresponding to A_{880nm} (or A_{873nm}) (1 mm) = 1, were employed for the measurement.

TABLES

TABLE 1. Strains and plasmids used in this study

Strain or plasmid	Relevant characteristics	Reference or source
E. coli		
RR28	Strain used for cloning routines, RecA$^-$ derivative of RR1	29
XL1MR	Δ(*mcrA*)183, Δ(*mcrCB-hsdSMR-mrn*173, *endA1*, *supE44*, *thi-1*, *recA1*, *gyrA96*, *relA1*, *lac*	Stratagene
R. rubrum		
S1	Wildtype	11
G9	Random carotenoid-less mutant (putative *crtB* mutant)[a]	11
ST2	S1-derived Tn*5*-mutant, carotenoid-less (putative *crtB* mutant)[a]	62
GPUHK1	G9-derived *puhA*-interposon mutant, *npt* in the same transcriptional orientation as the *puhA*-operon, PS$^-$ Kan^r	This study
GPUHK2	G9-derived *puhA*-interposon mutant, *npt* in the reverse transcriptional orientation as the *puhA*-operon, PS$^-$ Kan^r	This study
SPUHK1	S1-derived *puhA*-interposon mutant, *npt* in the same transcriptional orientation as the *puhA*-operon, PS$^-$ Kan^r	This study
SPUHK2	S1-derived *puhA*-interposon mutant, *npt* in the reverse transcriptional orientation as the *puhA*-operon, PS$^-$ Kan^r	This study
Plasmids		
pBsH2	pBsKSII(+) derivative, carries a 3.6 kb *Hin*dIII-fragment derived from a cosmid containing *puhA* and flanking genes	This study
pBsKSII+	high copy cloning vector, ColE1 Amp^r	Stratagene
pBsLGKAN	pBsKSII(+) derivative carrying the kanamycin resistance cassette, Kan^r	This study
pBsPUHK1	*puh* operon with a partial deleted *puhA* gene with the interposon in the same transcriptional orientation as the *puhA* operon in pBsKSII(+), Amp^r Kan^r	This study
pBsPUHK2	resistance cartridge in opposite orientation as in pBsPUHK1	This study
pRK2013	mobilizing helper plasmid, *tra*$^+$ Kan^r	19
pRK404	Derivative of pRK290, *mob*$^+$	13
pRKGP	*G115-puhA* subcloned into pRK404	This study
pRKΔGP	Δ*G115-puhA* subcloned into pRK404	This study
pRKOPUH1	3.6 kb *Hin*dIII-fragment subcloned into pRK404	This study
pSC21-7	pVK100 derivative containing ca. 20 kb of *R. rubrum* chromosomal DNA, carries the *puh* operon	50
pSUP202	suicide vector, ColE1, *mob*$^+$ Amp^r Cm^r Tet^r	55
pSUPPK1	*Hin*dIII fragment of pBsPUHK1 containing the deleted *puhA* gen on pSUP202, Amp^r Kan^r Cm^s Tet^r	This study
pSUPPK2	*Hin*dIII fragment of pBsPUHK2 containing the deleted *puhA* gen on pSUP202, Amp^r Kan^r Cm^s Tet^r	This study

[a] As shown by HPLC analysis the mutants G9 and ST2 are completely lacking carotenoids or their precursors (beginning with phytoene) (R. Ghosh, unpublished data).

TABLE 2. Relative amounts of the LH1 complexes in different culture media.

Strain	Relative intensity (±5 %) of the LH1 near-IR absorption maximum [a]					
	semi-aerobic growth medium					
	M		M2S		M2SF	
	A_{880nm} (or A_{873nm})[b]	%	A_{880nm} (or A_{873nm})[b]	%	A_{880nm} (or A_{873nm})[b]	%
S1	0.14	100	0.517	100	0.77	100
SPUHK1	0.13	93	0.197	38	0.64	83
SPUHK2	0.10	71	0.167	32	0.79	103
ST2	0.051	100	0.547	106	0.62	87
G9	0.051	100	0.517	100	0.71	100
GPUHK1	no peak	0	0.167	32	0.49	69
GPUHK2	no peak	0	0.137	26	0.63	89
S1 (pRKGP)	n. d.		0.517	100	0.76	99
SPUHK1 (pRKGP)	n. d.		0.317	61	0.65	84
	anaerobic growth medium[c]					
S1	0.274	100	n. d.		n. d.	
S1 (pRKGP)	0.224	82	n. d.		n. d.	
SPUHK1 (pRKGP)	0.214	78	n. d.		n. d.	

[a] The relative intensity of the LH1 near-IR absorption maximum was calculated from the ratio of the near-IR Q_y absorption maximum (λ= 880 nm for S1 or λ= 873 nm for G9/ST2) observed to that of the corresponding parental strain grown semi-aerobically in the same medium. The relative intensity obtained for ST2 has been calculated using G9 as a reference (n. d. not determined).

[b] In all cases cell suspensions were adjusted to the same A_{660nm} (turbidity) prior to the measurement.

[c] These strains were harvested in the mid-exponential phase.

TABLE 3. Relative amounts of the LH1 BChl and carotenoids in isolated chromatophores.[a]

Strain	Growth	Relative intensity (%)(± 10%) of the absorption maximum at	
		880 nm (or 873 nm)[b]	512 nm [c]
S1	anaerobic	100	100
S1	semi-aerobic	88	83
SPUHK1	semi-aerobic	86	83
SPUHK2	semi-aerobic	79	76
ST2	semi-aerobic	88	–
G9	anaerobic	100	–
GPUHK1	semi-aerobic	72	–
GPUHK2	semi-aerobic	78	–

[a] Normalized to identical amounts of protein, as judged from the A_{280nm}.

[b] The wavelength maximum in parentheses correspond to the Q_y absorption band of the carotenoid-less strains.

[c] Carotenoid absorption maximum.

FIGURES

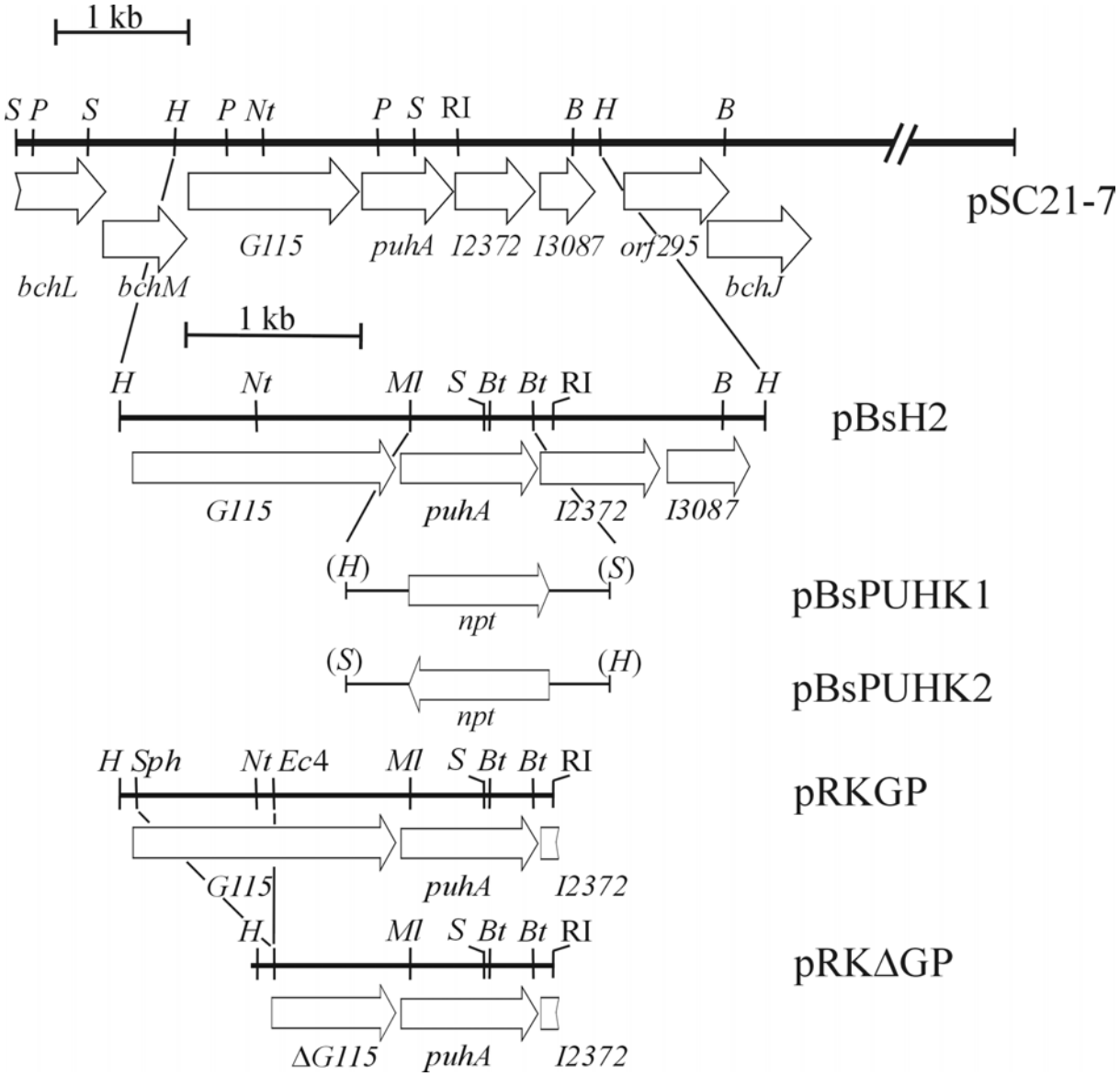

Figure 1

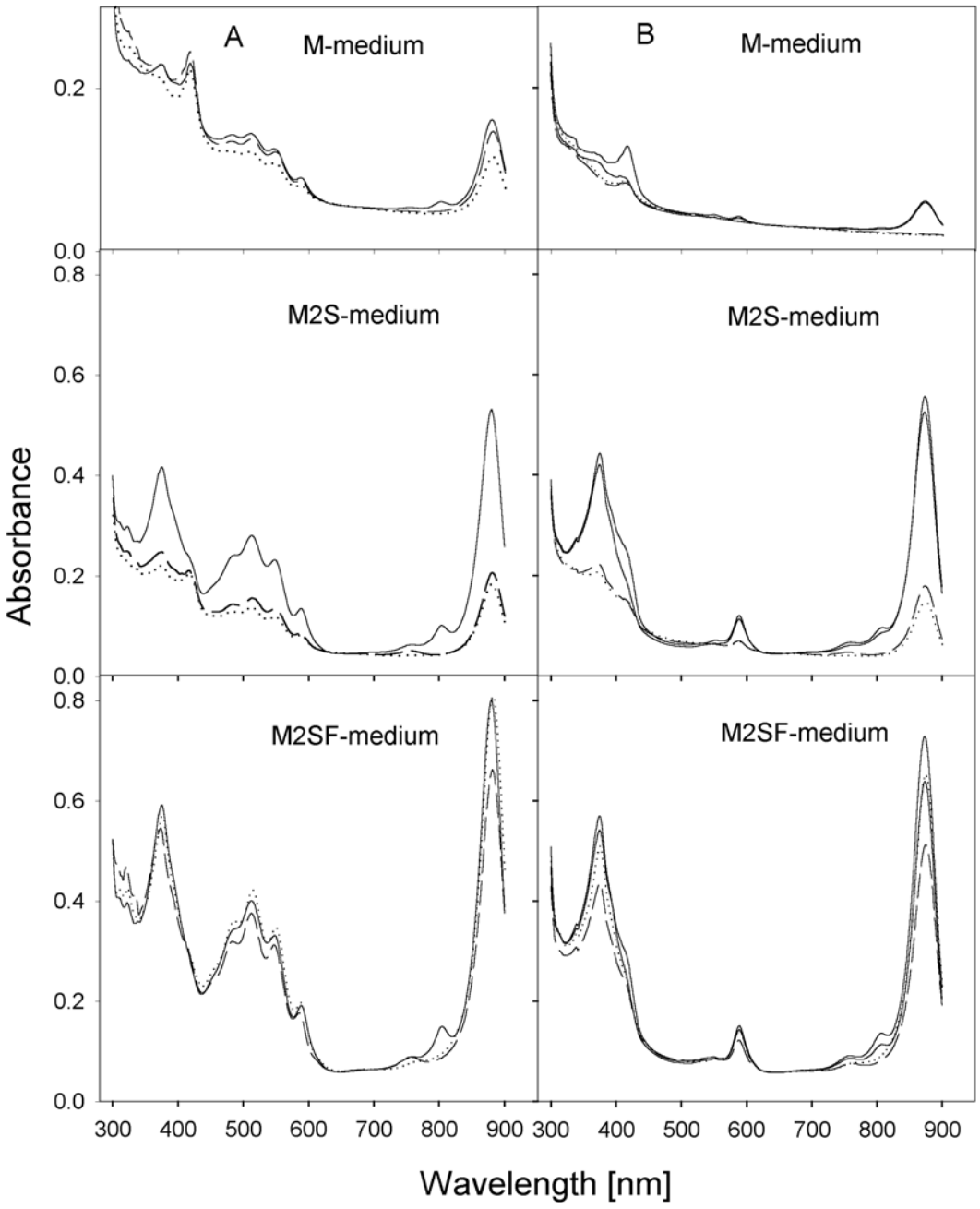

Figure 2

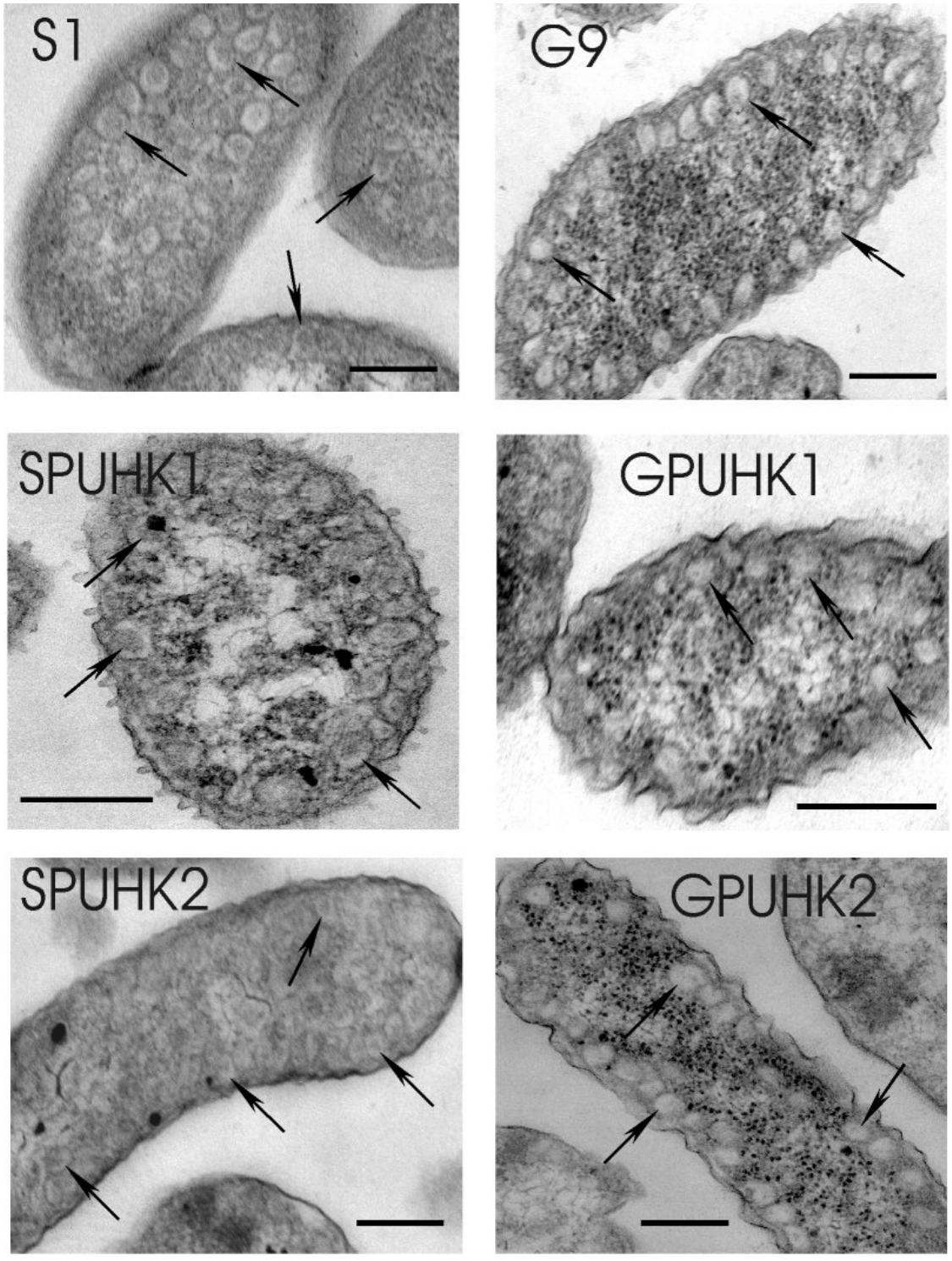

Figure 3

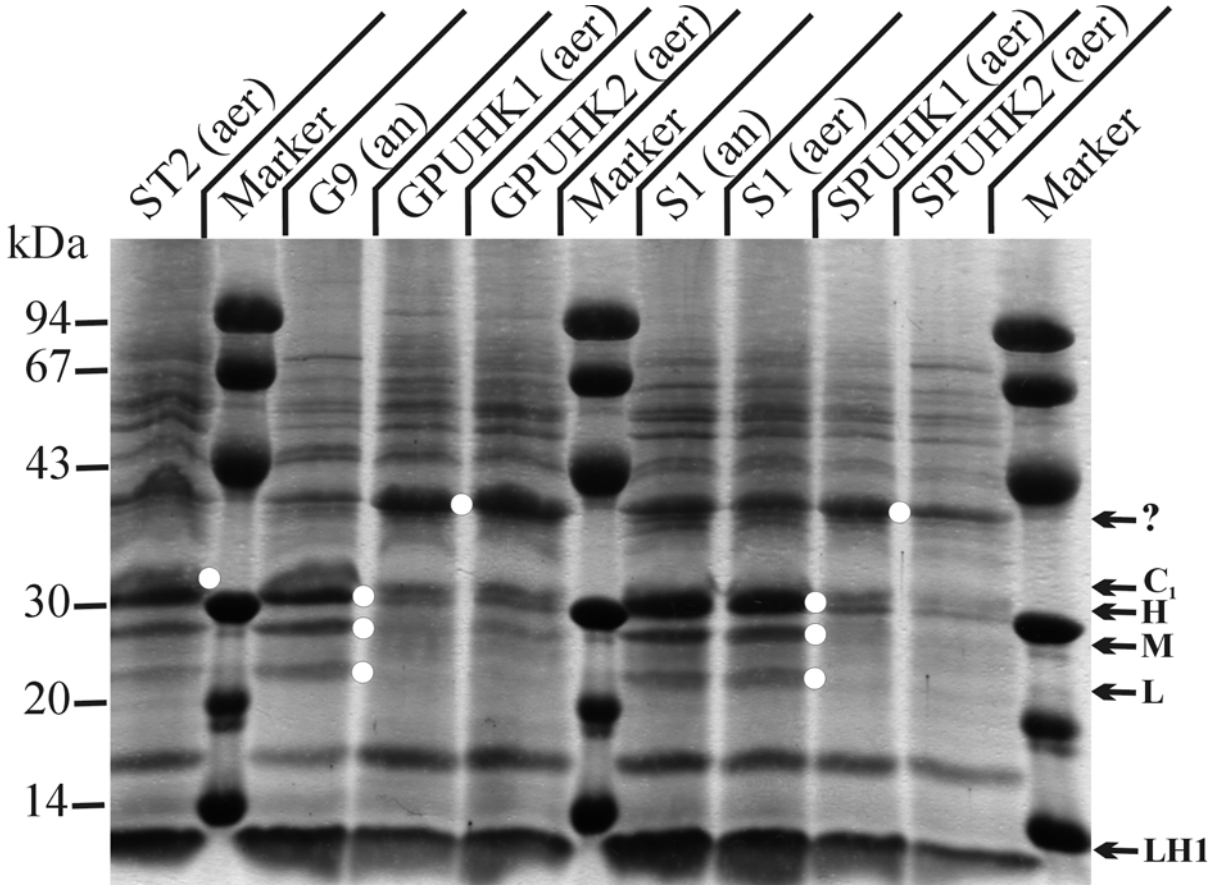

Figure 4

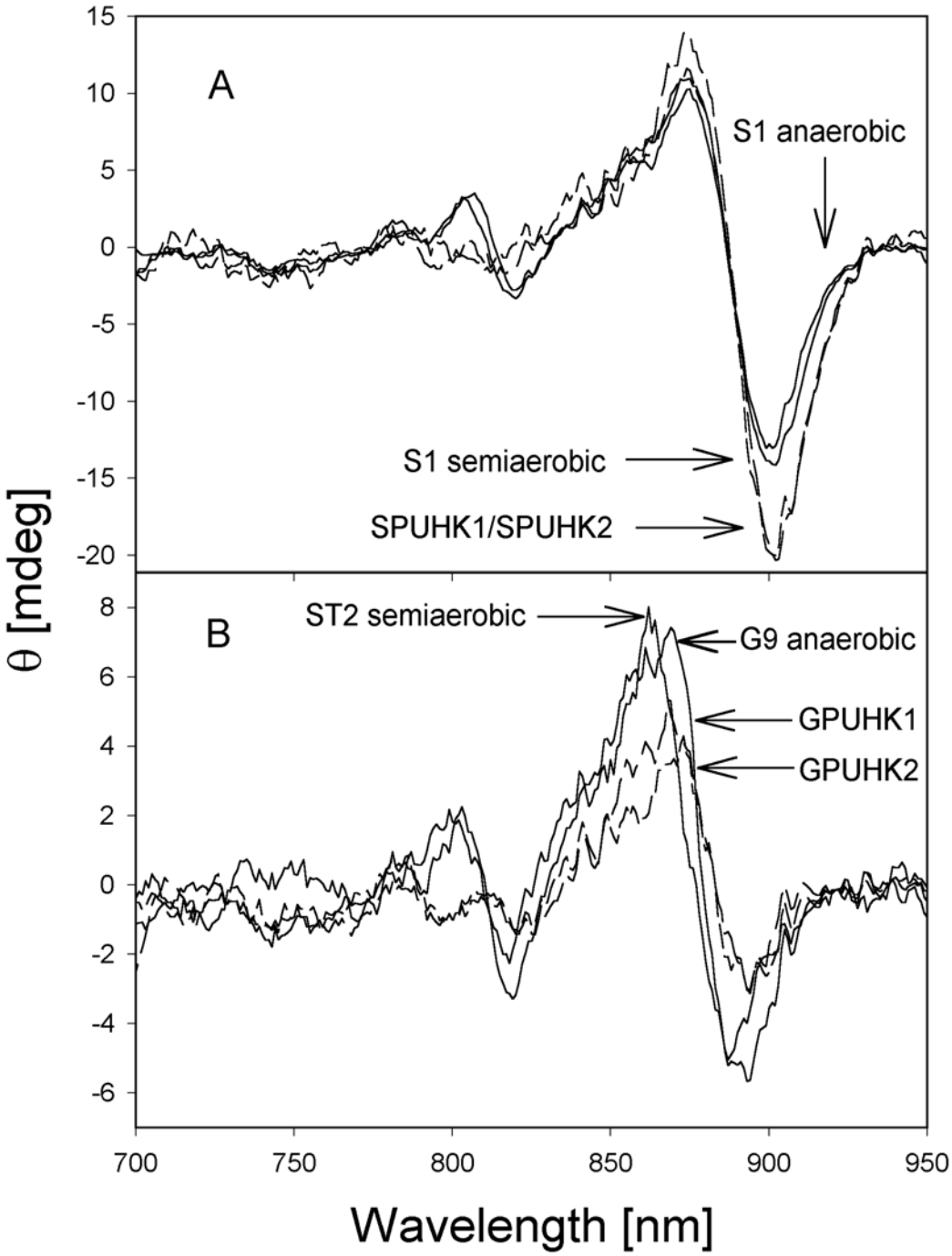

Figure 5

SUPPLEMENTARY DATA

FIGURE LEGENDS

Figure S1: Southern hybridization analysis of parental strains and mutants. For the indicated strains 4µg of chromosomal DNA were digested with (a) *Sal*I or (b) *Sph*I. Hybridization was performed using a digoxigenin labelled *puhA* probe or a digoxigenin-labelled *kan* (*npt*) probe as indicated. (c) Restriction map of the genomic fragment (upper part), the *puh* operon (magnification of HindIII fragment) and the PUHK1 and PUHK2 genotypes (lower parts), respectively. Abbreviations: *S*, *Sal*I; *P*, *Pst*I; *H*, *Hin*dIII; RI, *Nt*, *Not*I; *Eco*RI; *B*, *Bam*HI; *Sph*, *Sph*I; *Ml*, *Mlu*I; *Bt*, *Bst*EII.

Figure S2: Absorption spectra obtained from complemented (plasmid in parentheses) deletion mutants and their parental strains. The upper panel (A) shows absorption spectra obtained from *R. rubrum* S1 and the complemented mutant *R. rubrum* SPUHK1 (pRKOPUH1) and *R. rubrum* SPUHK2 (pRKOPUH1). And the lower panel (B) shows absorption spectra of *R. rubrum* G9, *R. rubrum* ST2 and the complemented mutants GPUHK1 (pRKOPUH1) and GPUHK2 (pRKOPUH1). Equal cell densities were measured in all cases as described in Fig. 2. All cultures used for this measurement were grown anaerobically (photoheterotrophically) in M-medium. Parental strains (–) and mutants (--) are indicated.

Figure S3: Absorption spectra of isolated chromatophores of parental and mutant strains. Spectra are shown for (A) *R. rubrum* S1 and corresponding mutants and (B) *R. rubrum* G9 and corresponding mutants as well as the Tn*5*-derived carotenoid-less strain *R. rubrum* ST2. Growth conditions are indicated for the parental strains and for *R. rubrum* ST2. All deletion mutants were grown semi-aerobically in M2SF-medium.

Figure S4: SDS-PAGE analysis of isolated chromatophores of parental strains and mutants. Upper panel: Each lane contains 20 µg of protein and has been stained with Coomassie Blue after SDS-PAGE. Growth conditions [aerobic (aer) and anaerobic (an)] are indicated as appropiate. Assignments of the known protein components, the H, M and L subunits of the RC as well as the cytochrome c_1 of the cytochrome bc_1 complex, and the LH1 complex (α and β polypeptides are not resolved in this system) are indicated. The lower panel shows a

densitometric analysis of lanes containing chromatophores of (A) *R. rubrum* S1 and corresponding mutants SPUHK1 and SPUHK2, and (B) *R. rubrum* G9 and corresponding mutants GPUHK1 and GPUHK2, as well as isolated chromatophores of *R. rubrum* ST2. For the parental strains *R. rubrum* S1 (lower panel A), *R. rubrum* G9 (lower panel B) and *R. rubrum* ST2 (lower panel B) the chromatophores obtained from (–) anaerobic and (--) semi-aerobic cultures are indicated. For the mutants the solid lanes represent either SPUHK1 and GPUHK1, as appropiate and the dotted lines represent SPUHK2 and GPUHK2, as appropiate.

Figure S5: SDS-PAGE analysis of WSP of parental strains and mutants.
Upper panel: Each lane contains 20 µg of protein and has been stained with Coomassie Blue after SDS-PAGE. Growth conditions [aerobic (aer) and anaerobic (an)] are indicated as appropiate. Assignment of the known neophosphotransferase protein (Npt), which mediates resistance to the antibiotics kanamycin is indicated. The lower panel shows a densitometric analysis of lanes containing WSP of (A) *R. rubrum* S1 and corresponding mutants SPUHK1 and SPUHK2, and (B) *R. rubrum* G9 and corresponding mutants GPUHK1 and GPUHK2, as well as the WSP of *R. rubrum* ST2. For the parental strains *R. rubrum* S1 (lower panel A), *R. rubrum* G9 (lower panel B) and *R. rubrum* ST2 (lower panel B) the WSP obtained from (–) anaerobic and (--) semi-aerobic cultures are indicated. For the mutants the solid lanes represent either SPUHK1 and GPUHK1, as appropiate and the dashed lines represent SPUHK2 and GPUHK2, as appropiate.

Figure S6: ESR spectra obtained from isolated chromatophores of parental strains and *puhA* deletion mutants. (A) Spectra obtained from *R. rubrum* S1 grown anaerobically (–) and semi-aerobically (–) as well as those obtained for the deletion mutants SPUHK1 (--) and SPUHK2 (--); (B) Spectra from *R. rubrum* G9 grown anaerobically (–), *R. rubrum* ST2 grown semi-aerobically and from the *puhA* deletion mutants GPUHK1 (--) and GPUHK2 (--). Equal amounts, corresponding to $A_{880nm/874nm}$ (4 mm) = 1, were employed for this measurement. The field strength increment (ΔB_0) shown in Gauss (G) is indicated on the x-axes.

FIGURES

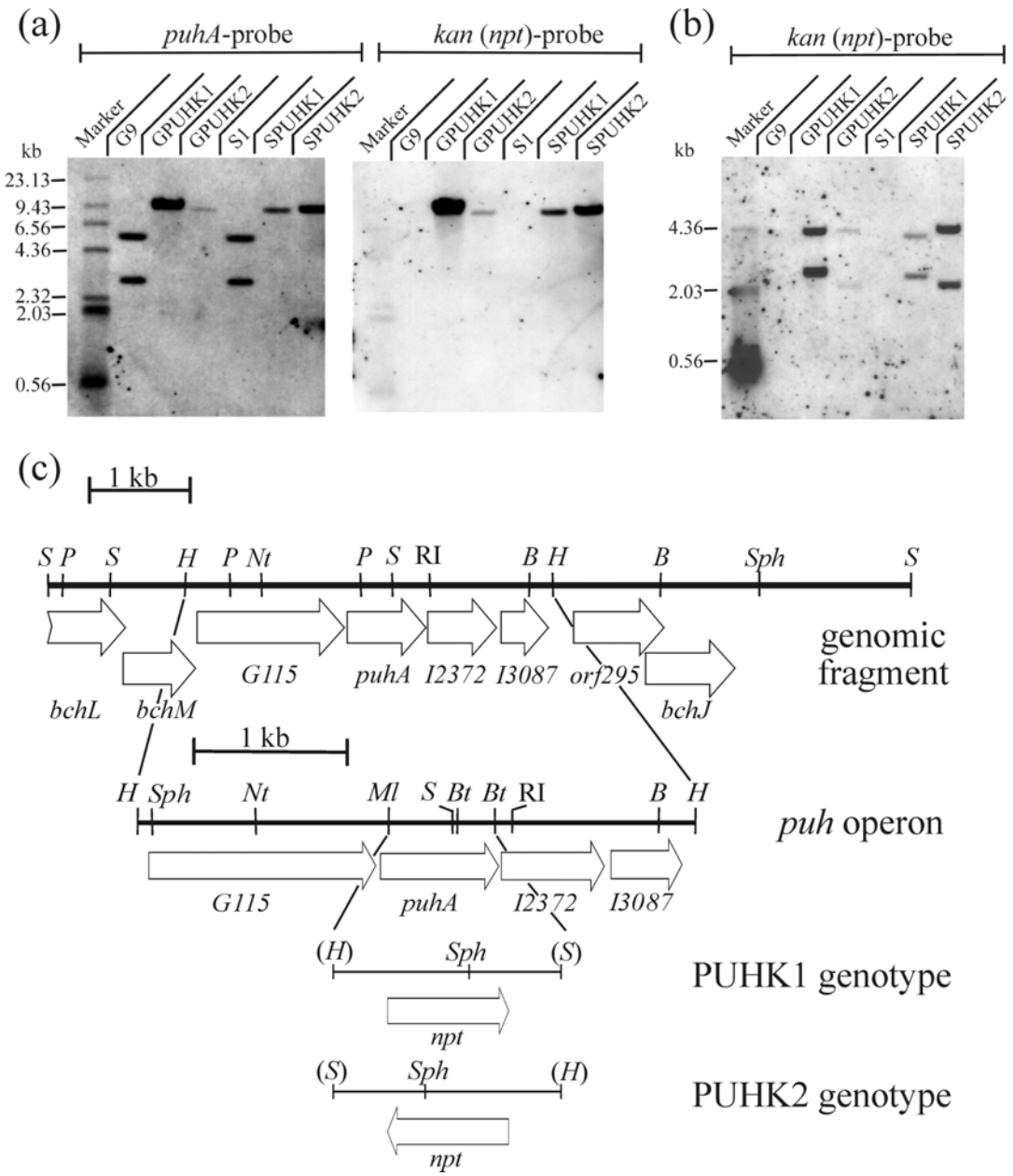

Figure S1

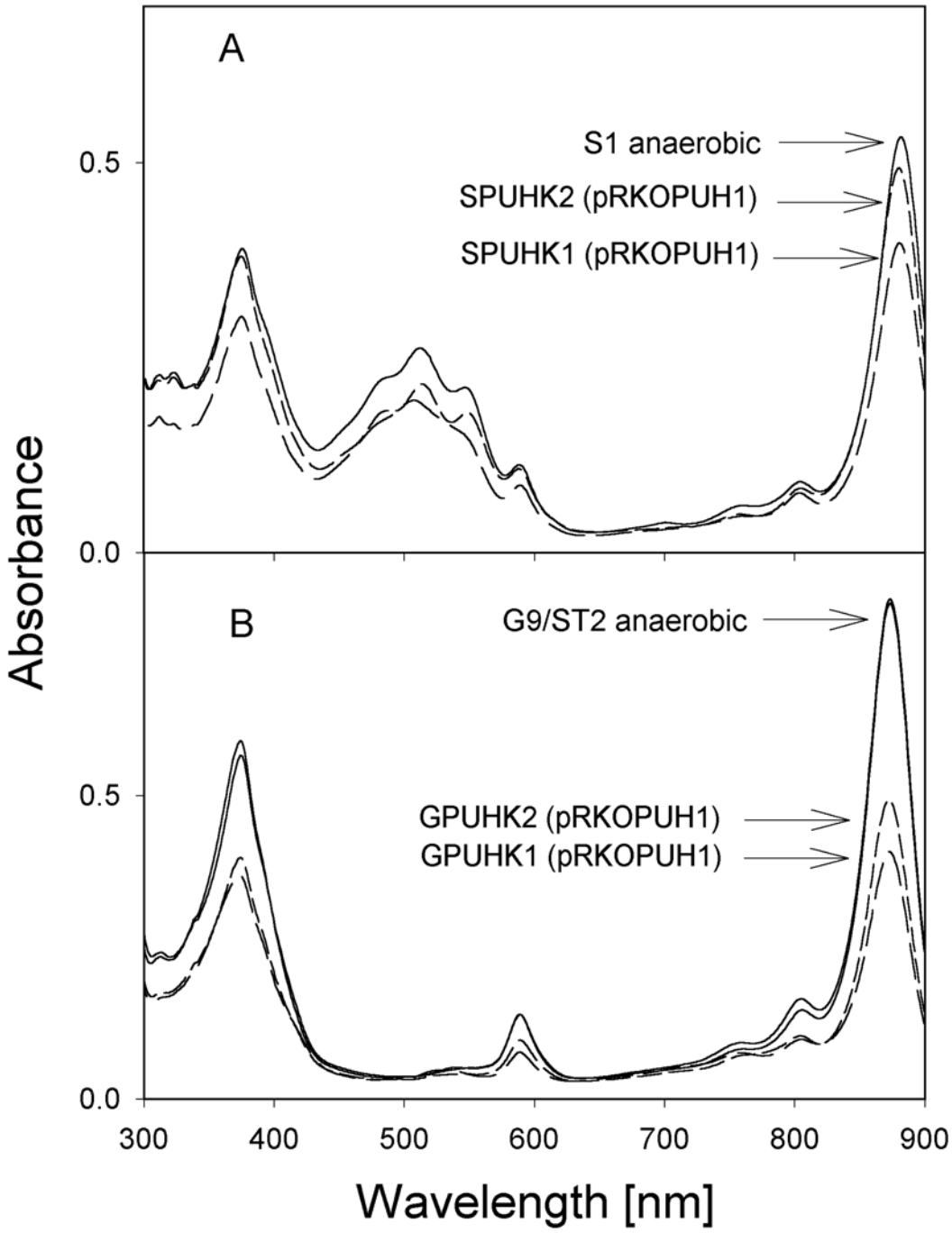
A
S1 anaerobic
SPUHK2 (pRKOPUH1)
SPUHK1 (pRKOPUH1)
0.5
0.0
B
G9/ST2 anaerobic
GPUHK2 (pRKOPUH1)
GPUHK1 (pRKOPUH1)
0.5
0.0
Absorbance
300
400
500
600
700
800
900
Wavelength [nm]

Figure S2

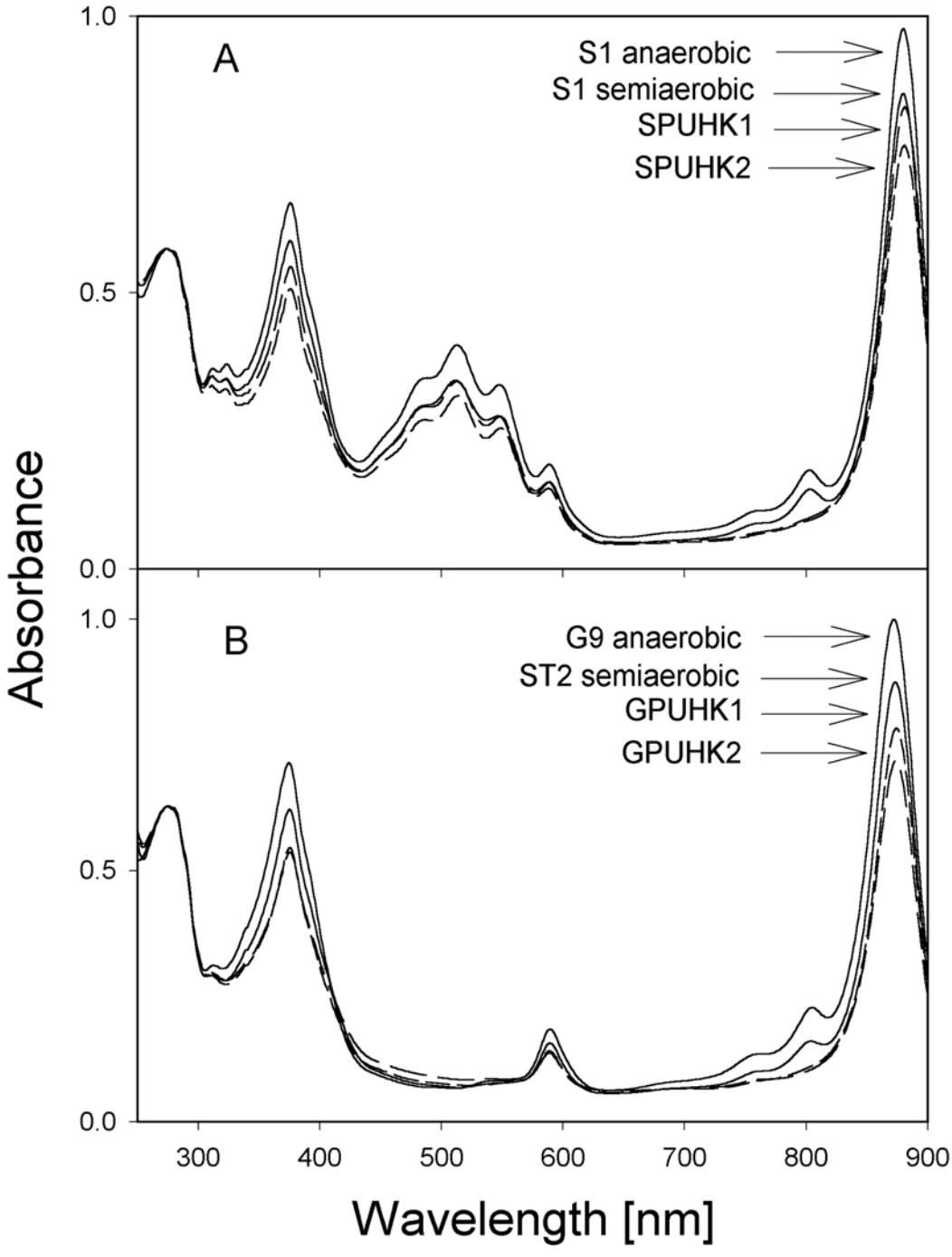
A
S1 anaerobic
S1 semiaerobic
SPUHK1
SPUHK2
B
G9 anaerobic
ST2 semiaerobic
GPUHK1
GPUHK2
Absorbance
1.0
0.5
0.0
300
400
500
600
700
800
900
Wavelength [nm]

Figure S3

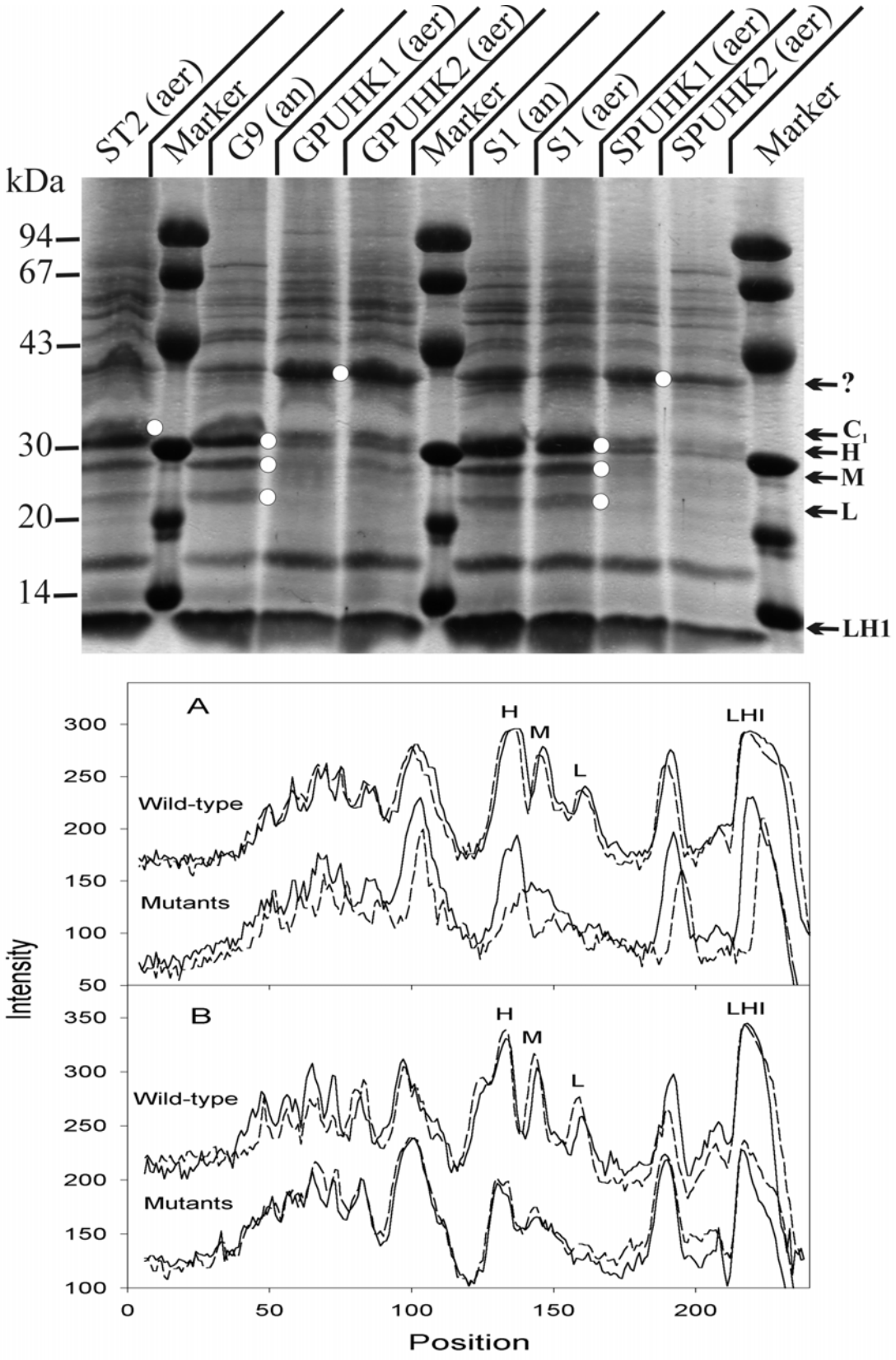
ST2 (aer)
Marker
G9 (an)
GPUHK1 (aer)
GPUHK2 (aer)
Marker
S1 (an)
S1 (aer)
SPUHK1 (aer)
SPUHK2 (aer)
Marker
kDa
94
67
43
30
20
14
?
C1
H
M
L
LH1
A
B
H
M
L
LHI
Wild-type
Mutants
Intensity
Position
0
50
100
150
200
300
250
350

Figure S4

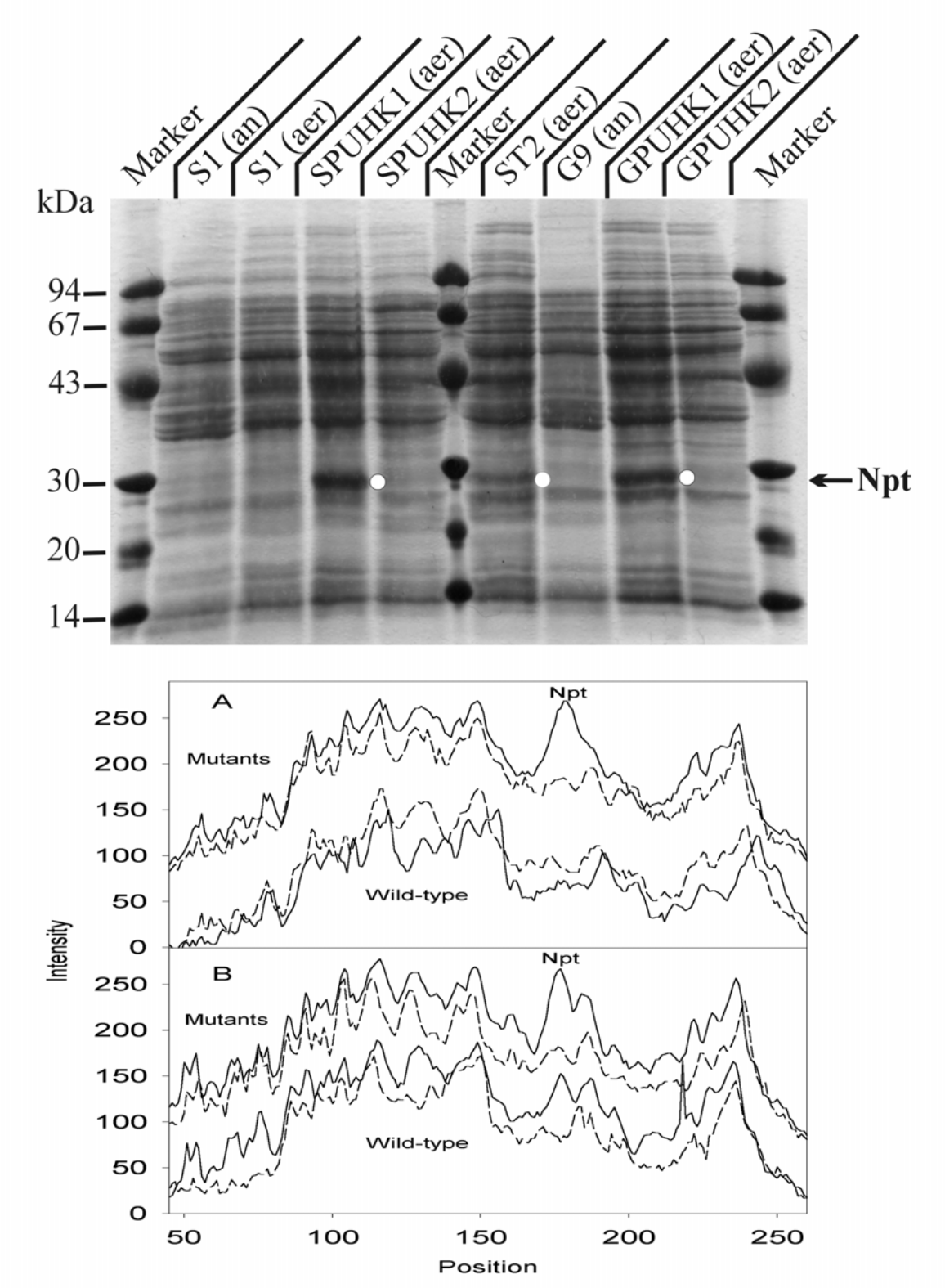
Marker
S1 (an)
S1 (aer)
SPUHK1 (aer)
SPUHK2 (aer)
Marker
ST2 (aer)
G9 (an)
GPUHK1 (aer)
GPUHK2 (aer)
Marker
kDa
94
67
43
30
20
14
Npt
A
Mutants
Wild-type
Npt
B
Mutants
Wild-type
Npt
Intensity
250
200
150
100
50
0
50
100
150
200
250
Position

Figure S5

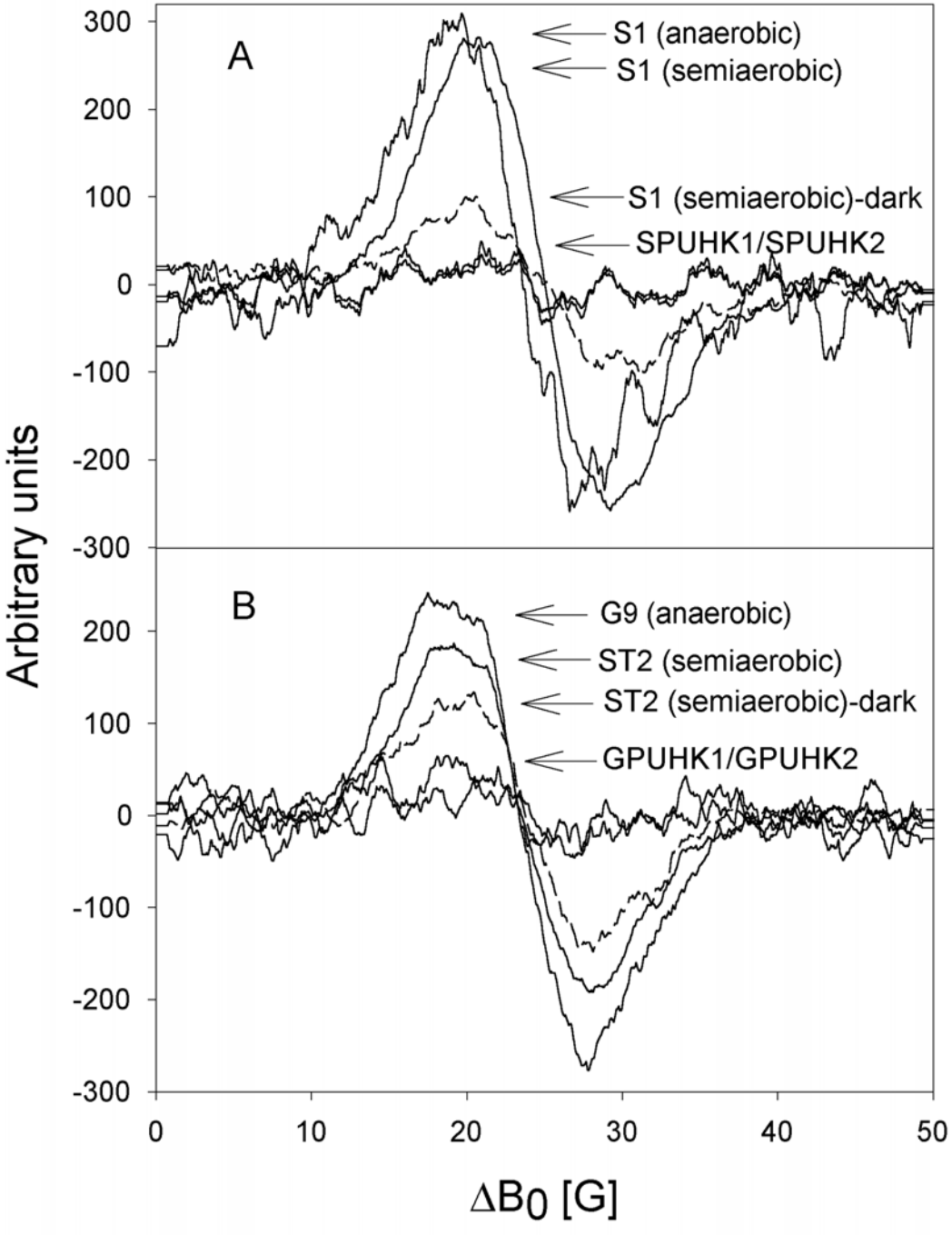
A
S1 (anaerobic)
S1 (semiaerobic)
S1 (semiaerobic)-dark
SPUHK1/SPUHK2
B
G9 (anaerobic)
ST2 (semiaerobic)
ST2 (semiaerobic)-dark
GPUHK1/GPUHK2
Arbitrary units
300
200
100
0
-100
-200
-300
0
10
20
30
40
50
ΔB0 [G]

Figure S6

MUTAGENESE DER H-UNTEREINHEIT

The Design and Expression of Independent Transmembrane and Cytoplasmic Domains of the H subunit of the Photosynthetic Reaction Center Demonstrates Synergistic Interaction with the Light-Harvesting 1 Complex

Domenico Lupo[1], Felix Autenrieth[1,2], Klaus Schulten[2], and Robin Ghosh[1*]

[1]Department of Bioenergetics, Institute of Biology, University of Stuttgart, Pfaffenwaldring 57, D-70550 Stuttgart, Germany

[2]Beckmann Institute, Theoretical and Computational Biophysics Group, University of Illinois 405 N Mathews Avenue, Urbana, IL 61801 USA

∗corresponding author: Tel. +49711/685-5047; Fax:+49711/685-5096;
E-mail: robin.ghosh@bio.uni-stuttgart.de

ABSTRACT

The molecular design of functional domains of the H subunit of the photosynthetic reaction center (RC) of the purple non-sulfur bacterium *Rhodospirillum rubrum* was performed by a three step procedure. First, the structure of the reaction center was deduced by modeling the amino acid sequences of the subunits L, M, and H, to the closely homologous subunits of reaction center from *Rhodobacter sphaeroides* and *Thermochromatium tepidum.* Secondly, the domain structure of the H subunit was analyzed by comparing the *R. rubrum* model to the known X-ray structures from the reaction centers of *Rb. sphaeroides*, *Blastochloris viridis* and *Th. tepidum*. At this stage, it appeared that the cytoplasmic (CY) domain of the H subunit could be composed of two subdomains: a putative light-harvesting (LH1-) interaction domain immediately following the transmembrane (TM) α-helix (which interacts principally with the M-subunit of the reaction centre) and a cytoplasmic domain which interacts principally with the L- and M-subunits of the reaction center. In a third step, the *puhA* gene encoding the H subunit, was redesigned as a two-gene cistron (*puhDM*) encoding the putative TM-LH1 interaction domain and the CY-LM-interaction domain, respectively, and expressed under control of the *puhA* promotor in a *puhA*-deletion mutant (SPUHK1) of *R. rubrum*. In addition, the individual TM- and CY-encoding genes were expressed singly in the same mutant. Coexpression of both domains restored the capability for photosynthetic growth and the assembly of a functional RC. Expression of the TM or CY domains singly enhanced the RC content when compared to the mutant, but the expression level was significantly lower than that of the wild-type. In the mutant expressing the 2-gene cistron almost wild-type levels of photosynthetic growth were observed, whereas in both strains expressing the single domains, photosynthetic growth occurred but was severely impaired compared to that of SPUHK1 expressing the *puhDM* construct. Aerobic growth of all strains was unimpaired compared to the wild-type.

INTRODUCTION

Purple non sulfur bacteria like *Rhodospirillum rubrum* show a very high metabolic versatility. They can grow in the dark chemoheterotrophic in the presence of oxygen or perform an anoxygenic photosynthesis under light conditions, when oxygen is absent. For photoheterotrophic growth these bacteria contain specialized membranes (20) called intracytoplasmic membranes (ICM) or in isolated form, chromatophores, which contain all the essential proteins required for photoinduced cyclic electron transport (25). The minimal photosynthetic unit (PSU) is thought to consist of a reaction centre complex (RC) enclosed by a light-harvesting complex (LH1). The minimal PSU is also called the RC-LH1 core complex. Additionally, some species contain an LH2 complex surrounding the RC-LH1 core. Light absorbed by the LH complexes is transferred to the RC, where a charge separation in the so-called special pair occurs ($P \rightarrow P^+$), which is used to reduce ubiquinone to ubiquinol ($UQ \rightarrow UQH_2$). Ubiquinol in turn diffuses through the membrane to the cytochrome bc_1 complex, which oxidises ubiquinol and reduces the mobile carrier cytochrome c_2, which is then able to rereduce the RC, thereby completing the reactions of cyclic electron transport. The transfer of protons across the ICM from the cytoplasm to the periplasm, induces a proton motive force, which is used by the ATPase to generate ATP. Biosynthesis of the ICM is highly regulated by a signal transduction network which respond to oxygen pressure and light intensities (for a review (56)). Because oxygen acts as the main signal for the induction of PSA expression, ICMs are produced even in the dark, when the oxygen pressure drops under a certain threshold (1). This makes these organisms well suited for creation of mutations in photosynthesis proteins and analysis of photosynthetic deficient strains. The heterotrimeric RC is composed of an L and M subunits, each composed of 5 transmembrane α-helices, which bind the pigments needed for the primary photosynthetic process of charge separation (16, 17) and the H subunit, composed of a single transmembrane α-helix and a large cytoplasmic domain. The LH1 complex of *R. rubrum* was shown to consists of 16 α/β-heterodimers, which form a ring around the RC (31, 33). From the first high resolution structures available for the RC from *Blastochloris viridis* (formerly *Rhodopseudomonas viridis*) (17), *Rhodobacter sphaeroides* (3, 4) and *Thermochromatium tepidum* (39) no function could be assigned to the H subunit. However, deletion studies of the H subunit in *Rb. sphaeroides* (46), *Rb. capsulatus* (54) and *R. rubrum* (12, 38) have indicated the requirement of the H subunit for the assembly of a functional RC. It was also shown by our group, that the observed reduction of LH1 and ICM in the *puhA* deletion strains of *R. rubrum* could be

overcome by cultivation with modified medium (38). Biochemical studies have indicated that the H subunit was involved in the protonation of UQ (15, 29, 48). This finding was confirmed by the high resolution structures of various RC crystals in different redox states (47). Amino acid sequence analysis and mainly structure comparison of available X-ray structures revealed a modular nature of the H subunit (23). A recent study (50) consisted in swapping these identified domains between the species of *B. viridis* and *Rb. sphaeroides*. This study found following correlations between the H subunit domains and their function. Periplasmic domain mutations resulted in impairment of membrane localization of the H subunit. Swapping of the transmembrane domain reduced the amount of functional RC complexes and finally the cytoplasmic domain turned out to be also involved in the membrane accumulation of the H subunit. On the basis of their results this group proposed a new model for RC complex assembly.

In the present study we have adopted a different approach to that of Beatty and coworkers (50). Whereas the latter study simply exchanged the complete cytoplasmic domain immediately following the transmembrane α-helix, we attempted to define a putative LH1-binding domain from elementary considerations and experimental observations as to the nature of the RC-LH1 interaction.

We show, that both, a modified H subunit containing an extended linker between the two putative cytoplasmic subdomains, and the separated, but co-expressed domains, retained the function of the native H subunit, thus restoring photosynthetic capability to the *puhA* deletion strain SPUHK1 (38). However, we also show that SPUHK1 containing plasmids encoding only one domain, either the transmembrane (TM) or the cytoplasmic (CY) domain is unable to grow photosynthetically even though small but significant amounts of functional RC are still expressed.

MATERIALS AND METHODS

Growth of bacteria. Bacterial strains and plasmids are listed in Table 1. *Escherichia coli* cultures were grown in Luria-Bertani medium (43) at 37°C. Antibiotics were added as required at the following concentrations: Na-ampicillin 100 µg/ml; kanamycin sulfate 50 µg/ml and tetracycline-HCl 10 µg/ml. *R. rubrum* strains were grown at 30°C in either Sistrom minimal medium A (M-medium, containing K-succinate (20 mM) and added glutamic acid (0.7 mM) and aspartic acid (0.3 mM)) as described previously (45) with antibiotics added as required in the following concentrations: kanamycin sulfate, 20 µg/ml; and tetracycline-HCl, 4 µg/ml or in M2SF (M-medium with following modifications, 40 mM NH_4^+-succinate (replaces K-succinate), 40 mM Na-phosphate and 20 mM HEPES, containing additionally 0.3 % (16.7 mM) fructose) (26).

Cultures were cultivated phototrophically in closed bottles (Pyrex) using M-medium at 30°C. *R. rubrum* was grown chemoheterotrophically in the dark in 250 ml baffled Erlenmeyer flasks in M2SF medium (100 ml) at 30°C, shaking at 150 rpm (Lab-Therm, 2 cm throw, Adolf Kühner Inc. Basel). For growth kinetics study under semiaerobic conditions flasks were incubated in an Incubator Shaker Model G25 (Brunswick Scientific Co. Inc., Edison New Jersey, USA); under anaerobic conditions serum bottles were employed.
For anaerobic, photoheterotrophic growth on M-agar plates an anaerobic jar (Oxoid) was employed under a controlled CO_2/H_2 atmosphere (GasPack from Oxoid no. BR 038B).

Molecular biological techniques. Production of ssDNA was performed by infecting *E.coli* XL1MRF' cells with the VCS-M13 helper phage (Stratagene). Plasmid DNA or ssDNA were isolated using kits from Qiagen, Eppendorf or Roche and cloned by standard procedures (43). Restriction enzymes were obtained from New England Biolabs and agarose for gel electrophoresis of DNA was obtained from Pharmacia Amersham.

Site-directed mutagenesis of the *puhA* gene. Our mutagenesis strategy (Fig. 3) involved a separation of the putative TM and CY domain by inserting a BamHI-NdeI linker at position 102 (see below) and an NcoI site at the ATG start codon of the *puhA*-TM domain. The NcoI present in the wild-type G115 was deleted (without changing the reading frame of the truncated ORF of *G115*) prior to mutagenesis of the *puhA* (TM) start codon (Table 2). For the construction of a *puhA*-containing vector where the TM and CY domains are expressed as a

two-gene cistron, a three step mutagenesis protocol was employed using the Transformer Site-Directed Mutagenesis Kit (Clontech), except that the strain *E. coli* Top10/MutS (A. Prilipov, unpublished data) was employed for amplification of mismatched hybrid plasmids. All mutagenesis steps were performed with pBsSKII(+)-derived plasmids. First, two codons were changed to modify Glu102 and Pro103 to Gly102 and Ser103, respectively creating a BamHI restriction site (Fig. 3a) and yielding plasmid pBsSLΔGNPNB. Insertion of the NdeI restriction site caused the insertion of amino acids His and Met at position 104 and 105, respectively, to yield plasmid pBsSLΔGNPNBNd. Finally insertion of a BamHI-NdeI linker containing a ribosomal binding site (RBS) adopted from the natural RBS present in the native *puhA* gene, which contains a RBS-ATG spacer of 10 basepairs (7), yielded plasmid pBsSLPuhDM. The BamHI-NdeI linker also encoded XhoI and XbaI sites (Fig. 3b) to facilitate subsequent cloning steps with the individual domains. Plasmids expressing only the puhTM or puhCY domains were constructed from pBsSLPuhDM by digestion with XhoI/BstEII or NcoI/BamHI, respectively, and then religating the restricted plasmid, to yield pBsSLPuhTM and pBsSLPuhCY, respectively (Fig. 3b). Finally, all resulting mutations were confirmed by sequence analysis.

Complementation of mutants. All derivatives of the *puhA* gene obtained from the site-directed mutagenesis were cloned as blunt-ended *Hin*dIII-*Eco*RI fragments into the broad-host-range vector pRK404 (19, 44) at the blunt-ended *Bam*HI site to yield the plasmids listed in Table 1. These plasmids were transferred separately either to *R. rubrum* S1 or to the *R. rubrum puhA*-deletion mutants (38) by triparental conjugation with *E. coli* RR28 (30), using the helper plasmid pRK2013 (24) contained in *E.coli* RR28, applying the filter-mating technique (53).

Isolation of chromatophores (intracytoplasmic membranes, ICM). The chromatophore preparation was performed as described previously (38). Finally, chromatophores were resuspended in 2 ml of 20 mM TrisHCl pH 8.0, frozen in liquid nitrogen and stored at – 85°C.

Absorption spectra. The absorption spectrum of intact cells as well as of chromatophores was measured using 2 mm path-length cuvettes in a Jasco V-560 UV/VIS spectrophotometer, equipped with a photodiode detector for turbid samples. Intact cells were measured after suspension in M-medium containing 80% glycerol. For the absorption measurements equal

amounts of cells and chromatophores were employed by adjusting the concentrations to yield the same absorption at λ = 660 nm (turbidity) or at λ = 280 nm (protein amount).

Photobleaching of RC. Photobleaching of the RC was measured by comparing the spectra measured before and after illumination with a halogen light source. For each sample the procedure was repeated to confirm reversible bleaching of the RC. Equal amounts A_{880nm}(2mm) = 0.6 of isolated chromatophores were suspended in 0.5 ml 20 mM TrisHCl pH 8.0 and absorption spectrum measured between 780-900 nm.

SDS-polyacrylamide gel electrophoresis (SDS-PAGE). SDS-PAGE was performed according to the method of Laemmli (36) using 12.5% acrylamide gels. In general, samples (20µg protein) were precipitated by the addition of 3 vol of methanol before solubilizing in SDS-PAGE sample buffer. This step is effective in reducing the BChl and lipid content of the sample, which can affect the final gel resolution. The gels were stained with Coomassie Brillant Blue R250 (Pharmacia). Heme staining was performed according to Goodhew *et al.* (27), and protein determination by the modified Lowry method of Peterson (41) using bovine serum albumin as standard.

Chaotropic treatment of chromatophores. Chromatophores were treated by a modified procedure employed previously (15) to deplete the H subunit from detergent-solubilized purified RCs. 2mg of chromatophores in 20 mM TrisHCl pH 8.0 were mixed to a final volume of 2 ml containing the chaotropic reagent (0,75 M Lithium-perchlorate ($LiClO_4$) and 50 mM $CaCl_2$) After 30 min incubation at room temperature the samples were centrifuged at 100 000 × g for 1 h at 4°C. The pellet was resuspended in 1 ml 20 mM TrisHCl pH 8.0 and potter homogenised and the supernatant was concentrated to a final volume of 200 µl by ultrafiltration with Nanosep spin tubes (Pall Filtron).

Near-infrared (Near-IR) fluorescence images. Near-IR fluorescence images were recorded at room temperature as decribed (55) using a Grundig model 873 digital CCD camera and a Wratten 87C gelatin filter from Kodak.

Homology modeling of the L, M and H chain. Amino acid sequence alignments for the RC sequences of the L and M chains were performed using the program ClustalX (51). The protein sequences from *R. rubrum* (6, 7) and the structures of *Rb. sphaeroides* (47), *T.*

tepidum (39) and *Blc. viridis* (37) were incorporated in the alignments. All the homology-modeling steps for the L, M and H chain were carried out with the program Modeller included in the InsightII package (InsightII (2000) Modeller Package, Molecular Simulations Inc., Burlington, Mass). The structure of *T. tepidum* (39) was employed as a template following the generation of the preliminary *R. rubrum* RC model. The sequence is more similar to the *R. rubrum* sequence than the *Rb. sphaeroides* sequence. Superimposition of the structures from *T. tepidum* (39), *Rb. sphaeroides* (47) and *Blc. viridis* (37) in InsightII yielded the same structurally conserved regions as before.

The subunits were assembled using the program Psfgen included in NAMD2 (32). The assembly procedure resulted in several “bad” contacts between the H subunit and the cytoplasmic site of the L and M chain. The “bad“ contact sites were fixed using the Builder Module and for minimization the Discover Module of InsightII. Two different approaches were employed. The first approach was employed when two loop regions interacted with each other in an inappropriate way. By changing the torsion angles at the edges of the “bad” contact loop the loop was rotated that it can move freely during the following minimization. The second approach was employed when long side chains such as those from arginine or glutamic acid are trapped within the protein structure. By mutating that residue to glycine the loops carrying this residue could move apart during minimization. The remutation to the initial residue always resulted in a structure with no steric hindrance, which was then subjected to another round of minimization. Hydrogen atoms were added to the resulting structure consisting of L, M and H and the resulting protein complex was subjected to 4 000 steps of minimization in NAMD2 (32) using the CHARMM22 force field (9). Refinement of the model was carried out using the program NAMD2 (32). Due to the empirical approach of loop generation described above the newly generated loops needed to be refined in order to exclude energy traps in the model. This refinement was carried out by a 10 ps simulated annealing run of the loops. The backbone and the side-chains of the structurally conserved regions were fixed during this run. The simulated annealing run included a heat-up phase from 300 K to 500 K and a cool-down phase from 500 K to 300 K. The temperature was changed in intervals of 50 K each interval lasting 1 ps. The refined protein complex was subjected to 4 000 steps of minimization in NAMD2 (32) using the CHARMM22 force field (9). A more detailed procedure and analysis of the RC model will be presented elsewhere.

Finally, the cofactors were added to the refined protein model: 4 bacteriochlorophylls (BChla), 2 bacteriopheophytins (BPh), 2 ubiquinones (UQ), 1 *cis*-carotenoid (sphaeroidene) and 1 iron ion (FERR). We used here *cis*-spheroidene from the RC of *Rb. sphaeroides* (21) as only these coordinates were available. The coordinates and the arrangement of the pigments were employed from the 2.2 Å RC structure of *Rb. sphaeroides* (47). For BChla and BPh, the CHARMM22 force field for photosynthetic pigments developed by Damjanović (14) was employed. The phytyl chain of the topology file was modified to *all-trans*-geranylgeraniol *R. rubrum* BChla (34). Force field parameters for spheroidene and ubiquinone were assigned with the program QUANTA (MSI QUANTA 4.0. (1994) Molecular Simulations Inc., Burlington, Mass). The parameters for iron are included in the standard CHARMM22 force field for protein and lipids (9). Hydrogen atoms were added to the cofactors using the program X-PLOR (10). The cofactors were placed into the refined homology model of *R. rubrum* using Psfgen (32). The Mg atom of each individual BChla has been coordinated with M-His217, M-His 264, L-His190 and L-His230 according to Allen *et al.* (3). The final RC model converged within 4 000 minimization steps using NAMD2 (32) and the CHARMM22 force field (9).

RESULTS

Design principles of the H subunit as deduced from homology modeling. The final model for the H subunit of the RC of *R. rubrum* (Fig. 1) shows the same basic domain structure observable in the X-ray structures of the H subunits from *Rb. sphaeroides* (22), *Blc. viridis* (18) and *T. tepidum* (39). In particular, the transmembrane (TM) α-helix, which interacts with the M-subunit of the RC, and a large cytoplasmic (CY) domain, containing a single long α-helix (shown in yellow and cyan in Fig. 1), which interacts with the L- and M-subunits at the cytoplasmic surface, as well as a β-barrel. The H subunit β-barrel domain has recently been designated the PRC-fold (5).

In this study we have attempted to define the H-domain structure responsible for interaction with the LH1 ring by the following strategy. A number of experimental observations help to define the nature of the RC-LH1 interaction: (1) it is known that the H subunit is stably associated with the RC in detergent and cannot be removed by high salt concentrations alone (15, 52), implying that the H-RC interaction is principally hydrophobic. All of the X-ray structures show the hydrophobic but poorly conserved TM α-helix to be tightly bound to L and M, but also to have very low B-values, consistent with limited mobility; (2) the RC can be quite specifically removed from the LH1 ring *in situ* by extraction with the zwitterionic detergent LDAO (52), but not so easily by neutral detergents, implying that charge interactions (affected by the zwitterionic head-group of LDAO) may be important for RC-LH1 interactions; (3) site-directed deletion of the L and M-subunits does not affect the localization of the H subunit to the LH1 ring in the isolated complex (K. Kittelmann and R. Ghosh, unpublished data), suggesting that a major RC interaction site is at the H subunit; (4) all of the studies reported so far (46, 54, 12) show that in minimal media, the levels of the LH1 subunit are much more profoundly affected by the presence of the H subunit than are observed for L- or M- or LM-deletion mutants (35); (5) early crosslinking studies showed that only a H-LH1 proximity can be demonstrated (40). We believe that these experimental observations allow us to draw the conclusion that the H subunit must contain an LH1 interaction domain that is at least partially charged in character, implying an involvement of the CY domain.

Visual inspection of the CY domains of both the *R. rubrum* model and the available X-ray structures suggested that two subdomains are actually present (Fig. 1). One of these begins at

position Glu44, immediately following a highly charged C-terminal end of the TM domain (see Fig. 2). In the *R. rubrum* model this TM C-terminal sequence is RREDRRGYPL which is perfectly conserved with the sequences from both *Blc. viridis* and *T. tepidum*. The charged nature of this domain makes it a strong candidate for a H-LH1 interaction domain. Immediately following this sequence is a long rather flexible domain containing an outer loop region and a number of charged and polar residues extending to the outer surface of the H subunit. If the TM C-terminal sequence described above interacts with the LH1 complex, then a number of residues of this first CY subdomain (CY subdomain 1) must also play a role in H-LH1 interaction. Finally, the CY subdomain 1 (ending at Pro103) is followed by the PRC fold (here designated CY subdomain 2) described in (Anantharaman 2002). The two CY subdomains seem to be interacting only minimally suggesting that they might be functionally separated by molecular biological techniques. We therefore chose to introduce a stop codon at position 104, with the concomitant mutation of Pro103 to Gly. In the model, Pro103 seems only to participate in a loop joining the 2 CY domains and is thus a good candidate for a cleavage site.

Design of the *puhA*-(TM-CY) cistron. Separation of the H subunit into two macro-domains by keeping a minimal interference with respect to the amino acid sequence, was obtained by designing of new restriction enzyme sites, so that each domain could be expressed from its own start codon and possessing an own RBS and stop codon (Figure 3). Expression was regulated from the native promotor located between 200 and 400 base pairs upstream of the start codon (7, 8). Starting with plasmid pBsSLGP (38) a *Bam*HI and an *Nde*I site were inserted into *puhA* at codon Glu102/Pro103 (Fig. 3a) after deleting the unique *Nco*I site in G115 and creating a *Nco*I site at the *puhA* start codon. Intermediate constructs with the mutagenesis primer used are listed in Table 2. Creation of an *Nco*I site at the start codon of *puhA* resulted in the exchange of Asn to Asp. The creation of *Bam*HI and the insertion of *Nde*I at GluH102/ProH103 changed the amino acid composition to Gly/Ser and His/Met, respectively. Finally, the synthetic linker sequence (Fig. 3b) was inserted into plasmid pBsSLGNPNBNd, which was double digested with *Bam*HI and *Nde*I, to obtain plasmid pBsSLGNPNBNdL. The linker separates the two domains by introducing a stop codon for the TM domain and an RBS upstream from the start codon of CY. As *G115* expression was shown to cause a 10 h lag phase when cells were grown under semi-aerobic conditions (38) all plasmids were depleted of *G115* by excision of a 751 bp *Sph*I-*Eco*47III fragment prior to subcloning the blunt-ended *Hin*dIII-*Eco*RI fragment into the broad-host-range vector

pRK404. Further derivatives were made from pBsSLPuhDM. Plasmid pBsSLPuhTM, which possesses only the TM domain with the CY domain excised by *Xho*I-*Bst*EII digestion. Plasmid pBsSLPuhCY contains only the CY domain with the TM domain eliminated by *Nco*I-*Bam*HI treatment.

Complementation-Phenotyping and physiology of complemented strains. In a first experiment the complementing capability of all pRK404-derivatives constructed, was tested by transfering these plasmids into either S1-derived (SPUHK1 and SPUHK2) or G9-derived *puhA* deletion strains (GPUHK1 and GPUHK2) using triparental mating. Plasmids containing the intact (pRKLΔGP), mutated (pRKLΔGPNB, pRKLΔGPNBNd) or separated H subunit (pRKLPuhDM) could complement the strains to allow photosynthetic growth (Fig. 3).

For further analysis plasmids pRKLΔGP, pRKLPuhDM, pRKLPuhTM and pRKLPuhCY were transferred either to the wild-type *R. rubrum* S1 or its *puhA* deletion derivative SPUHK1.

Anaerobic incubation on M-agar showed that SPUHK1 (pRKLPuhDM) had a longer generation time and appeared less pigmented when compared to the wild-type containing the same plasmids or SPUHK1 (pRKLΔGP). Only after 6 to 8 weeks of incubation these cells reached the same pigmentation intensity as the wild-type. Growth kinetics study with anaerobic cultures confirmed this observation (Fig. 4D). However, in contrast to the cultivation on agar-plates growth began after a lag-phase of 20 days. The plasmid-containing strains showed an OD_{880}/OD_{660} ratio of about 70-92 % of the wild-type (Fig. 4E) indicating that the LH1 levels (Table 3) per cell were about the same as in the wild-type strain. The characteristic peaks at 760 nm and 802 nm due to the presence of the RC (Fig. 4F) were clearly visible for the S1 derivatives and SPUHK1 complemented with pRKLΔGP, reaching 91 % of the wild-type signal. Interestingly, SPUHK1 (pRKLPuhDM) showed the peak at 760 nm, whereas the expected peak at 802 nm was reduced, flattened and red-shifted to 805 nm. In SPUHK1 strains expressing solely the TM- or CY domains, growth under photosynthetic conditions was detected only after more than 2 months incubation and cells immediately reached the stationary phase. Further incubation did not result in increasing cell mass or pigmentation.

Growth kinetics study under semi-aerobic conditions in M2SF medium (Fig. 4A) showed for the S1 cells containing plasmids pRKLΔGP, pRKLPuhDM or pRKLPuhCY (data not shown) an increase of the generation time up to 2.5 h (Table 3) and for the pRKLPuhTM (not shown in Fig. 4) containing cells a slightly increased generation time (Table 3). In contrast to the S1 strains the SPUHK1 cells containing the plasmids pRKLPuhTM or pRKLPuhCY showed the same growth kinetics as SPUHK1 cells (not shown in Fig. 4), whereas complemented cells with plasmid pRKLΔGP or pRKLPuhDM showed increased generation times of 1 and 2 hours (Table 3). The LH1-Q_y absorption maxima (Fig. 4C) of the S1 strains were slightly decreased (Table 3) for the cells with pRKLΔGP or pRKLPuhDM and significantly increased (Table 3) for cells expressing only one domain on plasmid pRKLPuhTM or pRKLPuhCY, respectively (spectra not shown), in addition to the H subunit present on the genome. The SPUHK1 cells showed an inverted scenario, with the strains expressing an intact or separated H subunit (Fig. 4C) showing increased LH1 peaks (Table 3) compared to S1 or the parental strain SPUHK1, and slightly decreased for the cells expressing only the TM- or CY-domain (Table 3). As observed for the anaerobic cells the strains which were complemented to be photosynthetic showed also under these conditions the characteristic RC peaks with SPUHK1 (pRKLPuhDM) showing again the same features seen under phototrophic growth conditions (Fig. 4C). The SPUHK1 cells expressing only one domain, on plasmid pRKLPuhTM or pRKLPuhCY also showed a very weak RC signal, similar in shape to the SPUHK1 (pRKLPuhDM) cells (data not shown).

Near-IR fluorescence images were recorded for *R. rubrum* S1 and SPUHK1 cells containing plasmids pRKLΔGP, pRKLPuhDM, pRKLPuhTM or pRKLPuhCY incubated on plates either under anaerobic or aerobic conditions (Fig. 5). Under phototrophic conditions all S1 derivatives as well as SPUHK1 containing pRKLΔGP showed low fluorescence, whereas SPUHK1 with the complementing plasmid pRKLPuhDM showed a strong fluorescence. The weak fluorescence signal emitted by the SPUHK1 cells bearing pRKLPuhTM or pRKLPuhCY indicated that these cells grew under anaerobic conditions and thus must possess a functional RC.

Localization of the TM- and CY domains and characterization of isolated chromatophores. Cells of S1 and SPUHK1 with pRKLΔGP, pRKLPuhDM, pRKLPuhTM and pRKLPuhCY were grown in 500 ml M2SF medium under semi-aerobic conditions to induce the production of high levels of intracytoplasmic membranes and photosynthesis

proteins. But an alteration in the expression level, judged by the LH1-Q_y peak at 880 nm, could be observed for the S1 strains containing additional copies of *puhA* and for all SPUHK1 derivatives, when compared to the cells cultivated for the growth kinetics study. We attributed this effect to the flask form, which has one baffle for the one used for growth kinetics and four baffles for cell production, indicating a susceptibility of these strains to slightly increased pO_2-levels.

The different samples obtained during the isolation of chromatophores by cell fractionation were analysed both by absorption spectroscopy and by SDS-PAGE. The fraction containing the WSP showed for all strains the same spectroscopic features as the wild-type spectrum (data not shown). Isolated chromatophores from S1-derived cells containing additional copies of *puhA* on pRKLΔGP or the separated domains co-expressed in tandem on pRKLPuhDM showed decreased levels of LH1 compared to the wild-type grown under the same conditions (data not shown). Expression of only one domain did not alter the LH1-Q_y peak intensity. In comparison to the S1-derived strains, the SPUHK1-derived strains showed significantly reduced levels of LH1 complexes (Fig. 4). As seen for intact cells the RC signal was clearly visible for the SPUHK1 (pRKLΔGP), but altered for SPUHK1 (pRKLPuhDM) and only rudimentary for the chromatophores isolated from the SPUHK1 carying either pRKLPuhTM or pRKLPuhCY. In order to confirm the presence of a functional RC the activity of the special pair at 870 nm was measured by photobleaching (Table 4). The SPUHK1 strains carrying pRKLPuhTM and pRKLPuhCY showed 31 % and 14 % of the wild-type RC, respectively.

SDS-PAGE analysis of the WSP fraction showed the same profile for all strains when compared to wild-type strain or SPUHK1 parental strain (data not shown), with the latter possessing an additional protein at 30 kDa attributed to the *npt* gene product (38). The CY domain expected to be located in this fraction for the strains containing pRKLPuhDM and especially for the pRKLPuhCY containing strains was undetectable.

SDS-PAGE analysis of isolated chromatophores (Fig. 6) from the S1-derived strains showed no alterations when compared to the wild-type profile, neither the CY- nor the TM-domains could be detected. The protein composition of SPUHK1(pRKLΔGP) was identical to the wild-type (Fig. 6), thus confirming the presence of an intact H subunit and the other RC polypeptides, which restored the photosynthetic phenotype. An additional protein of 19 kDa

appeared for SPUHK1(pRKLPuhDM), which is higher than the theoretical size of 16 kDa of the CY domain. In contrast, the TM domain 11 kDa in size could not be distinguished on the gel for this strain. The protein profiles of the SPUHK1 strains expressing only one domain showed no additional or overexpressed bands. The L and M subunits of the RC were present at very reduced levels.

As the CY domain was found associated with the membrane we performed a chaotropic treatment of isolated chromatophores from S1 and SPUHK1 carrying plasmids pRKLΔGP, pRKLPuhDM and pRKLPuhCY, by washing with 0.75 M $LiClO_4$. This procedure was modified from the protocol published previously by (15) for *in vitro* extraction of the H subunit. Absorption spectra were recorded for both the pellet and supernatant after treatment. While the spectra of the supernatants were identical for all strains showing mainly peaks attributable to cytochromes (data not shown), the spectra of the pellets showed two interesting results. The RC signal detected as a shoulder and red-shifted for the cells and for the isolated chromatophores from SPUHK1(pRKLPuhDM) appeared now firstly discrete, well defined and blue-shifted to 803 nm (Figure 7). SDS-PAGE analysis (Figure 7) of the pellet and supernatant obtained after the chaotropic treatment revealed the presence of the 19 kDa protein in the supernatant fraction from SPUHK1 containing pRKLPuhDM although pellet fraction also contained this protein.

DISCUSSION

In all the studies done so far (12, 38, 46, 54) deletion of the H subunit in *Rb. capsulatus*, *Rb. sphaeroides* and *R. rubrum*, resulted in the absence of a functional RC; thus underlining the structural requirement of this protein. In recent studies (2, 11, 47, 48) an additional role was assigned to the H subunit, being involved in the protonation of the Q_B, although the absence, by extracting the H subunit *in vitro* did not inhibit but only slow down this reaction (15, 29). Very recently, Beatty and coworkers (50) analysed the effects of domain swapping between *Rb. sphaeroides* and *Blc. viridis*. In our study we have performed the separation of the H subunit in a TM and CY domain and analysed the effects upon coexpression of the separated domains or expression of only one domain in either the wild-type *R. rubrum* S1 or the *puhA*-deletion strain SPUHK1.

Based on the molecular modelling of the RC from *R. rubrum* a hinge region was localized at codon 102/103, which was genetically modified. The construct pRKLΔGNPNBNd, which contains the newly designed and inserted restriction enzyme sites posses 4 non-native amino acids at this position. Interestingly, there were no detectable changes in the phenotype of complemented strain SPUHK1(pRKLΔGNPNBNd), when compared to the same strain containing pRKLΔGP (which expresses the native *puhA* gene). This indicates, that the putative hinge region tolerates significant changes, tending to confirm our model of the putative domain structure of the CY domain. Separated and co-expressed domains on plasmid pRKLPuhDM could complement the SPUHK1 strain, but photosynthetic growth was slowed. As this strain could nevertheless reach the same cell density and pigmentation of the wild-type, the increased generation time could be due to the reduced levels of RC observed from the absorption spectra, SDS-PAGE analysis and near-IR fluorescence images. SPUHK1 cells expressing only the TM or CY domain could also grow under phototrophic conditions. However, cell growth was detectable only after 2 months and further incubation did not increase cell density or pigmentation. This could be due to a reduced level of RC with impaired functionality. Cell fractionation analysis revealed that, in contrast to our expectations, that the CY domain would appear in the water-soluble fraction (as an highly expressed protein), we found it only in very low amounts in the membrane fraction of the pRKLPuhDM containing SPUHK1 strain. Although expression from the pRK-plasmids is under the control of the native *puhA* promotor and the broad-host-range vector is present in multiple copies in the cells (6 copies per cell (42)), the SDS-PAGE analysis of

SPUHK1(pRKLPuhCY) did not show the CY domain in either the ultracentrifugal supernatant or pellet fractions. We were also unable to localise the TM protein with its theoretical molar mass of 11 kDa on the SDS gel. These findings are in agreement with those of Beatty et al (49, 50), who found the H subunit to be absent in the soluble fraction. In contrast, they found high levels of the M and L subunits in the soluble fraction, although each contains 5 transmembrane helices and should be more hydrophobic than the H subunit. These findings could suggest, that the H subunit must be effectively inserted into the membrane otherwise it will be degraded. This could explain the small CY amounts found for the SPUHK1(pRKLPuhDM) cells, which could be due to interaction with the TM domain, thus anchoring the CY domain to the membrane, and the complete absence of CY in S1 or SPUHK1 expressing pRKLPuhCY. The dynamics of interaction of the coexpressed domains resulted in lowered amounts of functional RC, which showed altered spectroscopic characteristics. While the peak at 760 nm due to BPha of the RC was unaffected, the peak at 802 nm due to the accessory BChla molecules was red-shifted by 3 nm and appeared to be decreased. Quantification of the special pair using photobleaching resulted in 86% of the wild-type amount. As a consequence the SPUHK1 cells expressing plasmid pRKLPuhDM showed a longer generation time and a 20 days lag-phase under phototrophic cultivation. Interestingly, the chaotropic extraction of the CY domain from the chromatophores isolated from SPUHK1(pRKLPuhDM) resulted in a blue-shifted absorption maximum of the accessory BChla in the RC, which appeared now increased when compared to untreated chromatophores. The increased amounts of RC found in SPUHK1 cells expressing only the TM (31%) or CY (14%) domain when compared to parental strain SPUHK1 (6%), although undetectable by SDS-PAGE, could be explained suggesting an interaction with the L and M subunits. In contrast to the parental strain SPUHK1, cells containing a single domain were capable of photosynthetic growth. But the long time period until growth was detectable and the premature reaching of the stationary phase was not only due to a reduced RC content but resulted from an impaired RC function. This implicates that both domains carry amino acids which are required for the photosynthetic RC to be functional.

An interesting observation, which we are currently unable to explain, was that transfer of pRK plasmids carrying only one domain (pRKLPuhTM or pRKLPuhCY) in the wild-type strain S1 resulted in higher amounts of LH1 than the parental strain. This was also true for the SPUHK1 strain containing the pRK plasmid with either the intact *puhA* gene (pRKLΔGPuhA) or the separated and coexpressed domains (pRKLPuhDM), as judged from the LH1-Q_y peak

of total cells measured by absorption spectroscopy during growth kinetic experiments under semi-aerobic conditions in M2SF medium. Based on the results obtained for the H subunit deletion strains (38), which were shown to express wild-type levels of LH1 using the M2SF medium, and also based upon an analysis of the metabolic processes leading to a defined redox state of the cells in M2SF (28), it is intriguing to speculate, that overexpression of intact, separated or only single domains of the H subunit in the different genetic backgrounds (*puhA*$^{+}$/*puhA*$^{-}$) influences the LH1 expression by acting on a regulatory way in the redox state.

The susceptibility of the SPUHK1 strains containing pRKLΔGPuhA, pRKLPuhDM, pRKLPuhTM and pRKLPuhCY encountered during cultivation under large scale conditions and showing lesser amounts of LH1 will be the subject of a future study.

In this study, we not only established and confirmed the validity of a deletion/ complementation system for studying H subunit function in *R. rubrum*, in analogy to the work of Chen *et al.* (11), but have also extended this system to be suitable for studying the functional role of the domains of the H subunit. We believe that our study underlines the fact that the functional role of the H subunit has been poorly studied so far, as many of the observations above are unexpected and difficult to explain, thus making it in interesting object of future studies.

ACKNOWLEDGMENTS

We would like to thank Prof. Dr. Andreas Kuhn for providing sequencing facilities. We acknowledge the Landesgraduiertenförderung Baden-Württemberg (grant no. 7631.2) for financial assistance and the Deutsche Forschungsgemeinschaft (grant no. WR28/13-1) for financial assistance.

REFERENCES

1. Aargard, J., & Sistrom, W. R. **(**1972) Control of synthesis of reaction center bacteriochlorophyll in photosynthetic bacteria. *Photochem. Photobiol.* **15,** 209-225.
2. Abresch, E. C., Paddock M. L., Stowell, M. H. B., McPhillips, T. M., Axelrod, H. L., Soltis, S. M., Rees, D. C., Okamura, M. Y. & Feher, G. (1998) Identification of proton transfer pathways in the X-ray crystal structure of the bacterial reaction center from *Rhodobacter sphaeroides*. *Photosyn. Res.* **55,** 119-125.
3. Allen, J. P., Feher, G., Yeates, T. O., Komiya, H. & Rees, D. C. (1987) Structure of the reaction center from *Rhodobacter sphaeroides* R-26: the protein subunits. *Proc. Natl. Acad. Sci. U S A* **84,** 6162-6166.
4. Allen, J. P., Feher, G., Yeates, T. O., Rees, D. C., Deisenhofer, J., Michel, H. & Huber, R. (1986) Structural homology of reaction centers from *Rhodopseudomonas sphaeroides* and *Rhodopseudomonas viridis* as determined by x-ray diffraction. *Proc. Natl. Acad. Sci. U S A* **83,** 8589-93.
5. Anantharaman, V. & Aravind, L. (2002) The PRC-barrel: A widespread, conserved domain shared by photosynthetic reaction center subunits and proteins of RNA metabolism. *Genome Biol.* **3,** 0061.1-0061.9.
6. Belanger, G., Berard, J., Corriveau, P. & Gingras, G. (1988) The structural genes coding for the L and M subunits of Rhodospirillum rubrum photoreaction center. *J. Biol. Chem.* 263, 7632-7638.
7. Bérard, J. & Gingrás, G. **(**1990) The *puh* structural gene coding for the H subunit of *Rhodospirillum rubrum* photoreaction center. *Biochem. Cell Biol.* **69,** 122-131.
8. Bérard, J., Bélanger, G. & Gingrás, G. (1989) Mapping of the *puh* messenger RNAs from *Rhodospirillum rubrum* - evidence for tandem promoters. *J. Biol. Chem.* **265,** 10897-10903.
9. Brooks, B. R., Bruccoleri, R. E., Olafson, B. D., States, D. J., Swaminathan, S. & Karplus, M. (1983) CHARMM: a program for macromolecular energy, minimization, and dynamics calculations. *J. Comp. Chem.* **4,** 187-217.
10. Brünger, A. T. (1996) X-PLOR, Version 3.8: A System for X-ray Crystallography and NMR. (Yale University Press, New Haven).
11. Chen, X.-Y., Yurkov, V., Paddock, M. L., Okamura, M. Y. & Beatty, J. T. (1998) A *puhA* gene deletion and plasmid complementation system for facile site directed

mutagenesis studies of the reaction center H protein of *Rhodobacter sphaeroides*. *Photosyn. Res.* **55,** 369-373.

12. Cheng, Y. S., Brantner, C. A., Tsapin, A. & Collins, M. L. P. 2000. Role of the H protein in assembly of the photochemical reaction center and intracytoplasmic membrane in *Rhodospirillum rubrum*. *J. Bacteriol.* **182,** 1200-1207.
13. Cohen-Bazire, G., Sistrom, W. R. & Stanier, R. Y. (1956) Kinetic studies of pigment synthesis by non-sulfur purple bacteria. *J. Cell. Comp. Physiol.* **49,** 25–68.
14. Damjanović, A., Kosztin, I., Kleinekathoefer, U. & Schulten, K. (2002) Excitons in a photosynthetic light-harvesting system: A combined molecular dynamics, quantum chemistry and polaron model study. *Physical Review E* **65,** 031919.
15. Debus, R. J., Feher, G. & Okamura, M. Y . (1985) LM Complex of reaction centers from *Rhodopseudomonas sphaeroides* **R-26*:*** Characterization and reconstitution with the H subunit. *Biochemistry* **24,** 2488-2500.
16. Deisenhofer, J., Epp, O., Miki, K., Huber, R. & Michel, H. (1984) X-Ray structure analysis of a membrane protein complex: electron density map at 3 Å resolution and a model of the chromophores of the photosynthetic reaction center from *Rhodopseudomonas viridis*. *J. Mol. Biol.* **180,** 385–398.
17. Deisenhofer, J., Epp, O., Miki, K., Huber, R. & Michel, H. (1985) Structure of the protein subunits in the photosynthetic reaction centre of *Rhodopseudomonas viridis* at 3 Å resolution. *Nature* **318,** 618-624.
18. Deisenhofer, J., Epp, O., Sinning, I. & Michel, H. (1995) Crystallographic refinement at 2.3 Å resolution and refined model of the photosynthetic reaction centre from *Rhodopseudomonas viridis*. *J. Mol. Biol.* **246,** 429-457.
19. Ditta, G., Schmidhauser, T., Yakobson, E., Lu, P., Liang, X.-W., Finlay, D. R., Guiney, D. & Helinski, D. R. (1985) Plasmids related to the broad host range vector, pRK290, useful for gene cloning and for monitoring gene expression. *Plasmid* **13,** 149–153.
20. Drews, G. **(**1978) Structure and development of the membrane system of photosynthetic bacteria. *Curr. Top. In Bioenergetics* **8B,** 161-207.
21. Ducruix, A. & Reiss-Husson, F. (1987) Primary characterization by X-ray diffraction of crystals of photochemical reaction centers from wild-type *Rhodopseudomonas sphaeroides*. *J. Mol. Biol.* **193,** 419-421.

22. Ermler, U., Fritzsch, G., Buchanan, S. K.& Michel, H. (1994) Structure of the photosynthetic reaction centre from *Rhodobacter sphaeroides* at 2.65 A resolution: cofactors and protein-cofactor interactions. *Structure* **2,** 925-936.
23. Fathir, I., Mori, T., Nogi, T., Kobayashi, M., Miki, K. & Nozawa, T. (2001) Structure of the H subunit of the photosynthetic reaction center from the thermophilic purple sulfur bacterium, *Thermochromatium tepidum*. Implications for the specific binding of the lipid molecule to the membrane protein complex. *Eur. J. Biochem.* **268,** 2652-7.
24. Figurski, D. H. & Helinski, D. R. (1979) Replication of an origin-containing derivative of plasmid RK2 dependent on a plasmid function provided *in trans*. *Proc. Natl. Acad. Sci. USA* **76,** 1648-1652.
25. Ghosh, R. & Bachofen, R. (1989) Die molekulare Struktur der photosynthetischen Membranen bei anoxygenen phototrophen Bakterien. *Forum Mikrobiologie* **12,** 556-564.
26. Ghosh, R., Hardmeyer, A., Thoenen, I. & Bachofen, R. (1994) Optimization of the Sistrom culture medium for large-scale batch cultivation of *Rhodospirillum rubrum* under semi-aerobic conditions with maximal yield of photosynthetic membranes. *Appl. Environ. Microbiol.* **60,** 1698-1700.
27. Goodhew, C. F., Brown, K. R. & Pettigrew, G. W. (1986) Haem staining in gels, a useful tool in the study of bacterial *c*-type cytochromes. *Biochim. Biopys. Acta* **852,** 288-294.
28. Grammel, H., Gilles, E. D. & Ghosh, R. (2003) Microaerophilic cooperation of reductive and oxidative pathways allows maximal photosynthetic membrane biosynthesis in *Rhodospirillum rubrum*. *Appl. Environ. Microbiol.* **69,** 6577-6586.
29. Hara, M., Kaneko, T., Nakamura, C., Asada, Y. & Miyake, J. (1998) Redox properties of an H-subunit-depleted photosynthetic reaction center from *Rhodopseudomonas viridis*. *Biochim Biophys Acta* **1363,** 199-208.
30. Hennecke, H., Günther, I. & Binder, F. (1982) A novel cloning vector for the direct selection of recombinant DNA in *E. coli*. *Gene* **19,** 231-234.
31. Jamieson, S. J., Wang, P., Quian, P., Kirkland, J. Y., Conroy, M. J., Hunter, C. N. & Bullough, P. A. (2002) Projection structure of the photosynthetic reaction centre-antenna complex of *Rhodospirillum rubrum* at 8.5 Å resolution. *EMBO J.* **21,** 3927-3935.

32. Kalé, L., Skeel, R., Bhandarkar, M., Brunner, R., Gursoy, A., Krawetz, N., Phillips, J., Shinozaki, A., Varadarajan, K. & Schulten, K. (1999) NAMD2: Greater scalability for parallel molecular dynamics. *J. Comp. Phys.***151,** 283-312.
33. Karrasch, S., Bullough, P. A. & Ghosh, R. (1995) The 8.5 Å projection map of the light-harvesting complex I from *Rhodospirillum rubrum* reveals a ring composed of 16 subunits. *EMBO J.* **14,** 631-638.
34. Katz, J. J., Strain, H. H., A. Harkness, L., Studier, M. H., Svec, W. A., Janson, T. R. & Cope B. T. (1972) Esterifying alcohols in the chlorophylls of purple photosynthetic bacteria. A new chlorophyll, bacteriochlorophyll (gg), all-trans-geranylgeranyl bacteriochlorophyllide a. *J. Am. Chem. Soc.* 94, 7938-7939.
35. Klug, G. & Cohen S. N. (1988) Pleiotropic effects of localized *Rhodobacter capsulatus puf* operon deletions on production of light-absorbing pigment-protein complexes. *J. Bacteriol.* **170,** 5814-21.
36. Laemmli, U. K. (1970) Cleavage of structural proteins during the assembly of the head of bacteriophage T4. *Nature* **227,** 680-685.
37. Lancaster, C. R. & Michel, H. (1997) The coupling of light-induced electron transfer and proton uptake as derived from crystal structures of reaction centres from *Rhodopseudomonas viridis* modified at the binding site of the secondary quinone, Q_B. *Structure* **5,** 1339-1359.
38. Lupo, D. & Ghosh, R. (2004) The reaction center H subunit is not required for high levels of light-harvesting complex 1 in *Rhodospirillum rubrum* mutants. *J. Bacteriol.* **186,** 5585-5595.
39. Nogi, T., Fathir, I., Kobayashi, M., Nozawa, T. & Miki, K. (2000) Crystal structures of photosynthetic reaction center and high-potential iron-sulfur protein from *Thermochromatium tepidum*: Thermostability and electron transfer. *Proc. Natl. Acad. Sci. U S A* **97,** 13561-13566.
40. Peters, J., Takemoto, J. & Drews, G. (1983) Spatial relationships between the photochemical reaction center and the light-harvesting complexes in the membrane of *Rhodopseudomonas capsulata*. *Biochemistry* **22,** 5660-5667.
41. Peterson, G. L. (1977) A simplification of the protein assay method of Lowry *et al.* which is more generally applicable. *Anal. Biochem.* **83,** 346-356.
42. Saegesser, R. (1992) Identifikation und Charakterisierung des Photosynthese - Genclusters aus *Rhodospirillum rubrum*. Ph.D. thesis. University of Zurich, Switzerland.

43. Sambrook, J., Fritsch, E. F. & Maniatis, T. (1989) Molecular Cloning: a laboratory manual, 2nd ed. Cold Spring Harbor Laboratory Press. Cold Spring Harbor, N.Y.
44. Scott, H. N., Laible, P. D. & Hanson, D. K. (2003) Sequences of versatile broad-host-range vectors of the RK2 family. *Plasmid* **50,** 74-79.
45. Sistrom, W. R. **(**1960) A requirement for sodium in the growth of *Rhodopseudomonas sphaeroides*. *J. Gen. Microbiol.* **22,** 778-785.
46. Sockett, R. E., Donohue, T. J., Varga, A. R. & Kaplan, S. (1989) Control of photosynthetic membrane assembly in *Rhodobacter sphaeroides* mediated by *puhA* and flanking sequences. *J. Bacteriol.* **171,** 436-446.
47. Stowell, M. H. B., McPhillips, T. M., Rees, D. C., Soltis, S. M., Abresch, E. & Feher, G. (1997) Light induced structural changes and the mechanism of electron/proton transfer in the photosynthetic reaction center. *Science* **276,** 812–816.
48. Takahashi, E. & Wraight, C. A. (1996) Potentiation of proton transfer function by electrostatic interactions in photosynthetic reaction centers from Rhodobacter sphaeroides: First results from site-directed mutation of the H subunit. *Proc. Natl. Acad. Sci. U S A* **93,** 2640-5.
49. Tehrani, A. & Beatty, J. T. (2004) Effects of precise deletions in *Rhodobacter sphaeroides* reaction center genes on steady-state levels of reaction center proteins: a revised model for reaction center assembly. *Photosyn. Res.* **79,** 101-108.
50. Tehrani, A., Prince, R. C. & Beatty, J. T. (2003) Effects of photosynthetic reaction center H protein domain mutations on photosynthetic properties and reaction center assembly in *Rhodobacter sphaeroides*. *Biochemistry* **42,** 8919-8928.
51. Thompson, J. D., Gibson, T. J., Plewniak, F., Jeanmougin, F. & Higgins, D. G. (1997) The ClustalX windows interface: flexible strategies for multiple sequence alignment aided by quality analysis tools. *Nucleic Acids Research* **25,** 4876-4882.
52. Vadeboncoeur, C., Mamet-Bratley, M., & Gingras, G. (1979) Photoreaction center of photosynthetic bacteria. 2. Size and quaternary structure of the photoreaction centers from Rhodospirillum rubrum strain G9 and from Rhodopseudomonas sphaeroides strain 2.4.1. *Biochemistry.* **18,** 4308-4314.
53. Willetts, N. **(**1984) Conjugation. *Meth. Microbiol.* **17,** 33-59.
54. Wong, D. K.-H., Collins, W. J., Harmer, A., Lilburn, T. G. & Beatty, J. T. (1996) Directed mutagenesis of the *Rhodobacter capsulatus puhA* gene and *orf214*: pleiotropic effects on photosynthetic reaction center and light-harvesting 1 complexes. *J. Bacteriol.* **178,** 2334-2342.

55. Youvan, D. C., Hearst, J. E. & Marrs, B. L. (1983) Isolation and characterisation of enhanced fluorescence mutants of *Rhodopseudomonas capsulata*. *J. Bacteriol.* **154,** 748-755.
56. Zeilstra-Ryalls, J. H. & Kaplan, S. (2004) Oxygen intervention in the regulation of gene expression: the photosynthetic bacterial paradigm. *Cell. Mol. Life Sci.* **61,** 417-436.

FIGURE LEGENDS

Figure 1: Schematic representation of putative RC-LH1 interaction domains. The model of the H subunit from *R. rubrum* and the H subunits from the crystal structures of *Blc. viridis* (22), *T. tepidum* (39) and *Rb. sphaeroides* (18) are shown schematically. The two CY subdomains are indicated. Color code: red, TM domain; blue, highly conserved sequence; yellow, long α-helix; cyan, highly conserved sequence. Center: the model of the RC from *R. rubrum* is represented showing the interaction of the H subunit domains with the L and M subunits depicted space-filled in grey and white, respectively.

Figure 2: Sequence alignment of RC-H subunits using ClustalX. Amino acid sequences of the RC-H proteins from *R. rubrum* (RHORU), *Blc. viridis* (BLCVI), *T. tepidum* (THETE), *Rb. sphaeroides* (RHOSH) and *Rb. capsulatus* (RHOCA) were aligned using ClustalX. The shadowed and red-boxed amino acids represent the TM domain ending at Pro103 (numbering according to the H subunit sequence). The transmembrane α-helix is boxed in black and the highly conserved motif adjacent to this helix is boxed in blue. Amino acid sequence forming the long α-helix in the cytoplasmic domain is boxed in yellow, with the highly conserved charged amino acids boxed in cyan.

Figure 3: Construction of *puhA* derivatives for the separation and coexpression of the TM (red) and CY (green) domains. Left (a) the three step mutagenic strategy for separating the TM and CY domains is indicated (closed boxes indicate modified or altered amino acids at the TM-CY interface). The final DNA sequence containing the Shine-Dalgarno ribosomal binding side (RBS) immediately preceding the ATG start codon of CY is indicated; and the resulting ORFs are shown in (b). Also indicated in (b) are the constructions for the expression of the TM and CY domains singly. The plasmid designation of the constructs are indicated at the right-hand-side of (a) and (b). (Right) The growth phenotype under photosynthetic cultivation of the complementing plasmids above are indicated, as well as the presence of RC or LH1 under these conditions. (+++) indicates wild-type growth. Abbreviations: *H*, *Hin*dIII; *Nc*, *Nco*I; *S*, *Sal*I; *Bt*, *Bst*EII; RI, *Eco*RI; *B*, *Bam*HI; *Nd*, *Nde*I; *Xh*, *Xho*I; *Xb*, *Xba*I. A scale bar is shown and restriction enzyme sites, which were blunt-ended are shown in parentheses.

Figure 4: Growth kinetics (A-B, D-E) and absorption (C, F) spectra of *R. rubrum* cells grown either semi-aerobically or photosynthetically. Cells of *R. rubrum* S1 (pink ●), SPUHK1 (blue □), S1 (pRKLΔGP) (orange ▲), S1(pRKLPuhDM) (red ◆), SPUHK1 (pRKLΔGP) (violet ⬡) and SPUHK1(pRKLPuhDM) (darkblue ▽) are indicated. The growth kinetics have been followed by either OD_{660} (cell turbidity at 660 nm) or by the ratio OD_{880}/OD_{660} which reflects the amount of photosynthetic membranes (LH1-Q_y absoprtion peak at 880 nm) per cell.

Figure 5: Near-IR-fluorescence-images of *R. rubrum* (S1 and SPUHK1) cells cultivated phototrophically containing the complemented plasmids pRKLΔGP (ΔGP), pRKLPuhDM (PuhDM), pRKLPuhTM (PuhTM), pRKLPuhCY (PuhCY).

Figure 6: SDS-PAGE analysis (upper panel) and absorption spectra (lower panel) of isolated chromatophores obtained from S1 and SPUHK1 strains containing plasmids (see Fig. 5 for plasmid abbreviations). Each lane contains 20 µg protein and the gel was stained with Coomassie Brilliant Blue R250. The arrow indicates a 19 kDa protein, probably corresponding to the the CY domain. The lower panel shows the absorption spectra of isolated chromatophores obtained from SPUHK1 complemented with the plasmids pRKLΔGP (-·-), pRKLPuhDM (···), pRKLPuhTM (–) and pRKLPuhCY (---). Equal amounts of proteins were employed for the spectra.

Figure 7: Chaotropic treatment of isolated chromatophores obtained from S1 and SPUHK1 strains containing the plasmids indicated (abbreviations as in Fig. 5) after treatment with 0.75 M $LiClO_4$ and subsequent ultracentrifugation. The ultracentrifuged pellets (left lanes) and supernatants (right lanes) obtained were loaded onto the gel. The gel was stained initially for heme containing proteins (indicated by white circles) and then with Coomassie Brilliant Blue R250. The arrow indicates the 19 kDa protein (indicated also in Fig. 6). Lower panel (A) shows an expanded region between 750 nm and 850 nm of the absorption spectra of SPUHK1 (pRKLPuhDM) chromatophores (inset) before (solid line) and after the chaotropic treatment (dashed line). Panel (B) shows the difference spectrum obtained for the same region after chaotropic treatment. ΔA is calculated as Abs (after $LiClO_4$) – Abs (before $LiClO_4$).

FIGURES

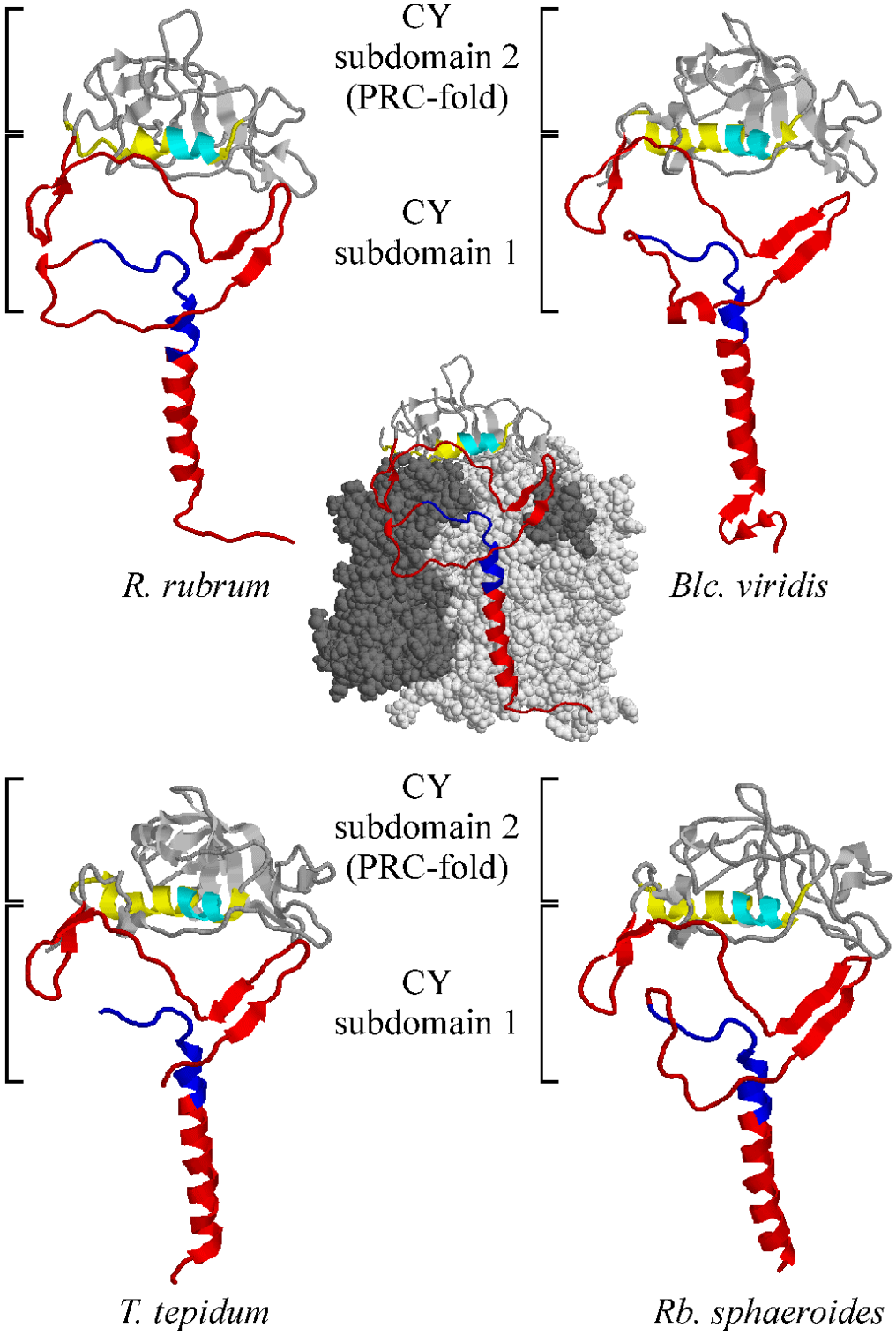

Figure 1

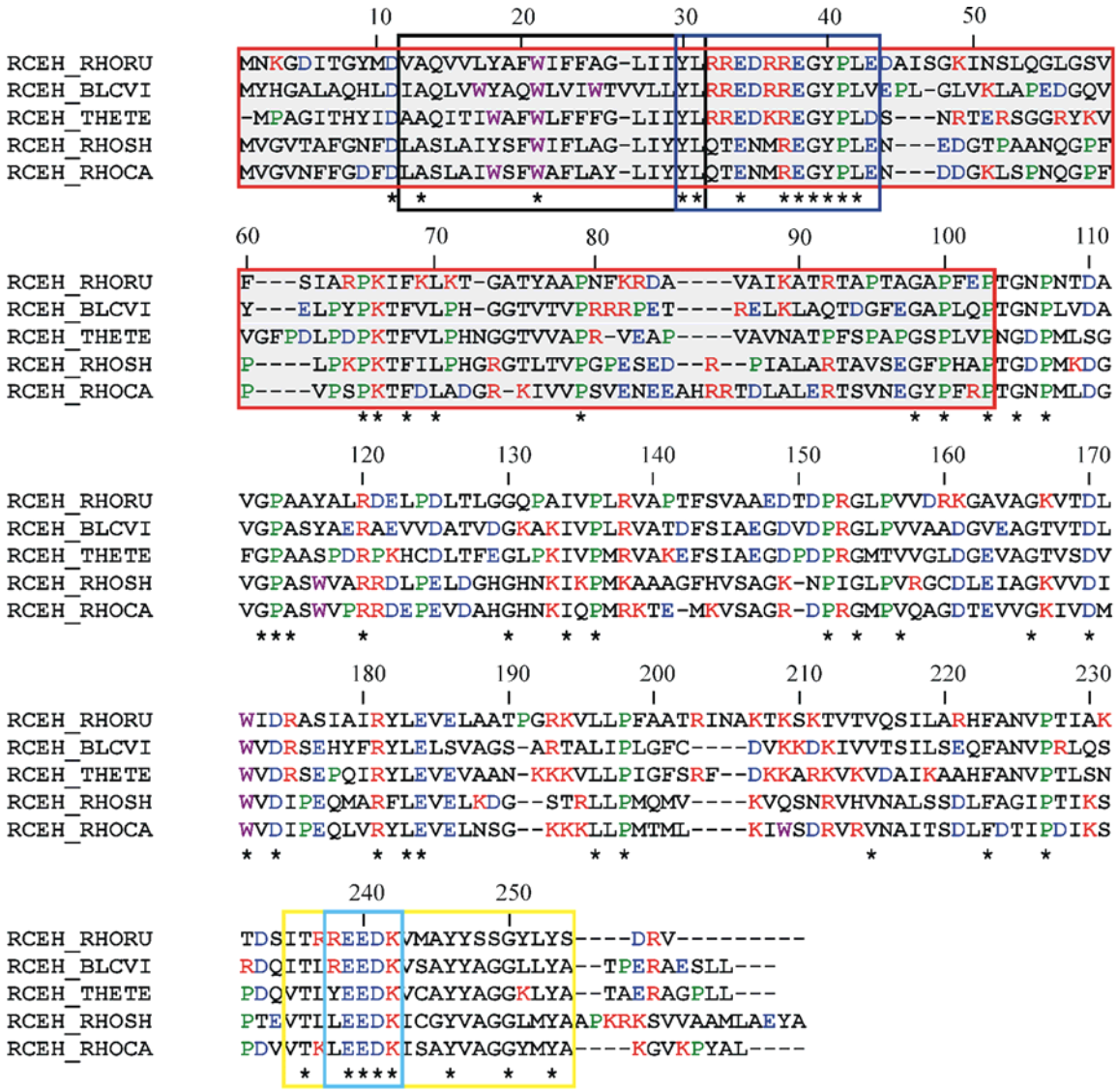
10 20 30 40 50
RCEH_RHORU MNKGDITGYMDVAQVVLYAFWIFFAG-LIIYLRREDRREGYPLEDAISGKINSLQGLGSV
RCEH_BLCVI MYHGALAQHLDIAQLVWYAQWLVIWTVVLLYLRREDRREGYPLVEPL-GLVKLAPEDGQV
RCEH_THETE -MPAGITHYIDAAQITIWAFWLFFFG-LIIYLRREDKREGYPLDS---NRTERSGGRYKV
RCEH_RHOSH MVGVTAFGNFDLASLAIYSFWIFLAG-LIYYLQTENMREGYPLEN---EDGTPAANQGPF
RCEH_RHOCA MVGVNFFGDFDLASLAIWSFWAFLAY-LIYYLQTENMREGYPLEN---DDGKLSPNQGPF
60 70 80 90 100 110
RCEH_RHORU F---SIARPKIFKLKT-GATYAAPNFKRDA----VAIKATRTAPTAGAPFEPTGNPNTDA
RCEH_BLCVI Y---ELPYPKTFVLPH-GGTVTVPRRRPET----RELKLAQTDGFEGAPLQPTGNPLVDA
RCEH_THETE VGFPDLPDPKTFVLPHNGGTVVAPR-VEAP----VAVNATPFSPAPGSPLVPNGDPMLSG
RCEH_RHOSH P----LPKPKTFILPHGRGTLTVPGPESED--R--PIALARTAVSEGFPHAPTGDPMKDG
RCEH_RHOCA P----VPSPKTFDLADGR-KIVVPSVENEEAHRRTDLALERTSVNEGYPFRPTGNPMLDG
120 130 140 150 160 170
RCEH_RHORU VGPAAYALRDELPDLTLGGQPAIVPLRVAPTFSVAAEDTDPRGLPVVDRKGAVAGKVTDL
RCEH_BLCVI VGPASYAERAEVVDATVDGKAKIVPLRVATDFSIAEGDVDPRGLPVVAADGVEAGTVTDL
RCEH_THETE FGPAASPDRPKHCDLTFEGLPKIVPMRVAKEFSIAEGDPDPRGMTVVGLDGEVAGTVSDV
RCEH_RHOSH VGPASWVARRDLPELDGHGHNKIKPMKAAAGFHVSAGK-NPIGLPVRGCDLEIAGKVVDI
RCEH_RHOCA VGPASWVPRRDEPEVDAHGHNKIQPMRKTE-MKVSAGR-DPRGMPVQAGDTEVVGKIVDM
180 190 200 210 220 230
RCEH_RHORU WIDRASIAIRYLEVELAATPGRKVLLPFAATRINAKTKSKTVTVQSILARHFANVPTIAK
RCEH_BLCVI WVDRSEHYFRYLELSVAGS-ARTALIPLGFC----DVKKDKIVVTSILSEQFANVPRLQS
RCEH_THETE WVDRSEPQIRYLEVEVAAN-KKKVLLPIGFSRF--DKKARKVKVDAIKAAHFANVPTLSN
RCEH_RHOSH WVDIPEQMARFLEVELKDG--STRLLPMQMV----KVQSNRVHVNALSSDLFAGIPTIKS
RCEH_RHOCA WVDIPEQLVRYLEVELNSG--KKKLLPMTML----KIWSDRVRVNAITSDLFDTIPDIKS
240 250
RCEH_RHORU TDSITRREEDKVMAYYSSGYLYS----DRV---------
RCEH_BLCVI RDQITIREEDKVSAYYAGGLLYA--TPERAESLL---
RCEH_THETE PDQVTIYEEDKVCAYYAGGKLYA--TAERAGPLL---
RCEH_RHOSH PTEVTILEEDKICGYVAGGLMYAAPKRKSVVAAMLAEYA
RCEH_RHOCA PDVVTKLEEDKISAYVAGGYMYA----KGVKPYAL----

Figure 2

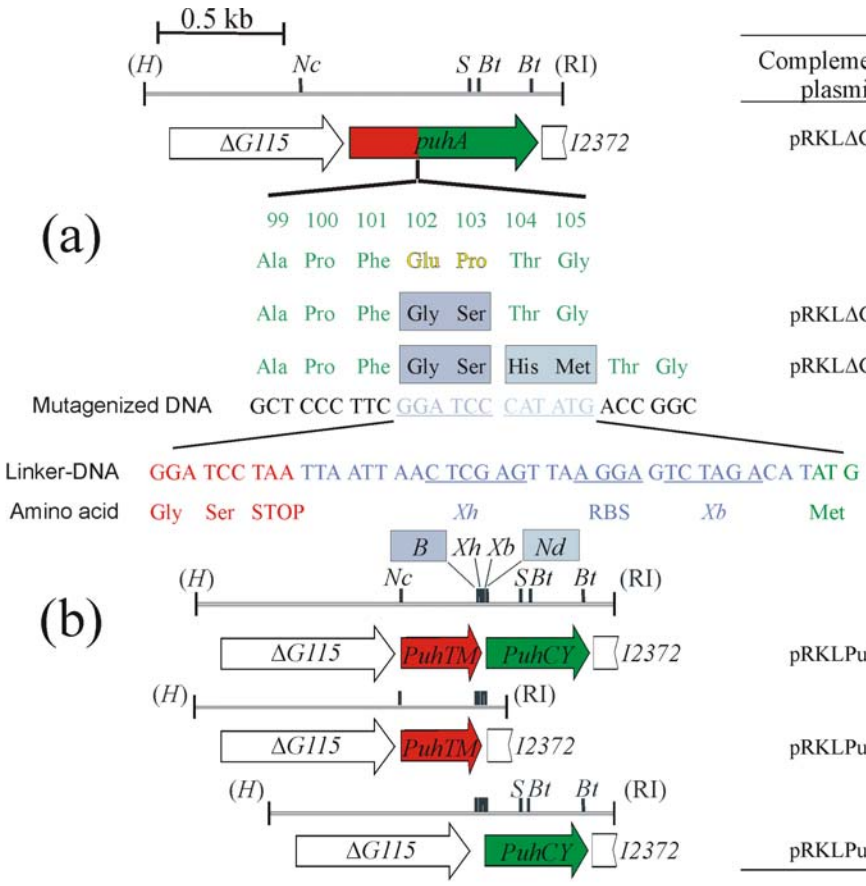

Complementing plasmid	PS Phenotype growth	RC	LH1
pRKLΔGP	+++	+++	+++
pRKLΔGNPNB	+++	+++	+++
pRKLΔGNPNBNd	+++	+++	+++
pRKLPuhDM	++	++	++
pRKLPuhTM1	(+)	(+)	(+)
pRKLPuhCY1	(+)	(+)	(+)

Figure 3

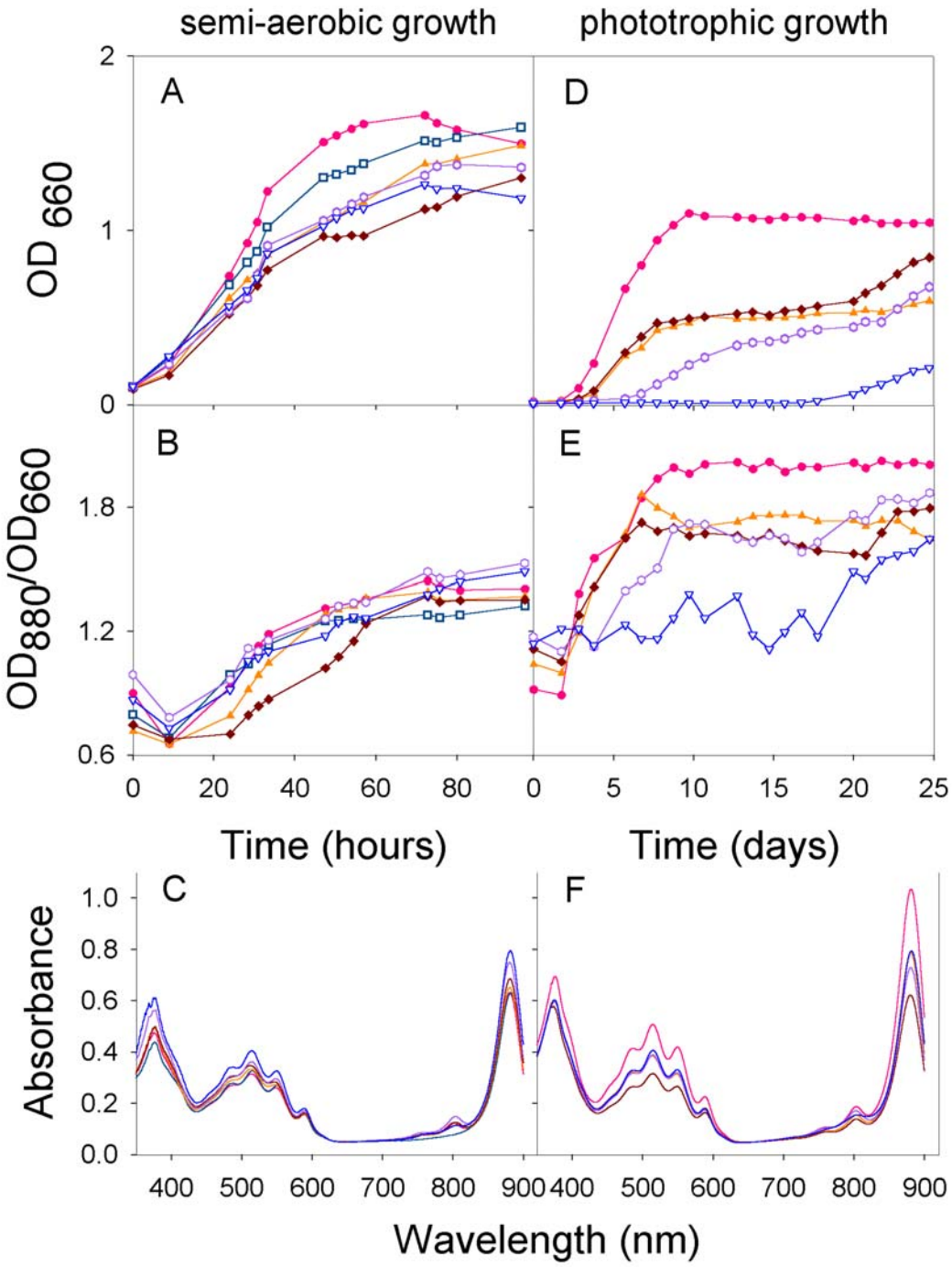
semi-aerobic growth
phototrophic growth
A
D
B
E
C
F
OD 660
OD880/OD660
Time (hours)
Time (days)
Absorbance
Wavelength (nm)

Figure 4

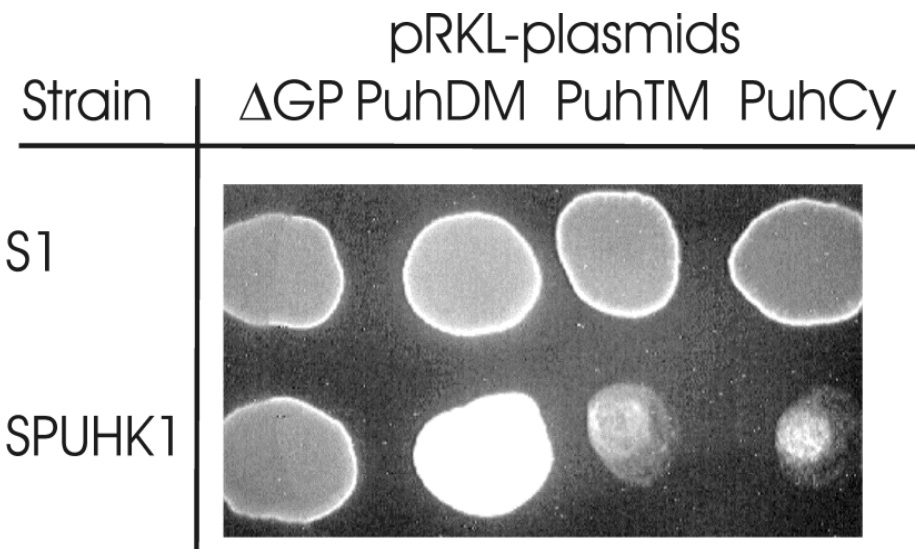

Figure 5

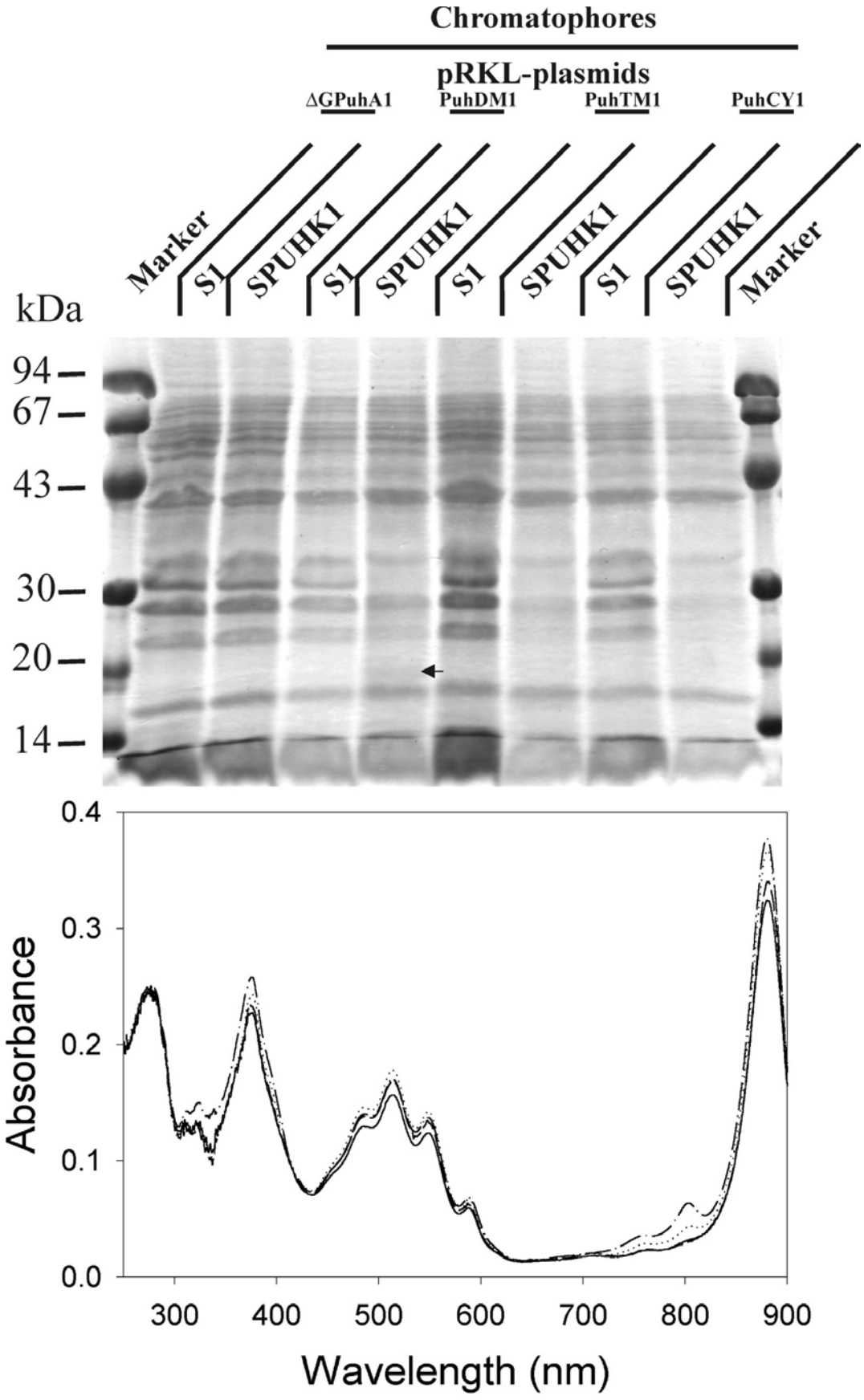
Chromatophores
pRKL-plasmids
ΔGPuhA1
PuhDM1
PuhTM1
PuhCY1
Marker
S1
SPUHK1
S1
SPUHK1
S1
SPUHK1
S1
SPUHK1
Marker
kDa
94
67
43
30
20
14
Absorbance
0.4
0.3
0.2
0.1
0.0
300
400
500
600
700
800
900
Wavelength (nm)

Figure 6

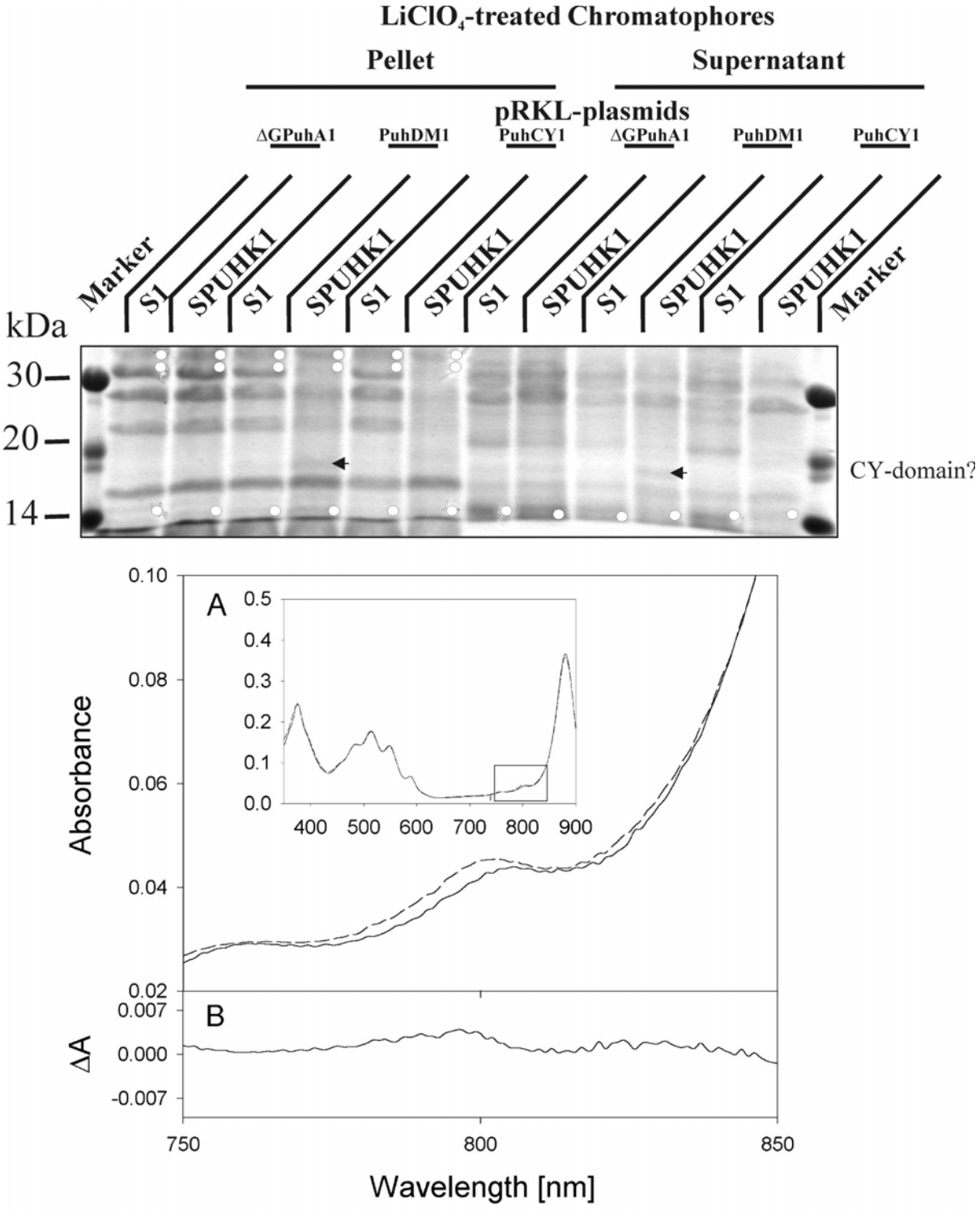
LiClO4-treated Chromatophores
Pellet
Supernatant
pRKL-plasmids
ΔGPuhA1
PuhDM1
PuhCY1
ΔGPuhA1
PuhDM1
PuhCY1
Marker
S1
SPUHK1
S1
SPUHK1
S1
SPUHK1
S1
SPUHK1
S1
SPUHK1
S1
SPUHK1
Marker
kDa
30
20
14
CY-domain?
A
B
Absorbance
ΔA
Wavelength [nm]

Figure 7

TABLES

TABLE 1. Strains and plasmids used in this study

Strain or plasmid	Relevant characteristics	Reference or source
E. coli strains		
Top10/MutS	F$^-$, *mcr*A Δ(*mrr-hsd*RMS-*mcr*BC) ϕ80*lac*ZΔM15 Δ*lac*X74 *rec*A1 *ara*D139 *gal*U *gal*K Δ(*ara-leu*)7697 *rps*L *end*A1 *nup*G (Str^R) *mut*S, (Tet^r)	unpublished
RR28	Strain used for cloning routines, RecA$^-$ derivative of RR1	30
XL1MR	Δ(*mcrA*)183 Δ(*mcrCB-hsdSMR*-mrn)173 *endA1 supE44 thi-1 recA1 gyrA96 relA1 lac*	Stratagene
XL1MRF'	Derivative of XL1MR [F' *pro*AB *lac*I^{q}ZΔM15 Tn10 (Tet^r)]	Stratagene
R. rubrum strains		
S1	Wildtype	13
SPUHK1	S1-derived *puhA*-interposon mutant, *npt* in the same transcriptional orientation as the *puhA*-operon, PS$^-$ Kan^r	38
SPUHK2	S1-derived *puhA*-interposon mutant, *npt* in the reverse transcriptional orientation as the *puhA*-operon, PS$^-$ Kan^r	38
GPUHK1	G9-derived *puhA*-interposon mutant, *npt* in the same transcriptional orientation as the *puhA*-operon, PS$^-$ Kan^r	38
GPUHK2	G9-derived *puhA*-interposon mutant, *npt* in the reverse transcriptional orientation as the *puhA*-operon, PS$^-$ Kan^r	38
Plasmids		
pBsSKII+	High copy cloning vector, ColE1 Amp^r	Stratagene
pBsSKΔBaXh	Derivative of pBsSKII+ with *Bam*HI and *Xho*I sites deleted	This study
pRK404	Derivative of pRK290, *mob*$^+$ Tet^r	19
pRK2013	Mobilizing helper plasmid, *tra*$^+$ Kan^r	24
pBsSLGP	*G115-puhA* subcloned into pBsSKII+	38
pBsSLΔGP	Δ*G115-puhA* subcloned into pBsSKII+	38
pBsSLΔGNP	Derivative of pBsSLΔGP with *Nco*I site in G115 deleted	This study
pBsSLΔGNPN	Derivative of pBsSLΔGNP with *Nco*I site at *puhA* start codon	This study
pBsSLΔGNPNB	Derivative of pBsSLΔGNPN with *Bam*HI site at codon 102 of *puhA*	This study
pBsSLΔGNPNBNd	Derivative of pBsSLΔGNPNB with *Nde*I site insertion 3' next to the *Bam*HI site.	This study
pBsSLPuhDM	*Hin*dIII-*Eco*RI fragment of pBsSLΔGNPNBNd subcloned into pBsSKΔBaXh, with synthetic linker sequence inserted	This study
pBsSLPuhTM	Derivative of pBsSLPuhDM with the CY domain excised as blunt-ended *Xho*I-*Bst*EII fragment	This study
pBsSLPuhCY	Derivative of pBsSLPuhDM with the TM domain excised as blunt-ended *Nco*I-*Bam*HI fragment	This study
pRKLGP	*G115-puhA* subcloned into pRK404 as blunt-ended *Hin*dIII-*Eco*RI fragment	38

pRKLΔGP	Δ*G115-puhA* subcloned into pRK404 as blunt-ended *Hin*dIII-*Eco*RI fragment	38
pRKLΔGNP	(*Hin*dIII)-(*Eco*RI) fragment into pRK404	This study
pRKLΔGNPN	(*Hin*dIII)-(*Eco*RI) fragment into pRK404	This study
pRKLΔGNPNB	(*Hin*dIII)-(*Eco*RI) fragment into pRK404	This study
pRKLΔGNPNBNd	(*Hin*dIII)-(*Eco*RI) fragment into pRK404	This study
pRKLPuhDM1	(*Hin*dIII)-(*Eco*RI) fragment into pRK404	This study
pRKLPuhTM1	(*Hin*dIII)-(*Eco*RI) fragment into pRK404	This study
pRKLPuhCY1	(*Hin*dIII)-(*Eco*RI) fragment into pRK404	This study

TABLE 2. Site-directed mutagenesis

Mutagenesis oligo	Mutation	Plasmid
5'-GGC GGC CCA CGG CCT GCT CG	CAT→ CAC deletion of *Nco*I site in G115, but His422 conserved	pBsSLΔGNP pRKLΔGNP
5'-GGA GGC CTT CCC ATG GAT AAA GGC GAC	CTC ATG AAT→ CCC ATG GAT creation of an NcoI site in *puhA*, AsnH2 to AspH2 exchange	pBsSLΔGNPN pRKLΔGNPN
5'-CCG CCG GCG CTC CCT TCG GAT CCA CCG GCA ACC CGA TGA CC	GAG CCC→GGA TCC creation of a *Bam*HI site, GluH102 to Gly and ProH103 to Ser exchange	pBsSLΔGNPNB pRKLΔGNPNB
5'-GCC GGC GCT CCC TTC GGA TCC CAT ATG ACC GGC AAC CCG ATG ACC GAC	CAT ATG insertion→creation of an *Nde*I site, insertion of His and Met	pBsSLΔGNPNBNd pRKLΔGNPNBNd

TABLE 3. Generation times and LH1-Q_y amounts.

Strain	Plasmid	Anaerobic		Semiaerobic	
		t_g [d]	A_{880nm} % WT	t_g [h]	A_{880nm} % WT
S1	none	1.78	100	8.5	100
SPUHK1		n.d.	n.d.	9.8	99.95
S1	pRKLΔGP	2.36	75.5	10.4	96
SPUHK1		4	69.9	10.9	108.4
S1	pRKLPuhDM1	2.57	59.4	11	95.2
SPUHK1		5.4	76	11.8	106.8
S1	pRKLPuhTM1	n.d.	n.d.	9.6	114
SPUHK1		n.d.	n.d.	9.7	98
S1	pRKLPuhCY1	n.d.	n.d.	11	115
SPUHK1		n.d.	n.d.	9.8	93

TABLE 4. Amounts of photoactive RC.

Strain	Plasmid	% RC
S1	none	100
SPUHK1		6
SPUHK1	pRKLΔGP	102
	pRKLPuhDM1	86
	pRKLPuhTM1	31
	pRKLPuhCY1	14

EINZELMOLEKÜLSPEKTROSKOPIE DER PSU

The circular symmetry of the light-harvesting 1 complex from *Rhodospirillum rubrum* is not perturbed by interaction with the reaction center

TITLE FOOTNOTE. Financial support was provided by the Volkswagen Foundation within the Priority Area "Physics, Chemistry and Biology with Single Molecules" and the Landesgraduiertenförderung Baden-Württemberg.

Uwe Gerken‡, Domenico Lupo§, Carsten Tietz‡, Jörg Wrachtrup‡ and Robin Ghosh§*

AUTHOR ADRESS. ‡Institute of Physics, University of Stuttgart, D-70550 Stuttgart, Germany

§Department of Bioenergetics, Institute of Biology, University of Stuttgart, D-70550 Stuttgart, Germany

*To whom correspondence should be addressed:

Tel. +49-711-685 5047; Fax +49-711-685 5096; email: robin.ghosh@bio.uni-stuttgart.de

RUNNING TITLE. Interaction of the reaction center with the LH1 complex.

Biochemistry; **2003;** *42*(35) pp 10354 - 10360; **Accelerated Publication**

DOI: 10.1021/bi034969m

ABBREVIATIONS

BChla, bacteriochlorophyll a, SM, single molecule; cryoEM, cryoelectronmicroscopy; LH, light-harvesting; RC, reaction center; PSU, photosynthetic unit; LDAO, lauryldimethylamine-N-oxide; DHPC, diheptanoyl-*sn*-phosphatidylcholine; DOPC, dioleoyl-*rac*-phosphatidyl-choline; CEO, collective electronic oscillator; ZPL, zero phonon line; PSB, phonon side band; AFM, atomic force microscopy.

ABSTRACT

The effect of the interaction of the reaction center (RC) upon the geometrical arrangement of the bacteriochlorophyll a (BChla) pigments in the light-harvesting complex 1 (LH1) from *Rhodospirillum rubrum* has been examined using single molecule spectroscopy. Fluorescence excitation spectra at 1.8 K obtained from single detergent-solubilized as well as single membrane-reconstituted LH1-RC complexes showed predominantly (>70%) a single broad absorption maximum at 880-900 nm corresponding to the Qy transition of the LH1 complex. This absorption band was independent of the polarization direction of the excitation light. The remaining complexes showed two mutually orthogonal absorption bands in the same wavelength region with moderate splittings in the range of ΔE = 30-85 cm^{-1}. Our observations are in agreement with simulated spectra of an array of 32 strongly coupled BChla dipoles arranged in perfect circular symmetry possessing only a diagonal disorder of 150 cm^{-1}. However, in contrast to LH1 complexes alone, excitation spectra which consists of a single absorption band were observed more frequently in the presence of the reaction center. Our results show that the interaction of the RC with the LH1 complex stabilizes the circular symmetric arrangement of the bacteriochlorophyll pigments, and are in contradiction to recent studies by other groups using single molecule spectroscopy as well as cryoelectronmicroscopy and atomic force microscopy indicating that the RC induces a elliptical distortion of the LH1 complex. Possible reasons for this discrepancy are discussed.

10.1021/bi034969m CCC: $25.00 © 2003 American Chemical Society Published on Web 08/14/2003

INTRODUCTION

The high efficiency of light-energy capture in photosynthetic purple bacteria is mediated by the membrane-bound light-harvesting (LH) complexes, designated LH1 and LH2. Both types of complexes are composed of two small (approx. 50 amino acids) non-identical polypeptides, α and β, which show significant homologies between species and bind the pigments bacterichlorophyll a (BChla) or BChlb and carotenoids (*1*). The absorption spectrum of the complexes is suited to their functional role *in vivo*. Thus, LH2 complexes show two strong absorption maxima in the near-IR region at 850 nm and 800 nm, respectively, and the LH1 complexes generally show a single absorption near-IR absorption maxima at 875-882 nm. As shown by spectroscopic studies (*2,3*) light energy can be passed preferentially from the LH2 to LH1 by radiationless energy transfer. The latter are then able to transfer energy to the reaction center (RC) which catalyzes the primary process. In recent years, the structure of the LH2 complexes for *Rhodopseudomonas acidophila* (*4*) and *Rhodospirillum molischianum* (*5*) have been elucidated at atomic resolution by X-ray crystallography. Both complexes are ring-like assemblies of the basic building block, the αβ heterodimer, arranged in a ring containing 9 and 8 αβ heterodimers for *Rps. acidophila* and *R. molischianum*, respectively. Each α and β polypeptide binds one BChla at a conserved histidine within the membrane bilayer, and the interaction between these pigments leads to the characteristic absorption maximum at 850 nm (*6*). A third, monomeric BChla, coordinated to the carboxyl group of a amino acid ligand present in the crystal structure and located close to the membrane surface, exhibits the absorption maximum at 800 nm (*6*).

The structure of the LH1 complex is not known at high resolution at the present time. However, medium-resolution projections at 0.85 nm have been obtained for 2D crystals of the LH1 complex from *Rhodospirillum rubrum* in the absence (*7*) and presence of the reaction center (*8*), both of which clearly show a ring-like symmetry of 32 transmembrane α-helices, assigned to α- and β –polypeptides, by analogy to the structural organization of the LH2 complexes. A membrane-bound conserved histidine on both polypeptide chains (homologous to those binding the B850- BChls of the LH2 complexes (1)) has been shown by both Raman spectroscopy (*9*) and by site-directed mutagenesis (*10*) to bind BChla. Biochemical analysis has shown that each αβ dimer of the LH1 complex binds two molecules of BChla and one molecule of carotenoid (spirilloxanthin in the wild-type *R. rubrum* S1) (*11,12*). In addition, detailed molecular modelling of the LH1 complexes of *Rhodobacter sphaeroides* (*13*) and *R.*

10.1021/bi034969m CCC: $25.00 © 2003 American Chemical Society Published on Web 08/14/2003

rubrum (*14*) using only the experimental pigment/αβ polypeptide stoichiometry and the assumption that $\alpha\beta(BChla)_2$ units are arranged in a ring with 16-fold symmetry showed rapid convergence to unique structures after energy minimization.

The observation of circular symmetry for both LH1 and LH2 complexes has been recently subjected to critical analysis by means of single molecule (SM) spectroscopy as well as by structural analysis using either cryoelectronmicroscopy (cryoEM) and atomic force microscopy (AFM). Single molecules of isolated LH2 complexes solubilized in detergent and immobilized in polyvinyl alcohol (PVA) spin-coated films have indicated they are not perfectly symmetrical but elliptically disordered (*15,16*). These results are of significance as they imply that the bulk near-IR spectra, for which a large body of spectral data exists (see (*17)*), are the sum of a large number of spectra arising from single LH complexes, each of which possesses shifted absorption maxima, which can be shifted by up to 116 cm-1 from the bulk absorption maxima. The shift of the near-IR absorption maxima is suggested to be due to static disorder of the pigments. These data also imply that the position of the pigments as obtained by X-ray crystallography (*4,5*) or modelling (*13,14*) is also the average of a number of statically disordered structures.

Recently, we have reexamined this question using SM spectroscopy of isolated LH1 complexes of the purple non-sulphur bacterium *R. rubrum* (*18*). Although our results also showed that detergent-solubilized LH1 complexes do indeed show a distribution of near-IR maxima about the bulk absorption maximum at 880 nm (at 1.8 K), the width of the distribution was significantly less than that observed for detergent-solubilized LH2 complexes (*18*). However, after reconstitution of the LH1 complexes into bilayer membranes, the fluorescence emission spectra show no preferential polarization, thus indicating unambiguously that the membrane environment maintains the LH1 complex in a circularly symmetric state, corresponding to the projection structure deduced from 2D crystals by cryoelectron microscopy (*7*). Very recently, Ketelaars *et al.* (*19*) have reported an SM study of detergent-solubilized LH1-RC complexes isolated from *Rps. acidophila* in which they show that a number of states with non-circular symmetry are present. In particular, they ordered the low temperature LH1 spectra into 4 classes (Types I to IV), where Type I (30% of the total) and Type II (17% of the total) were assigned to a circular symmetric and elliptically distorted exciton, respectively, Type III (17% of the total) was assigned to an “open” partial ring, and Type IV (36% of the total) was assigned to a dimeric LH1-RC aggregate. In this

10.1021/bi034969m CCC: $25.00 © 2003 American Chemical Society Published on Web 08/14/2003

previous study, the detergent lauryldimethylamine-N-oxide (LDAO) was employed as a solubilizing agent. They have argued that the interaction of the RC with the LH1 complex may stabilize a distortion of the LH1 ring, thus facilitating energy transfer to the RC *in vivo*. The results of SM spectroscopy in (*19*) are strikingly consistent with very recent structural studies of LH1-RC complexes using either cryoEM of 2D crystals (*8*) or AFM of natural membranes (*20*). In both of these studies (discussed in detail below) the LH1 rings showed an elliptical distortion with the major and minor axes differing by about 11% and 5 – 10%, respectively. In the AFM study it could also be shown that the removal of the RC *in situ*, caused the LH1 ring to revert to circular symmetry.

The present study, employing LH1-RC complexes purified with the detergent diheptanoyl-*sn*-phosphatidylcholine (DHPC) as detergent, which below a critical concentration, does not promote further dissociation of the LH1-RC complex to small subunits (*21*), contradicts these latter data. We show below that, in contrast to the conclusions drawn from the SM and structural studies mentioned above, even when solubilized in detergent (DHPC) the interaction of the RC with the LH1 *stabilizes* the circular symmetry of the latter complex, and when the LH1-RC complex is incorporated into lipid bilayers, these perfect circularly symmetric complexes are present almost exclusively. A rationale for this apparent contradiction will be presented.

10.1021/bi034969m CCC: $25.00 © 2003 American Chemical Society Published on Web 08/14/2003

MATERIALS AND METHODS

Preparation of phospholipids. 1,2-dioleoyl-*rac*-phosphatidylcholine (DOPC) was obtained from Avanti Polar Lipids (USA) or BACHEM (Switzerland). 100 mg DOPC dissolved in CHCl3 was dried under N2 as a thin film on to the surface of a round-bottomed flask. The film was then dried for 12 h under high vacuum ($\leq 10^{-3}$Torr) to remove all traces of solvent, and then suspended in 2 mL H2O by gentle shaking with glass beads. The suspension was then sonicated to translucency using a microtip probe (Branson) and aliquots taken from this homogeneous preparation for the phosphate determination, and the rest aliquoted into smaller volumes in Eppendorf tubes and frozen using liquid nitrogen, and then stored at –80°C. The phosphate determination, used for the calculation of the molar ratio below, was determined by the method of Ames and Dubin (*22*). The purity of the lipids was also routinely checked by thin-layer chromatography using silica gel plates and CHCl3/MeOH/H2O (80/30/4 (v/v/v)) as running solvent.

Isolation of the LH1-RC complexes. LH1-RC complexes were purified from isolated photosynthetic membranes of *R. rubrum* S1 (wild-type) with the exclusive use of the detergent DHPC (Avanti Polar Lipids, USA) as solubilizing agent as described previously (*21*). Reconstitution of the LH1-RC complexes into bilayer membranes comprised of (DOPC) at a LH1-RC/DOPC molar ratio of 1/4000 were also performed as described (*21*).

Sample preparation for SM spectroscopy. The detergent-solubilized complexes as well as the vesicles containing the LH1-RC complexes were immobilized (by spontaneous ionic interaction) onto a freshly cleaved mica (Goodfellow) surface. After preparation the samples were immediately transferred into the cryostat (Janis) and cooled down to 77 K within milliseconds and subsequently to 1.8 K.

Fluorescence Spectroscopy. All measurements were performed at 1.8 K with a home-built beam-scanning confocal microscope. Fluorescence excitation spectra from single LH1-RC complexes were obtained by positioning the focus of the microscope objective (Melles Griot) over a complex and subsequently stepwise scanning of the linearly polarized, continious wave excitation laser (Ti:Sa, Spectra Physics 3900-S) over the region of the $|k = \pm 1\rangle$ absorption bands. The fluorescence was detected at each step with an avalanche

10.1021/bi034969m CCC: $25.00 © 2003 American Chemical Society Published on Web 08/14/2003

photodiode (EG&G, SPCM) at wavelengths >905 nm. To determine a possible splitting of the excitonic states $|k = \pm 1\rangle$, a series of spectra in the range of 835 – 905 nm were recorded for each single complex, where the polarization direction of the excitation laser was turned by 30° between consecutive scans with a λ/2-waveplate. To improve the signal-to-noise ratio each scan was done twice and averaged afterwards.

For measuring fluorescence emission spectra the complexes were excited with the laser at 865 nm in their B880 absorption band. The fluorescence was recorded using a 30 cm-spectrograph (Acton Research SP-257) with a highly sensitive, liquid nitrogen-cooled back-illuminated CCD-camera (Princeton Instruments) as a detector.

10.1021/bi034969m CCC: $25.00 © 2003 American Chemical Society Published on Web 08/14/2003

RESULTS

Theory: Exciton Model of the B880 Ring. The exciton model of the B880 ring used here has been described in detail previously (18) and was used without modification. For brevity, however, we provide a shortened summary of the analysis used here again. The energy level diagram of the B880 ring consisting of 32 interacting BChla molecules, is calculated using the effective Hamiltonian for Frenkel excitons:

$$H = \sum_{i=1}^{32} E_0 |n\rangle\langle n| + \sum_{\substack{i=1 \\ m \neq n}}^{32} W_{mn} |m\rangle\langle n| \qquad (1)$$

where $|n\rangle$ is the product state of 32 two-level molecules where only one is in the excited state with energy E_0 and W_{mn} is the coupling strength among the states $|m\rangle$ and $\langle n|$. As the distances between all non-neighboring BChl*a* molecules are large enough to use the dipole-dipole approximation, the coupling strengths is :

$$W_{mn} = C_3 \left(\frac{\vec{d}_m \cdot \vec{d}_n}{r_{mn}^{\,3}} - \frac{3(\vec{r}_{mn} \cdot \vec{d}_m)(\vec{r}_{mn} \cdot \vec{d}_n)}{r_{mn}^{\,5}} \right) \qquad (2)$$

where $\vec{d}_n$ are the unit vectors of the BChla dipole moments and $\vec{r}_{mn}$ are the vectors connecting the Mg atoms of the BChla molecules. The unit vector $\vec{d}_n$, corresponds to the direction from the nitrogen atoms N_{21} to N_{23} (IUPAC nomenclature (*23*)) of the BChla tetrapyrrole ring, corresponding to the BChla Q_y transition dipole. The atomic positions were taken from the structural model for the LH1 complex of *R. rubrum* by Authenrieth *et al*. (*14*). The coupling strengths of the next but one pigments W_{13} were set to $W_{13} = -102\ \mathrm{cm}^{-1}$ leading to C_3 =415500 $\text{Å}^3\mathrm{cm}^{-1}$. This value for W_{13} was obtained previously (*18*) for the BChla molecules in the LH2 complex of *R. molischianum* using the collective electronic oscillator (CEO) approach (*24*). For the coupling strengths among the intra- and interdimeric pigments used here, the CEO calculations led to values of ν_1=363 cm^{-1} and ν_2=320 cm^{-1}, respectively. Due to the close sequence and structural homology of the apoproteins of LH2 and LH1, it is reasonable to suppose that the coupling strengths are comparable.

A calculated energy level spectrum is shown in Fig. 1A. All states except the lowest and the highest of both bands are 2-fold degenerate due to the circular arrangement of the pigments. For the case of perfect symmetry, the states $|k = \pm 1\rangle$ carry almost all of the oscillator strength

10.1021/bi034969m CCC: $25.00 © 2003 American Chemical Society Published on Web 08/14/2003

with orthogonal dipole moments, whereas the lowest state $|k=0\rangle$ carries no oscillator strength. Any disorder within the ring leads to a shift of the oscillator strength from $|k=\pm1\rangle$ to the other states, corresponding to a shift of the energy levels and thereby to a lifting of the degeneracies (Fig. 1B). Thus the introduction of ring disorder leads to a splitting (ΔE) of the fluorescence excitation maxima in the near-IR region. The splitting ΔE is also enhanced by a reduction of symmetry of the ring of BChla pigments, which in its simplest form could correspond to an elliptical deformation of the ring, thereby enhancing C_2-symmetry of the pigments (*15*). An elliptical deformation is usually characterized by the eccentricity ε:

$$\varepsilon = \sqrt{1-\left(\frac{b}{a}\right)^2} \qquad (3)$$

where a and b are the major and minor axes of the ellipse, respectively. The effect of diagonal disorder and ellipticity upon the energy states are shown for the three lowest energy levels ($|k=0\rangle$ and $|k=\pm1\rangle$, respectively) in Fig. 1C.

General considerations. For all SM experiments, the LH1-RC complexes were reconstituted into DOPC which has a phase transition temperature (T_m) at –20°C. The low T_m ensures that the bilayer membranes are maintained in the liquid-crystalline phase for all biochemical procedures, particularly reconstitution and the subsequent isolation of isolated complexes by means of sucrose gradient centrifugation, performed at 4°C. In our studies, we make the assumption that rapid freezing in liquid nitrogen prior to measurement, which occurs within milliseconds, ensures the transition to the solid state without transition through the gel ($L_{\beta'}$) phase. Instead, we believe that the membrane is frozen in a disordered state corresponding to a "snapshot" of the liquid-crystalline phase.

Functional state of the LH1-RC complexes

The activity of the RC was confirmed by following the bleaching of the RC P870 band due to the special pair, either by chemical oxidation with $K_3Fe(CN)_6$ or by photobleaching with actinic light as described in Noël *et al* (*25*).

Fluorescence emission spectra of single LH1-RC complexes. Fig. 2 shows 4 representative fluorescence emission spectra of single LH1-RC complexes membrane-reconstituted (Fig.

10.1021/bi034969m CCC: $25.00 © 2003 American Chemical Society Published on Web 08/14/2003

2A,B, 26 LH1-RC complexes measured) and detergent-solubilized (Fig. 2C,D, 32 LH1-RC complexes measured). In fact, for both types of samples, all spectra measured showed the same characteristics. The spectra in Fig.2(A,B) show a sharp spectral line on the short wavelength edge (zero phonon line (ZPL)) followed by a broad phonon side band (PSB). In the other spectra (Fig. 2D) the ZPL could not be clearly resolved because it is merged with the PSB. However, in general, we found more spectra with a resolved ZPL for membrane-reconstituted LH1-RC complexes than for the detergent-solubilized complexes. The spectral features of the emission spectra from the LH1-RC complexes described above are identical with the previously published emission spectra from the LH1 complex of *R. rubum* lacking the RC in detergent or reconstituted in membrane bilayers (*18*). Despite the fact that we performed excitation at 865 nm, which corresponds to the absorption maximum of the special pair, no spectral spectral features of the emission spectra are visible which differ from those obtained for LH1 complexes alone.

In principle, fluorescence might be observable for the relaxation processes following excitation of the special pair. The experimental lack of fluorescence due to the RC is probably due to charge separation in the RC resulting in the trapping of the electron by the long-lived Q_A^- state at low temperatures (26).

Fluorescence excitation spectra of single LH1-RC complexes. Typical fluorescence excitation spectra of the $|k = \pm 1\rangle$ states for membrane-reconstituted as well as for detergent-solubilized LH1-RC complexes are shown in Fig. 3 (A,B,C,D). The spectra measured with orthogonal polarization of the exciting light are shown in blue and red, respectively. Independent of the environment of the complexes, their excitation spectra showed a similar behaviour. Approximately 85% of all membrane-reconstituted and detergent-solubilized complexes, exhibited fluorescence excitation spectra consisting of a single broad absorption with peak maxima between 860 nm and 900 nm which did not depend upon the polarization direction of the excitation laser. The widths of these bands were in the range of 250 - 300 cm^{-1}. This value corresponds to a lifetime of the absorbing states of some tens of femtoseconds. All other complexes showed a single band at each polarization direction.

The observed splittings of these bands were in the range of ΔE = 30 - 85 cm^{-1}. In general, the fluorescence of the detergent-solubilzed complexes was weaker than for the membrane-

10.1021/bi034969m CCC: $25.00 © 2003 American Chemical Society Published on Web 08/14/2003

reconstituted complexes under comparable conditions, resulting in a lower signal-to-noise ratio in their excitation spectra. In seven (from 14 complexes investigated) excitation spectra of membrane reconstituted complexes we observed a narrow absorption line on the red wing of the excitation spectrum as shown in Fig. 3E which varied in intensity from complex to complex. A few spectra showed two and more narrow lines on their red wings, probably due to spectral diffusion. The widths of these narrow lines were $\leq$1 cm^{-1} and are therefore determined by the width of the excitation laser. For the detergent-solubilized complexes only 2 excitation spectra showed a clear narrow absorption line on the red wing, due to the low signal-to-noise ratio. These narrow absorption lines most probably represent the $|k = 0\rangle$ state from the Frenkel exciton picture used above. The mean energetic distance of this line from the $|k = \pm 1\rangle$ absorption maxima is 84 cm^{-1}, which is in good agreement with the calculated value of 75 cm^{-1} (as shown in Fig.1).

10.1021/bi034969m CCC: $25.00 © 2003 American Chemical Society Published on Web 08/14/2003

DISCUSSION

The stunning three-dimensional representations of the LH2 complexes from *Rps. acidophila* and *R. molischianum*, respectively, obtained by X-ray crystallography, have revealed arrays of $\alpha\beta(BChla)_3$ dimers arranged in a ring-like structure with perfect circular symmetry (*4,5*). The subsequent medium-resolution projection structures of the LH1 complexes from *R. rubrum* (*7*) and *Rb. sphaeroides* (*27*), obtained by cryoEM also showed larger arrays of 32 $\alpha\beta$ heterodimers with flawless circular symmetry (*7*). An exception to this rule has been reported (*28*) for the photosynthetic unit (PSU) of *Rb. sphaeroides* strain RCLH10. In this case, cryoEM analysis of intact membranes an "open" LH1 ring structure partially surrounding the RC. The intact PSU appeared to consist of a "dimer" of these units arranged with two-fold symmetry and with the RC accessible to the lipid bilayer. However, so far this organization seem to be exceptional and it is not clear whether it is attributable to the relatively low resolution of the images obtained after negative staining, or the highly unusual tubular morphology of the intracellular photosynthetic membranes in this exotic nitrate-utilizing strain. Certainly it is now well-established that the more commonly found strains of *Rb. sphaeroides* (with spheroidal intracellular membranes) contain closed LH1 rings with 16-fold symmetry (*27*). We will therefore limit ourselves to the 16-fold symmetric LH1 organization shown here to be present exclusively in *R. rubrum*.

Recent analysis of the geometry of the BChla pigments in LH2 rings using SM spectroscopy, which is exquisitely sensitive to small geometric deformations, seemed to indicate that the centrosymmetric view of the LH2 complexes may be severely biased by the averaging techniques employed by X-ray crystallography and cryoEM. Thus, the fluorescence excitation spectra obtained at low temperature for the ring of BChla pigments contributing to the B850 band of the LH2 complexes from *Rps. acidophila* show 2 or more absorption bands in the 850 nm region with a characteristic energy spitting between the $|k = \pm 1\rangle$ states of approximately 110 cm^{-1} (*15*). In this previous work, it has been argued that the characteristic splitting of the B850 absorption band at low temperature is not a matrix effect but is due to a correlated disorder of the pigments, which could be explained by an elliptical deformation with an eccentricity of $\varepsilon = 0.52$ (b/a = 0.85). More recent experiments (*19*) on detergent (LDAO)-solubilized LH1-RC complexes have indicated that also these exhibit a variety splittings in the fluorescence excitation spectra, with only about 30% of the LH1-RC complexes showing

10.1021/bi034969m CCC: $25.00 © 2003 American Chemical Society Published on Web 08/14/2003

a clear signature of a circular symmetric ring-like arrangement of their pigments. The remaining 70% of the complexes (from a population of 24 complexes) show excitation spectra which are only compatible with a gross deviation from circular symmetry (Type II spectra in (*19*)), and have been attributed either to an "open" ring or a partial ring of BChla pigments (Type III spectra in (*19*)), or or a dimeric LH1-RC aggregate (Type IV spectra in (*19*)). The assignment of elliptical distortion with C_2 symmetry to the BChla pigments of the LH1 ring in LH1-RC complexes has been suggested to be compatible with the 2-fold symmetry of the RC, which might act as a "mould" for the LH1.

To long-term workers in the field, the distortion of the LH1 ring, due to a site-specific interaction with the RC or even the presence of partial LH1 rings are attractive for a number of reasons, First, a distortion of the LH1 ring stabilized by interaction with the RC would allow a localization of excitation energy at a fixed point of the ring and thus facilitate energy transfer to the special pair. Secondly, considerable controversy exists concerning the molecular homogeneity of the LH1 complex. In several cases, additional polypeptides, such as PufX in *Rb. sphaeroides* (*29*) and *Rb. capsulatus* (*30*), the γ-polypeptide in *Rps. viridis* (*31*), and the Ω-polypeptide in *R. rubrum* (*32*) have found to be associated with the LH1 complex. At least in one case, PufX, this additional polypeptide component seems to be essential for functional electron transfer from the RC to the cytochrome bc_1 complex, presumably by forming a "pore" with the "closed" LH1 ring (*33*). An excellent summary of these data is given in Ketelaars *et al.* (*19*).

Thirdly, evidence from structural analyses of LH1 or LH1-RC complexes has also repeatedly indicated that the LH1 ring may be susceptible to elliptical distortion. Thus, although the medium-resolution projection of the *R. rubrum* LH1 ring was calculated by 16-fold averaging, necessarily generating circular symmetry, it was noted that unit cells were also present showing a noticeable ellipticity (7). More recent images of the *R. rubrum* LH1-RC complexes in 2D crystals showed an elliptic deformation, with the major and minor axes differing by about 11% (8), corresponding to an a/b ratio of 1.12.

In our calculations we have not included possible influences of the RC special pair or accessory BChls upon the energy levels of the LH1 BChls as there are not observed experimentally. In addition modelling studies which "dock" the RC into the LH1 ring show that the distances between the special pair and the accessory Bchla pigments to those of the

10.1021/bi034969m CCC: $25.00 © 2003 American Chemical Society Published on Web 08/14/2003

LH1 ring are rather large (approx. 42 Å and 36 Å for the Mg-Mg distances, respectively (*34,35*)). At these distances theory indicates that no energetic interactions are expected (*36*).

The exciton model for a ringlike aggregate with perfect symmetry predicts that the lowest state of the exciton manifold $|k=0\rangle$ carries no oscillator strength, thus preventing the appearance of fluorescence at low temperature, when only the lowest state is occupied. Nevertheless, strong low temperature fluorescence emission (Fig. 2) are experimentally observed for in bulk (*37*) and SM measurements ((*19*) and this study) of single LH1-RC complexes, indicating that a minimal distortion of the ring must be present.
This disagreement between the experimental results and the theory is overcome by assuming that the BChla molecules in the ring are distributed with a diagonal disorder (σ), which correspond to the full width half maximum (σ) of the Gaussian distribution of excitation energies about E_o. In fact, bulk measurements have also indicated that a diagonal disorder of about 200 cm^{-1} of the BChls must be present (*37,38*). The diagonal disorder not only leads to a shift of oscillator strength to the state $|k=0\rangle$ but also causes a splitting of the degenerated excitonic states. The fact that the excitation spectra mostly showed only a single broad line independent of the polarization, suggests that the B880 ring is only weakly perturbed so that the states $|k=\pm 1\rangle$ remain nearly degenerate. Our experimentaly observed distributions of splittings ΔE of the states $|k=\pm 1\rangle$ (Fig.3F) are compatible with a moderate diagonal disorder of $\sigma \leq 150$ cm^{-1}.

In an impressive study of intact photosynthetic membranes from *Rps. viridis* using AFM, Scheuring *et al*. (*20*) have very recently presented data which indicates that the LH1 ring is elliptical in shape when present as a complex with the RC. In this latter study, intact LH1 rings containing no RC (which had been extracted in some cases as a consequence of the AFM measurement) reverts to circular symmetry. Thus, both AFM and cryoEM studies appear to lead to the same conclusion, namely that the LH1 rings of LH1-RC complexes present in bilayer membranes possess elliptical geometry. The (a/b) ratios obtained in these two experiments were similar (a/b= 1.12 and 1.05 – 1.11 for the cryoEM and AFM studies, respectively (see Fig. 1C).

By contrast, our own data show unambiguously that not only LH1 rings in LH1-RC complexes exhibit a minimal distortion from perfect circular symmetry when reconstituted

10.1021/bi034969m CCC: $25.00 © 2003 American Chemical Society Published on Web 08/14/2003

into lipid bilayers, but also, even more strikingly, that the circular symmetry is *stabilized* by the interaction with the RC, even when the LH1-RC particles are present in the detergent-solubilized state.

How can the discrepancy between our study here and the structural and spectroscopic studies be rationalized. On the one hand, we note that both the cryoEM (*8*) and the AFM (*20*) studies have been performed using 2D crystalline arrays, where the LH1-RC complexes are closely packed. Thus, it seems likely that the observed ellipticity is a consequence of a packing artefact and is not attributable to a fundamental property of the LH1-RC interaction. The study of Scheuring *et al.* (*20*) may indicate that an elliptical ring geometry is physiologically meaningful only for a photosynthetic membrane where the complexes are packed in an almost perfect 2D crystal, such as those from *Rps. viridis* (*39*) or *Ectothiorhodospira halochloris* (*40*). However, this perfect packing is exceptional. In most photosynthetic membranes from bacteria such as *R. rubrum*, *Rb. sphaeroides* or *Rhodobacter capsulatus*, both kinetic and structural evidence exists that most LH1-RC complexes exist in domains (varying from approx. 100 LH1-RC complexes at high light intensities, to as little as 4 LH1-RC complexes at low light intensities (*3*)) which are significantly less well ordered than in *Rps. viridis* or *E. halochloris*. Although a preliminary AFM study of one such example (from *Rps. acidophila*) has been performed, the resolution obtained in this earlier study was not sufficient to obtain information concerning the ellipticity of the LH1-rings (*41*).

We believe that the apparent correspondence of the SM data of Ketelaars *et al*. (*19*) with the cryoEM (*8*) and AFM (*20*) data refers to a different molecular phenomenon than a packing effect. We have observed repeatedly that the formation of regular 2D crystalline arrays for isolated LH1 (Karrasch *et al*. (*7*)) or LH1-RC complexes (*21*) requires the presence of 1-2 mol phospholipid /αβ domain (*11,42*)) to be present. We speculate that the large number of distorted or "open" LH1 complexes observed by Ketelaars *et al*. (*19*) may be due to their use of LDAO as a detergent. In our hands, as judged by Gaussian analysis of the absorption spectra obtained from LH1-RC complexes in this latter detergent (R. G., unpublished data) it has not been possible to obtain "perfect" absorption spectra of either isolated LH1 or LH1-RC rings without evidence of "non-native" spectral contributions not observed for LH1 rings *in vivo* or for reassembled complexes obtained after extensive dialysis. This is not true when the detergent DHPC (a short-chain phospholipid) is employed as a solubilizing agent, provided that a critical detergent concentration (usually between 0.07 – 0.09% (w/v)) is not exceeded

10.1021/bi034969m CCC: $25.00 © 2003 American Chemical Society Published on Web 08/14/2003

(see Materials and Methods). The phosphocholine head-group may stabilize interactions between αβ chains, similiar to that observed in 2D crystals and probably in vivo as well. Under these conditions, “native” (which we interpret as corresponding to LH1 rings showing no detergent-induced destabilization or dissociation) absorption spectra (and near-IR CD spectra, data not shown) are obtained.

In conclusion, our data demonstrates unambiguously that the LH1 ring present in a homogenous two-dimensional potential of the lipid bilayer exhibits near-perfect circular symmetry, even when interacting with the reaction center. The stabilization of a circularly symmetric LH1 by interaction with an intrinsically asymmetrical RC points to an unusual and subtle structural/thermodynamic phenomenon which we will pursue in future studies.

ACKNOWLEDGEMENTS

We thank Ms. Gerasimoula Gerasimidou for expert technical assistance. We thank Dr. Fedor Jelezko for fruitfull discussion and critical reading of the manuscript.

10.1021/bi034969m CCC: $25.00 © 2003 American Chemical Society Published on Web 08/14/2003

REFERENCES

1. Zuber, H. (1986) *Encycl. Plant Physiol*., 19, 238 – 251.
2. Monger , T. G., and Parson, W. W. (1977) *Biochim. Biophys. Acta*, 460, 393 – 407.
3. Vos, M., van Grondelle, R., and Duysens, L. N. M. (1986) *Biochim. Biophys. Acta,* 850, 501 - 512
4. McDermott, G., Prince, S. M., Friend, R.H., Hawthornthwaite-Lawless, A. M., Papiz, A. M., Cogdell, R. J. , and Isaacs, N. W. (1995) *Nature*, 374, 517 – 521.
5. Koepke, J., Hu, X., Muenke, C., Schulten, K., and Michel, H. (1996) *Structure*, 4, 581 – 597.
6. Kramer, H. J. M., Pennoyer, J. D., van Grondelle, Niederman, R. A., and Amesz, J. (1984) *Biochim. Biophys. Acta*, 767, 335 – 344.
7. Karrasch, S., Bullough, P. A. ,and Ghosh, R. (2000) *EMBO J*., 14, 631 – 638.
8. Jamieson, S. J., Wang, P., Qian, P., Kirkland, J. Y., Conroy, M. J., Hunter, C. N., and Bullough, P. A. (2002) *EMBO J.,* 21, 3927 – 3035.
9. Robert, B. and Lutz, M. (1985) *Biochim. Biophys. Acta,* 807, 10 – 23.
10. Hu, Q., Sturgis, J. N., Robert, B., Delagrave, S., Youvan, D. C., and Niederman, R. C. (1998) *Biochemistry*, 37, 10006 – 10015.
11. Picorel, R., Belanger, G., and Gingras, G. (1983) *Biochemistry*, 22, 2491 – 2497.
12. Cogdell, R. J., Lindsay, J. G., Valentine, J., and Durant I. (1982) FEBS Letts. 150, 151 154.
13. Hu, X., Schulten, K. (1998) *Biophys J.*, 75, 683 – 694.
14. Authenrieth, F., Ritz, T., Schulten, K., and Ghosh, R. (2002) submitted.
15. van Oijen, A. M., Ketelaars, M., Köhler, J., Aartsma, T. J., and Schmidt, J. (1999) *Science*, 285, 400 – 402.
16. Bopp, M. A., Jia, Y., Li, L., Cogdell, R., and Hochstrasser, R. (1997) *Proc. Natl. Acad. Sci. USA*, 94, 10630 – 10635.
17. Dekker, J. P., Gilbro, T., and Sundström, V. (1994) *Biochim. Biophys. Acta,* 1187, 1 – 65.
18. Gerken, U., Jelezko, F., Götze, B., Branschädel, M., Tietz, C., Ghosh, R., and Wrachtrup, J. (2003) *J. Phys. Chem. B*, 107, 338 – 343.
19. Ketelaars, M. , Hoffmann, C., Koehler, J., Howard, T. D., Cogdell, R .J., Schmidt, J**.,** and Aartsma, T. J., (2002) *Biophys J.*, 83, 1701 – 1714.

10.1021/bi034969m CCC: $25.00 © 2003 American Chemical Society Published on Web 08/14/2003

20. Scheuring, S., Seguin, J., Marco, S., Levy, D., Robert, B., and Rigaud, J.-L. (2003) *Proc. Natl. Acad. Sci. USA*, 100, 1690 – 1693.
21. Stahlberg, H., Dubochet, J., Vogel, H., Ghosh R. (1998) *J. Mol. Biol.*, 282, 819 – 831.
22. Ames, B. N. and Dubin, D. T. (1960) *J. Biol. Chem.*, 235, 769 – 775.
23. Moss, G.P. (1987) *Pure Appl. Chem.*, 59, 779 – 832.
24. Tretiak, S., Middleton, C., Chernyak, V., and Mukamel, S. (2000) *J. Phys. Chem. B*, 104, 9540 – 9553.
25. Noël, H., van der Rest, M., and Gingras, G. (1972) *Biochim. Biophys. Acta,* 275, 219-230.
26. Paschenko, V. V., Gorokhov, V. V., Grishanova, N. P., Goryacheva, E. A., Korratovsky, B.N., Knox, P.P., Zakharova, N. I., and Rubin, A. B. (1998) *Biochim. Biophys. Acta,* 1364, 361 – 372.
27. Walz, T., Jamieson, S. J., Bowers, C.M., Bullough, P.A., and Hunter, C. N. (1998) *J. Mol. Biol.*, 282, 833 – 845.
28. Jungas, C., Ranck, J. L., Joliot, P., Rigaud, J.-L, and Vermeglio, A. (1999) *EMBO J.*, 18, 524 – 543.
29. Farchaus, J.W., Barz, W.P., Grünberg, H., and Oesterhelt, D. (1992) *EMBO J.*, 11, 2779 – 2788.
30. Youvan, D. C., Bylina, E. J., Alberti, M., Begusch, H., and Hearst, J. E. (1984), *Cell*, 37, 949 – 957.
31. Jay, F., Lambillote, M., Stark, W., and Mühlenthaler, K. (1984) *EMBO J.*, 3, 773 – 776.
32. Ghosh, R., Ghosh-Eicher, S., Di Berardino, M., and Bachofen, R. (1994) *Biochim. Biophys. Acta,* 1148, 28 – 36.
33. Barz, W. P., Vermeglio, A., Francia, F., Venturoli, G., Melandri, B. A., and Oesterhelt D. (1995) *Biochemistry*, 34, 15248 – 15258.
34. Papiz, M.Z., Prince, S.M., Hawthornthwaite-Lawless, A. M., McDermott, G., Freer, A. A., Isaacs, N. W., and Cogdell, R. J. (1996) *Trends Plant Sci*., 1 , 198 – 206.
35. Hu, X., Damjanovic, A., Ritz, Th., and Schulten, K. (1998) *Proc. Natl. Acad. Sci. USA*, 95, 5935 – 5941.
36. Novoderezkhin, V. I., Razjivin, A.P. (1994) *Photosynth. Res.*, 42, 9 – 15.
37. Monshouwer R., Abrahamsson, M., van Mourik, F., van Grondelle, R. (1997) *J. Phys. Chem. B*, 101, 7241 – 7248.

10.1021/bi034969m CCC: $25.00 © 2003 American Chemical Society Published on Web 08/14/2003

38. Visser, H. M., Somsen, O. J. G., van Mourik, F., and van Grondelle, R. (1996) *J. Phys. Chem*., 100, 18859 – 18867.
39. Miller, R. M. (1982) *Nature*, 300, 53 – 55.
40. Engelhardt, H., Engel, A., and Baumeister, W. (1986) *Proc. Natl. Acad. Sci. USA*, 83, 8972 – 8976.
41. Scheuring, S., Reiss-Husson, F., Engel, A., Rigaud, J.-L., Ranck, J-L. (2001) *EMBO J.*, 12, 3029 – 3035.
42. Ghosh, R, Hauser, H., and Bachofen, R. (1988) *Biochemistry*, 27, 1004 – 1014.

10.1021/bi034969m CCC: $25.00 © 2003 American Chemical Society Published on Web 08/14/2003

FIGURE LEGENDS

Fig. 1: (A) Energy level diagram of the B880 ring simulated without any kind of disorder and (B) simulated with a diagonal disorder of $\sigma = 175$ cm^{-1}. (C) Effect of elliptical deformation, expressed as the axis ratio of the ellipse a/b, upon the 3 lowest energy states simulated without diagonal disorder (black lines) and with an additional diagonal disorder of $\sigma = 150$ cm^{-1} (grey lines). (D) The splitting (ΔE) of the $|k = \pm 1\rangle$ states taken from (C) and plotted against the axis ratio a/b (the axis ratio a/b is the inverse of the ratio used in Eqn. 3). The symbols show data taken from the SM study (*19*) ((○), ΔE= 116 cm^{-1}), from the cryoEM study (*8*)((□), a/b=1.12) and from the AFM study (*20*) ((Δ), a/b=1.05). (■) depicts the mean ΔE value measured here.

Fig. 2: Typical fluorescence emission spectra (excitation wavelength 870 nm) of membrane-reconstituted (A,B) and detergent-solubilized (C,D) single LH1-RC complexes.

Fig. 3: Typical fluorescence excitation spectra of membrane-reconstituted (A,B) and detergent-solubilized (C,D) isolated LH1-RC complexes. The red and the blue spectra were measured at orthogonal polarization directions (arrows, inset) of the exciting light. In (E) the fluorescence excitation spectra of an membrane-reconstituted isolated complex showing a pronounced narrow absorption line on the red wing (arrow). (F) Histogram of the splitting ΔE of the $|k = \pm 1\rangle$ states for the membrane-reconstituted (red) and detergent-solubilized (green) LH1-RC complexes. To emphasize how the presence of the RC influences the energetic positions of the $|k = \pm 1\rangle$ states the corresponding histogram obtaind for single LH1 complexes from *R. rubrum* (without RC, taken from Gerken *et al.* (*18*)) is shown in the inset.

10.1021/bi034969m CCC: $25.00 © 2003 American Chemical Society Published on Web 08/14/2003

FIGURES

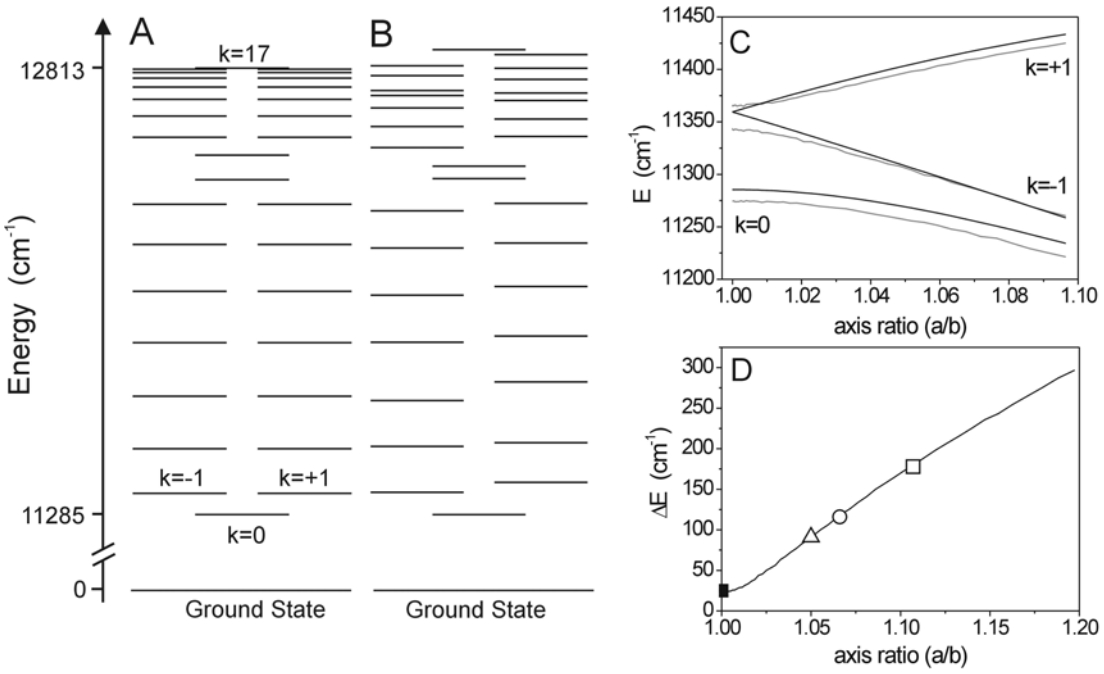

Figure 1

10.1021/bi034969m CCC: $25.00 © 2003 American Chemical Society Published on Web 08/14/2003

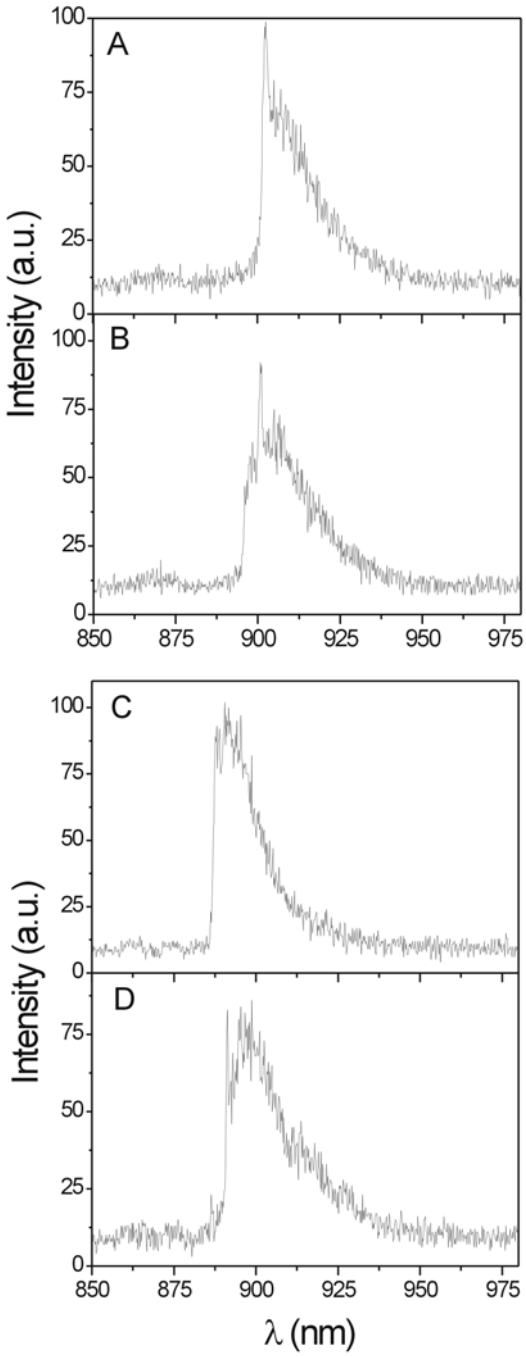

Figure 2

10.1021/bi034969m CCC: $25.00 © 2003 American Chemical Society Published on Web 08/14/2003

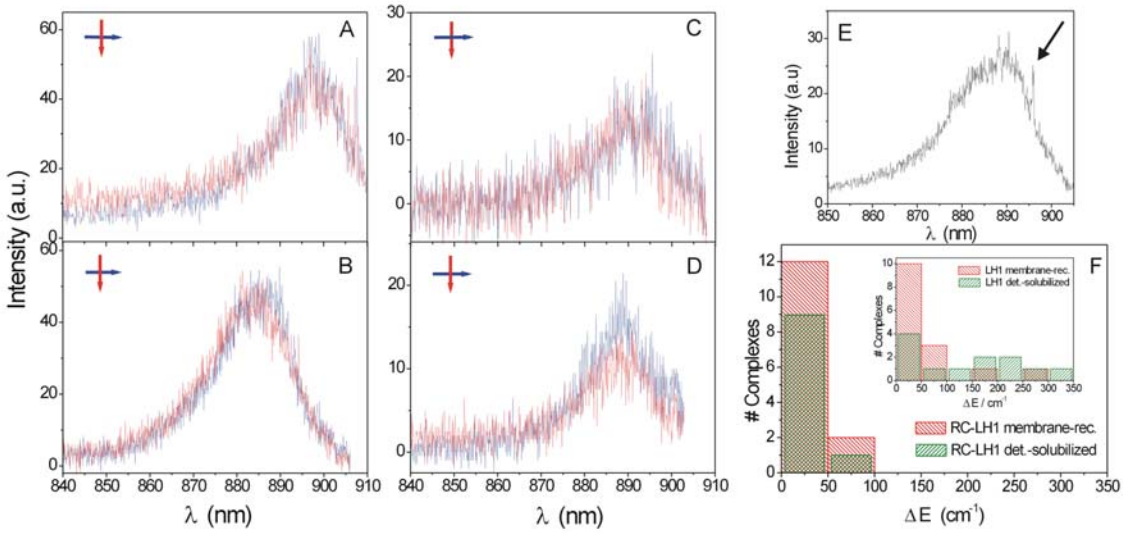

Figure 3

10.1021/bi034969m CCC: $25.00 © 2003 American Chemical Society Published on Web 08/14/2003

CHARAKTERISIERUNG UND KRISTALLISATION DER PSU

The photosynthetic unit of *Rhodospirillum rubrum* associates strongly with an outer membrane porin *in vitro*

by

Domenico Lupo[1], Katharina Kittelmann[1], Bianca Naumann[2], Michael Hippler[2] and Robin Ghosh[1]*

[1]Dept. of Bioenergetics
Institute of Biology,
University of Stuttgart,
Pfaffenwaldring 57,
D-70550 Stuttgart,
Germany

[2]Department of Biology,
101 Mudd Building,
University of Pennsylvania,
Philadelphia, PA 19104, USA

*Corresponding author: Tel.: (+711) 685 5047; Fax: (+711) 685 5096; Email: robin.ghosh@bio.uni-stuttgart.de

Running title: Tight binding of an outer membrane porin to the photosynthetic unit *in vitro*

ABBREVIATIONS

DHPC, diheptanoyl-*sn*-phosphatidylcholine; DOPC, dioleoyl-*sn*-phosphatidylcholine; LH1, light-harvesting complex 1; βOG, n-octyl-β-glucopyranoside; PSU, photosynthetic unit; Crt, carotenoid; BChla, bacteriochlorophyll a

ABSTRACT

The photosynthetic unit (PSU) from the purple non-sulphur bacterium, *Rhodospirillum rubrum* S1 was purified using several ion-exchange chromatographic steps in the presence of the detergent diheptanoyl-*sn*-phosphatidylcholine (DHPC). The final preparation contained principally 8 major bands when analysed by SDS-PAGE, corresponding to the 2 polypeptides of the light-harvesting complex 1, the L, M, H subunits of the reaction center, as well as 2 additional bands with molecular weights of approximately 18 kDa and 40 kDa, respectively. In this study we focussed on the 40 kDa protein, as this component quantitatively copurified with the PSU through all the chromatographic steps and was also shown to be present within 2D crystals obtained from the final preparation. This component was also present in PSU preparations obtained from an carotenoid-less mutant *R. rubrum* GKΔLM, which lacked the L and M subunits of the reaction centre. Amino acid sequences of the SDS-PAGE upper bands were obtained using mass spectrometry, and showed that the 40 kDa band observed for PSUs from both S1 and GKΔLM is an outer membrane porin (Por41). A fragment of the same porin is also associated with the H-subunit, even after denaturation in SDS. The association of the H-subunit with the Por41 protein in DHPC was confirmed by sucrose gradient analysis of the purified PSU. In this experiment it could also be demonstrated that a minor fraction of the PSU is not bound to Por41. The tight binding of Por41 to the PSU, probably to the H-subunit, is a major factor in determining the quality of 2D and 3D crystals of this complex.

INTRODUCTION

It is now well-established that purple non-sulphur bacteria contain specialised intracellular membranes which contain all of the components necessary for photosynthetic cyclic electron transport (8, 9). In recent years, it has become increasingly clear that the photosynthetic membranes possess a high level of structural organisation (2, 6, 8, 33, 39, 40, 41, 42, 43, 49). In particular, a major organising influence seems to be the minimal photosynthetic unit (PSU), composed principally of a reaction centre (RC), which mediates the primary process, and the light-harvesting complex 1 (LH1), which enhances the efficiency of excitation energy transfer to the RC (20). The LH1 complex from *Rhodospirillum rubrum* is composed of 2 non-identical polypeptides, α and β, which bind two bacteriochlorophyll a (BChla) molecules and 1-2 carotenoids (Crt) (7, 36). It has been demonstrated using electron microscopy of negatively stained 2D crystals (50) or cryoelectron microscopy (cryoEM) (21, 24) of unstained 2D crystals, that the *R. rubrum* LH1 complex is assembled from 16 $\alpha\beta(BChla)_2Crt$ subunits (5) into a ring-like structure which encircles the RC. This organization has also been confirmed recently by high-resolution atomic force microscopy (AFM) (13).

In most purple bacteria, the PSU is also associated with a second LH complex (LH2) which is composed of 2 further non-identical polypeptides (also designated α and β) which bind 2 BChla molecules within the membrane bilayer (at a homologous position to those of the LH1 complex) and a third BChla close to the membrane polar interface, as well as 2 Crt molecules. The LH2 complex is also a ring-like structure composed of 8- or 9-$\alpha\beta(BChla)_3(Crt)_2$ oligomers (26, 31). In some bacteria, such as *R. rubrum*, *Blastochloris viridis* or *Ectothiorhodospira halochloris*, which contain only a single LH complex, studies using either low-angle X-ray diffraction of oriented membranes (47), EM, cryoEM (10, 21, 32) or AFM of native membranes (41) have shown that the PSUs are packed quasi-hexagonally in a well-organised long-range lattice. On the other hand, very recent high-resolution AFM studies of native or detergent-treated membranes from *Rhodobacter sphaeroides* (2) which contain LH1 and LH2 complexes, have provided visual evidence that the PSUs in these organisms may be packed in dimeric rows. Additionally, cryoEM data from *Rb. sphaeroides* (23) as well as medium-resolution X-ray diffraction data from the PSU of *Rhodopseudomonas palustris* (37) have indicated that the LH1 ring is not completely closed. In *Rb. sphaeroides* and *Rhodobacter capsulatus*, it has been demonstrated that a further protein, PufX (not present in single LH-organisms) interrupts the ring and facilitates the passage of ubiquinone between the

RC and the cytochrome bc_1 complex (3, 11, 29, 39). It is thought that in most purple bacteria the packing defects of the PSU-lattice are sufficient to allow the insertion of large membrane complexes (e.g. the cytochrome bc_1 complex, or the ATP-synthase) necessary for maintaining functional cyclic electron transport from the RC.

Despite the recent advances in understanding the structural organisation of the photosynthetic membrane, it has proved difficult to visualise the intact (RC-LH1)-PSU at atomic resolution. So far, 2D crystals of both isolated LH1 and RC-LH1 from several sources have not yielded diffraction data with a resolution of greater than approximately 6-8 Å (21, 24, 45, 51), and in a recent X-ray diffraction study of the PSU from *Rhodopseudomonas palustris*, diffraction to only 4.8 Å was achieved (37), far short of that necessary for visualising atomic interactions. The slow progress in obtaining high-quality PSU crystals is partly due to the usual difficulties in crystallising membrane proteins, but also to the special problems associated with maintaining the integrity of the unusual pigment protein interactions within the complex. In particular, many studies have shown that the BChla and Crt molecules are bound rather loosely to many complexes, and can be easily depleted by detergent treatment (14, 16, 17). In particular, the PSU from many sources, including *R. rubrum*, examined here, is sensitive to pigment depletion by some common chromatographic techniques, particular gel filtration (see Discussion).

Some years ago, we showed (25) that the PSU from *R. rubrum* is particular stable in the presence of the short-chain phospholipid detergent diheptanoyl-*sn*-phosphatidylcholine (DHPC) and that the DHPC-purified complex yields good 2D crystals from the carotenoid-less mutant, *R. rubrum* G9, diffracting to approximately 13.5 Å after negative staining (45). This detergent was subsequently employed to produce 2D crystals of the the PSU from the wild-type *strain (R. rubrum* S1) which diffracted to 8.5 Å (21). So far, 3D crystals obtained using a DHPC-purified PSU have not been reported.

The initial aim of the present study was to develop a large-scale purification of the *R. rubrum* PSU which minimises the use of the prohibitively expensive detergent DHPC but which also eliminates the need for gel filtration in the procedure. In the course of this work, performed with PSUs obtained from different *R. rubrum* strains, we repeatedly observed the presence of apparently stoichiometric amounts of an unknown 40 kDa protein in nearly all of the

preparations. This 40 kDa protein was also present in the G9-PSU crystallised previously (45). Here, we have identified this component to be an outer membrane porin (see below), which we believe to be tightly bound to the PSU during purification, and we present evidence that even when the 40 kDa protein is absent, fragments of the same porin may still be bound to the complex. We believe that the identification of this component, involving the first systematic mass spectrometry study of the 23-40 kDa region of purified PSUs reported so far, may be of consequence for the crystallisation of the PSU complex, and will stimulate workers in this area to examine the purity of their preparations more critically.

MATERIALS AND METHODS

Growth of bacteria and chemicals. The wild-type *R. rubrum* S1 (ATCC no. 11170) and a site-directed interposon mutant, designated GKΔLM (38), of the carotenoid-less mutant G9, were grown at 30°C microaerophilically in the dark using a minimal medium (Sistrom medium A (44)) which has been modified for maximal expression of photosynthetic genes (15). GKΔLM was grown in the presence of kanamycin sulfate (20 µg/ml) to select for the *npt* interposon. All chemicals were obtained from Fluka AG (Buchs, Switzerland) or Merck (USA) with the exception of DEAE-cellulose (DE-52, Whatman), dioleoyl-*sn*-phosphatidylcholine (DOPC) and the DHPC (Avanti Polar Lipids, Alabaster, AL), soybean phosphatidylcholine (soybean-PC, Lipid Products, UK) and n-octyl-β-glucopyranoside (βOG) (Bachem, Switzerland). The concentration of the stock suspensions of phospholipids (DHPC, soybean-PC and DOPC) were determined by the ammonium molybdate method (1).

Isolation of chromatophores (intracytoplasmic membranes, ICM). The preparation of chromatophore membranes was performed as described (30). Pellets were resuspended in 2 ml of 20 mM TrisHCl pH 8.0, frozen in liquid nitrogen and stored at –85°C. Isolation, extraction, purification and crystallisation steps were done in dim light and under a nitrogen-enriched atmosphere. All buffer solutions were purged with nitrogen gas prior to use.

Absorption spectra. Absorption spectra of chromatophores, purified PSU or 2D crystals were measured using 2 mm path-length cuvettes in a Jasco V-560 UV/VIS spectrophotometer, equipped with a photodiode detector for turbid samples. The sample concentration was adjusted to the same absorption at the LH1-Q_y band (either at 880 nm for wild-type carotenoid-containing strain S1 or at 874 nm for the carotenoid-less strain GKΔLM).

SDS-polyacrylamide gel electrophoresis (SDS-PAGE). SDS-PAGE was performed according to the method of Laemmli (28) using 12.5% acrylamide gels. In general, samples (20 µg protein) were precipitated by the addition of 3 volumes of methanol before solubilizing in SDS-PAGE sample buffer. This step is effective in reducing the BChla and lipid content of the sample, which can affect the final gel resolution. The gels were stained with Coomassie Brilliant Blue R250 (Pharmacia). Heme staining was performed according to Goodhew *et al.*

(18), and protein determination by the modified Lowry method of Peterson (35) using bovine serum albumin as standard.

Determination of the molar PSU/DOPC ratio. The molar PSU/DOPC ratio was determined as follows. Previous studies (R. Ghosh, unpublished data) have established that 100 μg purified LH1 complex yield an A_{880}(1cm) = 0.144 (after correction for turbidity). We assume that the effective PSU molecular weight is approximately 389.5 kDa (14.6 kDa (LH1α/β) + 100.4 kDa (RC) + 37.5 kDa (Por41) + 18 kDa (unknown component)) Assuming an oligomer of 16 αβ$(BChla)_2$Crt units, the LH1/PSU ratio is 0.60. We also assume that the reassociation of PSU is principally due to phospholipid-LH1 interactions. Thus, the LH1 molar value is 0.6 × (PSU protein concentration (as determined by the Lowry method)/(14 600).

Extraction and purification of PSU from S1 and GKΔLM. The solubilisation and purification of RC-LH1 complexes was performed by a modification of the procedures we established previously (25, 45). Chromatophores were suspended in extraction buffer (10 mM TrisHCl, pH 8.0, 140 mM NaCl, 2 mM $MgCl_2$ and 10 mM Na-ascorbate) to an A_{880nm}(1cm) = 20. DHPC was added to a final concentration of 18 mM and the solution was allowed to equilibrate with stirring for 30 minutes at room temperature. Subsequently, the extraction cocktail was diluted 9-fold and centrifuged at 100 000 × g for 1h at room temperature. PSU complexes were obtained quantitatively in the pellet, which was resuspended in extraction buffer to A_{880}(1cm) = 20 containing 2 mM DHPC. After stirring for 10 minutes at room temperature the solution was applied to a DEAE-cellulose column equilibrated in the buffer indicated. Two separate DEAE-cellulose chromatographic procedures (yielding the batches B1-PSU and B2-PSU, respectively) were employed to purify PSUs from S1. B1-PSU was purified on a column pre-equilibrated with purification buffer (10 mM TrisHCl, 150 mM NaCl, 2 mM $MgCl_2$ and 2 mM DHPC). This batch was collected as a flow-through fraction and reapplied to a further DEAE-cellulose column (also equilibrated with purification buffer) to which it bound. B1-PSU was then washed with 2 column volumes of purification buffer and then eluted with the same buffer containing 200 mM NaCl and 0.3% (w/v) βOG. For the purification of B2-PSU, the DHPC-solubilised pellet obtained after the 100 000 × g centrifugation step above, was applied to a DEAE-cellulose column, which had been pre-equilibrated with purification buffer containing 0.3% βOG instead of 2 mM DHPC. Initially, the DHPC-solubilised PSU-pellet was bound to the matrix, but was eluted by washing the column with 2 volumes of equilibration buffer. Both the B1-PSU and B2-PSU eluted fractions

were reconstituted with the phospholipid DOPC in a molar DOPC/LH1 ratio of 2:1 (determined as described below). The lipid suspension was sonicated to clarity immediately prior to mixing with the samples obtained from the DEAE-cellulose columns. Dialysis was performed for 2 days at 6°C against 50 mM NH_4HCO_3 pH 8.0 and for additional 3 days at 6°C against 20 mM Tris-HCl pH 8.0. Dialysed samples were centrifuged at 100 000 × g for 1h at 8°C and the pellets resuspended by Potter homogenisation in 20 mM Tris-HCl pH 8.0.

For the purification of "PSU" from the RC-LM$^-$ mutant GKΔLM, chromatophores were obtained from semi-aerobic cells as described above. The chromatophores, equilibrated to room temperature, were adjusted to an A_{874}(1 cm) = 20 with extraction buffer and then DHPC was added dropwise to a final concentration of 16 mM. The extraction cocktail was incubated for 20 min and then diluted to a final DHPC concentration of 2 mM, and stirred for a further 20 min at 4°C. Finally, the preparation was centrifuged at 100 000 × g for 1 h at 6°C. The resulting pellet was resuspended to a final A_{874}(1cm) of 20 with extraction buffer and DHPC added to 2 mM, followed by an equilibration time of 20 min and ultracentrifugation at 100 000 × g. The blue pigment-proteins were obtained quantitatively in the pellet. The blue pellet was resuspended in extraction buffer to A_{874}(1cm) of 20 containing 1.9 mM DHPC and then applied to a DEAE-cellulose column equlibrated with extraction buffer containing 1.9 mM DHPC. In contrast to the PSU complexes from S1, the GKΔLM "PSU" complexes did not bind to the column but were collected in the "flow-through" fraction. The PSU complexes were reconstituted with 1-2 mol soybean-PC/mol LH1 as described above and the resuspended pellet resolubilised in 2 mM DHPC and reapplied to a further DEAE-cellulose column. Once again, no binding to the matrix was observed, even after this step was repeated using only 20 mM TrisHCl pH 8.0 containing 2 mM DHPC instead of extraction buffer. "PSU" complexes were therefore purified routinely using 3 sequential DEAE-cellulose columns, collecting each "PSU" fraction in the "flow-through" eluate, and reconstituting with soybean PC prior to the subsequent column or dialysis to yield the final preparation.

Sucrose gradient of solubilised B2-PSU. 200 µg of B2-PSU were solubilised with 0.5 % (w/v) DHPC in a total volume of 1 ml (20 mM TrisHCl pH 8.0) and then centrifuged at 100 000 × g for 1h at 8°C. The supernatant was loaded onto a linear sucrose gradient (0.4 M - 2 M sucrose in 20 mM TrisHCl pH 8.0 and 0.09 % (w/v) DHPC) and centrifuged for 40 hours at 100 000 × g at 8°C. The colored bands observed in the gradient were collected, diluted 10-

fold in 20 mM TrisHCl pH 8.0 and then pelleted by ultracentrifugation at 100 000 × g. The pellets obtained were suspended in 20 mM TrisHCl pH 8.0 and analysed by SDS-PAGE.

Two-dimensional crystallisation of purified B1-PSU. Purified B1-PSU was reconstituted with DOPC in a series of molar ratios (0.8:1 to 1:1) and then adjusted to a volume of 200 µl with crystallisation buffer (20 mM TrisHCl pH 8.0, 10mM $MgCl_2$ and 2 mM DHPC). Dialysis was performed for 3 days at 8°C in microdialysis setups against 2.5 ml reservoir buffer (50 mM NH_4HCO_3 pH 7.9, 200 mM NaCl and 10 mM $MgCl_2$) containing 0.8 % βOG. A further dialysis for 5 days was then performed using fresh reservoir buffer. Crystallisation procedures were performed in a Plexiglas box, which allowed the entire handling to be done in dim light and under a nitrogen-enriched atmosphere. Crystals were immediately analysed by electron microscopy and then stored at 4°C. As judged from their diffraction patterns, the 2D crystals were stable for up to 3 weeks.

Transmission electron microscopy of 2D crystals. The 2D crystals solution (4 µl) were adsorbed for 30 seconds on carbon-coated grids, which had been treated by glow discharge prior to use. The samples were stained twice for 20 seconds with 1 % uranyl acetate, blotted and then air-dried prior to analysis. Transmission electron microscopy was carried out with a Zeiss EM 10 operated at 60 kV. Images were recorded using Kodak EM-Film 4489 at a nominal magnification of 50 000 ×. The diffraction pattern from film negatives was obtained using an optical bench. The negatives were scanned at a resolution of 1000 ppi for presentation purposes.

Characterisation of purified PSU by mass spectrometry.

For amino acid sequence analysis 20 µg of B2-PSU and H-LH1 ("PSU") from GKΔLM were loaded onto separate 12.5 % SDS gels and the higher molecular protein species were cut, transferred into 1.5 ml reaction vials and dried under high vacuum after freezing in liquid nitrogen. In-gel tryptic digestion was carried out essentially as in (19), with acetonitrile as the organic phase. Autosampling and chromatography were done essentially as described in (46). With the following change: Samples were first injected onto a µ-Precolumn (PepMapTM C18, 5 µm, 100 Å 300 µm i.d. × 5 mm) (LC-Packings, Sunnyvale, California, USA), and washed for 4 min at a flow rate of 0.25 µl/min with the aqueous phase. A nano-column switching device (Switchos, LC-Packings, Sunnyvale, California, USA) was used to direct the flow either to waste or to the analytical column. A fused silica needle with 8 µm aperture

(FS360-75-8-N-5-C12; New Objective, Woburn, Mass.) was used for ionization of peptides. Mass spectra were measured with an LCQ Deca XP Plus ion trap mass spectrometer (Thermo Electron, San Jose, California). Acquisition of mass spectra and sequence identification using Sequest software (Thermo Electron, San Jose, California) were done as described in (46) by using a database which contained the unfinished genome sequence of *R. rubrum* (Accession: NZ_AAAG00000000).

RESULTS

Strategy of the PSU purification. Although we have isolated PSUs here using ion-exchange chromatography as described previously (25, 45), we have added an important modification which allows a significant purification. We have shown previously that highly purified LH1 complexes will reversibly aggregate to form proteinaceous vesicles following detergent removal (17) and that the formation of these vesicles is dependent on the presence of 1-2 mol tightly-bound phospholipid (R. Ghosh, unpublished data). By contrast, detergent removal from ion-exchange-purified PSUs leads only to non-specific aggregates, although the absorption spectrum is still characteristic of native complexes. We reasoned that possibly the detergent DHPC had displaced the LH1-bound phospholipid, thus preventing protein vesicle formation, and that if we added 1-2 mol phospholipid (here DOPC) prior to detergent removal we would allow the vesicles to be formed, facilitating the stabilization of the complex and concentration by centrifugation. We note that this amount of phospholipid is too small to allow the formation of significant phospolipid vesicles and allow membrane protein reconstitution to occur in the usual way. Since protein vesicle formation is a characteristic property of the LH1 complex, other membrane proteins are expected to clump together and no longer be well-separated by a subsequent DEAE-cellulose chromatography step. Thus, we should also be able to achieve a significant purification step by this procedure. We also knew that the LH1 proteinaceous vesicles require only very small amounts of detergent for resolubilisation, which is a highly cooperative process, in contrast to typical reconstituted membranes, which usually require much larger amounts of detergent for resolubilisation than is required for maintaining the solubility of the isolated membrane protein. Consequently, the successful solubilisation of the proteinaceous vesicle in a low concentration of detergent (here 2 mM DHPC) should confirm our reconstitution strategy.

Purification of PSUs from S1 and GKΔLM. We also introduced a further modification of the previously described protocol, in that we chose to dilute the PSUs isolated after initial extraction with 18 mM or 20 mM DHPC to a final concentration of 2 mM DHPC. The rationale for this step was that, as judged by the spectra in the near-IR region, the PSUs have only a limited stability (several hours) in 20 mM DHPC, whereas as they are very stable (days) in 2mM DHPC. Surprisingly, the PSUs from both S1 and GKΔLM were obtained quantitatively in the pellet after centrifugation at 100 000 × g at room temperature, but could be easily resolubilised by adding extraction buffer containing 2 mM DHPC.

The DHPC-solubilised PSU preparations from S1 and GKΔLM behaved very differently when chromatographed with DEAE-cellulose. The S1 PSUs bound well to the DEAE-matrix equilibrated with buffer containing 150 mM NaCl, but were eluted by raising the salt concentration to 200 mM and changing the detergent to 0.3 % βOG (this concentration is insufficient to cause dissociation of LH1 complexes (17)). The change of detergent was not only essential for elution, but facilitates the rapid removal of detergent by dialysis in the following dissociation step. In contrast, PSUs isolated from GKΔLM, also diluted to 2 mM DHPC, pelleted and resolubilised in the same detergent, were not bound to the DEAE-matrix, even in the absence of salt. We conclude, therefore that the binding of the PSU complexes to the DEAE-matrix is due to interaction with the L and M subunits of the RC. In the event, we were able to utilise this property, as most membrane proteins from *R. rubrum* do in fact bind well to DEAE-cellulose at low salt concentrations (R. Ghosh, unpublished).

For both types of complexes, our strategy of reconstitution, resolubilisation and re-chromatography using the same (fresh) matrix appeared to work well. As judged by SDS-PAGE (see below), passage of the PSUs from both strains through 3 DEAE-cellulose columns as described above led to preparations with a high purity, though the purity of the GKΔLM PSU is somewhat less than that from S1, as judged by SDS-PAGE. In addition, the spectral profiles of both types of complexes (Fig.1) showed them to be essentially indistinguishable from those determined from intact chromatophores of the parent strain. The PSU complexes showed LH1-Qy/carotenoid ratio of 2.6 (for B1-PSU) and 2.7 (for B2-PSU), respectively, which is identical to that of S1 chromatophores (2.57). Strikingly, spectra taken from equal amounts of protein (as determined from the A_{280}) showed almost identical peak intensities due to BChla, with the exception of the peaks at 760 nm and 802 nm, which arise from the bacteriophaeophytin a (BPha) and the accessory BChla of the RC and are thus not present in PSUs from GKΔLM. The data in Fig. 1a also shows that the Qy band of the LH1 complex in chromatophores from GKΔLM is blue-shifted by about 6 nm compared to that of the LH1 in those from S1, and red-shifted by about 2 nm from the parent strain G9. A second-derivative analysis of the spectrum from chromatophores of both strains (Fig.1b) shows clearly that only the Q_y band and neither the Q_x nor the Soret band are wavelength-shifted. This is also true for the purified PSU complexes (Fig. 1c).

The SDS-PAGE profile of the isolated PSU from S1 revealed 8 major bands, with a number of very minor bands (Fig. 2). The bands due to LH1 α and β (both located under the 14 kDa

marker), as well as L (23 kDa) and M (26 kDa) subunits of the RC (48) were clearly distinguishable. Above the M subunit were two bands at 30 and 34 kDa of about equal intensity. We have observed these 2 bands in all of our PSU preparations so far. We assigned the 30 kDa band to the H-subunit (48). The 34 kDa band did not correspond to cytochrome c_1, as this was not detectable by heme staining (data not shown). Finally, 2 bands (18 kDa and 40 kDa) could not be assigned at this stage. In this study, we have focussed on the 40 kDa protein, as it appears in every PSU preparation we have isolated from *R. rubrum* so far (see also (45)) in stoichiometric amounts to those of the RC and LH1, as confirmed here by densitometric analysis of the SDS-PAGE profiles (Fig. 3), whereas the 18 kDa component is variable (see below). We could exclude the possibility that the 40 kDa protein is a cytochrome b, as no redox spectrum due to this protein could be detected for any of the purified PSUs from S1.

Strikingly, the purified PSU from GKΔLM also showed a strong 40 kDa component (in addition to major bands at 34 kDa, 18 kDa and less than 14 kDa (LH1 α and β), in roughly the same amounts relative to the LH1 polypeptides (Fig. 3) as for the S1-PSU. As expected, the L and M polypeptides of the RC were missing, but also apparently only a single band at 34 kDa and not at 30 kDa was observed, suggesting that the H-subunit may have been removed by the purification (Fig. 2).

Finally, the B1-PSU and B2-PSU preparations showed an interesting difference in that for the latter, the 18 kDa polypeptide appeared to be depleted, despite the fact that the absorption spectra of both complexes were identical. Thus it appears that the exchange of 2 mM DHPC for 0.3 % βOG in the second DEAE-step is effective in achieving the removal of the 18 kDa component, without causing pigment dissociation from the PSU.

2D crystallisation of the B1-PSU and B2-PSU complexes and analysis of the crystal composition. Despite the fact that large amounts of PSU complexes with high purity could be isolated routinely, we were unable to obtain 2D crystals diffracting to below approximately 24 Å with these preparations. An electron micrograph of a representative 2D crystal of B1-PSU, after staining with 1% uranyl acetate, is shown in Fig. 4a. Even at this low resolution, the LH1 rings, as observed previously (45, 50) are clearly visible. The diffraction pattern (Fig. 4b) indicates two superimposed lattices, arising from two crystal forms present in the same preparation. The absorption spectrum of the crystal, obtained after pelleting the 2D crystals by

spinning in a bench-top centrifuge for 5 min, followed by resuspension in reservoir buffer, shows identical spectral features to those of intact chromatophores, with the exception of a small red-shift (approximately 1 nm) in the LH1-Qy band of the crystals (Fig. 4c). In general, the B2-PSU crystals were of lesser quality (as judged by their optical diffraction pattern) than those obtained from B1-PSU, despite the apparently higher purity.

SDS-PAGE analysis (Fig. 2) of the crystals obtained from both B1-PSUs and B2-PSUs showed that all the major protein components, in particular the 40 kDa protein, observed after column chromatography, are retained in the crystals (Fig.2 and Fig. 3).

Mass spectrometry of the major 25-40 kDa bands. In order to identify the major protein components in the 25-40 kDa region of PSUs from both S1 and GKΔLM, the corresponding bands were excised from a Coomassie Blue-stained gel and subjected to mass spectrometry. For the S1-PSU, the assignment of the major polypeptides confirmed that the 25 kDa and 30 kDa bands correspond to the M- and H-subunits of the RC as expected. However, the 34 kDa band contained peptides arising from the major outer membrane proteins Por41, and the porin-associated protein (PAP), as well as the H-subunit. The clear separation of the 34 kDa from the 30 kDa band suggests that the H-subunit is comigrating with a Por41 fragment, as the native PAP protein also has the same molecular weight (34) so that a H-PAP complex would migrate at a molecular weight of 60 kDa, which is not observed. As the molecular weight of the H-Por41 complex differs from the H-subunit by only 4 kDa, we conclude that a proteolytic fragment of Por41 is bound to the H-subunit. Finally, the 40 kDa band could be assigned to the Por41 protein (34). No polypeptide corresponding to cytochrome c_1 was observed.

For the GKΔLM "PSU", both the 30 kDa and the 34 kDa bands yielded major peptides corresponding to Por41 and PAP. The 34 kDa band also contained a peptide arising from cytochrome c_1, which was confirmed by heme staining of the SDS-gels (data not shown). As above, the only major peptides arising from the 40 kDa band were due to Por41.

Separation of the 40 kDa porin from the PSU. To assess whether the S1 PSU was exclusively bound to the Por41 porin, the B2-PSU was analysed by sucrose gradient centrifugation in the presence of 2 mM DHPC. In the event, 4 coloured bands (1-4) were observed, banding at both heavy and light densities, with the major band corresponding to band 2 (Fig. 5). All of the bands exhibited absorption spectra characteristic of intact PSU

(data not shown). However, SDS-PAGE analysis revealed that whereas all bands contained components corresponding to the H, M and L subunits of the RC, as well as the α and β subunits of the LH1 complex, the Por41/PSU ratios appeared to differ significantly between the bands, with band 3 lacking this component completely. This result shows that the porin is not just serendipitously copurified in our procedure, but is physically bound, but not obligatorily so, to the PSU complex. As only the coloured bands have been examined here, it remains unclear as to whether free Por41 is still present in the final preparation. The heaviest PSU fraction also contains a low molecular weight component (approximately 14 kDa) not present in the other complexes, which lacks the unknown 18 kDa component. We suspect that the heaviest band corresponds to PSU-porin complexes forming higher aggregates, as centrifugation at 100 000 × g yielded a pellet showing a somewhat similar protein profile (Fig. 5), enriched in the lower molecular weight components (in particular the 18 kDa protein). This also indicates that the lower molecular weight components are not intrinsic to the minimal PSU.

DISCUSSION

In initiating the present study, we were motivated by the necessity to develop a purification procedure for the *R. rubrum* PSU which allows the isolation of large quantities of protein suitable for 2D- and 3D-crystallization, but avoids the use of excessively large quantities of the expensive detergent DHPC. Our choice of DHPC as the major purification detergent is due to the observation that this detergent allows the pigment-protein integrity of the PSU to be retained in a long-term stable form. DHPC has the useful property that it is dialyzable, due to its high CMC, and is conducive to crystallisation. Additionally we wanted to avoid gel filtration in the purification protocol, as we have repeatedly observed, not only for PSU but also for isolated LH1, that this procedure tends to remove small amounts of pigments (both BChla and Crt) from the complexes. This is also observable in the recent 2D crystallisation study of Jamieson *et al.* (21) where the absorption spectrum of gel-filtration-purified PSU from *R. rubrum* showed a A_{880}/Crt ratio of approximately 3.5, significantly larger than our value for all of the purified complexes reported here of 2.6, indicating that a significant fraction of the PSU complexes reported in the former study were carotenoid-depleted. In fact, in addition, to the orthorhombic crystal form of the PSU which is equivalent to the 2D cystals obtained from purified *R. rubrum* LH1 (24), these authors also reported a tetragonal crystal form, which we have only observed for the carotenoid-less LH1 and PSU complexes (45).

A further goal of our study was to identify the 40 kDa protein, which is present in purified preparations of S1-PSU, as well as those of GKΔLM "PSU", and was also present in PSU preparations from the carotenoid-less mutant G9, reported previously (45). The latter preparation also yield excellent tetragonal crystals, diffracting after negative stain to about 13.5 Å. Unfortunately, the protein composition of these latter crystals was not examined. Nevertheless, the co-purification of this component in all of our preparations, led us to suspect that it might be functionally important for the PSU complex. Two candidates for a functionally coupled 40 kDa protein suggest themselves from the literature. The first, is the cytochrome b_{565} component of the cytochrome bc_1 complex, which has been shown to migrate with an apparent molecular weight of 35 kDa on SDS-gels (27). The supramolecular association of the cytochrome bc_1 complex with the PSU has been the subject of intense discussion in recent years (12, 22, 23) and it has been suggested from image analysis of natural 2D-crystals from a nitrate-fixing strain of *Rb. sphaeroides* (23) that this complex is probably physically associated with the PSU. In this latter study, the SDS-PAGE analysis

revealed a plethora of protein components present in the membrane, so that the functional interpretation of the diffraction data remains difficult. A second candidate, was the LhaA protein encoded by the *puh* operon (4, 52) which also encodes the H-subunit of the RC. Beatty and coworkers (52) have shown that this protein, which has a nominal molecular weight of approximately 45 kDa, enhances the expression of the LH1 complex in *Rb. capsulatus*. Initially we hypothesised that the LhaA protein may migrate with an apparent molecular weight of 40 kDa on SDS-PAGE and could also be associated with the LH1 complex. However, the mass spectrometric data shows clearly that the LhaA protein in not present in purified PSU in the molecular weight region between 23 kDa and 40 kDa in detectable quantitites.

The mass spectrometric analysis clearly shows that the 40 kDa protein corresponds to the outer membrane porin Por41. Physiologically, the outer membrane porins and the PSU do not occupy the same compartment, the PSU being localised in the inner membrane and the OMPs in the outer membrane, so it is likely that the strong association detected here is an artefact of purification. Nevertheless, the strong binding of porin to the PSU is of significance for crystallisation attempts, as contamination with this protein, which is clearly present in 2D crystals of the PSU, may lead to poorer crystal quality. Even more disturbing is the finding that fragments of this porin, presumably present after proteolytic degradation during purification, are still bound strongly to the H subunit. We predict that the presence of these fragments will probably reduce the success of 3D crystallisation attempts, as the H-subunit with its large cytoplasmic domain is the most obvious candidate for protein-protein contacts in crystal packing.

In this study we have not examined the lower molecular weight region in detail. Nevertheless, we note that the 18 kDa protein is also present in most of our preparations, and this component appears to be removed by sucrose gradient centrifugation with no effect upon the spectral properties of the PSU. It is likely therefore, that this protein is not an essential component of the minimal PSU. In this context, it is interesting to note that the mass spectrometry data of the PSU from *Rps. palustris* (shown in the Supplementary Data section of (37)), for which crystals diffracting to 4.8 A were recently reported, also shows a strong peak at approximately 17 kDa. The mass spectrometry profile is interesting as the lower molecular weight region was strongly overrepresented, making the assessment of the PSU purity using this criterion difficult.

Finally, we believe that the identification of OMPs as contaminating proteins which are tightly-bound to the PSU, is a significant step forward in understanding the factors leading to poor crystals of these complexes. Our study shows that any purification procedure designed to provide high quality PSU from *R. rubrum*, will require a stringent step at an early stage to ensure the complete removal of OMPs. We believe that none of the published procedures so far fulfil this prerequisite. Our demonstration that sucrose gradient centrifugation is partially successful in achieving this goal, suggests that the binding of Por41 is not irreversible. We are presently attempting new purification strategies to achieve this goal on a quantitative basis.

ACKNOWLEDGEMENTS

We acknowledge the Landesgraduiertenförderung Baden-Württemberg (grant no. 7631.2) and the Deutsche Forschungsgemeinschaft (grant no. WR28/13-1) for financial support. We thank Janet Vonck and Deryck Mills from the Max-Planck-Institute of Biophysics in Frankfurt for performing optical diffraction.

REFERENCES

1. Ames, B. N. (1966) Assay of inorganic phosphate, total phosphate and phosphatases, *Method. Enzymol*. *8*, 115-118.
2. Bahatyrova, S., Frese, R. N., Siebert, C. A., Olsen, J. D., van der Werf, K. O., van Grondelle, R., Niederman, R. A., Bullough, P. A., Otto, C., and Hunter, C. N. (2004) The native architecture of a photosynthetic membrane, *Nature 430*, 1058-1062.
3. Barz, W., Vermeglio, A., Francia, F., Venturoli, G., Melandri, B., and Oesterhelt, D. (1995) Role of the PufX protein in photosynthetic growth of *Rhodobacter sphaeroides*. 2. PufX is required for efficient ubiquinone/ubiquinol exchange between the reaction center Q_B site and the cytochrome bc_1 complex, *Biochemistry 34*, 15248-15258.
4. Bérard, J., and Gingrás, G. (1990) The *puh* structural gene coding for the H subunit of *Rhodospirillum rubrum* photoreaction center, *Biochem. Cell Biol. 69*, 122-131.
5. Chang, M.C., Callahan, P.M., Parkes-Loach, P.S., Cotton, T.M., and Loach, P.A. (1990) Spectroscopic characterization of the light-harvesting complex of *Rhodospirillum rubrum* and its structural subunit, *Biochemistry 29*, 421-429.
6. Cogdell, R. J., Fyfe, P. K., Barrett, S. J., Prince, S. M., Freer, A. A., Isaacs, N. W., McGlynn, P., and Hunter, C. N. (1996) The purple bacterial photosynthetic unit, *Photosynth.Res*. *48*, 55-63.
7. Cogdell, R. J., Isaacs, N. W., Howard, T. D., McLuskey, K., Fraser, N. J., and Prince, S. M. (1999) How photosynthetic bacteria harvest solar energy, *J. Bacteriol. 180*, 3869-3879.
8. Cogdell, R. J., Lindsay, J. G., Valentine, J., and Durant, I. (1982) A further characterization of the B890 light-harvesting pigment-protein complex from *Rhodospirillum rubrum*, *FEBS Letts. 150*, 151-154.
9. Drews, G. (1978) Structure and development of the membrane system of photosynthetic bacteria, *Curr. Top. Bioenerg. 8B*, 161-207.
10. Engelhardt, H., Engel, A., and Baumeister, W. (1986) Stoichiometric model of the photosynhtetic unit of *Ectothiorhodospira halochloris*, *Proc. Natl. Acad. Sci. U.S.A. 83*, 8972-8976.
11. Farchaus, J. W., Barz, W., Grünberg, H., and Oesterhelt, D. (1992) Studies on the expression of the pufX polypeptide and its requirement for photoheterotrophic growth in *Rhodobacter sphaeroides*, *EMBO J. 11*, 2779-2788.

12. Fernandez-Valesco, J., and Crofts, A. R. (1991) Complexes or super complexes: inhibitor titrations show that electron transfer in chromatophores from Rhodobacter sphaeroides involves a dimeric UQH_2:cytochrome c_2 oxidoreductase, and is delocalized, *Biochem. Soc. Trans. 19*, 588-593.
13. Fotiadis, D., Qian, P., Phillipsen, A., Bullough, P. A., Engel, A., and Hunter, C. N. (2004) Structural analysis of the reaction center light-harvesting complex I photosynthetic core complex of *Rhodospirillum rubrum* using atomic force spectroscopy, *J. Biol. Chem. 279*, 2063-2068.
14. Fraser, N. J., Dominy, P. J., Ucker, B., Simonin, I., Scheer, H., and Cogdell, R. J. (1999) Selective release, removal, and reconstitution of bacteriochlorophyll a molecules into the B800 sites of LH2 complexes from *Rhodopseudomonas acidophila* 10050, *Biochemistry 38*, 9684-9692.
15. Ghosh, R., Hardmeyer, A., Thoenen, I., and Bachofen, R. (1994) Optimization of the Sistrom culture medium for large-scale batch cultivation of *Rhodospirillum rubrum* under semi-aerobic conditions with maximal yield of photosynthetic membranes, *Appl. Environ. Microbiol. 60*, 1698-1700.
16. Ghosh, R., Hauser, H., and Bachofen, R. (1988) Reversible dissociation of the B873 light-harvesting complex from *Rhodospirillum rubrum* G9+, *Biochemistry 27*, 1004-1014.
17. Ghosh, R., Rosatzin, T., and Bachofen, R. **(**1988) Subunit structure and reassembly of the light-harvesting complex from *Rhodospirillum rubrum* G9+, in *Photosynthetic Light-Harvesting Systems* (Scheer, H., and Schneider, S., Eds.), pp 93-102, Walter de Gruyter, Berlin.
18. Goodhew, C. F., Brown, K. R., and Pettigrew, G. W. (1986) Haem staining in gels, a useful tool in the study of bacterial *c*-type cytochromes*, Biochim. Biopys. Acta 852*, 288-294.
19. Hippler, M., Klein, J., Fink, A., Allinger, T., and Hoerth, P. (2001) Towards functional proteomics of membrane protein complexes: analysis of thylakoid membranes from *Chlamydomonas reinhardtii*, *Plant J. 28*, 595-606.
20. Hu, X., Damjanovic, A., Ritz, T., and Schulten, K. (1998) Architecture and function of the light harvesting apparatus of purple bacteria, *Proc. Natl. Acad. Sci. U.S.A. 95*, 5935-5941.

21. Jamieson, S. J., Wang, P., Qian, P., Kirkland, J. Y., Conroy, M. J., Hunter, C. N., and Bullough, P. (2002) Projection structure of the photosynthetic reaction centre-antenna complex of *Rhodospirillum rubrum* at 8.5 Å resolution, *EMBO J. 21*, 3927-3935.
22. Joliot, P., Vermeglio, A., and Joliot, A. (1996) Supramolecular organization of the photosynthetic chain in chromatophores and cells of *Rhodobacter sphaeroides*, *Photosynth. Res. 48*, 291-299.
23. Jungas, C., Ranck, J., Rigaud, J.-L., Joliot, P., and Verméglio, A. (1999) Supramolecular organization of the photosynthetic apparatus of *Rhodobacter sphaeroides*, *EMBO 18*, 534-542.
24. Karrasch, S., Bullough, P.A., and Ghosh, R. (1995) The 8.5 Å projection map of the light-harvesting complex 1 from *Rhodospirillum rubrum* reveals a ring composed of 16 subunits, *EMBO J. 14*, 631-638.
25. Kessi, J., Ghosh, R. and Bachofen, R. (1995) Purification of an LHI-RC-complex of *Rhodospirillum rubrum* by solubilization of chromatophores with a short-chain lecithin, *Photosynth. Res. 46*, 353-362.
26. Koepke, J., Hu, X., Muenke, C., Schulten, K., and Michel, H. (1996) The crystal structure of the light-harvesting complex II (B800-850) from *Rhodospirillum molischianum*, *Structure 4*, 581-597.
27. Kriauciunas, A., Yu, L., Yu, C.-A., Wynn, R. M., and Knaff, D. B. (1989) The *Rhodospirillum rubrum* cytochrome bc_1 complex: peptide composition, prosthetic group content and quinone binding, *Biochim. Biophys. Acta 976*, 70-76.
28. Laemmli, U. K. (1970) Cleavage of structural proteins during the assembly of the head of bacteriophage T4, *Nature 227*, 680-685.
29. Lilburn, T.G., Haith, C. E., Prince, R. C., and Beatty, J. T. (1992) Pleiotropic effects of the *pufX* gene deletion on the structure and function of the photosynthetic apparatus of *Rhodobacter capsulatus Biochim. Biophys. Acta 1100*, 160-170.
30. Lupo, D., and Ghosh, R. (2004) The reaction center H subunit is not required for high levels of light-harvesting complex 1 in *Rhodospirillum rubrum* mutants, *J. Bacteriol. 186*, 5585-5595.
31. McDermott, G., Prince, S. M., Freer, A. A., Hawthornthwaite-Lawless, A. M., Papiz, M. Z., Cogdell, R. J., and Isaacs, N. W. (1995) Crystal structure of an integral membrane light-harvesting complex from photosynthetic bacteria, *Nature 374*, 517-521.

32. Miller, K. R. (1982) Three-dimensional structure of a photosynthetic membrane, *Nature 300*, 53-55.
33. Monger, T. G., and Parson, W. W. (1977) Singlet triplet fusion in *Rhodopseudomonas sphaeroides*: a probe of the photosynthetic apparatus, *Biochim. Biophys. Acta 460*, 393-407.
34. Neumann, U., Benz, R., Rosenbusch, J. P., Stahl, B., and Weckesser, J. (1995) Porin and porin-associated protein (PAP) from *Rhodospirillum rubrum* FR1, *Microbiology 141*, 3155-3160.
35. Peterson, G. L. (1977) A simplification of the protein assay method of Lowry *et al.* which is more generally applicable, *Anal. Biochem. 83*, 346-356.
36. Picorel, R., Bélanger, G. and Gingras, G. (1983) Antenna holochrome B880 of *Rhodospirillum rubrum* S1. Pigment, phospholipid and polypeptide composition, *Biochemistry 22*, 2491-2497.
37. Roszak, A. W., Howard, T. D., Southall, J., Gardiner, A., Law, C. J., Isaacs, N. W., and Cogdell, R. J. (2003) Crystal structure of the RC-LH1 core complex from *Rhodopseudomonas palustris*, *Science 302*, 1969-1972.
38. Saegesser, R. (1992) Identifikation und Charakterisierung des Photosynthese - Genclusters aus *Rhodospirillum rubrum*, Ph.D. thesis, University of Zurich, Switzerland.
39. Scheuring, S., Francia, F., Busselez, J., Melandri, B. A., Rigaud J.-L., and Levy, D. (2004) Structural role of PufX in the dimerization of the photosynthetic core complex of *Rhodobacter sphaeroides*, *J. Biol. Chem. 279*, 3620-3626.
40. Scheuring, S., Reiss-Husson, F., Engel, A., Rigaud, J.-L., and Ranck, J.L. (2001) High-resolution AFM topographs of *Rubrivivax gelatinosus* light-harvesting complex LH2, *EMBO J. 20*, 3029-3035.
41. Scheuring, S., Rigaud, J.-L., and Sturgis, J. N. (2004) Variable LH2 stoichiometry and core clustering in native membranes of *Rhodospirillum photometricum*, *EMBO J. 23*, 4127-4133.
42. Scheuring, S., Seguin, J., Marco, S., Levy, D., Robert, B., and Rigaud, J.-L. (2003) Nanodissection and high-resolution imaging of the *Rhodopseudomonas viridis* photosynthetic core complex in native membranes by AFM. Atomic force microscopy, *Proc. Natl. Acad. Sci. U.S.A. 100*, 1690-1693.

43. Scheuring, S., Sturgis, J. N., Prima, V., Bernadac, A., Levy, D., and Rigaud, J.-L. (2004) Watching the photosynthetic apparatus in native membranes, *Proc. Natl. Acad. Sci. U.S.A. 101*, 11293-11297.
44. Sistrom, W. R. (1960) A requirement for sodium in the growth of *Rhodopseudomonas sphaeroides*, *J. Gen. Microbiol. 22*, 778-785.
45. Stahlberg, H., Dubochet, J., Vogel, H., and Ghosh, R. (1998) Are the light-harvesting I complexes from *Rhodospirillum rubrum* arranged around the reaction centre in a square geometry? *J. Mol. Biol. 282*, 819-831.
46. Stauber, E. J., Fink, A., Markert, C., Kruse, O., Johanningmeier, U., and Hippler, M. (2003) Proteomics of *Chlamydomonas reinhardtii* light-harvesting proteins, *Eukaryot. Cell 2*, 978-994.
47. Ueki, T., Kataoka, M., and Mitsui, T. (1976) Structural order in chromatophore membranes of *Rhodospirillum rubrum*, *Nature 262*, 809-810.
48. Vadeboncoeur, C., Mamet-Bratley, M., and Gingras, G. (1979) Photoreaction center of photosynthetic bacteria. 2. Size and quaternary structure of the photoreaction centers from *Rhodospirillum rubrum* strain G9 and from *Rhodopseudomonas sphaeroides* strain 2.4.1. *Biochemistry 18*, 4308-4314.
49. Vos, M., van Grondelle, R., van der Kooij, F. W., van der Poll, D., Amesz., J., and Duysens, L. N. M. (1986) Singlet-singlet annihiliation at low temperatures in the antenna of pruple bacteria, *Biochim. Biophys. Acta 850*, 501-502.
50. Walz, T., and Ghosh, R. (1997) Two-dimensional crystallization of the light-harvesting I reaction centre photounit from *Rhodospirillum rubrum*, *J. Mol. Biol. 265*, 107-111.
51. Walz, T., Jamieson, S. J., Bowers, C. M., Bullough, P. A., and Hunter, C. N. (1998) Projection structures of three photosynthetic complexes from *Rhodobacter sphaeroides*: LH2 at 6 Å, LH1 and RC-LH1 at 25 Å, *J. Mol. Biol. 282*, 833-845.
52. Young, C. S., Reyes, R. C., and Beatty, J. T. (1998) Genetic complementation and kinetic analyses of *Rhodobacter capsulatus orf1696* mutants indicate that the Orf1696 protein enhances assembly of the light-harvesting I complex, *J. Bacteriol. 180*, 1759-1765.

FIGURE LEGENDS

Fig. 1: (a) Absorption spectra comparison of isolated chromatophores from *R. rubrum* S1 (solid line) and GKΔLM (dashed line). (b) Second derivatives (F.D.(Abs)) of the absorption spectra shown in (a). (c) Absorption spectra comparison of B1-PSU and H-LH1. Spectra were normalised to the same A_{880nm} (or A_{874nm}) (2 mm).

Fig. 2: SDS-PAGE analysis. (left) SDS-gel of isolated chromatophores (Chr) from *R. rubrum* S1, the purified PSU from batch 1 (B1-PSU) and two 2D crystallisation trials (B1-2D Xlst1 and B1-2D Xlst2) from batch 1, and 2D crystals from PSU batch 2 (B2-2D Xlst). (right) SDS-gels of isolated chromatophores from GKΔLM (Chr) and purified H-LH1 complexes (H-LH1). Each lane contains 20 µg of protein and has been stained with Coomassie Brilliant Blue R250. Assignments of the known protein components, the H, M and L subunits of the RC as well as the LH1 complex (α and β polypeptides are not resolved in this system) are indicated. Two unknown proteins with a mass corresponding to 40 kDa and 34 kDa are also indicated.

Fig. 3. Densitometric analysis. Protein profiles obtained by grey-scale densitometry of the SDS-gels shown in Fig. 2. Spectra are shown with the same intensity scaling and assignments of the components corresponding to Fig. 2. The 40 kDa peak has been shaded for clarity. The molecular weights of the marker proteins are indicated on the horizontal bar.

Fig. 4 (a) TEM images of negatively stained crystallisation preparations from B1-PSU. (a) Negatively stained electron microscopy image of the 2D crystals. A series of molar DOPC/LH1 ratios as indicated, were employed. Scale bar represents 100 nm; (b) Diffraction pattern of the 2D crystals shown in (a) obtained by Fourier transform of the image; (c) Absorption spectra comparison of *R. rubrum* S1 chromatophores and the 2D crystals of the B1-PSU.

Fig. 5. Sucrose gradient and SDS-PAGE analysis of DHPC-solubilised B2-PSU. (A) B2-PSU (200 µg) was solubilised in 2 mM DHPC and the supernatant after centrifugation at 100 000 × g was banded on a linear sucrose gradient. (b) SDS-PAGE of the pellet after ultracentrifugation of the solubilised B2-PSU (42k-Pellet). The four colored bands visible in the sucrose gradient (Band 1 to Band 4) are indicated.

TABLES

Table 1. Mass spectrometric analysis of higher molecular weight proteins present in the PSU

Band	Assignment	Accession no.
S25	RC-M	gi|48766019
S30	RC-H	gi|48763353
	PAP	gi|48764070
S34	RC-H	gi|48763353
	PAP	gi|48764070
	Por41	gi|48763120
S40	Por41	gi|48763120
GK30	Por41	gi|48763120
	PAP	gi|48764070
GK34	Por41	gi|48763120
	PAP	gi|48764070
	RC-H	gi|48763353
	Cytochrome c_1	gi|48763600
	OmpA-like	gi|48763524
GK40	Por41	gi|48763120

Only the major polypeptides have been listed. The original sequence data has been tabulated in the Supplementary Data.

FIGURES

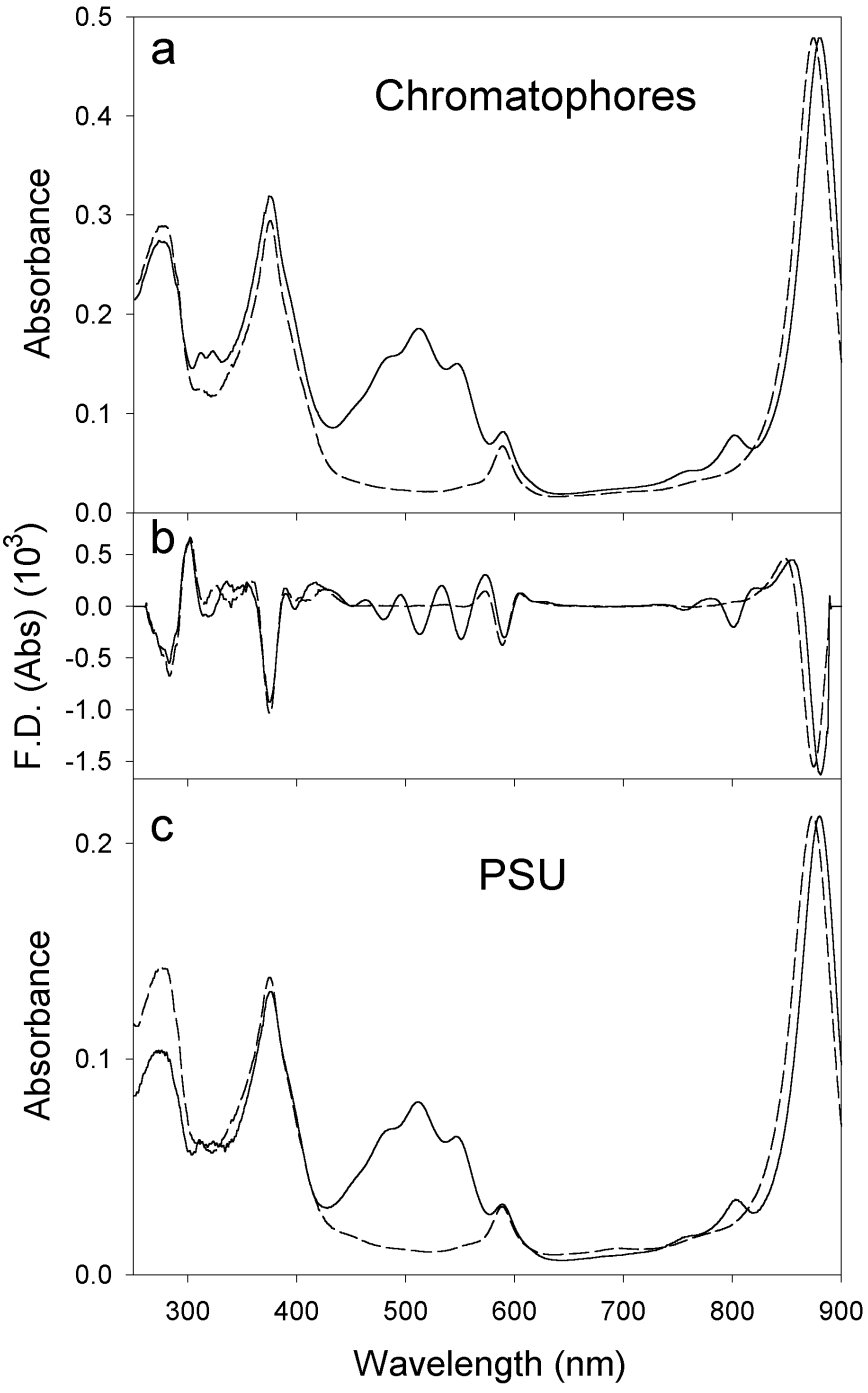

Figure 1

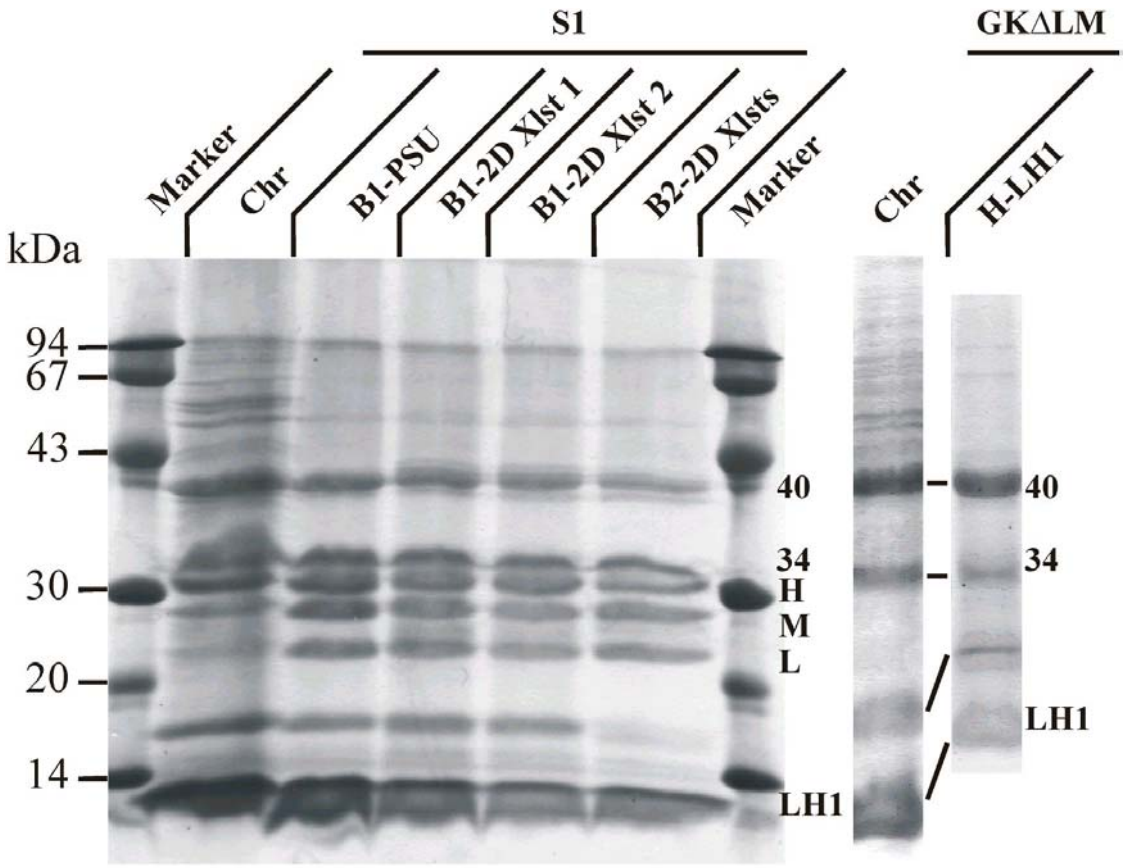
S1
GKΔLM
Marker
Chr
B1-PSU
B1-2D Xlst 1
B1-2D Xlst 2
B2-2D Xlsts
Marker
Chr
H-LH1
kDa
94
67
43
30
20
14
40
34
H
M
L
LH1
40
34
LH1

Figure 2

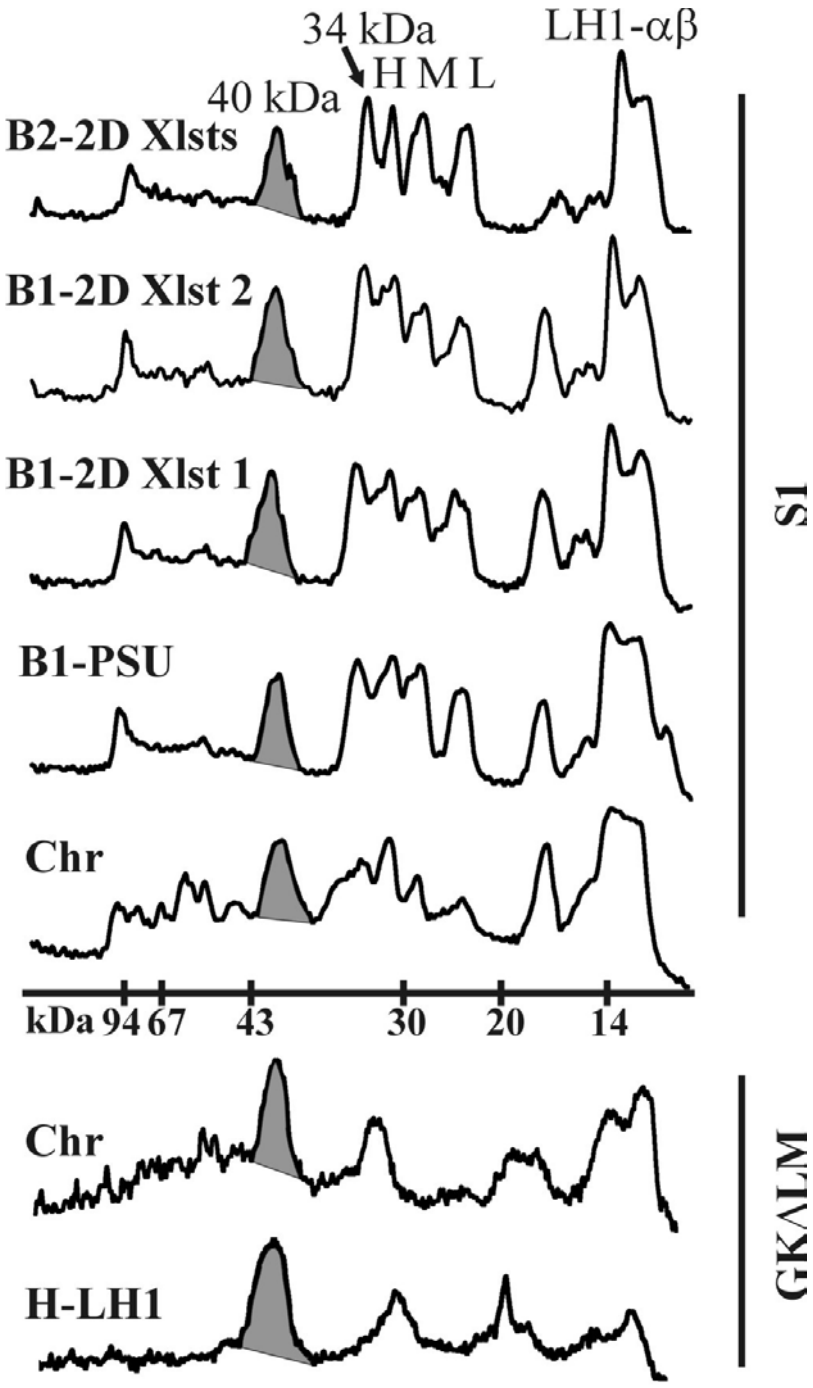
34 kDa
LH1-αβ
H M L
40 kDa
B2-2D Xlsts
B1-2D Xlst 2
B1-2D Xlst 1
B1-PSU
Chr
S1
kDa 94 67 43 30 20 14
Chr
H-LH1
GKΛLM

Figure 3

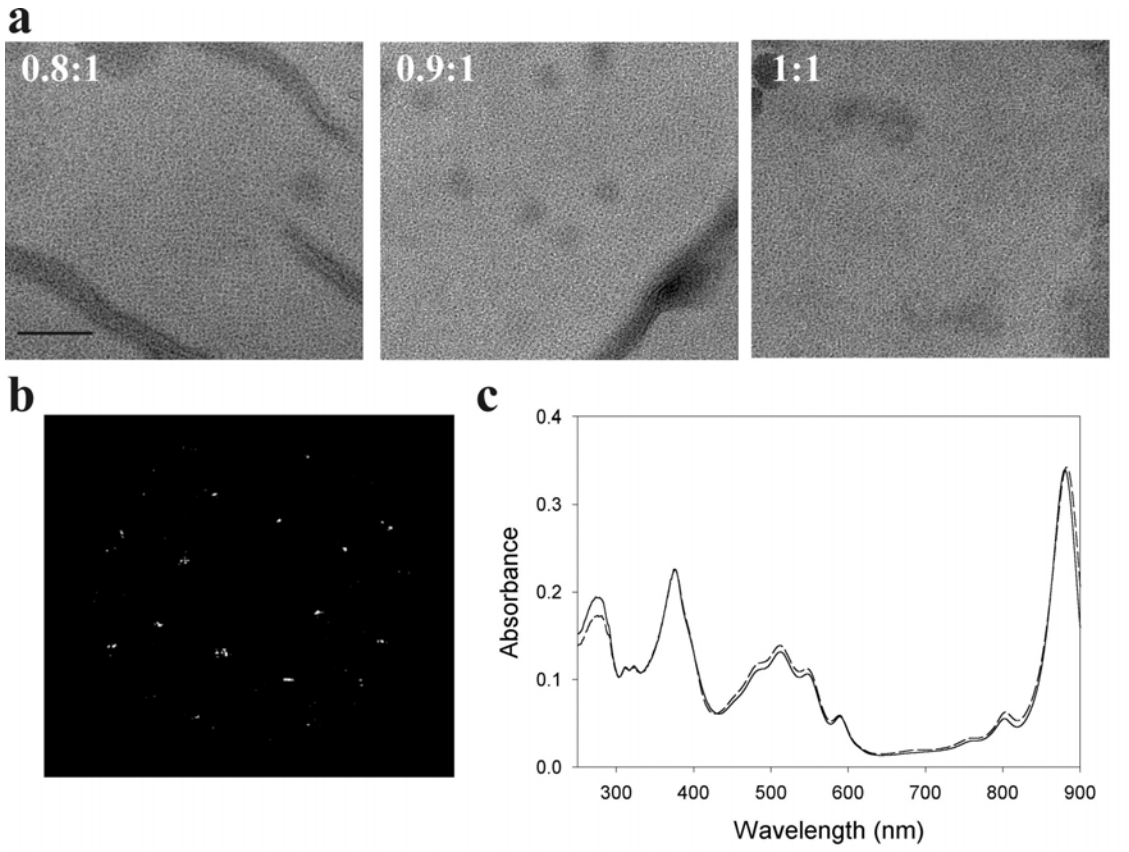
a
0.8:1
0.9:1
1:1
b
c
Absorbance
0.0
0.1
0.2
0.3
0.4
300
400
500
600
700
800
900
Wavelength (nm)

Figure 4

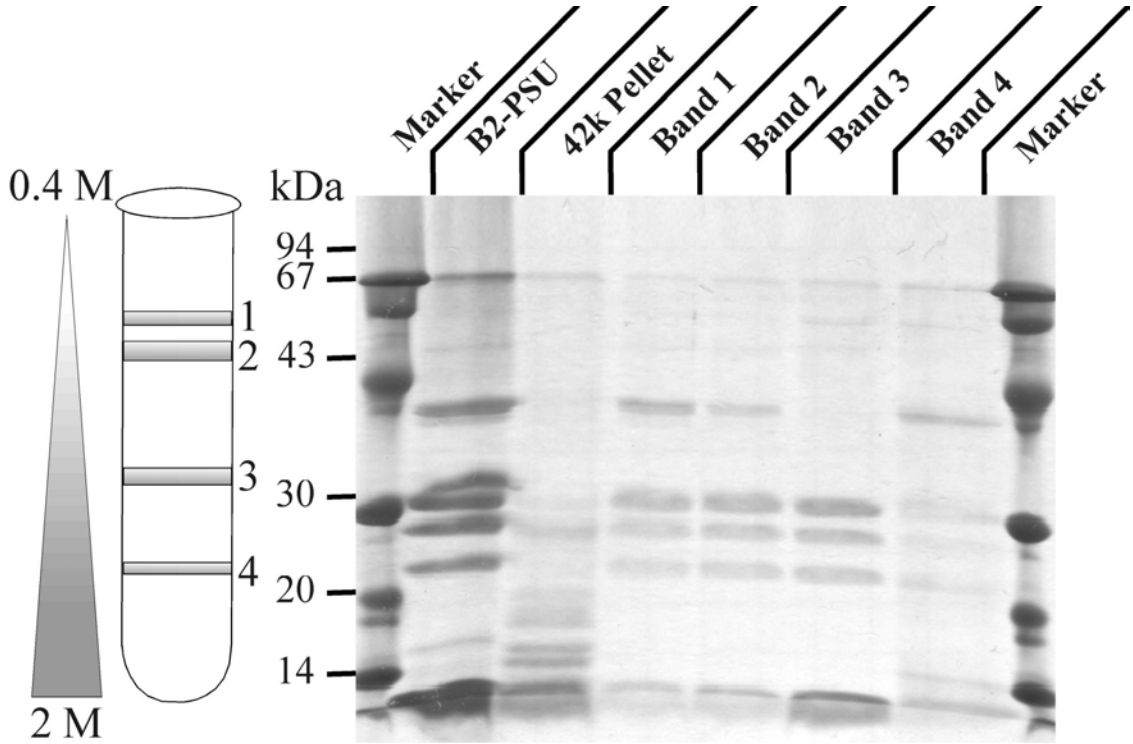
Marker
B2-PSU
42k Pellet
Band 1
Band 2
Band 3
Band 4
Marker
0.4 M
2 M
kDa
94
67
43
30
20
14
1
2
3
4

Figure 5

SUPPLEMENTARY DATA

Major polypeptides found by mass spectrometry

	Peptides	Assignment	Accession no.
S1-PSU			
S25			
	(R)WTMGFNATMESIHR		
	(R)LGKPGFSYWLGK		
	(R)LGGDREVEQITDR	M-subunit of the reaction centre	gi|48766019|ref|ZP_00270569.1|
	(K)PGFSYWLGK		
	(R)LGKPGFSYWLGK		
S34			
	(R)DELPDLTLGGQPAIVPLR		
	(K)VMAYYSSGYLYSDR		
	(R)TAPTAGAPFEPTGNPMTDAVGPAAYALR		
	(K)INSLQGLGSVFSIAR		
	(R)DELPDLTLGGQPAIVPLR		
	(K)VMAYYSSGYLYSDRV		
	(K)INSLQGLGSVFSIARPK		
	(R)VAPTFSVAAEDTDPR		
	(R)EEDKVMAYYSSGYLYSDRV		
	(K)TGATYAAPNFK		
	(K)VTDLWIDR	H-subunit of the reaction centre	gi|48763353|ref|ZP_00267908.1|
	(R)YLEVELAATPGR		
	(K)TVTVQSILAR		
	(R)YLEVELAATPGRK		
	(R)GRDMAFEILSREADQAMYGAK		
	(R)HFANVPTIAK		
	(R)YLEVELAATPGR		
	(K)VKDEAEVANRAK		
	(K)TGATYAAPNFK		
	(K)VTDLWIDR		
	(R)REGYPLEDAISGK		
	(R)TVYQQLMETTTPGGYPVLQHVR		
	(K)GPLGWDASSVSLGR	linocin/CFP29 homolog	gi|48765217|ref|ZP_00269768.1| COG1659:
	(R)GVDGPYALVLGR		
	(R)SALVTALGAGAPSSNPTVAAK		
	(R)LAVPTADGVVEQQNR	Porin-associated protein (PAP)	gi|48764070|ref|ZP_00268623.1| COG2885:
	(K)LAAAGQTPAPTAMAER		
S30			
	(K)DYVALAAHEANYGDWDDTAYYTNK	PAP	gi|48764070|ref|ZP_00268623.1| COG2885:
	(K)QNFEIAMNALGGAPAPAVVSEGFK		
	(R)GIASEVLTLEAYGEER		
	(R)SALVTALGAGAPSSNPTVAAK		
	(K)LAAAGQTPAPTAMAER		
	(R)ELGSYTGELTAAR		
	(R)LAVPTADGVVEQQNR		
	(K)VFFALDSAR		
	(R)LSPESEATLDR		
	(K)DYVALAAHEANYGDWDDTAYYTNK		
	(R)ELGSYTGELTAAR		
	(R)LSPESEATLDR		

	(K)VFFALDSAR		
	(K)INSLQGLGSVFSIAR (R)DELPDLTLGGQPAIVPLR (K)VMAYYSSGYLYSDRV (K)VMAYYSSGYLYSDR (R)EEDKVMAYYSSGYLYSDR (R)EEDKVMAYYSSGYLYSDRV (R)TAPTAGAPFEPTGNPMTDAVGPAAYALR (K)INSLQGLGSVFSIARPK (R)EEDKVMAYYSSGYLYSDR (K)SKTVTVQSILAR (R)VAPTFSVAAEDTDPR (R)EEDKVMAYYSSGYLYSDRV (K)INSLQGLGSVFSIARPK (R)YLEVELAATPGRK (R)YLEVELAATPGR (R)VAPTFSVAAEDTDPR (K)VTDLWIDRASIAIR (R)HFANVPTIAK (K)TGATYAAPNFK (R)HFANVPTIAK (K)TGATYAAPNFK (R)YLEVELAATPGR (R)REGYPLEDAISGK (R)EGYPLEDAISGK (R)YLEVELAATPGR (K)VTDLWIDR	H-subunit of the reaction centre	gi|48763353|ref|ZP_00267908.1|
	(R)TVYQQLMETTTPGGYPVLQHVR (R)GASDADLDPVIEAAR (K)GPLGWDASSVSLGR (R)GTLTVTLAAR (R)GVDGPYALVLGR (K)AWAEIETEAR	linocin/CFP29 homolog	gi|48765217|ref|ZP_00269768.1| COG1659:
S40			
	(R)DLVQMAVGYDAEFGDVGLK (R)DLVQMAVGYDAEFGDVGLK (K)VTYVTPQFYGFSAGVSYTPNVGGPR (R)SGVFDEFMVVAPTVGSVSLDDSK (K)MGPGIDLVGNVFYGETGIGSSNVDASR (K)MGPGIDLVGNVFYGETGIGSSNVDASR (R)IELEAEADNANNADK (K)DGGREDGFGIDTDTEVYFSGSTTLDNGITVAAR (K)LGGKQEQYFGGVASTK (R)VWTAGLSYAVGPYSVGFTYGQTDNDSK (R)VWTAGLSYAVGPYSVGFTYGQTDNDSK (K)LGGKQEQYFGGVASTK (K)QEQYFGGVASTK (R)EGFGAVTGIVLAF (R)VWTAGLSYAVGPYSVGFTYGQTDNDSK (K)QWVTVSGAFGK (K)QEQYFGGVASTK (R)SGVFDEFMVVAPTVGSVSLDDSK (K)QWVTVSGAFGK	Outer membrane porin (Por41)	gi|48763120|ref|ZP_00267676.1| COG3203:
GKΔLM -"PSU"			
GK34			
	(R)DLVQMAVGYDAEFGDVGLK (R)DLVQMAVGYDAEFGDVGLK (K)MGPGIDLVGNVFYGETGIGSSNVDASR	Por41	gi|48763120|ref|ZP_00267676.1| COG3203:

	(K)MGPGIDLVGNVFYGETGIGSSNVDASR (R)EGFGAVTGIVLAF (R)VWTAGLSYAVGPYSVGFTYGQTDNDSK (K)QWVTVSGAFGK (K)QWVTVSGAFGK		
	(K)QNFEIAMNALGGAPAPAVVSEGFK (K)DYVALAAHEANYGDWDDTAYYTNK (R)GIASEVLTLEAYGEER (R)SALVTALGAGAPSSNPTVAAK (R)LAVPTADGVVEQQNR (K)LAAAGQTPAPTAMAER (K)VFFALDSAR (R)LSPESEATLDR (K)VFFALDSAR (R)ELGSYTGELTAAR (R)LSPESEATLDR (R)VEVVFGG	PAP	gi|48764070|ref|ZP_00268623.1| COG2885:
	(K)TDTGYAAGGAAGYAFGGGPR (K)ADYDAYYNHTVLVGLR (K)ADYDAYYNHTVLVGLR (R)SGGDAYNLALSK (R)RAEAVVGELER (R)FLGTTGLDFK (K)GEADPLVPTPDGVR (R)RAEAVVGELER (R)LELEGTWR (R)AEAVVGELER (R)LELEGTWR (R)FLGTTGLDFK	OmpA-like protein	gi|48763524|ref|ZP_00268078.1| COG2885:
	(K)VMAYYSSGYLYSDRV	H-subunit of the reaction centre	gi|48763353|ref|ZP_00267908.1|
	(K)GLEVAFNEAK (K)AAAAANGGAAPPDLSLLAK (K)GLEVAFNEAK	Cytochrome c_1	gi|48763600|ref|ZP_00268154.1| COG2857:
GK30			
	(R)DLVQMAVGYDAEFGDVGLK (K)MGPGIDLVGNVFYGETGIGSSNVDASR	Por41	gi|48763120|ref|ZP_00267676.1| COG3203:
	(R)SALVTALGAGAPSSNPTVAAK (R)LSPESEATLDR (K)VFFALDSAR (R)LSPESEATLDR	PAP	gi|48764070|ref|ZP_00268623.1| COG2885:
GK40			
	(R)DLVQMAVGYDAEFGDVGLK (R)DLVQMAVGYDAEFGDVGLK (K)MGPGIDLVGNVFYGETGIGSSNVDASR (R)SGVFDEFMVVAPTVGSVSLDDSK (K)LGGKQEQYFGGVASTK (K)DGGREDGFGIDTDTEVYFSGSTTLDNGITVAAR (R)EGFGAVTGIVLAF (R)VWTAGLSYAVGPYSVGFTYGQTDNDSK (K)QEQYFGGVASTK (K)SWLGAGNGINGSVTQLYLDQSLDDDDAK (R)VWTAGLSYAVGPYSVGFTYGQTDNDSK (K)SGVDAAIYK (K)QWVTVSGAFGK	Por41	gi|48763120|ref|ZP_00267676.1| COG3203:

ÜBERSICHTSARTIKEL

Is the light-harvesting complex 1 of *Rhodospirillum rubrum* circularly symmetric? An overview of the controversy

by

Robin Ghosh*[1], Domenico Lupo[1], Uwe Gerken[2], Jörg Wrachtrup[3], Andreas Kuhn[2], Felix Autenrieth[1,4] and Klaus Schulten[4]

[1]Dept. of Bioenergetics, Institute of Biology, University of Stuttgart, Pfaffenwaldring 57, D-70550 Stuttgart, Germany

[2]Institute of Microbiology, University of Hohenheim, Garbenstraße 30, D-70599 Stuttgart, Germany

[3]Institute of Physics, University of Stuttgart, Pfaffenwaldring 57, D-70550 Stuttgart, Germany

[4]Beckmann Institute, Theoretical and Computational Biophysics Group, University of Illinois 405 N Mathews Avenue, Urbana, IL 61801 USA

*corresponding author: tel.: (+49711) 685 5047; fax: (+49711) 685 5096;
email: robin.ghosh@bio.uni-stuttgart.de

Running title: Is the light-harvesting complex 1 circularly symmetric?

ABSTRACT

Image analysis of cryoelectron micrographs of light-harvesting complex 1 (LH1) from *Rhodospirillum rubrum* reconstituted into lipid bilayers has indicated that deviations from circular symmetry is common. High-resolution data obtained from 2D crystals of the LH1 complex in combination with the reaction center using both cryoelectron microscopy (cryoEM) and atomic force microscopy have also indicated that the LH1 complex may have an elliptical geometry *in vivo*. On the other hand, single molecule spectroscopy of single LH1 complexes reconstituted into lipid bilayers at high lipid-to-protein ratios, performed in our group, indicates that the complexes are predominantly circularly symmetric. The circular symmetry is stabilized when the LH1 complexes are associated with reaction centers. These latter studies indicate that the asymmetry of the LH1 complexes in 2D crystals may be due to packing effects. A new circular symmetric model of the LH1 complex reveals a simple design of interaction domains responsible for intra- and interdimeric interaction.

KEYWORDS

Light-harvesting complex, reaction center, photosynthesis, single molecule spectroscopy, 2D crystallization

A SHORT OVERVIEW OF THE PRESENT CONTROVERSY

The light-harvesting complex 1 (LH1) from the purple non-sulphur bacterium *Rhodospirillum rubrum* has been well-characterized both biochemical and biophysical techniques. The basic building block of the LH1 complex contains 2 non-identical transmembrane polypeptides, α and β, composed of 52 and 54 amino acids, respectively, 2 bacteriochlorophyll a (BChla) molecules and 1 carotenoid (Crt, in the wild-type complex, spirilloxanthin) (2, 12). Early studies using cryoelectron microscopy of two-dimensional crystals showed the functional complex to be assembled from 16 $\alpha\beta(BChla)_2Crt$ subunits assembled in a closed ring (8). More recent studies using both cryoEM (7) as well as atomic force microscopy (3) have shown that the closed ring-like structure (see Fig. 1 for a more recent projection obtained at resolution of 5Å) is also present in the intact photosynthetic unit (PSU), which is composed of a LH1 complex associated with a reaction center (RC). All of these studies have indicated that the LH1 ring is not truly circularly symmetric but possesses a pronounced ellipticity (3, 7, 8). In fact, the AFM work has suggested further that the ellipticity is enhanced in the presence of the RC. An RC-induced distortion of the ring is tempting from the point of view of function, as it would induce a localized excitonic "focus" for excitation energy to be passed efficiently to the RC (15). In an alternative approach, Ketelaars *et al.* (9) have examined the *R. rubrum* RC-LH1 complex solubilized in lauryldimethylamine-N-oxide (LDAO), using single molecule spectroscopy, and shown that up to 5 oligomeric forms may be present, all of which show a pronounced ellipticity, thus tending to confirm the structural biological studies.

However, set against these latter studies is our recent work using single molecule spectroscopy of single LH1 complexes and PSUs (also designated here as RC-LH1 complexes) incorporated into lipid bilayers at very high lipid-to-protein ratios (4, 5). Single molecule fluorescence polarization spectroscopy is exquisitely sensitive to very small deviations from circular geometry and thus provides a stringent test of symmetry in the presence of the homogenous potential of the lipid bilayer. A critical aspect in interpreting these studies is the biochemical procedure necessary for gently dissociating the RC-LH1 complexes from the chromatophore membrane (see Fig 1b for a high resolution AFM image of the native *R. rubrum* chromatophore membrane) without inducing pigment-protein dissociation. So far, only a single detergent, diheptanoyl-*sn*-phosphatidylcholine (DHPC) seems to fulfill this criterium (14), and then only at a critical detergent concentration (generally 20 mM) . As is usual in membrane protein biochemistry, subsequent to extraction, detergent concentration must be rapidly reduced to a concentration (2mM) necessary for

maintaining the RC-LH1 complexes in stable form. A convenient measure of the integrity of the RC-LH1 complex is the intensity width, and absorption maximum of the LH1-Q_y. The detergent concentration is usually adjusted so that the highest concentration immediately prior to loss of A_{880} intensity is employed. At this concentration only single LH1 rings (containing RCs) are present (see (5)). Higher concentrations cause loss of A_{880} intensity, with attendant dissociation of the complexes. In our hands, other commonly used detergents (e. g. β-octyl glucoside, LDAO) do not allow RC-LH1 dissociation to be achieved without simultaneously affecting the pigment-protein structural integrity of the complex.

A particular striking measure of the asymmetry of the complex is the splitting of the near-IR excitation maxima observed when single LH1 or RC-LH1 molecules immobilized at 1.8 K are excited with two orthogonal polarization directions and monitored by fluorescence emission. Theoretical calculations show that the splitting (ΔE) is exquisitely sensitive to small changes of pigment geometry deviating from circular symmetry (see (5) for details). The deviation from circular geometry (or ellipticity) is conveniently measured by the (a/b) ratios of the major (a) and minor (b) axes. In a recent paper (4), we have shown that in the absence of RC, the orthogonal excitation maxima of 70% of the total LH1 reconstituted into lipid bilayers show perfect correspondence (see Fig. 1c insert in Fig. 1d) i. e. this fraction is present in circularly symmetric form. LH1 isolated in detergent, however, shows a much broader distribution of splittings, with only about 30% showing perfect correspondence of the excitation maxima. Strikingly, in the presence of bound RC, almost all of the LH1 complexes examined showed a perfect correspondence of the orthogonal excitation maxima, even when solubilized in detergent (see Fig. 1d and (5) for details). These studies show unambiguously that the LH1 complex is predominantly circularly symmetric when immersed in a lipid bilayer exerting a homogeneous lateral potential, and that the symmetry is stabilized by the presence of the RC, in stark contrast to the results obtained from cryoEM and AFM. In this context, we note that the accuracy of the excitation maxima spitting is easily able to detect a/b variations measured by cryoEM and AFM (see Fig. 1e). We also suggest that the ellipticity and different oligomeric forms of the *R. rubrum* complex solubilized in LDAO, as described by Ketelaars *et al.* (9) is due to a different effect, namely that the latter detergent is unsuitable for preparation of a RC-LH1 complex without attendant disruption of pigment-protein interaction. We intend to examine this aspect further in the future.

Our confirmation of circularly symmetric symmetry of the LH1 complex in a lipid bilayer, has allowed us to now construct a sophisticated model for the complex. Although other models are available, for *R. rubrum*, only the model of the $\alpha\beta(BChla)_2$ dimer has been presented, at a considerably lower level of sophistication than that presented here. Although full details of model construction will be presented elsewhere, it suffices to report that after initial "threading" to the $\alpha\beta(BChla)_2$ dimer to the dimer model from *Rhodobacter sphaeroides*, the dimer was energy minimized at 300 K and a dielectric constant of 1-10 for 10 000 steps using X-PLOR (1) and assembled into the 16-fold ring and minimized with heating and cooling for a further 3 600 steps. The complete procedure was performed with and without carotenoid. The final projection structure is shown in Fig 1f. A careful examination of the tetramer ($(\alpha\beta(BChla)_2)_2$) which is the minimal unit necessary for defining all intra (IA)- and inter-(IE)-dimeric domains of the final structure revealed a very simple design principle, probably common to all LH1 complexes. In particular, only 5 small protein-protein interaction domains (shown in Fig 1g) are sufficient to assemble the final structure. 3 of these domains are involved in α-β (IA) interaction, and two domains (one at each end of the transmembrane helix, involved in α-α or β-β interaction, respectively) are involved in interdimeric interaction. All of the IA and IE domains defined by our model appear to be highly conserved in other LH1 complexes, as judged from sequence homologies (see (16)). The other major interaction domains involve BChl-protein interaction, as has been observed for the LH2 structures determined by X-ray crystallography (10, 11). Full details of this model, which we hope will become a useful tool in the design of new mutagenesis experiments to examine structure function relationships, will be presented elsewhere.

Our results are consistent with the simple result for elementary physics, that a closed structure assembled from identical units and existing in a homogenous potential shows an energy minimum at a point where all energetic interactions between adjacent subunits are numerically equal (i. e. the structure is circularly symmetric). The results also indicate that the elliptical effects observed by cryoEM and AFM may arise from packing interactions between PSU complexes. The latter may correspond more closely to the physiological situation (see Fig. 1b) and in view of its potential functional importance, deserves more attention.

ACKNOWLEDGMENTS

We acknowledge the Landesgraduiertenförderung Baden-Württemberg (grant no. 7631.2) and the Deutsche Forschungsgemeinschaft (grant no. WR28/13-1) for financial support.

REFERENCES

1. Brünger AT (1996) X-PLOR, version 3.8: a system for X-ray crystallography and NMR. Yale University Press, New Haven, CT
2. Cogdell, RJ, Lindsay JG, Valentine J and Durant I (1982) A further characterization of the B890 light-harvesting pigment-protein complex from *Rhodospirillum rubrum*. FEBS Letts 150: 151-154.
3. Fotiadis D, Qian P, Philippsen A, Bullough PA, Engel A and Hunter CN (2004) Structural analysis of the reaction center light-harvesting complex I photosynthetic core complex of *Rhodospirillum rubrum* using atomic force microscopy. J Biol Chem 279: 2063-2068
4. Gerken U, Jelezko F, Götze B, Branschädel M, Tietz C, Ghosh R and Wrachtrup J (2003) The membrane environment reduces the accessible conformational space available to an integral membrane protein. J Phys Chem B 107: 338-343
5. Gerken U, Lupo D, Tietz C, Wrachtrup J and Ghosh R (2003) Circular symmetry of the light-harvesting 1 complex from *Rhodospirillum rubrum* is not perturbed by interaction with the reaction center. Biochemistry 42: 10354-10360
6. Humphrey W, Dalke A and Schulten K (1996) VMD: visual molecular dynamics. J Mol Graph 14: 33-38
7. Jamieson SJ, Wang P, Quian P, Kirkland JY, Conroy MJ, Hunter CN and Bullough PA (2002) Projection structure of the photosynthetic reaction center-antenna complex of *Rhodospirillum rubrum* at 8.5 Å resolution. EMBO J 21: 3927-3935
8. Karrasch S, Bullough PA and Ghosh R (1995) The 8.5 Å projection map of the light-harvesting complex I from *Rhodospirillum rubrum* reveals a ring composed of 16 subunits. EMBO J 14: 631-638
9. Ketelaars M, Hofmann C, Köhler J, Howard TD, Cogdell RJ, Schmidt J and Aartsma TJ (2002) Spectroscopy on individual light-harvesting 1 complexes of *Rhodopseudomonas acidophila*. Biophys J 83: 1701-15
10. Koepke J, Hu X, Muenke C, Schulten K and Michel H (1996) The crystal structure of the light-harvesting complex II (B800-850) from *Rhodospirillum molischianum*. Structure 4: 581-597
11. McDermott G, Prince SM, Freer AA, Hawthornthwaite-Lawless AM, Papiz MZ, Cogdell RJ and Isaacs NW (1995) Crystal structure of an integral membrane light-harvesting complex from photosynthetic bacteria. Nature 374: 517-521

12. Picorel R, Bélanger G and Gingras G (1983) Antenna holochrome B880 of *Rhodospirillum rubrum* S1. Pigment, phospholipid and polypeptide composition. Biochemistry 22: 2491-2497
13. Scheuring S, Seguin J, Marco S, Levy D, Robert B and Rigaud JL (2003) Nanodissection and high-resolution imaging of the *Rhodopseudomonas viridis* photosynthetic core complex in native membranes by AFM. Atomic force microscopy. Proc Natl Acad Sci USA 100: 1690-1693
14. Stahlberg H, Dubochet J, Vogel H and Ghosh R (1998) Are the light-harvesting I complexes from *Rhodospirillum rubrum* arranged around the reaction center in a square geometry? J Mol Biol 282: 819-831
15. van Grondelle R (1985) Excitation energy transfer, trapping and annihilation in photosynthetic systems. Biochim Biophys Acta Reviews 811: 147-195
16. Zuber H and Cogdell RJ (1995) Structure and organisation of purple bacterial antenna complexes. In: Blankenship RE, Madigan MT and Bauer CE (ed) Anoxygenic photosynthetic bacteria, pp 315-348. Kluwer Academic Publishers, Dordrecht, The Netherlands

FIGURE LEGENDS

Fig. 1: (a) Projection map at 5 Å resolution obtained by cryoelectron microscopy of 2D crystals of purified LH1 (wild-type complex) reconstituted into DOPC and embedded in amorphous ice as described in (8). Crystals belong to the space group p22121 and the unit cell is a = 129 Å and b = 195 Å; (b) high-resolution AFM images of native chromatophore membranes obtained from the carotenoid-less mutant *R. rubrum* G9. Membranes were immobilized by adsorption to mica immediately prior to the measurement. The tightly packed particles visible in both panels correspond to the PSUs (full details will be presented elsewhere); (c) typical fluorescence excitation spectra of membrane-reconstituted isolated LH1-RC complexes. The red and the blue spectra were measured at orthogonal polarization directions (arrows, inset) of the exciting light. The figure has been adapted from (5); (d) histogram of the splitting ΔE of the $|k = \pm 1\rangle$ states for the membrane-reconstituted (red) and detergent-solubilized (green) LH1-RC complexes. To emphasize how the presence of the RC influences the energetic positions of the $|k = \pm 1\rangle$ states the corresponding histogram obtained for single LH1 complexes from *R. rubrum* (without RC, adapted from Gerken *et al.* (4)) is shown in the inset; (e) Variation of the splitting (ΔE) of the $|k = \pm 1\rangle$ states with elliptical deformation, expressed as the axis ratio of the ellipse a/b. The symbols show data taken from the SM study (9) ((○), ΔE= 116 cm^{-1}), from the cryoEM study (7) ((□), a/b=1.12) and from the AFM study (13) ((Δ), a/b=1.05) (■) depicts the mean ΔE value measured for the complexes obtained in our laboratory (f) Our model of the *R. rubrum* LH1 ring assembled from 16 αβ$(BChla)_2$Crt subunits and energy minimized as described in the text (drawn with VMD (6)). Colors: blue, α-subunit; red, β-subunit; cyan, BChla; yellow, Crt; (g) schematic representation of the inter-and intra dimeric interactions deduced from our model of the $(\alpha\beta(BChla)_2Crt)_2$ dimer. The amino acid sequences of the interaction domains are shown in the closed boxes.

FIGURES

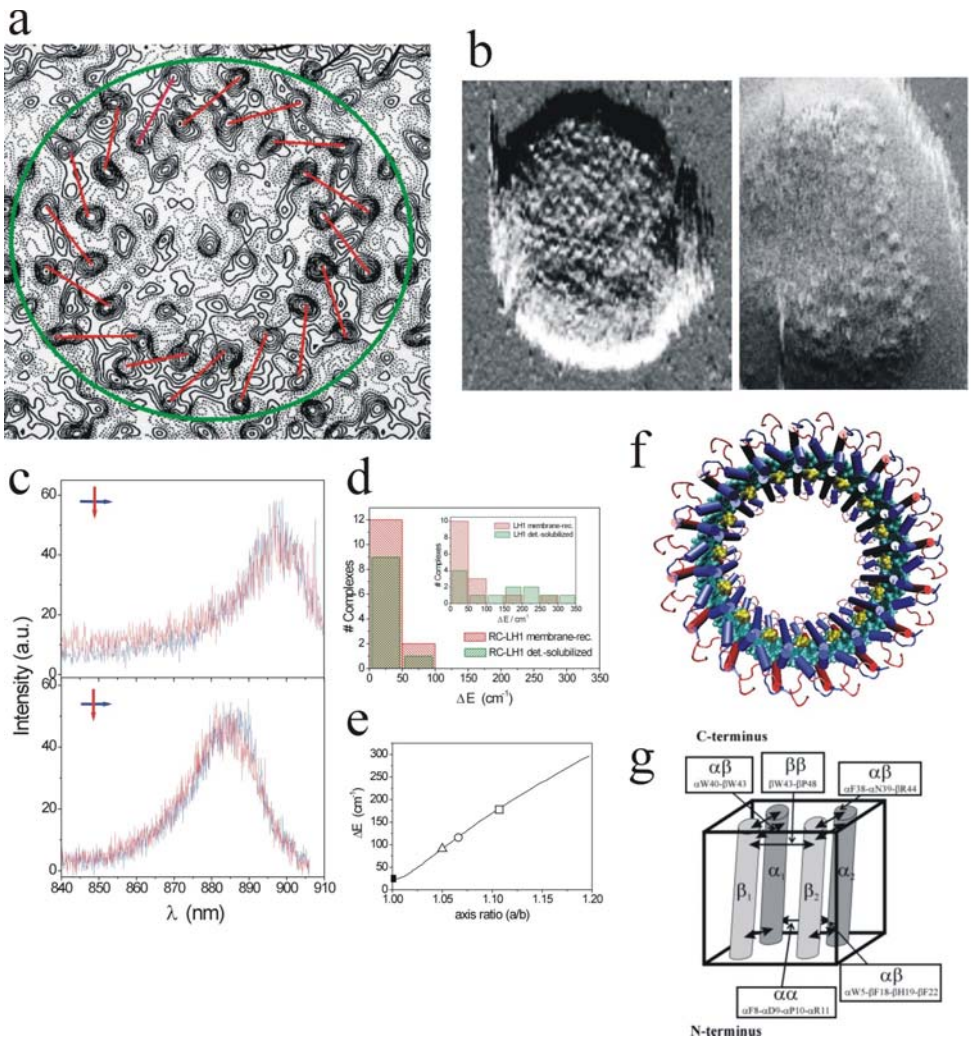

Figure 1

APPENDIX

A provoking hypothesis: does the H-subunit participate directly in the LH1 ring?

by

R. Ghosh and D. Lupo, Dept of Bioenergetics, Institute of Biology, University of Stuttgart

We propose here a new hypothesis for the interaction of the reaction center (RC) with the light-harvesting 1 (LH1) complex. We believe that the resolution so far achieved by structural biological means (cryoEM (2), AFM (1) and X-ray crystallography (4)) is still insufficient to precisely position the RC and particularly the H-subunit of the RC within the LH1 complex. We base our hypothesis on the following observations:

(1) the circular symmetry of the complex is *stabilized* by the interaction with the RC. Since the RC cannot bind simultaneously at all equivalent binding sites (due to its irregular geometry), this observation would seem to contradict the simple physical argument present in the main paper, namely that a circularly symmetric structure can only be maintained in a homogeneous restoring potential provided by the lipid bilayer. Binding of an RC to particular LH1 sites would cause the binding energies between subunits to be unequally distributed thus inducing a local asymmetry.

(2) We have recently reported an H-subunit-deletion mutant of *R. rubrum* (3) which expresses and assembles photosynthetic levels of LH1 complexes. The integrity of pigment-pigment interaction in the LH1 complex, as monitored by absorption spectroscopy and near-IR circular dischroism seem to be unchanged when compared to the wild-type LH1. The mutant still expresses 4% functional RC (presumably as an LM complex) but is completely unable to grow photosynthetically, even after several months. Recently we discovered (using ulrafast transient spectroscopy (in collaboration with Josef Wachtveitl, University of Frankurt) that the microscopic details of LH1 pigment-pigment interaction have indeed been significantly affected by the lack of an H-subunit (full details will be published elsewhere), suggesting that the H-subunit is interacting strongly with the subunits of the LH1 ring.

We are presently examining the hypothesis that the transmembrane (TM) α-helix of the RC-H subunit is not binding to the inner surface of the LH1 ring but is *integrated into the ring structure*, possibly replacing one of the inner α-subunits of the ring. The integration of the H-TM-helix into the LH1 ring would still allow a nearly homogenous distribution of binding energies, and would probably only minimally affect the absorption and near-IR-CD spectrum,

but may still affect the microscopic details of excitation energy transfer, as detected by ultrafast transient spectroscopy.

The lack of an α-subunit may be sufficient to allow more efficient transfer of reducing equivalents between the reduced ubiquinone "trapped" in the ring and oxidized ubiquinone in the surrounding environment, possibly by a collisional mechanism.

The integration of the H-subunit into the LH1 ring would also provide a simple way of providing a "growth point"for the LH1 ring which simultaneously requires the assembly of the RC.

This hypothesis is testable experimentally, and efforts to do this are currently underway in our laboratory.

REFERENCES

1. Fotiadis D, Qian P, Philippsen A, Bullough PA, Engel A and Hunter CN (2004) Structural analysis of the reaction center light-harvesting complex I photosynthetic core complex of *Rhodospirillum rubrum* using atomic force microscopy. J Biol Chem 279: 2063-2068
2. Jamieson SJ, Wang P, Quian P, Kirkland JY, Conroy MJ, Hunter CN and Bullough PA (2002) Projection structure of the photosynthetic reaction center-antenna complex of *Rhodospirillum rubrum* at 8.5 Å resolution. EMBO J 21: 3927-3935
3. Lupo D and Ghosh R (2004) The reaction center H subunit is not required for high levels of light-harvesting complex 1 in *Rhodospirillum rubrum* mutants. J Bacteriol 186: 5585-5595
4. Roszak, AW, Howard TD, Southall J, Gardiner A, Law CJ, Isaacs NW and Cogdell RJ (2003) Crystal structure of the RC-LH1 core complex from *Rhodopseudomonas palustris*. Science 302: 1969-1972

ANHANG

Auf den folgenden Seiten sind alle Plasmide aufgeführt, die in den Manuskripten und Publikationen zwar aufgelistet wurden aber nicht abgebildet werden konnten. Außerdem sind die Konstrukte, die im Ausblick erwähnt wurden und für zukünftige Projekte schon zur Verfügung stehen, abgebildet.
An erster Stelle steht die Abbildung des Cosmids pSC21-7, dessen Kartierung und Subklonierung vor der Veröffentlichung des teilsequenzierten Genoms aus *R. rubrum* erfolgte.

Abbildung-A1: Kartierung und Subklonierung des Cosmids pSC21-7. a: Die durch HindIII- und EcoRI-Verdau erhaltenen Fragmente aus pSC21-7 wurden in pBsKSII(+)-Vektoren subkloniert und durch Restriktionsanalysen mit verschiedenen Enzymen physikalisch kartiert. Das Plasmid pBsH2 trägt das *puh*-Operon mit dem *puhA*-Gen, welches für die H-Untereinheit kodiert. Einige Fragmente wurden auch ansequenziert, um die flankierende Region des *puh*-Operons näher zu definieren. b: Nach der Veröffentlichung des unvollständigen Genoms aus *R. rubrum* wurde das Cosmid pSC21-7 abgeglichen. Die Kartierung aus (a) entsprach vollständig der Abfolge auf dem Genom. Wobei das Genom noch zwei Lücken auf diesem Abschnitt vorwies. Die offenen Leserahmen wurden gegen Datenbankeinträge verglichen und entsprechen annotiert.

Abbildung-A2: Plasmidkarten der *puh*-Operon flankierenden Gene. Die 3'-flussabwärts folgende Gene *orf295* und *bchJ* (siehe Abbildung-A1) wurden im Verbund in den broad-host-range Vektor pRK404 subkloniert (oberer Teil). Für die zukünftige Komplementation einer Bakteriochlorophyllbiosynthese-Mutante wurde ein Konstrukt hergestellt auf dem *orf295* deletiert wurde (unterer Teil). Die Zahlen 1 und 2 in der Plasmidbezeichnung zeigen die Orientierung der Gentranskription im bezug auf die Transkriptionsrichtung vom lacZ-promotor an.

Abbildung-A3: Plasmidkarten der Komplementationskonstrukte. Weitere Erläuterungen siehe Publikation zum Deletions/Komplementationssystem bzw. Manuskript zur Mutagenese der H-Untereinheit.

Abbildung-A4: Plasmidkarten der Mutagenesekonstrukte, siehe Manuskript zur Mutagenese der H-Untereinheit.

Abbildung-A5: Herstellung von Fusionsproteine. a: Das “red-shift green-fluorescent“-Protein, aus dem Plasmid psmRS-GFP stammend – ein Konstrukt von Seth J. Davis (siehe Literaturverzeichnis), welches die Abteilung Molekularbiologie und Virologie der Pflanzen freundlicherweise zur Verfügung gestellt hatte – wurde an den C-Terminus der TM-Domäne im gleichen Leserahmen fusioniert. Die erfolgten Klonierungsschritte sind dargestellt. b: Fusion von sechs Histidinresten an den C-Terminus der CY-Domäne. Zuvor wurden zwei neue Restriktionsschnittstellen durch zielgerichteter Mutagenese in die CY-Sequenz eingebracht, um nachfolgend die synthetisch hergestellte Linker-DNA (mit der kodierenden His_6-Sequenz) mit der CY-Domäne im gleichen Leserahmen zu verknüpfen.

Abbildung-A6: Plasmidkarten der in Abbildung-A5 beschriebenen Konstrukte und zusätzlich ein Derivat von pRKLPuhCY1 (siehe Abbildung-A4).

Abbildung-A7: Plasmidkarten der Cysteinderivate. In den Komplementationsplasmiden, die in Abbildung-A4 und Abbildung-A6 aufgeführt sind, wurde die Aminosäure Threonin-104 gegen ein Cystein ausgetauscht. Threonin-104 befindet sich an der Oberfläche der CY-Domäne und der Austausch gegen Cystein soll für Quervernetzungsexperimente bzw. Fluoreszenzmarkierungen eingesetzt werden. Im unteren Bereich der Abbildung ist das Ergebnis der DNA-Sequenzierung der aufgeführten Plasmide im Vergleich zur Originalsequenz gezeigt, die den erfolgten Austausch bestätigte.

ABBILDUNGEN

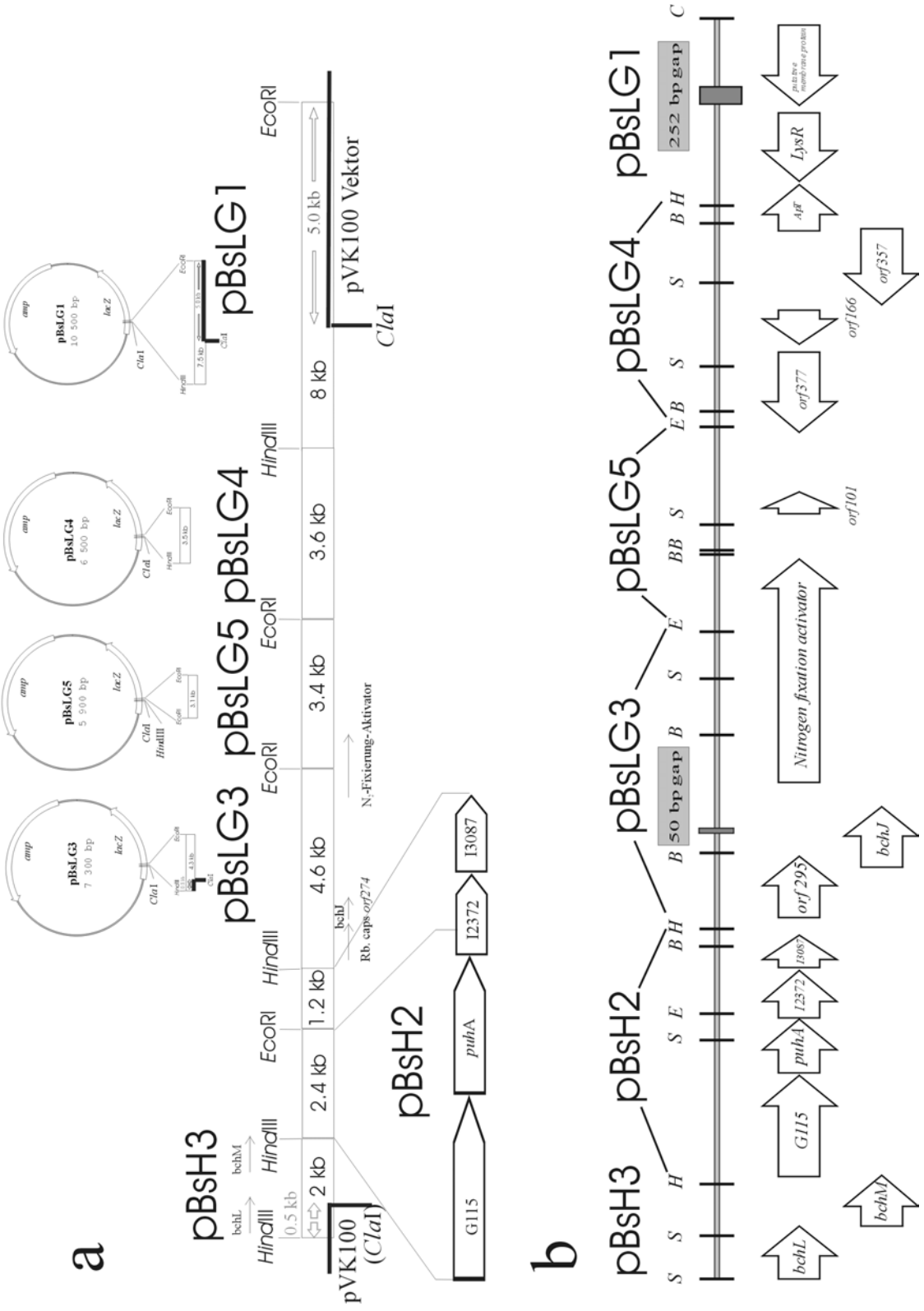

Abbildung-A1

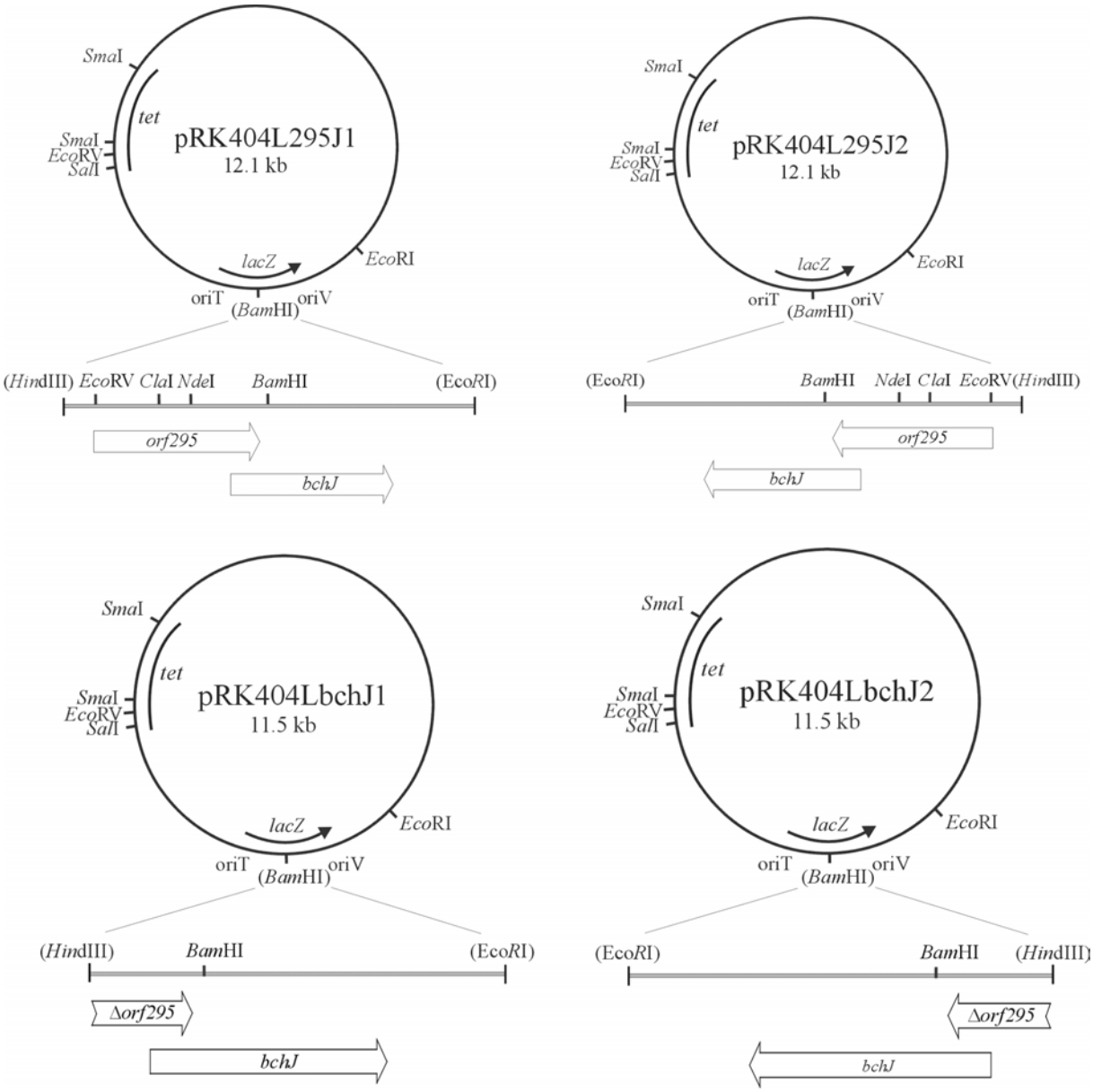

Abbildung-A2

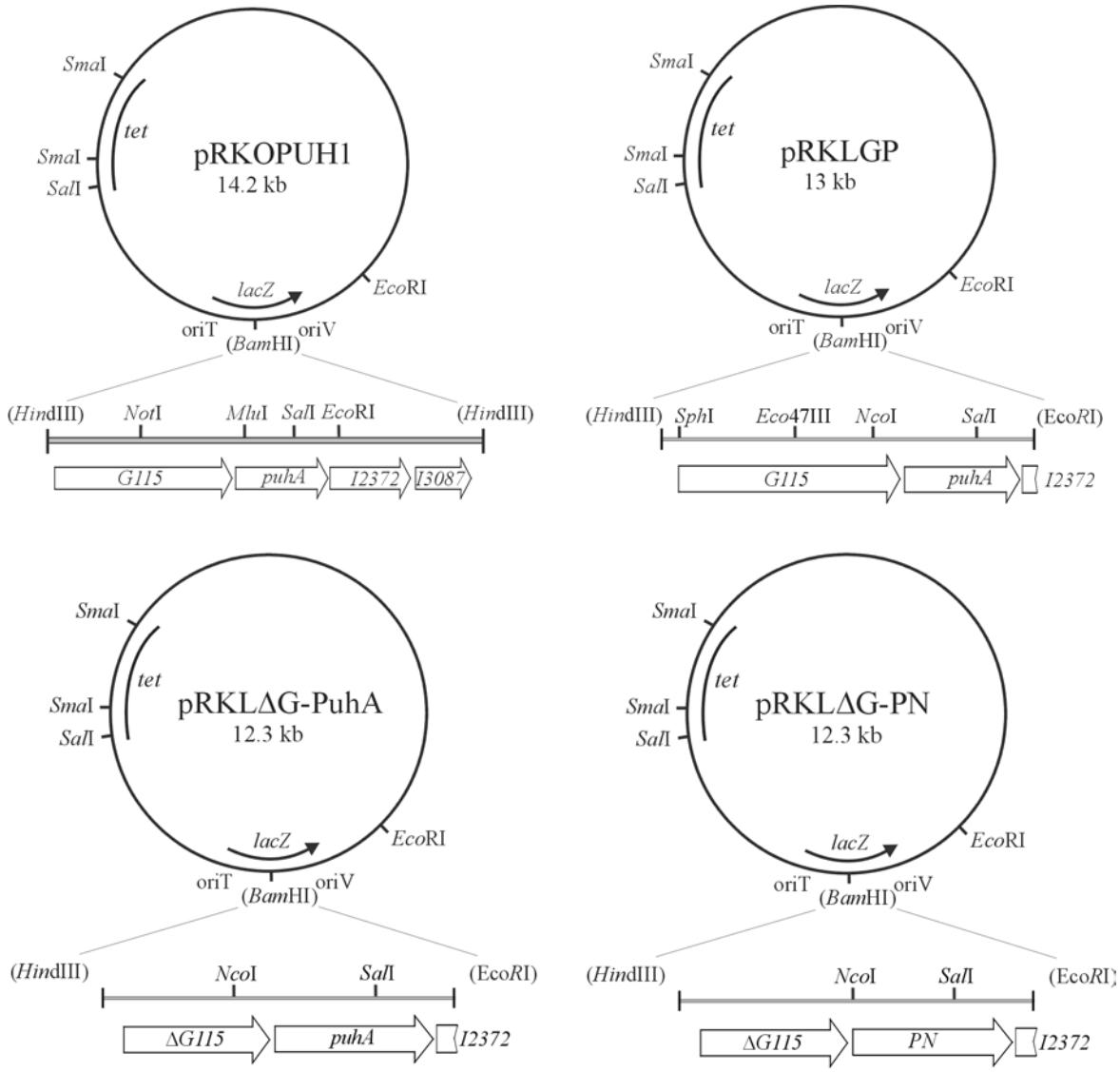

Abbildung-A3

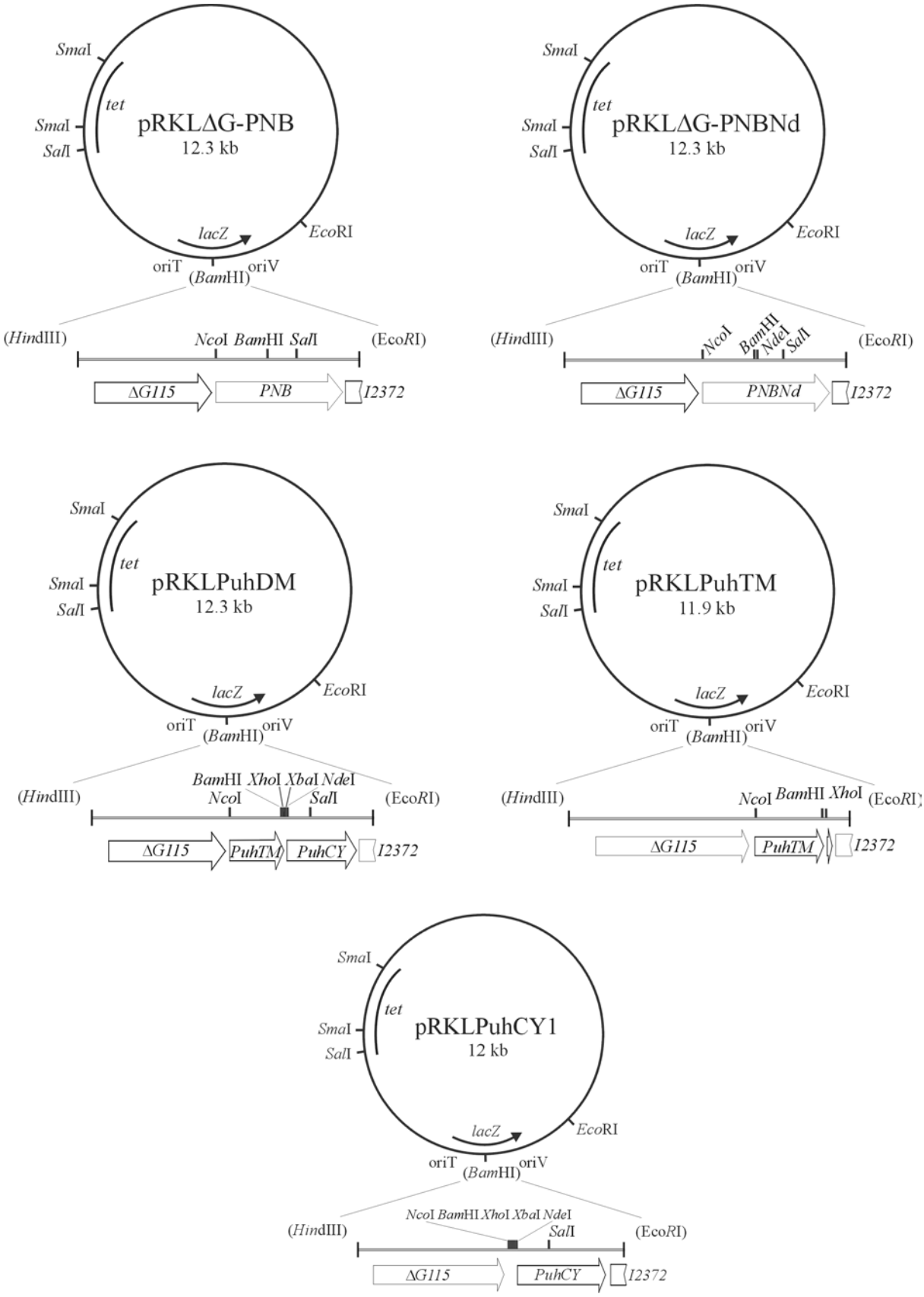

Abbildung-A4

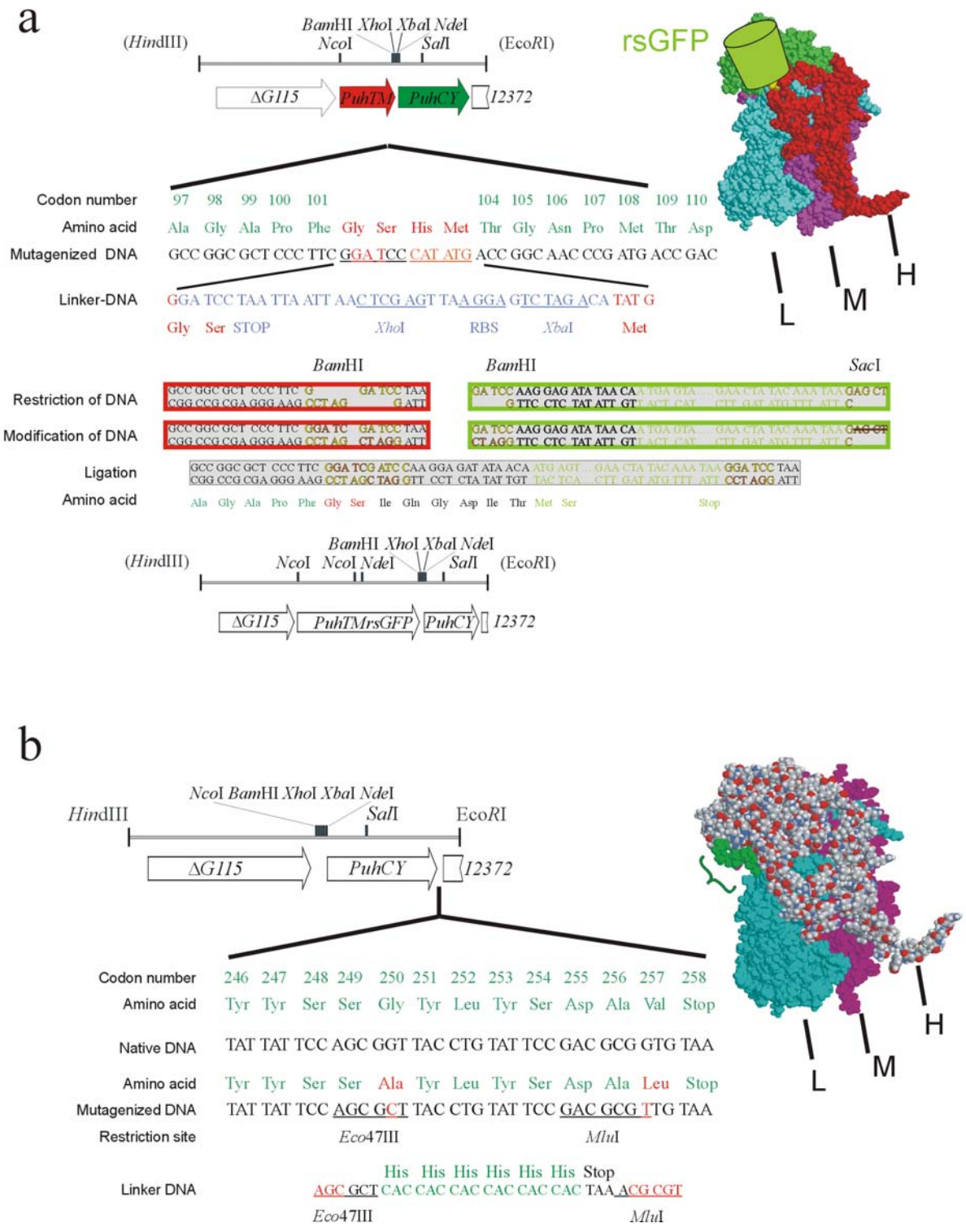

Abbildung-A5

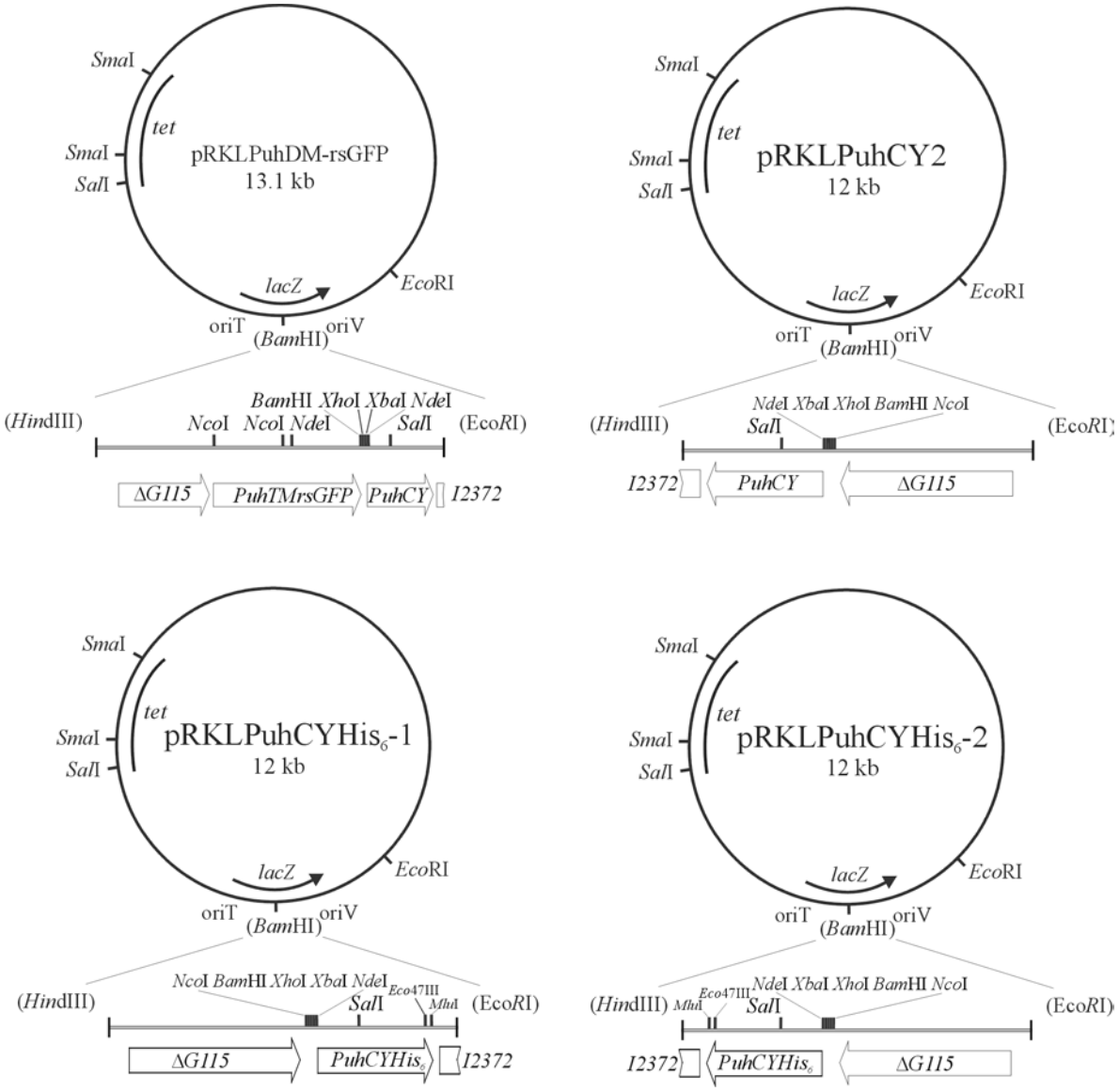

Abbildung-A6

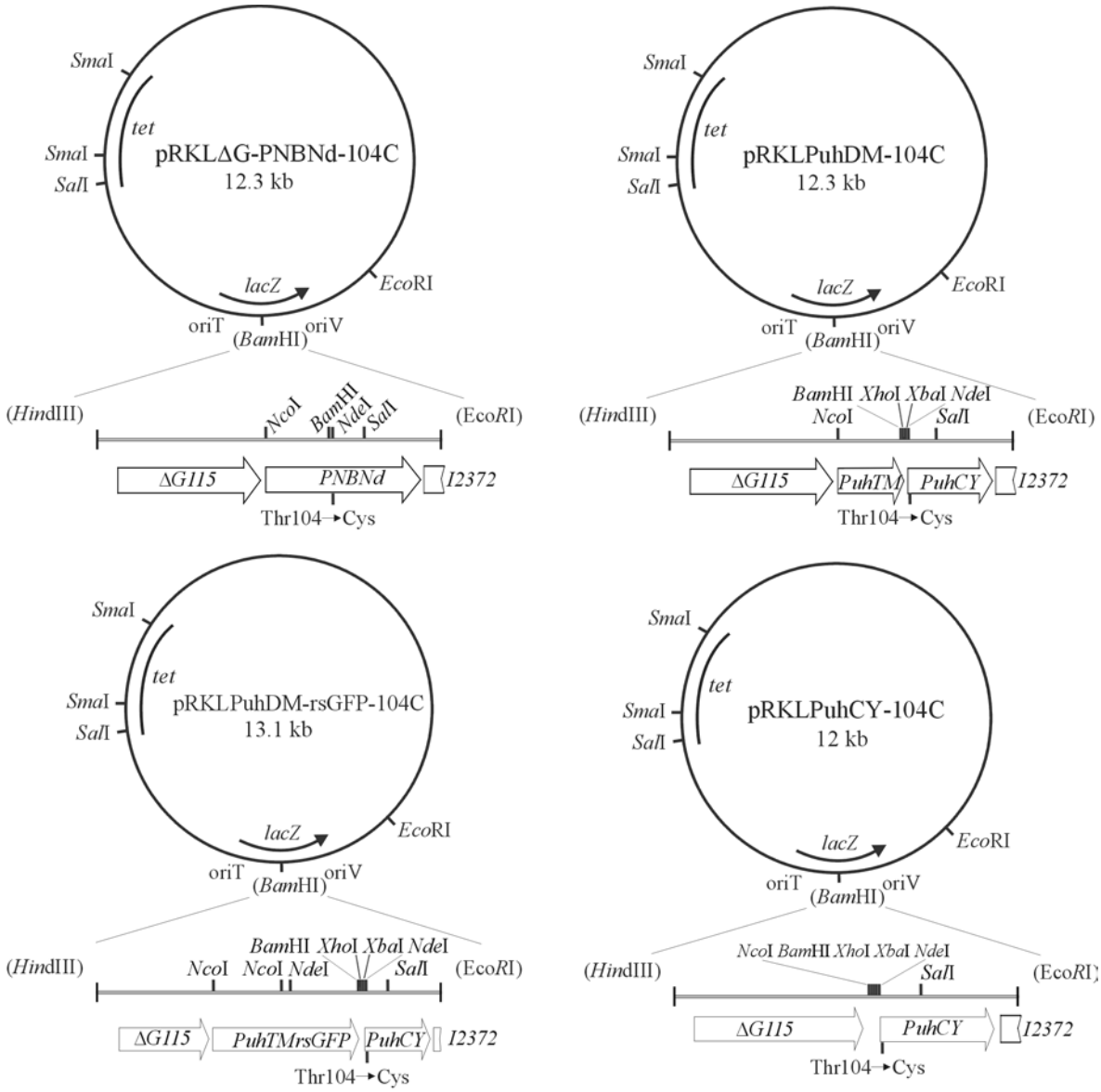

PuhCY

Met Thr Gly Asn Pro
ATG ACC GGC AAC CCG

pRKLΔGNPNBNd-104C
pRKLPuhDM-104C
pRKLPuhDMrsGFP-104C
pRKLPuhCY-104C

Met Cys Gly Asn Pro
ATG **TG**C GGC AAC CCG
ATG **TG**C GGC AAC CCG
ATG **TG**C GGC AAC CCG
ATG **TG**C GGC AAC CCG

Abbildung-A7

LITERATURVERZEICHNIS

⇒ Aargard, J., & Sistrom, W. R. **(**1972) *Photochem. Photobiol.* **15,** 209-225.

⇒ Abresch, E. C., Paddock M. L., Stowell, M. H. B., McPhillips, T. M., Axelrod, H. L., Soltis, S. M., Rees, D. C., Okamura, M. Y. & Feher, G. (1998) *Photosyn. Res.* **55,** 119-125.

⇒ Aklujkar, M., Harmer, A. L., Prince, R. C. & Beatty, J. T. **(**2000) *J. Bacteriol.* **182,** 5440-5447.

⇒ Allen, J. P., Feher, G., Yeates, T. O., Komiya, H. & Rees, D. C. (1987) *Proc. Natl. Acad. Sci. U S A* **84,** 6162-6166.

⇒ Allen, J. P., Feher, G., Yeates, T. O., Rees, D. C., Deisenhofer, J., Michel, H. & Huber, R. (1986) *Proc. Natl. Acad. Sci. U S A* **83,** 8589-93.

⇒ Ames, B. N. & Dubin, D. T. (1960) *J. Biol. Chem.* **235,** 769 – 775.

⇒ Ames, B. N. (1966) *Method. Enzymol*. **8,** 115-118.

⇒ Anantharaman, V. & Aravind, L. (2002) *Genome Biol.* **3,** 0061.1-0061.9.

⇒ Authenrieth, F., Ritz, T., Schulten, K. & Ghosh, R. (2002) submitted.

⇒ Bahatyrova, S., Frese, R. N., Siebert, C. A., Olsen, J. D., van der Werf, K. O., van Grondelle, R., Niederman, R. A., Bullough, P. A., Otto, C. & Hunter, C. N. (2004) *Nature* **430,** 1058-1062.

⇒ Barz, W. P., Vermeglio, A., Francia, F., Venturoli, G., Melandri, B. A. & Oesterhelt, D. (1995) *Biochemistry* **34,** 15248 – 15258.

⇒ Beck, E., Ludwig, G., Auerswald, E. A., Reiss, B. & Schaller, H. (1982) *Gene* **19,** 327-336.

⇒ Belanger, G., Berard, J., Corriveau, P. & Gingras, G. (1988) *J. Biol. Chem.* **263,** 7632-7638.

⇒ Ben-Shem A., Frolow, F. & Nelson, N. (2003) *Nature* **426,** 630-635.

⇒ Bérard, J. & Gingrás, G. **(**1990) *Biochem. Cell Biol.* **69,** 122-131.

⇒ Bérard, J., Bélanger, G. & Gingrás, G. (1989) *J. Biol. Chem.* **265,** 10897-10903.

⇒ Berman H. M., Westbrook, J., Feng, Z., Gilliland, G., Bhat, T. N., Weissig, H., Shindyalov, I. N. & Bourne, P. E. (2000) *Nucleic Acids Res.* **28,** 235-242.

⇒ Bhatia G. E. (1981) Ph.D. thesis, University of California San Diego, USA.

⇒ Boonstra, A. F., Visschers, R. W., Calkoen, F., van Grondelle, R., van Bruggen, E. F. J. & Boekema, E. J. **(**1994) *Biochim. Biophys. Acta.* **1142,** 181-188.

⇒ Bopp, M. A., Jia, Y., Li, L., Cogdell, R. & Hochstrasser, R. (1997) *Proc. Natl. Acad. Sci. USA* **94,** 10630 – 10635.

⇒ Brooks, B. R., Bruccoleri, R. E., Olafson, B. D., States, D. J., Swaminathan, S. & Karplus, M. (1983) *J. Comp. Chem.* **4,** 187-217.

⇒ Brünger, A. T. (1996) X-PLOR, Version 3.8: A System for X-ray Crystallography and NMR. (Yale University Press, New Haven).

⇒ Buggy J. J., Sganga, M. W. & Bauer, C. E. (1994) *J. Bacteriol.* **176,** 6936-6943.

⇒ Bylina, E. J., Robles, S. J. & Youvan, D. C. **(**1988) *Israel J. Chem.* **28,** 73-78.

⇒ Camara-Artigas A., Brune, D. & Allen, P. (2002) *Proc. Natl. Acad. Sci. U S A* **99,** 11055-11060.

⇒ Chang, M.C., Callahan, P.M., Parkes-Loach, P.S., Cotton, T.M. & Loach, P.A. (1990) *Biochemistry* **29,** 421-429.

⇒ Chen, X.-Y., Yurkov, V., Paddock, M. L., Okamura, M. Y. & Beatty, J. T. (1998) *Photosyn. Res.* **55,** 369-373.

⇒ Cheng, Y. S., Brantner, C. A., Tsapin, A. & Collins, M. L. P. 2000. *J. Bacteriol.* **182,** 1200-1207.
⇒ Cogdell, R. & Scheer, H. (1985) *Photochem. Photobiol.* **42,** 669-678.
⇒ Cogdell, R. J., Fyfe, P. K., Barrett, S. J., Prince, S. M., Freer, A. A., Isaacs, N. W., McGlynn, P. & Hunter, C. N. (1996) *Photosynth.Res*. ***48*,** 55-63.
⇒ Cogdell, R. J., Isaacs, N. W., Howard, T. D., McLuskey, K., Fraser, N. J. & Prince, S. M. (1999) *J. Bacteriol.* **180,** 3869-3879.
⇒ Cogdell, R. J., Lindsay, J. G., Valentine, J., and Durant, I. (1982) *FEBS Letts.* **150,** 151-154.
⇒ Cohen-Bazire, G., Sistrom, W. R. & Stanier, R. Y. (1956) *J. Cell. Comp. Physiol.* **49,** 25–68.
⇒ Damjanović, A., Kosztin, I., Kleinekathoefer, U. & Schulten, K. (2002) *Physical Review E* **65,** 031919.
⇒ DaPra, E., Snozzi, M. & Bachofen, R. (1982) *Arch Microbiol.* **133,** 23-27.
⇒ Davis, S. J. & Vierstra, R. D. (1998) *Plant Mol. Biol.* **36,** 521-528.
⇒ Debus, R. J., Feher, G. & Okamura, M. Y . (1985) *Biochemistry* **24,** 2488-2500.
⇒ Deisenhofer, J., Epp, O., Miki, K., Huber, R. & Michel, H. (1984) *J. Mol. Biol.* **180,** 385–398.
⇒ Deisenhofer, J., Epp, O., Miki, K., Huber, R. & Michel, H. (1985) *Nature* **318,** 618-624.
⇒ Deisenhofer, J., Epp, O., Sinning, I. & Michel, H. (1995) *J. Mol. Biol.* **246,** 429-457.
⇒ Dekker, J. P., Gilbro, T. & Sundström, V. (1994) *Biochim. Biophys. Acta* **1187,** 1 –65.
⇒ Ditta, G., Schmidhauser, T., Yakobson, E., Lu, P., Liang, X.-W., Finlay, D. R., Guiney, D. & Helinski, D. R. (1985) *Plasmid* **13,** 149–153.
⇒ Donohue, J. T., Hoger, J. H. & Kaplan, S. (1986) *J. Bacteriol.* **168,** 953-961.
⇒ Dörge, B., Klug, G., Gad'on, N., Cohen, S. N. & Drews, G. (1990) *Biochemistry* **29,** 7754-7758.
⇒ Drews, G. & Golecki, J. R. (1995) p. 231–257. *In* R. E. Blankenship, M. T. Madigan, and C. E. Bauer (ed.), Anoxygenic photosynthetic bacteria. Kluwer Academic Publishers, Dordrecht, The Netherlands.
⇒ Drews, G. & Oelze, J. **(**1981) *Adv. Microb. Physiol.* **22,** 1-92.
⇒ Drews, G. **(**1978) *Curr. Top. In Bioenergetics* **8B,** 161-207.
⇒ Ducruix, A. & Reiss-Husson, F. (1987) *J. Mol. Biol.* **193,** 419-421.
⇒ Engelhardt, H., Engel, A. & Baumeister, W. (1986) *Proc. Natl. Acad. Sci. USA* **83,** 8972 – 8976.
⇒ Eraso, J. M. & Kaplan, S. (2000) *Biochemistry* **39,** 2052-2062.
⇒ Ermler, U., Fritzsch, G., Buchanan, S. K. & Michel, H. (1994) *Structure* **2,** 925-936.
⇒ Farchaus, J.W., Barz, W.P., Grünberg, H. & Oesterhelt, D. (1992) *EMBO J.* **11,** 2779 – 2788.
⇒ Fathir, I., Mori, T., Nogi, T., Kobayashi, M., Miki, K. & Nozawa, T. (2001) *Eur. J. Biochem.* **268,** 2652-7.
⇒ Fernandez-Valesco, J. & Crofts, A. R. (1991) *Biochem. Soc. Trans.* **19,** 588-593.
⇒ Ferreira K. N., Iverson, T. M., Maghlaoui, K., Barber, J. & Iwata, S. (2004) *Science* **303,** 1831-1838.
⇒ Figurski, D. H. & Helinski, D. R. (1979) *Proc. Natl. Acad. Sci. USA* **76,** 1648-1652.
⇒ Fotiadis, D., Qian, P., Phillipsen, A., Bullough, P. A., Engel, A. & Hunter, C. N. (2004) *J. Biol. Chem.* **279,** 2063-2068.
⇒ Francke, C. & Amesz, J. **(**1995) *Photosyn. Res.* **46,** 347-352.

⇒ Fraser, N. J., Dominy, P. J., Ucker, B., Simonin, I., Scheer, H. & Cogdell, R. J. (1999) *Biochemistry* **38,** 9684-9692.
⇒ Garcia, A. F., Mäntele, W., Gad'on, N., Tadros, M. H. & Drews, G. **(**1991) *Arch. Microbiol.* **155,** 205-209.
⇒ Gerken, U., Lupo, D., Tietz, C., Wrachtrup, J. & Ghosh, R. (2003) *Biochemistry* **42,** 10354-10360.
⇒ Gerken, U. 2003. Doktorarbeit, Universität Stuttgart, Deutschland.
⇒ Gerken, U., Jelezko, F., Götze, B., Branschädel, M., Tietz, C., Ghosh, R. & Wrachtrup, J. (2003) *J. Phys. Chem. B* **107,** 338 – 343.
⇒ Ghosh, R, Hauser, H. & Bachofen, R. (1988) *Biochemistry* **27,** 1004 – 1014.
⇒ Ghosh, R. & Bachofen, R. (1989) *Forum Mikrobiologie* **12,** 556-564.
⇒ Ghosh, R., Ghosh-Eicher, S., Di Berardino, M. & Bachofen, R. (1994) *Biochim. Biophys. Acta* **1148,** 28 – 36.
⇒ Ghosh, R., Hardmeyer, A., Thoenen, I. & Bachofen, R. (1994) *Appl. Environ. Microbiol.* **60,** 1698-1700.
⇒ Ghosh, R., Hoenger, A., Hardmeyer, A., Mihailescu, D., Bachofen, R., Engel, A. & Rosenbusch, J. P. (1993) *J. Mol. Biol.* **231,** 501-504.
⇒ Ghosh, R., Rosatzin, T. and Bachhofen, R. (1988) p. 93-102. *In* H. Scheer and S. Schneider (ed.), Photosynthetic light-harvesting systems. Walter de Gruyter and Co., Berlin-New York.
⇒ Gomelsky, M. & Kaplan, S. (1995) *J. Bacteriol.* **177,** 4609-4618.
⇒ Goodhew, C. F., Brown, K. R. & Pettigrew, G. W. (1986) *Biochim. Biopys. Acta* **852,** 288-294.
⇒ Grammel, H., Gilles, E. D. & Ghosh, R. (2003) *Appl. Environ. Microbiol.* **69,** 6577-6586.
⇒ Hara, M., Kaneko, T., Nakamura, C., Asada, Y. & Miyake, J. (1998) *Biochim Biophys Acta* **1363,** 199-208.
⇒ Hartigan N., Tharia, H. A., Sweeney, F., Lawless, A. M. & Papiz, M. Z. (2002) *Biophys. J.* **82,** 963-977.
⇒ Heller H. (1993) Doktorarbeit Technische Universität München, Deutschland.
⇒ Heller H., Schäfer, M. & Schulten, K. (1993) *J. Phys. Chem.* **97,** 8343-8360.
⇒ Hennecke, H., Günther, I. & Binder, F. (1982) *Gene* **19,** 231-234.
⇒ Hippler, M., Klein, J., Fink, A., Allinger, T. & Hoerth, P. (2001) *Plant J.* **28,** 595-606.
⇒ Holt, S. C. & Marr, A. G. **(**1965) *J. Bacteriol.* **52,** 1421-1429.
⇒ Hu X., T. Ritz, Damjanovic, A., Autenrieth, F. & Schulten, K. (2002) *Q. Rev. Biophys.* **35,** 1-62.
⇒ Hu, Q., Sturgis, J. N., Robert, B., Delagrave, S., Youvan, D. C. & Niederman, R. C. (1998) *Biochemistry* **37,** 10006 – 10015.
⇒ Hu, X. & Schulten, K. (1998) *Biophys J.* **75,** 683 – 694.
⇒ Hu, X., Damjanovic, A., Ritz, T. & Schulten, K. (1998) *Proc. Natl. Acad. Sci. USA* **95,** 5935 – 5941.
⇒ Humphrey W, Dalke, A. & Schulten, K. (1996) *J. Mol. Graph.* **14,** 33-38.
⇒ Hunter, C. N., van Grondelle, R. & van Dorssen, R. J. (1989) *Biochim. Biophys. Acta* **973,** 383-389.
⇒ Igarashi N., Harada, J., Nagashima, S., Matsuura, K., Shimada, K. & Nagashima, K. V. (2001) *J. Mol. Evol.* **52,** 333-341.
⇒ Jamieson, S. J., Wang, P., Quian, P., Kirkland, J. Y., Conroy, M. J., Hunter, C. N. & Bullough, P. A. (2002) *EMBO J.* **21,** 3927-3935.
⇒ Jay, F., Lambillote, M., Stark, W. & Mühlenthaler, K. (1984) *EMBO J.* **3,** 773 – 776.

⇒ Joliot, P., Vermeglio, A. & Joliot, A. (1996) *Photosynth. Res.* ***48,*** 291-299.
⇒ Jones, M. R., Fowler, G. J. S., Gibson, L. C. D., Grief, G. G., Olsen, J. D., Crielaard, W. & Hunter, C. N. (1992) *Mol. Microbiol.* **6,** 1173-1184.
⇒ Jones, M. R., Visschers, R. W., van Grondelle, R. & Hunter, C. N. (1992) *Biochemistry* **31,** 4458-4465.
⇒ Jordan, P., Fromme, P., Witt, H. T., Klukas, O., Saenger, W. & Krauss, N. (2001) *Nature* **411,** 909-917.
⇒ Joshi, H. M. & Tabita, F. R. (1996) *Proc. Natl. Acad. Sci. U S A* **93,** 14515-14520.
⇒ Jungas, C., Ranck, J., Rigaud, J.-L., Joliot, P. & Verméglio, A. (1999) *EMBO* **18,** 534-542.
⇒ Kagawa, R., Montgomery, M. G., Braig, K., Leslie, A. G. and Walker, J. E. (2004) *EMBO J.* **23,** 2734-2744.
⇒ Kalé, L., Skeel, R., Bhandarkar, M., Brunner, R., Gursoy, A., Krawetz, N., Phillips, J., Shinozaki, A., Varadarajan, K. & Schulten, K. (1999) *J. Comp. Phys.***151,** 283-312.
⇒ Karrasch, S., Bullough, P. A. & Ghosh, R. (1995) *EMBO J.* **14,** 631-638.
⇒ Katiliene Z., Katilius, E. and Woodbury, N. W. (2003) *Biophys J.* **84,** 3240-3251.
⇒ Katz, J. J., Strain, H. H., A. Harkness, L., Studier, M. H., Svec, W. A., Janson, T. R. & Cope B. T. (1972) *J. Am. Chem. Soc.* **94,** 7938-7939.
⇒ Kessi, J., Ghosh, R. & Bachofen, R. (1995) *Photosynth. Res.* **46,** 353-362.
⇒ Ketelaars, M. , Hoffmann, C., Koehler, J., Howard, T. D., Cogdell, R .J., Schmidt, J**.** & Aartsma, T. J. (2002) *Biophys J.* **83,** 1701 – 1714.
⇒ Klug, G. & Cohen S. N. (1988) *J. Bacteriol.* **170,** 5814-5821.
⇒ Koepke, J., Hu, X., Muenke, C., Schulten, K. & Michel, H. (1996) *Structure* **4,** 581-597.
⇒ Kohl, D. H., Townsend, J., Commoner, B., Crespi, H. L., Dougherty, R. C. & Katz, J. J. (1965) *Nature* **12,** 1105-1110.
⇒ Kramer, H. J. M., Pennoyer, J. D., van Grondelle, Niederman, R. A. & Amesz, J. (1984) *Biochim. Biophys. Acta* **767,** 335 – 344.
⇒ Kriauciunas, A., Yu, L., Yu, C.-A., Wynn, R. M. & Knaff, D. B. (1989) *Biochim. Biophys. Acta* **976,** 70-76.
⇒ Laemmli, U. K. (1970) *Nature* **227,** 680-685.
⇒ Lancaster, C. R. & Michel, H. (1997) *Structure* **5,** 1339-1359.
⇒ Lilburn, T.G., Haith, C. E., Prince, R. C. & Beatty, J. T. (1992) *Biochim. Biophys. Acta* **1100,** 160-170.
⇒ Liu Z., Yan, H., Wang, K., Kuang, T., Zhang, J., Gui, L., An, X. & Chang, W. (2004) *Nature* **428,** 287-292.
⇒ Lupo, D. & Ghosh, R. (2004) *J. Bacteriol.* **186,** 5585-5595.
⇒ Lupo, D. (2000) Diplomarbeit, Universität Stuttgart, Deutschland.
⇒ Masuda, S. & Bauer, C. E. (2002) *Cell* **110,** 613-623.
⇒ Mazodier, P., Cossart, P., Giraud, E. & Gasser, F. (1985) *Nucleic Acids Res.* **13,** 195-205.
⇒ McAuley K. E., Fyfe, P. K., Ridge, J. P., Isaacs, N. W., Cogdell, R. J. & Jones. M. R. (1999) *Proc. Natl. Acad. Sci. U S A* **96,** 14706-14711.
⇒ McDermott, G., Prince, S. M., Freer, A. A., Hawthornthwaite-Lawless, A. M., Papiz, M. Z., Cogdell, R. J. & Isaacs, N. W. (1995) *Nature* **374,** 517-521.
⇒ McLuskey K., Prince, M., Cogdell, R. J. & Isaacs. N. W. (2001) *Biochemistry* **40,** 8783-8789.
⇒ Miller, K. R. (1982) *Nature* **300,** 53-55.
⇒ Monger, T. G. & Parson, W. W. (1977) *Biochim. Biophys. Acta* **460,** 393-407.

⇒ Monshouwer R., Abrahamsson, M., van Mourik, F. & van Grondelle, R. (1997) *J. Phys. Chem. B* **101,** 7241 – 7248.
⇒ Mosley C. S., Suzuki, J. Y. and Bauer, C. E. (1994) *J. Bacteriol.* **176,** 7566-7573.
⇒ Moss, G.P. (1987) *Pure Appl. Chem.*, 59, 779 – 832.
⇒ Naylor G. W., Addlesee, H. A., Gibson, L. C. D. & Hunter, C. N. (1999) *Photosyn. Res.* **62,** 121–139.
⇒ Neumann, U., Benz, R., Rosenbusch, J. P., Stahl, B. & Weckesser, J. (1995) *Microbiology* **141,** 3155-3160.
⇒ Noël, H., van der Rest, M. & Gingras, G. (1972) *Biochim. Biophys. Acta,* **275,** 219-230.
⇒ Nogi, T., Fathir, I., Kobayashi, M., Nozawa, T. & Miki, K. (2000) *Proc. Natl. Acad. Sci. U S A* **97,** 13561-13566.
⇒ Novoderezkhin, V. I. & Razjivin, A.P. (1994) *Photosynth. Res.* **42,** 9 – 15.
⇒ Oh, J. I. & Kaplan, S. (2000) *EMBO J.* **19,** 4237-4247.
⇒ Oh, J. I. & Kaplan, S. (2001) *Mol. Microbiol.* **39,** 1116-1123.
⇒ Okamura M. Y., Steiner, L. A. & Feher, G. (1974) *Biochemistry* **13,** 1394-1403.
⇒ Ormerod, J. G., Ormerod, K. S. & Gest, H. (1961) *Arch. Biochem. Biophys.* **94,** 449–463.
⇒ Papiz, M. Z., Prince, S. M., Hawthornthwaite-Lawless, A. M., McDermott, G., Freer, A. A., Isaacs, N. W. & Cogdell, R. J. (1996) *Trends Plant Sci*. **1,** 198 – 206.
⇒ Paschenko, V. V., Gorokhov, V. V., Grishanova, N. P., Goryacheva, E. A., Korratovsky, B.N., Knox, P.P., Zakharova, N. I. & Rubin, A. B. (1998) *Biochim. Biophys. Acta,* **1364,** 361 – 372.
⇒ Pemberton J. M., Horne, I. M. & A. McEwan, G. (1998) *Microbiology* **144,** 267 - 278.
⇒ Peters, J., Takemoto, J. & Drews, G. (1983) *Biochemistry* **22,** 5660-5667.
⇒ Peterson, G. L. (1977) *Anal. Biochem.* **83,** 346-356.
⇒ Philipson, K. D. & Sauer, K. (1973) *Biochemistry* **12,** 535-539.
⇒ Picorel, R., Bélanger, G. and Gingras, G. (1983) *Biochemistry* **22,** 2491-2497.
⇒ Ponnampalam S. N., Buggy, J. J. & Bauer, C. E. (1995) *J. Bacteriol.* **177,** 2990-2997.
⇒ Richter, P. & Drews, G. (1991) *J. Bacteriol.* **173,** 5336-5345.
⇒ Richter, P., Brand, M. & Drews, G. **(**1992) *J. Bacteriol.* **174,** 3030-3041.
⇒ Robert, B. & Lutz, M. (1985) *Biochim. Biophys. Acta* **807,** 10 – 23.
⇒ Roszak, A. W., Howard, T. D., Southall, J., Gardiner, A., Law, C. J., Isaacs, N. W. & Cogdell, R. J. (2003) *Science* **302,** 1969-1972.
⇒ Saegesser, R. (1992) Ph.D. thesis. University of Zurich, Switzerland.
⇒ Saegesser, R., Ghosh, R. & Bachofen, R. (1992) *FEMS Microbiol. Lett.* **95,** 7-12.
⇒ Sambrook, J., Fritsch, E. F. & Maniatis, T. (1989) Molecular Cloning: a laboratory manual, 2nd ed. Cold Spring Harbor Laboratory Press. Cold Spring Harbor, N.Y.
⇒ Schertler, G. F. X. (1992) *Curr. Opin Struct. Biol.* **2,** 534-544.
⇒ Scherz, A., & Parson, W. W. (1984) *Biochim. Biophys. Acta.* **766,** 653-665.
⇒ Scheuring, S., Francia, F., Busselez, J., Melandri, B. A., Rigaud J.-L. & Levy, D. (2004) *J. Biol. Chem.* **279,** 3620-3626.
⇒ Scheuring, S., Reiss-Husson, F., Engel, A., Rigaud, J.-L. & Ranck, J. L. (2001) *EMBO J.* **20,** 3029-3035.
⇒ Scheuring, S., Rigaud, J.-L. & Sturgis, J. N. (2004) *EMBO J.* **23,** 4127-4133.
⇒ Scheuring, S., Seguin, J., Marco, S., Levy, D., Robert, B. and Rigaud J. L. (2003) *Proc. Natl. Acad. Sci. USA* **100,** 1690-1693
⇒ Scheuring, S., Sturgis, J. N., Prima, V., Bernadac, A., Levy, D. & Rigaud, J.-L. (2004) *Proc. Natl. Acad. Sci. U.S.A.* **101,** 11293-11297.

⇒ Scott, H. N., Laible, P. D. & Hanson, D. K. (2003) *Plasmid* **50,** 74-79.
⇒ Sganga, M. W. & Bauer, C. E. (1992) *Cell* **68,** 945-954.
⇒ Simon, R., Priefer, U. & Pühler, A. **(**1983) p. 98-105. *In* A. Pühler (ed.) Molecular genetics of the bacteria-plant interaction. Springer-Verlag Berlin Heidelberg.
⇒ Sistrom, W. R. **(**1960) *J. Gen. Microbiol.* **22,** 778-785.
⇒ Sockett, R. E., Donohue, T. J., Varga, A. R. & Kaplan, S. (1989) *J. Bacteriol.* **171,** 436-446.
⇒ Spurr, A. R. (1969) *J. Ultrastruct. Res.* **26,** 31-43.
⇒ Stahlberg, H., Dubochet, J., Vogel, H., and Ghosh, R. (1998) *J. Mol. Biol.* **282,** 819-831.
⇒ Stark, W., Kühlbrandt, W., Wildhaber, I., Wehrli, E. & Mühlethaler, K. (1984) *EMBO J.* **3,** 777-783.
⇒ Stauber, E. J., Fink, A., Markert, C., Kruse, O., Johanningmeier, U. & Hippler, M. (2003) *Eukaryot. Cell* **2,** 978-994.
⇒ Stowell, M. H. B., McPhillips, T. M., Rees, D. C., Soltis, S. M., Abresch, E. & Feher, G. (1997) *Science* **276,** 812–816.
⇒ Swem L. R., Elsen, S., Bird, T. H., Swem, D. L., H. Koch, G., Myllykallio, H., Daldal, F. & Bauer, C. E. (2001) *J. Mol. Biol.* **309,** 121-138.
⇒ Takahashi, E. & Wraight, C. A. (1996) *Proc. Natl. Acad. Sci. U S A* **93,** 2640-5.
⇒ Tehrani, A. & Beatty, J. T. (2004) *Photosyn. Res.* **79,** 101-108.
⇒ Tehrani, A., Prince, R. C. & Beatty, J. T. (2003) *Biochemistry* **42,** 8919-8928.
⇒ Thompson, J. D., Gibson, T. J., Plewniak, F., Jeanmougin, F. & Higgins, D. G. (1997) *Nucleic Acids Research* **25,** 4876-4882.
⇒ Tretiak, S., Middleton, C., Chernyak, V. & Mukamel, S. (2000) *J. Phys. Chem. B* **104,** 9540 – 9553.
⇒ Ueki, T., Kataoka, M. & Mitsui, T. (1976) *Nature* **262,** 809-810.
⇒ Vadeboncoeur, C., Mamet-Bratley, M., & Gingras, G. (1979) *Biochemistry.* **18,** 4308-4314.
⇒ van Grondelle, R. (1985) *Biochim Biophys Acta Reviews* **811,** 147-195.
⇒ van Oijen, A. M., Ketelaars, M., Köhler, J., Aartsma, T. J. & Schmidt, J. (1999) *Science* **285,** 400 – 402.
⇒ Various authors. (1995) In R. E. Blankenship, M. T. Madigan, and C. E. Bauer (ed.) Anoxygenic photosynthetic bacteria. Kluwer Academic Publishers, Dordrecht, The Netherlands.
⇒ Visser, H. M., Somsen, O. J. G., van Mourik, F. & van Grondelle, R. (1996) *J. Phys. Chem*. **100,** 18859 – 18867.
⇒ Vos, M., van Grondelle, R., van der Kooij, F. W., van der Poll, D., Amesz., J. & Duysens, L. N. M. (1986) *Biochim. Biophys. Acta* **850,** 501-512.
⇒ Walz, T. & Ghosh, R. (1997) *J. Mol. Biol.* **265,** 107-111.
⇒ Walz, T., Jamieson, S. J., Bowers, C. M., Bullough, P. A. & Hunter, C. N. (1998) *J. Mol. Biol.* **282,** 833-845.
⇒ Wiggli, M., Cornacchia, L., Saegesser, R., Bachofen, R. & R. Ghosh. (1996) *Microbiol. Res.* **151,** 57-62.
⇒ Willetts, N. **(**1984) *Meth. Microbiol.* **17,** 33-59.
⇒ Wong, D. K.-H., Collins, W. J., Harmer, A., Lilburn, T. G. & Beatty, J. T. (1996) *J. Bacteriol.* **178,** 2334-2342.
⇒ Yankovskaya, V., Horsefield, R., Tornroth, S., Luna-Chavez, C., Miyoshi, H., Leger, C., Byrne, B., Cecchini, G. and Iwata, S. (2003) *Science* **299,** 700-704.
⇒ Yeliseev, A. A. & Kaplan, S. (1995) *J. Biol. Chem.* **270,** 21167-21175.

⇒ Young, C. S. & Beatty, J. T. (1998) *J. Bacteriol.* **180,** 4742-4745.
⇒ Young, C. S., Reyes, R. C. & Beatty, J. T. (1998) *J. Bacteriol.* **180,** 1759-1765.
⇒ Youvan, D. C., Bylina, E. J., Alberti, M., Begusch, H. & Hearst, J. E. (1984) *Cell* **37,** 949-957.
⇒ Youvan, D. C., Hearst, J. E. & Marrs, B. L. (1983) *J. Bacteriol.* **154,** 748-755.
⇒ Zeilstra-Ryalls, J. H. & Kaplan S. (1995) *J. Bacteriol.* **177,** 6422-6431.
⇒ Zeilstra-Ryalls, J. H. & Kaplan, S. (2004) *Cell. Mol. Life Sci.* **61,** 417-436.
⇒ Zeilstra-Ryalls, J., Gomelsky, M., Eraso, J. M., Yeliseev, A., O'Gara, J. & Kaplan, S. (1998) *J. Bacteriol.* **180,** 2801-2809.
⇒ Zhang, Z., Huang, L., Shulmeister, V. M., Chi, Y. I., Kim, K. K., Hung, L. W., Crofts, A. R., Berry, E. A. & Kim, S. H. (1998) *Nature* **392,** 677-684.
⇒ Zuber, H. & Cogdell, R. J. (1995) pp 315-348. In: Blankenship RE, Madigan MT and Bauer CE (ed) Anoxygenic photosynthetic bacteria, Kluwer Academic Publishers, Dordrecht, The Netherlands
⇒ Zuber, H. (1986) *Encycl. Plant Physiol*. **19,** 238-251.

DANKSAGUNG

Allen, die bisher an meiner persönlichen, wie auch wissenschaftlichen Entwicklung beteiligt waren, möchte ich an dieser Stelle gebührend danken:

- Meine Eltern, die mich geformt und stets unterstützt haben, danke ich dafür, mir die Möglichkeit gegeben zu haben der großen Leidenschaft für die Wissenschaft zu folgen. Mit ihrer großen Lebensfreude und ihrem Erfahrungsschatz haben sie nicht nur mir vorgelebt und gezeigt, welche Dinge erstrebenswert sind.
- Den Mitgliedern meiner großen Familie gilt mein Dank für ihren unschätzbaren Beitrag zu meiner Entwicklung. Da deren namentlichen Auflistung den Rahmen sprengen würde, seien an dieser Stelle, stellvertretend auch für die erhaltene Unterstützung, meine Schwester, ihr Ehemann und ihre beiden Kinder erwähnt.
- Den vielen Freunden und Bekannten danke ich für die einzigartigen Begegnungen und den unvergesslichen Unterhaltungen.
- Danken möchte ich auch denjenigen, die für immer in unserer Erinnerung bleiben werden.
- Angefangen bei denen, die den Grundstein gelegt haben, möchte ich allen danken, die an meiner schulischen Ausbildung beteiligt waren.
- Allen Lehrenden der Universität Stuttgart und besonders denen des Studienganges Technische Biologie spreche ich an dieser Stelle, für ihre Begeisterung und ihre Wissensvermittlung, ein großes Danke aus.
- Prof. Dr. Robin Ghosh danke ich nicht nur für die Bereitstellung dieses interessanten und vielfältigen Forschungsprojektes, sondern vor allem dafür, dass er mir einen Einblick in seinen Methoden- und Wissensschatz gewährt hat. Des weiteren möchte ich mich bei ihm für die exzellente Betreuung und die wissenschaftliche, wie auch nicht-wissenschaftliche Vorbereitung für die Zeit nach der Promotion danken.
- Allen früheren und heutigen Mitgliedern der Abteilung Bioenergetik, Blanquita Schreiter, Khaled Abou-Aisha, Maria Tsichouridou, Henrik Sommer, Gerasimoula Gerasimidou, Caroline und Felix Autenrieth, Katharina Kittelmann, Simon Stutz, Jörg Hammel und Christian Flogaus danke ich für die stimulierende Arbeitsatmosphäre.
- Für das Modell des photosynthetischen Reaktionszentrums aus *R. rubrum* möchte ich Felix Autenrieth erneut danken, der im Rahmen seiner Diplomarbeit beim Prof. Dr. K. Schulten am Beckman Institut der Universität Illinois die Berechnungen durchgeführt hat.
- Herrn Prof. Dr. H. Jeske gilt mein Dank, da er sich persönlich für dieses Forschungsvorhaben als Gutachter verbürgt hat. Danke auch, dass er meine weitere wissenschaftliche Laufbahn unterstützt hat und danke für die wertvollen Vorschlägen zu den publizierten Manuskripten und anderen Teilen dieser Doktorarbeit.
- Prof. Dr. U. Kull möchte ich für die Unterstützung danken, die er mir während meines Studiums und während der Promotion gegeben hat. Für die vielen Ratschläge, für seine Hilfsbereitschaft und für die Korrekturen der deutschsprachigen Teile der vorliegenden Arbeit ein großes Dankeschön. Aber damit ist Herrn Kull nicht genügend gedankt, denn auch sein breites und profundes Fachwissen, mit welchem er uns alle bereichert hat, muss genannt werden und sein großes Allgemeinwissen, das ihn zum Vorbild für uns alle macht.
- Für die Bereitstellung von Verbrauchsmaterial für die Elektronenmikroskopie und für die Einführung bzw. Benutzung der Bedampfungsanlage und des “glow discharge“-Gerätes möchte ich den Mitarbeitern der Abteilung Biophysik, der Abteilung

- Molekularbiologie und Virologie der Pflanzen sowie der Abteilung Zoologie und Tierphysiologie danken.
- Für das nachbarschaftliche Aushelfen mit verschiedenen Chemikalien und Gerätschaften ein herzliches Dankeschön an alle Mitarbeiter der Abteilung Botanik.
- Michael Schweikert danke ich für seine Zeit und seine Geduld, die er aufgebracht hat, mich in die Benutzung des Elektronenmikroskops einzuführen. Auch für die Herstellung der Schnitte möchte ich ihm erneut danken. Es war mir eine Freude mit ihm arbeiten zu dürfen.
- Marzia Sidri danke ich für die schönen Unterhaltungen und der Erkenntnis, dass meine Sprachkenntnisse verbesserungswürdig sind; außerdem ein großes Danke für die Korrektur der italienischen Zusammenfassung.
- Prof. Dr. J. Wrachtrup vom 3. Physikalisches Institut und vor allem Uwe Gerken danke ich für die Einzelmolekülspektroskopiemessungen und für die gute Zusammenarbeit.
- Prof. Dr. H. Port und seinem Mitarbeiter Peter Gärtner vom 3. Physikalisches Institut gilt mein Dank für die gute Kooperation und den ausführlichen Erläuterungen zu den verschiedenen Energietransferwegen und Anregungszuständen in den verschiedenen photosynthetischen Komplexen aus *R. rubrum*.
- Prof. Dr. D. Schweitzer 3. Physikalisches Institut, seinen Mitarbeitern Wolfgang Schmidt und Belal Salame möchte ich für die ESR-Messungen danken.
- Prof. Dr. A. Kuhn vom Instiut für Mikrobiologie der Universität Hohenheim, sowie seinen Mitarbeitern möchte ich für die Bereitstellung des Sequenziergerätes und des nahen-IR CD-Spektrophotometers ganz herzlich danken.
- Prof. Dr. W. Kühlbrandt vom Max-Planck-Institut für Biophysik und seinen Mitarbeitern Deryck Mills und Janet Vonck danke ich für die hochauflösenden EM-Aufnahmen bzw. für die Diffraktionsbilder von der optischen Bank.
- Prof. Dr. M. Hippler und seiner Mitarbeiterin Bianca Naumann von der biologischen Abteilung der Universität Pennsylvania, gilt erneut mein Dank für die Sequenzierung der Proteine aus der isolierten photosynthetischen Einheit mittels Massenspektrometrie.
- Prof. Dr. J. Wachtveitl vom Institut für physikalische und theoretische Chemie der Universität Frankfurt und seinen Mitarbeitern Sergiu Amarie, Martin Lenz, Thomas Köhler und Karsten Neumann danke ich für die sehr freundliche Aufnahme und ihre Einführung in die Ultrakurzzeitspektroskopie. Aber vor allem danke ich ihnen für die kurzfristige Messung der verschiedenen *R. rubrum* Stämme.

LEBENSLAUF

Domenico Lupo

geboren am 07.12.1975 in Bietigheim-Bissingen

SCHULAUSBILDUNG

1982-1986: Grundschule (Burgfeldschule) in Sachsenheim.

1986-1995: Allgemeinbildendes Gymnasium (Ellentalgymnasien I und II) in Bietigheim Bissingen, naturwissenschaftliche Richtung. Abschlussprüfungen in Chemie, Latein, Mathematik und Religion. Schulabschluss: Allgemeine Hochschulreife.

1995-2000: Hochschulstudium. Studiengang Technische Biologie an der Universität Stuttgart.

1.-4. Semester Grundstudium: Experimentalphysik, anorganische und organische Chemie, biophysikalische Chemie, Biochemie, Mathematik, Informatik, Molekularbiologie, Mikrobiologie, Zellbiologie, Immunologie, Genetik, Physiologie, Zoologie und Botanik.
Prüfungen in Chemie I, Chemie II, Biologie I, Biologie II, Experimentalphysik und Mathematik.
Abschluss: Vordiplom.

5. Semester: Verfahrenstechnik, Bioverfahrenstechnik, Regelungstechnik und Technische Biochemie. Abschlussklausuren in allen aufgeführten Fächern.

6.-7. Semester Hauptstudium: Besuch von Spezialvorlesungen in: Technischer Biochemie, Proteinbiochemie, Strukturbiologie, Molekularbiologie, Mikrobiologie, Virologie, Immunologie, Zellbiologie und industrieller Genetik.

Diplomprüfung in Biochemie und Mikrobiologie (Nebenfach).

Extraordinäre Vorlesungen in: Molekularspektroskopie und Quantenmechanik für Technische Biologen; Statistische Thermodynamik von Proteinen.

8./9. Semester: Studienarbeit: Deletion der H-Untereinheit im Reaktionszentrum des phototrophen Bakteriums *Rhodospirillum rubrum* durch zielgerichtete Mutagenese.

Diplomprüfung in Experimentelle Biologie-molekulare Richtung (Hauptfach) und Experimentelle Biologie-physiologische Richtung (Nebenfach).

10./11. Semester: Diplomarbeit: Funktion der H-Untereinheit des photosynthetischen Reaktionszentrums aus *Rhodospirillum rubrum*.
Studienabschluss: Diplom-Biologe technisch orientiert (t.o.).

2001-2004: Promotion. Studienfach Technische Biologie an der Universität Stuttgart.